



**A University of Sussex PhD thesis**

Available online via Sussex Research Online:

<http://sro.sussex.ac.uk/>

This thesis is protected by copyright which belongs to the author.

This thesis cannot be reproduced or quoted extensively from without first obtaining permission in writing from the Author

The content must not be changed in any way or sold commercially in any format or medium without the formal permission of the Author

When referring to this work, full bibliographic details including the author, title, awarding institution and date of the thesis must be given

Please visit Sussex Research Online for more information and further details

# **Asymptotic Safety: From Perturbatively Exact Models to Particle Physics**

**Tom Steudtner**

Submitted for the degree of Doctor of Philosophy  
University of Sussex  
June 2020

# Declaration

I hereby declare that this thesis has not been and will not be submitted in whole or in part to another University for the award of any other degree.

This thesis consists of several peer-reviewed and published (including minor adaptations) as well as unpublished works which have been completed in various collaborations:

- **Ch. 2 is based on [1]:** I. Schienbein, F. Staub, T. Steudtner and K. Svirina, *Revisiting RGEs for general gauge theories*, *Nucl. Phys.* **B939** (2019) 1 [1809.06797]
- **Ch. 3 and Ch. 4** are based on unpublished works in collaboration with Daniel Litim.
- **Ch. 5 is based on [2]:** A. D. Bond, D. F. Litim, G. Medina Vazquez and T. Steudtner, *UV conformal window for asymptotic safety*, *Phys. Rev.* **D97** (2018) 036019 [1710.07615]
- **Ch. 6 derives of [3]:** A. D. Bond, D. F. Litim and T. Steudtner, *Asymptotic safety with Majorana fermions and new large  $N$  equivalences*, *Phys. Rev.* **D101** (2020) 045006 [1911.11168]
- **Ch. 7** is based unpublished work in cooperation with Gudrun Hiller, Clara Hormigos-Feliu and Daniel Litim.
- **Ch. 8** is submitted for publication with a preprint available as [4], a prelude section has been prepended in this thesis: G. Hiller, C. Hormigos-Feliu, D. F. Litim and T. Steudtner, *Anomalous magnetic moments from asymptotic safety*, 1910.14062

I have led or corroborated the original research presented in this thesis.

Signature:

Tom Steudtner

UNIVERSITY OF SUSSEX

TOM STEUDTNER, DOCTOR OF PHILOSOPHY

ASYMPTOTIC SAFETY: FROM PERTURBATIVELY EXACT MODELS TO PARTICLE PHYSICS

SUMMARY

The behaviour of quantum field theories at different energy scales is encoded by its renormalisation group (RG) flow. To be physical and fundamental, their high-energy limit needs to be controlled by an ultraviolet fixed point – a property called asymptotic safety. Recent developments have proven that in strictly four spacetime dimensions and beyond the well-known case of asymptotic freedom, a family of theories with weakly interacting UV fixed points exists in a perturbatively exact setting. This thesis is dedicated to further investigate this phenomenon. Following a thorough introduction, this work consist of three main parts.

The first part is concerned with technical aspects of computing perturbative renormalisation group equations. We revisit literature results and correct several long-standing errors. Moreover, we present a novel software package to facilitate these calculations, and highlight its advantages over existing tools.

The second part is focused on the phenomenon of perturbatively exact asymptotic safety. We systematise the search for such theories to identify new classes of models. For an important benchmark model with unitary gauge symmetry and Dirac fermions, we extend the RG analysis to the highest available loop order. We determine the size of the conformal window and the mechanisms limiting it. Furthermore, we find two novel classes of asymptotically safe theories involving orthogonal or symplectic gauge groups and Majorana fermions. We also discover new large- $N$  equivalences amongst seemingly different quantum field theories, leading to new dualities, and a triality amongst asymptotically safe theories.

In the third part, realistic models of particle physics are constructed. The Standard Model is coupled to an extended sector via electroweak, Yukawa and Higgs portal interactions. We demonstrate that safety until the Planck scale and stability of the Higgs potential is achieved in these theories. Moreover, we show that both discrepancies of electron and muon anomalous magnetic moments can be accounted for simultaneously without explicit lepton flavour violation.

## Acknowledgements

First of all, I am very grateful to my family and their support throughout these studies. During my time at Sussex, I was fortunate to work with many great people. With none have I shared my office longer than Luke and Wissarut, to whom I am thankful for many interesting discussions about programming, history and pop culture. I owe my gratitude to Sandra for her clever advice and delightful company. As for Gustavo, I will never forget the valuable lesson he taught me about the consumption of alcohol in connection with public transportation. Moreover, I am grateful to Jack and Sonali for introducing me to a magic potion called coffee, as well as academic excursions about linguistics, feminism and many random things. My other doctoral siblings Tuğba, Andy, Charlie and Yannick have proven to be reliable allies in all daily challenges, and their contributions shall not be forgotten. We are all thankful to Boris for setting a new benchmark on PhD duration and paper output. To Iberê, who still owes us beer, to Basem, whose voice would rock these walls, as well as Luiz, for joining martial arts classes with me. Many thanks to Dan, Jonathan and Alex for organising the internal seminar, and more importantly coffee and cookies. To Folkert, who stalks me even abroad, and Charanjit, for not abandoning our house (and me in it) during the quarantine. I would like to thank my seniors Kirsty, Djuna, both Chrises, Heather, Alba and Barry, as well as the younger generation including Brad, Eric, Ryan, Chloe, Mike and Reuben for creating a friendly working atmosphere — although some of you have not been around a lot due to being abroad or in the *exile* annex. I apologise to all my colleagues who have shared the lunch table with me and suffered through my humour as well as infrequent complaining about various british issues (although I am still convinced my criticisms are justified). Moreover, I would like to thank Daniel Litim for supervising my research efforts, as well as Gian Paolo Vacca and Gudrun Hiller for hosting me during research placements – and in this regard, also the entire HEP group at TU Dortmund for integrating me so seamlessly. I am grateful to all my collaborators who have contributed to the publications contained herein: Daniel, Andy, Gudrun, Clara, Florian, Ingo and Kseniia. I also owe gratitude to my friends Patrick, Janina and Kevin, as well as my actual brother Mark for proof-reading chapters of this thesis. Parts of the works have been supported by the Grant 57314657 of the *Deutscher Akademischer Austauschdienst (DAAD)*, the ACRI visitor program, and the School of Mathematical and Physical Sciences at the University of Sussex.

# Contents

<b>1</b>	<b>Introduction</b>	<b>8</b>
1.1	Motivation . . . . .	8
1.2	Renormalisation group . . . . .	11
1.3	Fixed points . . . . .	14
1.4	Perturbation theory . . . . .	17
1.5	Simple gauge-Yukawa theories . . . . .	19
1.6	Exact asymptotic safety . . . . .	25
1.7	Outline . . . . .	30
<b>2</b>	<b>Revisiting RGEs</b>	<b>33</b>
2.1	Introduction . . . . .	33
2.2	The Lagrangian for a general gauge theory . . . . .	33
2.3	Renormalisation Group Equations . . . . .	34
2.4	The dummy field method . . . . .	35
2.5	Beta functions for dimensionful parameters . . . . .	36
2.5.1	Fermion mass . . . . .	39
2.5.2	Trilinear coupling . . . . .	42
2.5.3	Scalar mass . . . . .	44
2.6	Comparison with supersymmetric RGEs . . . . .	46
2.7	Numerical impact . . . . .	53
2.7.1	Running of fermion mass terms . . . . .	53
2.7.2	Off-diagonal wave-function renormalisation . . . . .	55
2.8	Conclusions . . . . .	57
2.9	Appendix: Dummy field method at two-loop . . . . .	58
2.9.1	Fermion mass . . . . .	58
2.9.2	Cubic scalar coupling . . . . .	60
2.9.3	Bilinear scalar . . . . .	64
2.10	Appendix: Full two-loop RGEs . . . . .	69
2.10.1	Gauge couplings . . . . .	69
2.10.2	Quartic scalar couplings . . . . .	69
2.10.3	Yukawa couplings . . . . .	72
2.10.4	Fermion mass terms . . . . .	73
2.10.5	Trilinear scalar couplings . . . . .	73
2.10.6	Scalar mass terms . . . . .	75

<b>3</b>	<b>ARGES</b>	<b>78</b>
3.1	Overview . . . . .	78
3.2	Design & comparison with other frameworks . . . . .	78
3.3	Setup . . . . .	80
3.4	ARGES by example . . . . .	80
3.4.1	Defining a model . . . . .	80
3.4.2	Obtaining output . . . . .	82
3.4.3	Advanced capabilities . . . . .	83
3.5	Conclusion . . . . .	86
<b>4</b>	<b>Theorems for exact asymptotic safety</b>	<b>87</b>
4.1	Introduction . . . . .	87
4.2	Classification . . . . .	87
4.2.1	Uncharged scalars . . . . .	88
4.2.2	Uncharged fermion . . . . .	90
4.2.3	Two-index fermion . . . . .	91
4.2.4	Two-index scalar . . . . .	92
4.2.5	All fields 2-index gauged . . . . .	93
4.3	Discussion . . . . .	94
<b>5</b>	<b>UV conformal window for asymptotic safety</b>	<b>99</b>
5.1	Introduction . . . . .	99
5.2	Asymptotic safety . . . . .	100
5.2.1	The model . . . . .	100
5.2.2	Veneziano limit . . . . .	101
5.2.3	Renormalisation group . . . . .	101
5.2.4	Anomalous dimensions . . . . .	103
5.2.5	Systematics . . . . .	103
5.2.6	Away from four dimensions . . . . .	105
5.3	Results at 2NLO' . . . . .	105
5.3.1	Fixed points . . . . .	106
5.3.2	Vacuum stability . . . . .	106
5.3.3	Anomalous dimensions . . . . .	107
5.3.4	Scaling exponents . . . . .	108
5.4	UV conformal window . . . . .	108
5.4.1	Limits for interacting fixed points . . . . .	109
5.4.2	Bounds from fixed points and exponents . . . . .	110
5.4.3	Stabilising vs destabilising fluctuations . . . . .	110
5.4.4	Bounds from beta functions . . . . .	111
5.4.5	Bounds from strong coupling . . . . .	113
5.4.6	Implications for model building and cosmology . . . . .	113
5.5	Discussion . . . . .	115

<b>6</b>	<b>Majorana fermions and large-N equivalences</b>	<b>119</b>
6.1	Introduction . . . . .	119
6.2	Majorana fermions . . . . .	120
6.3	Dirac fermions . . . . .	123
6.4	Large N equivalences . . . . .	125
6.5	Discussion and conclusions . . . . .	130
<b>7</b>	<b>Asymptotic safety beyond the Standard Model</b>	<b>131</b>
7.1	Model . . . . .	131
7.2	Running couplings . . . . .	134
7.2.1	Top-down approach . . . . .	134
7.2.2	Bottom-up approach . . . . .	136
7.3	Phenomenology . . . . .	142
7.4	Conclusion . . . . .	147
<b>8</b>	<b>Anomalous magnetic moments from asymptotic safety</b>	<b>148</b>
8.1	Prelude . . . . .	148
8.2	Introduction . . . . .	150
8.3	New vector-like fermions and scalar matter . . . . .	150
8.4	Explaining anomalous magnetic moments . . . . .	151
8.5	Running of couplings up to the Planck scale . . . . .	153
8.6	Collider production and decay . . . . .	154
8.7	Discussion . . . . .	156
<b>9</b>	<b>Conclusion</b>	<b>157</b>



# 1 Introduction

## 1.1 Motivation

Quantum field theory (QFT) is the backbone of our modern understanding of high-energy physics in the quantum regime and beyond. Fusing the bizarre principles of quantum mechanics and special relativity, it provides the language that spells out the state-of-the-art notion of particle physics. The crown jewel of this framework is the Standard Model (SM) [5–9], which lays claim to describe most of the observable physics within the quantum realm of our universe. The SM incorporates three of the four most fundamental forces of nature: the electromagnetic, weak and strong interactions, mediated by photon,  $W^\pm$  and  $Z^0$  bosons, as well as gluon exchanges. Moreover, it contains all known elementary building blocks of matter: leptons and quarks. With the Higgs boson [10–12], the last postulated piece to render the SM a consistent QFT [13] has been discovered [14–16].

However, this does not mean the theory is complete. In spite of its success in capturing and appropriately quantifying many phenomena in particle physics, the SM does not paint a full picture of our universe. An ideal theory would contain all fundamental forces and elementary particles, be valid at all energy scales, and correctly predict all of nature. By design, the SM is foremost a minimal and effective rather than fundamental description of measurable physics, omitting aspects that are experimentally inaccessible. This includes all phenomena at energy scales beyond our current technological reach. For instance, it does not incorporate the fundamental interaction of gravity. While the macroscopic nature of gravity is on solid theoretical ground owing to general relativity, its consistent and predictive quantum description has remained a controversial topic. Nevertheless, quantum gravity effects are expected to take hold around the Planck energy scale, unaccounted for by the SM. Therefore, it is not surprising that the theory fails to answer important cosmological questions regarding the nature of dark matter, dark energy, inflation and the matter-antimatter asymmetry [17, 18]. Other than gravity, no new physics beyond the Standard Model (BSM) is predicted in the vast energy range between the electroweak and the Planck scale. This is at tension with certain discrepancies between experimental and SM predictions, such as neutrino masses [19], lepton anomalous magnetic moments [20–22], various flavour anomalies [20] and arguably the metastability of the Higgs potential [23–25]. From a more philosophical perspective, the SM is also not satisfactory as a fundamental theory of nature. It contains several parameters that are determined by measurements but not predicted by an underlying mechanism. This includes the flavour textures in the Yukawa sector, as well as the hierarchy and strong CP problem [26]. Moreover, the existence of Landau poles [27] suggests that the physics contained by the theory has strongly coupled ultraviolet (UV) dynamics [28, 29], which is at odds with being a fundamental description in this regime – a systematic bug that cannot be avoided by any valid choice of model parameters (quantum triviality) [30].

From this perspective, the Standard Model can be interpreted as a low-energy approximation of a more complete theory. In order to establish consistency with observations and to make predictions at higher energies, it is in dire need of an extension. However, neither theoretical concerns nor experimental data point towards a definite direction for constructing such a BSM theory. This lack of an unified guiding principle has led to a philosophical schism in model building. Many ansätze rely on assumptions of symmetry or mathematical elegance, e.g. supersymmetry, but have so far either failed to make verifiable predictions or are excluded by experimental data [20].

In this thesis, we will champion the paradigm of *asymptotic safety*. At its core, the principle dictates for a QFT to be consistent and well-defined at all scales [31]. In particular, the paradigm demands that theories are physical and predictive even in the high-energy limit. This is achieved if all their couplings remain at finite values as the energy scale approaches infinity. Hence, the objective is to construct theories that exhibit such an UV fixed point of couplings, controlling the high-energy dynamics of the model. As a paradigm for constructing SM extensions, asymptotic safety is completely based on physical assumptions. In fact, it is by definition the only true principle of UV completion. While other ansätze merely shift the range of validity towards a higher energy scale, asymptotic safety is devoid of such a constraint.

Moreover, a theory capturing all fundamental physics of the universe is expected to be asymptotically safe. In that sense, the concept has originally been developed as a criterion for a theory of quantum gravity [32]. Utilising functional renormalisation group methods [33, 34], evidence for the existence of a UV fixed point in various approximations of quantum gravity has been gathered. This includes minimal Einstein-Hilbert theories [35–37], extensions with higher orders of the Ricci scalar [38–44] and other curvature terms [45–48] as well as gravity coupled to matter [49–52]. A more sophisticated overview is provided by the reviews [37, 53–59] and the references therein. Alternatively, UV fixed points of gravity have also been identified with diagrammatic methods slightly above two spacetime dimensions [32, 60, 61] or a large number of matter fields [62–64]. Further examples of asymptotic safety are also known away from four space-time dimensions, including Yang-Mills theories in  $d = 4 + \epsilon$  dimensions [65–67], four-fermion Gross-Neveu models either slightly above two [68, 69] or exactly three dimensions for a large number of flavours [70, 71], as well as  $\mathcal{O}(N)$  scalar theories in  $d = 3$  [72–74] and non-linear  $\sigma$  models [75–78] in  $d = 2 + \epsilon$ , both with a large- $N$  limit.

If no new physics is present between the electroweak and the Planck scale, the onset of asymptotically safe quantum gravity can predict parameters in the SM [79–83]. However, in order to address its drawbacks by a BSM theory within an experimentally verifiable energy regime, we will employ the asymptotic safety scenario to particle theories without gravity and in exactly four space-time dimensions. If all couplings are to remain sufficiently weak, this implies a strict canon of possible interactions among scalar fields, fermions and gauge bosons. For such a QFT, the asymptotic safety paradigm is well-established in form of the older concept of *asymptotic freedom* – a special case where the UV fixed point is non-interacting. Most famously, the discovery of asymptotic freedom in Quantum Chromodynamics (QCD) [84, 85] has been pivotal in understanding the strong interaction. Moreover, the concept has also been employed to construct UV complete SM extensions. However, these models are constrained by their non-interacting

high-energy dynamics in gauge group, matter content and coupling strengths [86–88].

Although explored almost as early as asymptotic freedom [89], interacting UV fixed points have remained a mystery in theories of particle physics. On the other hand, infrared (IR) fixed points have been studied extensively in the context of the conformal window of QCD. That is, the parameter range in the number of quarks flavours  $N_f$  for which the strong gauge coupling reaches the Banks-Zaks fixed point [90, 91] in the IR, instead of giving rise to chiral symmetry breaking and confinement. The window spans from an upper limit which is perturbatively determined by the loss of asymptotic freedom to  $N_f \leq 16$ , towards a lower bound marked by the onset of strong dynamics, estimated to  $N_f \geq 12 \dots 6$  by various methods [92–109], whereby  $N_f = 6$  is realised in QCD.

More recently, a new milestone has been established when the existence of weakly-interacting UV fixed points has been proven in non-abelian gauge theories with suitable Yukawa interaction [110, 111]. The progress was spear-headed by the construction of QCD-like theory, where the existence of an UV fixed point can be guaranteed [112, 113]. The discovery has sparked many investigations of various aspects [2, 3, 67, 114–120], and represents a promising new direction for BSM model building [4, 121–125]. This novel ansatz marks the entry of asymptotic safety beyond freedom into the realm of particle physics, and is also the starting point of this thesis. We will mostly neglect a second mechanism proposing a UV fixed point in the presence of a large number of matter fields [126–135], as its validity has been questioned [136].

The *modus operandi* of this work is to investigate QFTs for weakly coupled fixed points of their renormalisation group flow. However, almost all fixed points can be described by a conformal field theory (CFT) [137, 138]. This invites a complementary strategy, focusing on the fixed points themselves and leveraging their potent conformal symmetry, independently of the models wherein the points occur. Each CFT description is determined by conformal data such as scaling dimensions and structure constants, for which unitarity bounds [139] apply. The data can be extracted e.g. from the renormalisation group [140] or the conformal bootstrap [141–143]. The latter technique has recently been retrofitted to four dimensions [144] with progress being made towards gauge theories [145], see [146, 147] for reviews. Furthermore, the renormalisation group flow among conformal fixed points is constrained by the  $a$ -theorem [148–151] and Weyl consistency conditions [152, 153].

**Outline.** The remaining part of this introduction is dedicated to briefly review the theoretical underpinnings of this thesis. First, we will recall the renormalisation group as fundamental feature of any QFT, and highlight how it encodes the scale dependence. After that, we will formally introduce fixed points of this flow and the terminology surrounding them. This will lead us to a definition of asymptotic safety, and how it insures UV completion and predictivity. Subsequently, it is argued how the picture is simplified in a weak coupling regime and how perturbation theory is a powerful instrument of investigation. We arrive at theorems that outline necessary features of a theory to exhibit asymptotic safety. Next, the most basic example of such a model, a simple gauge-Yukawa theory, is investigated in a general manner. Cataloguing its fixed points and phases, the mechanism of asymptotic safety is uncovered. Thereafter, we will develop a program to guarantee the existence of the UV fixed point, and arrive at the Litim-Sannino model. In the last section, we will then provide an outlook for the main part of the thesis.

## 1.2 Renormalisation group

**Scales.** Most physical systems look different depending on what scale they are investigated at, which may be a characteristic length, energy or similar. In particular, even if the classical action is scale invariant, quantum fluctuation may introduce such a parameter (e.g. dimensional transmutation [154]). Hence, it is possible to understand a system at a certain scale, but not at another: nuclear physics can be formulated effectively without a notion of quantum chromodynamics. In particular, high-energy details of a theory wash out in the low-energy limit, unless they are protected by a symmetry [155].

To connect the physics between the scales we can measure, and extrapolate beyond them, the understanding of how a system changes as we vary the scale is crucial. This is encoded in the renormalisation group (RG). The need for such a formalism was first encountered with the development of Quantum Electrodynamics (QED) by Tomonaga [156], Schwinger [157–160], Feynman [161–163] and Dyson [164,165] which required a renormalisation procedure that introduced an associated cut-off scale. An RG theory around transformations of this cut-off was first introduced by Stückelberg and Petermann [166], but went unnoticed, until explored by Gell-Mann and Low [167]. The formalism has been modernised by Callan and Symmanzik [168,169], and we will give an overview in this section. Based on the work of Kadanoff [170], a more intuitive picture of the RG was developed by Wilson [171–174], which has led to functional formalisms [33, 34, 175] discussed below.

**Renormalisation Group Equations.** In Quantum Field Theory (QFT), the introduction of a renormalisation scale  $\mu$  is a consequence of the regularisation of UV divergences from momentum integrals. Consider a generic theory with action  $S$ , containing the fields  $\phi_a$  and corresponding currents  $J_a$ . All physical information is contained in correlation functions of the shape

$$\langle \phi_{a_1}(x_1) \dots \phi_{a_n}(x_n) \rangle = i^{-n} \mathcal{Z}[J]^{-1} \left( \frac{\delta}{\delta J_{a_1}(x_1)} \dots \frac{\delta}{\delta J_{a_n}(x_n)} \right) \mathcal{Z}[J] \Big|_{J=0} \quad (1.1)$$

where

$$\mathcal{Z}[J] = \int \mathcal{D}\phi \, e^{iS[\phi] + i \int d^4x J_a(x) \phi_a(x)} \quad (1.2)$$

is the partition function. However, (1.1) will in general involve momentum integrals that are (UV) divergent for large values. In a multiplicative renormalisation procedure,

$$\lambda_i^{\text{bare}} \mapsto \lambda_i(\mu) + \delta\lambda_i^{\text{ct}}, \quad \phi_a^{\text{bare}} \mapsto \left( \sqrt{Z}_{ab}(\mu) + \delta\sqrt{Z}_{ab}^{\text{ct}} \right) \phi_b, \quad (1.3)$$

the classical (bare) couplings  $\lambda_i^{\text{bare}}$  and fields  $\phi_a^{\text{bare}}$  are replaced by renormalised quantities  $\lambda_i(\mu)$ ,  $\sqrt{Z}_{ab}\phi_b$ , depending on a renormalisation scale  $\mu$ , and counter-terms  $\delta\lambda_i^{\text{ct}}$ ,  $\delta\sqrt{Z}_{ab}^{\text{ct}}$  absorbing the UV divergences. Note that  $\sqrt{Z}$  is called field strength renormalisation. The renormalisation group equations (RGEs) can then be formulated using  $\beta$  and  $\gamma$  functions [168,169] describing the running of these renormalised quantities with a change of  $\mu$

$$\beta_i(\lambda_j) = \frac{\partial \lambda_i}{\partial \ln \mu}, \quad \gamma_{ab}(\lambda_j) = \sqrt{Z}_{ac}^{-1} \frac{\partial \sqrt{Z}_{cb}}{\partial \ln \mu}. \quad (1.4)$$

Besides the ambiguity of the regularisation mechanism, many renormalisation schemes exist as the counter terms  $\delta\lambda_i^{\text{ct}}$  and  $\delta\sqrt{Z}_{ab}^{\text{ct}}$  may contain arbitrary finite parts. This dependency, as well as the choice of the renormalisation scale  $\mu$ , drops out when computing physical quantities  $\mathcal{O}$ :

$$\frac{d\mathcal{O}}{d\ln\mu} = \left( \frac{\partial}{\partial\ln\mu} + \beta_i \frac{\partial}{\partial\lambda_i} + \int d^4x \phi_b(x) \gamma_{ab} \frac{\delta}{\delta\phi_a(x)} \right) \mathcal{O} = 0. \quad (1.5)$$

However, the physical interpretation of the renormalisation group highly depends on these aforementioned details. Throughout this work, we will use dimensional regularisation, computing quantum fluctuations at  $d = 4 - \epsilon$  and the modified minimal subtraction or in short  $\overline{MS}$  scheme [176]. Therein, counter-terms only contain the regularised UV singularities as  $\epsilon \rightarrow 0$  as well as a universal constant that can be absorbed in a redefinition of the scale  $\mu$ , leading to the expansion

$$\lambda_i^{\text{bare}} = \mu^{\epsilon\kappa_i} \left[ \lambda_i + \delta\lambda_i^{\text{ct}}(\lambda_j) \right], \quad \delta\lambda_i^{\text{ct}} = \sum_{n=1}^{\infty} c_n^{(i)} \epsilon^{-n}. \quad (1.6)$$

Here,  $\kappa_i$  is a number that mere depends on the type of coupling  $\lambda_i$ . As the bare coupling is independent of the renormalisation scale, the condition

$$\frac{d}{d\ln\mu} \lambda_i^{\text{bare}} = \left[ \frac{\partial}{\partial\ln\mu} + \sum_j \beta_j \frac{\partial}{\partial\lambda_j} \right] \lambda_i^{\text{bare}} = 0, \quad (1.7)$$

together with (1.6) and  $\beta$  functions being UV finite implies that the latter can be extracted from the first order poles of the coupling counter-terms

$$\beta_i = -\epsilon\kappa_i\lambda_i - \kappa_i c_1^{(i)} + \sum_j \kappa_j \lambda_j \frac{\partial c_1^{(i)}}{\partial\lambda_j}, \quad (1.8)$$

suggesting an intimate link between the removal of UV divergencies via counter-terms and the renormalisation group. The same argument relates the anomalous dimensions  $\gamma_{ab}$  to the poles of the field strength renormalisation counter-terms:

$$\delta\sqrt{Z}^{\text{ct}} = \sum_{n=1}^{\infty} z_n \epsilon^{-n}, \quad \gamma = - \sum_i \kappa_i \lambda_i \frac{\partial z_1}{\partial\lambda_i}. \quad (1.9)$$

Following the conventions (1.3), each bare interaction vertex

$$v_i^{abc\dots} = \lambda_i \phi^a \phi^b \phi^c \dots \quad (1.10)$$

requires a counter-term  $\delta v_i$  to cancel infinities from proper vertex corrections, relating to counter-terms for both the field strength renormalisation of external legs and the coupling

$$\delta v_i = \left[ \delta\lambda_i^{\text{ct}} + \lambda_i \sum_{\text{legs}} \left( \delta\sqrt{Z}^{\text{ct}} \right) \left( \sqrt{Z}^{-1} \right) \right]. \quad (1.11)$$

This relation is reflected by the general shape of the  $\beta$  functions

$$\beta_{\lambda_i} = \beta_{v_i} + \sum_{\text{legs}} \gamma \cdot v, \quad (1.12)$$

retaining terms that are either vertex ( $\beta_{v_i}$ ) or leg corrections ( $\gamma \cdot v$ ).

In spite of this simple connection to the first-order poles of counterterms cancelling UV divergencies, a strong physical interpretation of this scheme is difficult, other choices provide a better understanding of the renormalisation group. But this lack of attachment to the physical world is a virtue – the scale  $\mu$  can be considered a free parameter, which choice does not change the theory, as defined by its observables. However, this does not mean that  $\mu$  is completely spurious, and the renormalisation group physically irrelevant. The Wilsonian renormalisation group provides an alternative formulation allowing for a more straightforward interpretation.

**Wilsonian renormalisation group.** The concept of the renormalisation group and its interpretation has been generalised by Wilson [173] on quantum actions  $S_\Lambda$  containing all possible operators. Therein, UV divergences are regulated by choosing a momentum cut-off scale  $\Lambda$

$$\mathcal{Z}_\Lambda[J] = \int_{p^2 < \Lambda^2} \mathcal{D}\phi e^{iS_\Lambda[\phi] + i \int d^4x J(x)\phi(x)}. \quad (1.13)$$

A renormalisation group transformation then amounts to changing the cut-off. If the new scale is lower,  $\Lambda' < \Lambda$ , the fields are decomposed into soft and hard modes  $\phi = \phi' + \varphi$  with momenta below and above  $\Lambda'$ , and the hard modes integrated out

$$\begin{aligned} \mathcal{Z}_{\Lambda'}[J'] &= \int_{p^2 < \Lambda'^2} \mathcal{D}\phi' \int_{\Lambda'^2 \leq p^2 < \Lambda^2} \mathcal{D}\varphi e^{iS_\Lambda[\phi' + \varphi] + i \int d^4x J'(x)\phi'(x)} \\ &= \int_{p^2 < \Lambda'^2} \mathcal{D}\phi' e^{iS_\Lambda[\phi'] + i \int d^4x J'(x)\phi'(x)}. \end{aligned} \quad (1.14)$$

Hence, each renormalisation point corresponds to a different QFT, retaining a unique number of momentum modes, related by the renormalisation group. As the cut-off is sent to infinity  $\Lambda \rightarrow \infty$ , the action becomes sensitive to high-energy effects. This is the key difference to the procedure introduced before – although cut-off schemes are also available therein – where scale is considered a regularisation parameter of the very same theory, no degrees of freedom are integrated out by changing it.

A slight generalisation of the Wilsonian ansatz represents the Polchinski RG [175], where the cut-off is replaced by a smooth UV regulator  $C_\Lambda^{-1}$

$$\mathcal{Z}_\Lambda[J] = \int \mathcal{D}\phi e^{iS_{\text{int}}[\phi] + i \int d^4x \left[ \frac{1}{2} \phi C_\Lambda^{-1} (-\partial^2) \phi + J\phi \right]}, \quad C_\Lambda(p^2) = \begin{cases} p^{-2} & \text{for } p^2 \ll \Lambda^2 \\ 0 & \text{for } p^2 \gg \Lambda^2 \end{cases}. \quad (1.15)$$

This approach is considered more practical to implement, as it leads to an exact flow equation

$$\frac{\partial S_{\text{int}}}{\partial \ln \Lambda} = \frac{1}{2} \int d^4p \left[ \text{tr} \frac{\partial C_\Lambda(p^2)}{\partial \ln \Lambda} \frac{\delta^2 S_{\text{int}}}{\delta \phi(p) \delta \phi(-p)} - \frac{\delta S_{\text{int}}}{\delta \phi(p)} \frac{\partial C_\Lambda(p^2)}{\partial \ln \Lambda} \frac{\delta S_{\text{int}}}{\delta \phi(-p)} \right] \quad (1.16)$$

for the interaction part of the action  $S_{\text{int}}$ .

Taking a complementary perspective to the Wilsonian approach of a low-energy action, the functional renormalisation group is formulated in terms of an effective action, which is generated by the UV modes that are integrated out. In order to separate those degrees of freedom, an infrared (IR) regulator  $R_k$  has to be introduced instead. After Wick rotation, the euclidean partition function

$$\mathcal{Z}_k[J] = \int \mathcal{D}\phi e^{-S[\phi] - \int d^4x \left[ \frac{1}{2} \phi R_k(-\partial^2) \phi - J\phi \right]}, \quad R_k(p^2) = \begin{cases} k^2 & \text{for } p^2 \ll k^2 \\ 0 & \text{for } p^2 \gg k^2 \end{cases}, \quad (1.17)$$

can be Legendre-transformed to obtain the quantity

$$\Gamma_k[\varphi] = -\ln \mathcal{Z}_k[J] + \int d^4x \left[ J\varphi - \frac{1}{2} \varphi R_k(-\partial^2) \varphi \right], \quad (1.18)$$

which is called effective average action, and functional of the classical field  $\varphi$  (averaged over the unregulated momentum space). If the scale  $k$  is lowered to zero, the regulator disappears and the full effective action  $\Gamma_0[\varphi] = \Gamma[\varphi]$  is obtained. In the opposite limit  $k \rightarrow \infty$ , the average action only contains high-energy quantum fluctuations and becomes the bare action  $\Gamma_\infty[\varphi] = S[\varphi]$ . Transformations of the RG scale towards this limit are reminiscent of changing the coarse-graining of  $\Gamma_k$ , by averaging only over shorter and shorter distances. This flow can be described by the exact Wetterich equation [33, 34]

$$\frac{\partial \Gamma_k[\varphi]}{\partial \ln k} = \frac{1}{2} \text{tr} \int d^4p \left[ \frac{\partial R_k(p^2)}{\partial \ln k} \left( \frac{\delta^2 \Gamma_k}{\delta \varphi(-p) \delta \varphi(p)} + R_k(p^2) \right)^{-1} \right]. \quad (1.19)$$

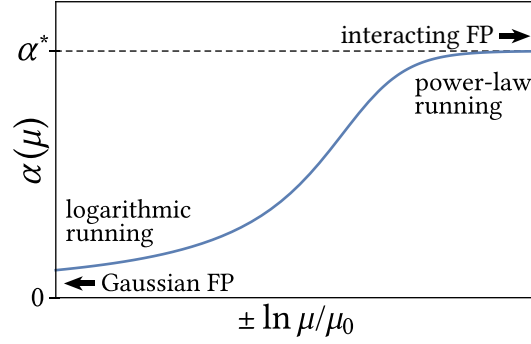
The Wetterich (1.19) and Polchinski (1.16) flows are UV finite due to the properties of the regulator. In fact, both formalisms are related by a Legendre transformation [34].

Both notions of the renormalisation group are self-consistent and arise from different methods of regularising the UV dynamics of the same physical systems within a QFT descriptions. Hence, both approaches are in fact equivalent formulations of the same physics. Practically, each procedure comes with its own advantages and disadvantages, but all physical phenomena must appear in each of them. This includes also the notion of UV completion, which means taking the limit  $\Lambda \rightarrow \infty$  in the Wilsonian renormalisation group picture, and is intertwined with the consistency of the renormalisation procedure  $\mu \rightarrow \infty$  in the other formulation (or equivalently to zero if it is a length scale). These considerations will lead us to discuss fixed points next.

### 1.3 Fixed points

After having established that quantum fluctuations of a theory induce renormalisation group running, we will now review the exception from this phenomenon: fixed points. In the following, we will collect some general properties and then highlight the importance of fixed points for UV completion.

**Definition.** Fixed points are a set of couplings  $g_i^*$  at which the renormalisation group flow ter-



**Figure 1.1:** Renormalisation group running of coupling  $\alpha$  with the renormalisation scale  $\mu$  (blue line) via  $\partial\alpha/\partial\ln\mu = -B\alpha^2 + C\alpha^3$  between the non-interacting, Gaussian fixed point  $\alpha = 0$  (lower left) to an interacting fixed point  $\alpha = \alpha^* = B/C$  (top right). Close to the Gaussian, the flow follows a logarithmic behaviour as in (1.22), while power-law running as in (1.23) is found in the vicinity of  $\alpha^*$ . The direction of the flow is immaterial in this plot, the sign of the abscissa is arbitrary.

minates. They can be formally identified by a collective zero point of all  $\beta$  functions

$$\beta_i(g_j^*) = \left. \frac{\partial g_i}{\partial \ln \mu} \right|_{g_j=g_j^*} = 0. \quad (1.20)$$

Therefore, trajectories in coupling space can only reach a fixed point in an asymptotic limit  $\mu \rightarrow \pm\infty$ , so that they can be classified as UV or IR. At such a point, the QFT becomes scale invariant even at quantum level, with each operator  $\mathcal{O}_\Lambda = \left(\frac{\Lambda}{\Lambda'}\right)^{\Delta_\mathcal{O}} \mathcal{O}_{\Lambda'}$  transforming via its scaling dimension  $\Delta_\mathcal{O}$ , which are physical observables. In most cases the theories even exhibit a complete conformal symmetry [137, 138]. As correlators at a fixed point become  $\langle \phi(0)\phi(r) \rangle \propto r^{-\Delta_\phi}$ , no finite correlation length exists, and microscopic phenomena extend to macroscopic scales. Hence, critical phenomena such as second order phase transitions [171, 172] are associated with fixed points. In consequence, close to criticality all physical systems can be categorised into universality classes, in which the fixed points correspond to the same conformal field theory, leading to some features being universal within each class.

**Attractivity, Predictivity.** To quantify if a fixed point is UV or IR, trajectories in coupling space have to be investigated around it. Unless the fixed point is in an extremum of the  $\beta$  function, it can be expanded via

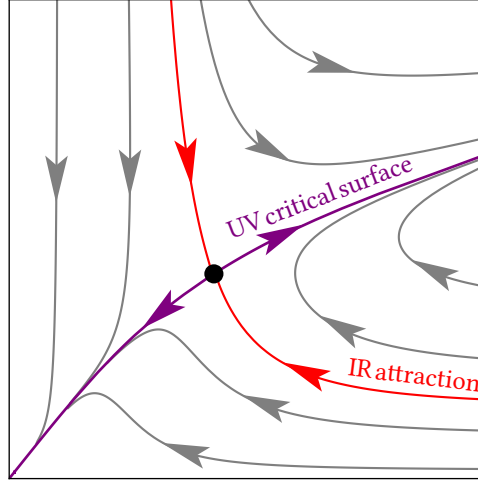
$$\beta_i(g) = M_{ij}(g_j - g_j^*) + C_{ijk}(g_j - g_j^*)(g_k - g_k^*) + \mathcal{O}[(g - g^*)^3], \quad (1.21)$$

where  $M_{ij} = \partial\beta_i/\partial g_j|_{g=g^*}$  is called the stability matrix. Its eigenvalues, the critical exponents  $\vartheta_i$  indicate that the RG flow around the fixed point is given by a power law

$$g_i(\mu) = g_i^* + \vec{c} \cdot \vec{v}_i \left( \frac{\mu}{\mu_0} \right)^{\vartheta_i} + \dots, \quad (1.22)$$

where  $\vec{v}_i$  are the corresponding eigenvectors, and  $\vec{c}$  is a direction in coupling space. Trajectories with  $\vartheta_i < 0$  are called relevant, they are UV attractive or IR repulsive. On the other hand, irrelevant eigendirections have  $\vartheta_i > 0$ , and are IR attractive or UV repulsive. The case  $\vartheta_i = 0$  is called





**Figure 1.2:** Example flow diagram in the space of two couplings, arrows are directed from the UV to the IR. The fixed point (black dot) has one relevant (purple) and one irrelevant (red) eigendirection. The high-energy complete theories live on the UV critical surface, which is one-dimensional (purple line).

marginal; the RG evolution is then logarithmically in the scale parameter

$$g_i(\mu) = g_i^* + a_i \ln \left( \frac{\mu}{\mu_0} \right) + \dots, \quad (1.23)$$

where  $a_i$  as well as the couplings  $g_i$  are obtained by diagonalising (1.21). An example trajectory in the two-loop approximation exhibiting both regimes is displayed in Fig. 1.1.

Critical exponents are physical observables and invariant under a suitable reparametrisation  $g_i \mapsto g'_i$  as

$$\begin{aligned} M'_{ij} &= \frac{\partial}{\partial g'_j} \beta'_i \Big|_* = \frac{\partial g_l}{\partial g'_j} \frac{\partial}{\partial g_l} \left( \frac{\partial g'_i}{\partial g_k} \frac{\partial g_k}{\partial \ln \mu} \right) \Big|_* \\ &= \frac{\partial g_l}{\partial g'_j} \left( \frac{\partial g'_i}{\partial g_k} \frac{\partial}{\partial g_l} \beta_k + \beta_k \frac{\partial^2 g'_i}{\partial g_k \partial g_l} \right) \Big|_* = \left( \frac{\partial g'_i}{\partial g_k} \right) M_{kl} \left( \frac{\partial g_l}{\partial g'_j} \right), \end{aligned} \quad (1.24)$$

since all  $\beta$  functions vanish at the fixed points regardless of the parametrisation. Hence, the transformation  $M' \mapsto T M T^{-1}$  leaves the eigenvalue spectrum invariant.

Further, the submanifold in coupling space containing all trajectories attracted to a fixed point are referred to as its critical surface. Its dimension corresponds to the number of parameters that can be chosen freely while still being attracted to the fixed point. The dimensionality of the repulsive submanifold however corresponds to the number of parameters that are predicted in terms of the critical surface ones. An example is displayed in Fig. 1.2, featuring a system of two couplings, which represent the coordinate axes. UV complete theories require RG trajectories that lie in the critical surface, which is one-dimensional (purple line). Hence, one coupling is completely predicted by the other.

**UV completion and asymptotic safety.** An essential criterion for UV completion of a theory is that the limit  $\mu \rightarrow \infty$  of the renormalisation scale must be well-defined and physical. As all physical observables are independent of  $\mu$ , it is a parameter free to be chosen – including the limit  $\mu \rightarrow \infty$ . Hence, this notion of UV completion of a theory reflects the consistency of its

renormalisation group procedure. In the Wilsonian renormalisation group, the limit implies that a theory exists where all high-momentum modes  $p^2 \rightarrow \infty$  are included, that is free of unphysical properties such as poles. This is indeed a reasonable definition of UV completion. Excluding the possibility of limit cycles [31], this requires the following ingredients:

- a) A UV fixed point  $g_i^*$  of all dimensionless couplings exist. This requires (1.20) with  $g_i = \mu^{-d_i} G_i$ , where the coupling  $G_i$  in the action has the mass dimension  $d_i$ . Hence, any quantity computed in terms of  $g_i^*$  is UV finite.
- b) Its UV critical surface is finite-dimensional. Otherwise, the theory might still be UV complete, but non-predictive as an infinite set of open parameters exist.
- c) The UV fixed point needs to be situated in a physical regime and connects to the IR through trajectories that are physical as well.

Theories that exhibit these properties are called *asymptotically safe*. The concept has been named by Weinberg [32] as a non-perturbative generalisation of renormalisability. It is a general criterion for UV completion for quantum field theories, and can be used for predictive model building. In that sense, restricting the parameter space onto the UV critical surface is not fine-tuning, but a prediction by UV completion. Hence, the concept is in contraposition to effective field theory approaches, where all couplings are fixed by (in principle, infinitely many) measurements in the IR instead.

Many studies have been conducted regarding asymptotic safety of quantum gravity in various approximations, as well as many other theories, using Wilsonian renormalisation group techniques, large- $N$  limits and  $\epsilon$  expansions around critical dimensions, see [58] for a review and references therein.

Here, we will mostly be interested in asymptotic safety in strictly  $d = 4$  and a weak coupling regime, excluding gravity. In such a regime, the phenomenon of *asymptotic freedom* [84, 85] is well known and even predates the notion of asymptotic safety. In fact, it is a special case of asymptotic safety where the UV fixed point is non-interacting ( $g_i^* = 0$ ). However, for a long time no weakly coupled theory exhibiting asymptotic safety beyond freedom has been identified, leaving the latter as the only viable mechanism for UV completion. This has led to the development of GUT extension of the SM, embedding away abelian gauge groups that are incompatible with complete asymptotic freedom [86–88]. The situation has changed only recently with the seminal work [112], demonstrating safety beyond freedom in a gauge-Yukawa theory that is perturbatively exact. As these developments form the foundations of this work, they will be discussed in more detail in the following sections, starting with implications of the weak coupling regime.

## 1.4 Perturbation theory

In the context of Quantum Field Theory, the spirit of perturbation theory is to expand the action of a system around that of a free theory, treating all interactions as small fluctuations that can be systematically arranged as convergent series. For example, consider an interacting theory  $\mathcal{L}(\phi) = \mathcal{L}_0(\phi) + g I(\phi)$  with  $\mathcal{L}_0$  being the free field theory, and  $g I$  the interaction Lagrange density. The full partition function  $\mathcal{Z}$  is expanded around the exactly solvable partition function

of the free field theory  $\mathcal{Z}_0$

$$\begin{aligned}\mathcal{Z}[J] &= \int \mathcal{D}\phi e^{i \int d^4x \mathcal{L}(\phi(x)) + J(x)\phi(x)} \\ &= e^{ig \int d^4x I\left[\frac{\delta}{\delta J(x)}\right]} \mathcal{Z}_0[J] \\ &= \left(1 + ig \int d^4x I\left[\frac{\delta}{\delta J(x)}\right] - \frac{1}{2}g^2 \iint d^4x d^4x' I\left[\frac{\delta}{\delta J(x)}\right] I\left[\frac{\delta}{\delta J(x')}\right] + \dots\right) \mathcal{Z}_0[J].\end{aligned}\tag{1.25}$$

The argument is that for the series to converge, the coupling constant  $g$  needs to be sufficiently small. Hence, terminating the series at a finite (loop) order is a good approximation. This approach has been very successful for weakly coupled theories, especially due to the technique of Feynman diagrams.

**Canonical scaling.** Moreover, this implies an ordering principle for operators in the action. As quantum fluctuations are assumed to be small, the scaling behaviour of each operator is given by its canonical dimension. Couplings with classically positive mass dimensions are relevant, quantum fluctuations do not change its scaling. On the other hand, higher order operators are considered irrelevant. Merely for classically marginal couplings, where the scaling exponents are solely determined by quantum fluctuations, the situation is unclear *a priori*. Hence, for finite field content, the number of marginal and relevant operators is finite as well, rendering such a theory predictive.

**Perturbative renormalisability.** By definition, each perturbative expansion, including the one for the RG flow equations, is a power series in the coupling constants. Hence, dimensional analysis suggests that perturbative theories defined in terms of classically marginal and relevant couplings in the UV, only require the same kind of operators to measured in the IR to determine the relevant RG flow. Such theories are called (perturbatively) renormalisable.<sup>1</sup> As the renormalisation scale dependence is entirely absorbed in those couplings, renormalisable actions are self-similar under RG transformations [177, 178]. On the other hand, if arbitrary operators with negative mass dimension (non-renormalisable operators) are involved, each loop order of a perturbative expansion requires the knowledge of operators of couplings with even lower mass dimension.

**Template theory and master formulas.** The set of renormalisable operators is highly dependent on the number of spacetime dimensions. For  $d = 4$ , only gauge couplings  $g$ , Yukawa interactions  $Y$  and scalar quartic couplings  $\lambda$  are dimensionless. Moreover, scalar  $\mu$  and fermion masses  $m$  as well as scalar cubic interactions  $h$  have a positive mass dimension. This allows the bare Lagrangian of a template theory to be formulated as

$$\begin{aligned}\mathcal{L} &= -\frac{1}{4}F_A^{\mu\nu}F_{\mu\nu}^A + \frac{1}{2}D^\mu\phi_a D_\mu\phi_a + i\psi_j^\dagger \sigma^\mu D_\mu\psi_j + \mathcal{L}_{\text{gh}} + \mathcal{L}_{\text{gf}} \\ &\quad - \frac{1}{2}\left(Y_{jk}^a \psi_j \varepsilon \psi_k \phi_a + Y_{jk}^{a*} \psi_j^\dagger \varepsilon \psi_k^\dagger \phi_a\right) - \frac{1}{4!}\lambda_{abcd} \phi_a \phi_b \phi_c \phi_d \\ &\quad - \frac{1}{2}\left[m_{jk} \psi_j \varepsilon \psi_k + m_{jk}^* \psi_j^\dagger \varepsilon \psi_k^\dagger\right] - \frac{\mu_{ab}^2}{2!}\phi_a \phi_b - \frac{h_{abc}}{3!}\phi_a \phi_b \phi_c.\end{aligned}\tag{1.26}$$

<sup>1</sup>There are additional requirements, such as a gauge symmetry for spin one fields.

where  $\mathcal{L}_{\text{gf, gh}}$  are gauge fixing and ghost terms and  $\psi_i, \phi_a$  being Weyl fermions and real scalar fields, with universal indices running over all particle species, generations, flavours, colours and so on. In the same spirit, a sum over all gauge groups is implied. More details will be provided in Ch. 2. The ansatz is extremely powerful, as any renormalisable theory can be embedded into this template. In fact, RG equation can be extracted in this general form, resolving only momentum integral and spinor contractions, but retaining the universal index structure. Early works up to two-loop order in gauge, Yukawas and quartics and field strength anomalous dimensions in the  $\overline{\text{MS}}$  scheme [179–184] have been recomputed and extended for masses and scalar cubic [1, 185]. For gauge couplings, the full three-loop results are available [186–190]. Moreover, the running of vacuum expectation values (VEVs) has been computed up to two-loop order [191, 192]. For the pure scalar part of (1.26), general RGEs have been determined at three and four loops [150, 193]. Constraints on four-loop gauge and three-loop Yukawa RG equations are provided in [190]. A handy introduction into universal index contraction is given in [194]. In more specialised cases, higher order corrections have also been computed. For  $\mathcal{N} = 1$  supersymmetric theories a similar template approach exists for the  $\overline{\text{DR}}$  scheme, with all results available at two-loop order [191, 192, 195–198] and even three-loop for gauge couplings and superpotential parameters [199–201]. In non-supersymmetric simple gauge theories with charged fermions, gauge  $\beta$  functions are known up to 5-loop [202–205]. Moreover, four-loop RG equations are available in some scalar-Yukawa theories [206–208] and 6-loops in  $O(N)$  [209–211] and  $O(N) \times O(M)$  scalar theories [212–214]. For the Standard Model, all  $\beta$  functions have been computed up to three-loop [215–220], and four-loop [221] for all gauge couplings.

**Theorems of asymptotic safety.** The universal structure of weakly coupled  $\beta$ -functions in four dimensions implies strict theorems on the existence of asymptotic safety in a weakly coupled regime:

1. Gauge interactions are strictly required for asymptotic safety. [111, 222]
2. In order to achieve asymptotic freedom, all gauge subgroups must be non-abelian. [222]
3. In order to achieve asymptotic safety beyond freedom, non-abelian gauge interactions, with or without abelian subgroups, as well as Yukawa interactions are required. This implies that gauge bosons, fermions and scalars have to be present in the theory. [110, 111]

These theorems hold for arbitrary gauge and global symmetries and representations. The last point, depending on global and local symmetries, often implies that besides gauge and Yukawa couplings scalar quartic interactions must also be taken into account. In the next section, we will demonstrate these theorems for simple gauge-Yukawa theories.

## 1.5 Simple gauge-Yukawa theories

Now, we will consider a QFT with single but arbitrary gauge group with interaction  $g$ , that can contain both scalar and fermionic matter, weaved together in a single Yukawa coupling  $y$ . The number of scalar quartic interactions  $\lambda_i$  on the other hand depends on gauge and global symmetries and representations. Using the definitions

$$\alpha_g = \frac{g^2}{(4\pi)^2}, \quad \alpha_y = \frac{y^2}{(4\pi)^2}, \quad \alpha_i = \frac{\lambda_i}{(4\pi)^2}, \quad (1.27)$$

the general structure of the RGEs  $\beta_{g,y,i} = \partial \alpha_{g,y,i} / \partial \ln \mu$  at leading, non-trivial order (2-loop in gauge couplings, 1-loop in Yukawas, quartics) is:

$$\begin{aligned}\beta_g &= \alpha_g^2 (-B + C \alpha_g - D \alpha_y), \\ \beta_y &= \alpha_y (E \alpha_y - F \alpha_g), \\ \beta_i &= H^{ijk} \alpha_j \alpha_k - I_g^{ij} \alpha_g \alpha_j + I_y^{ij} \alpha_y \alpha_j + J_g^i \alpha_g^2 - J_y^i \alpha_y^2.\end{aligned}\tag{1.28}$$

Here, the coefficients  $B, C, D, E, F, H^{ijk}, I_{g,y}^{ij}$  and  $J_{g,y}^i$  depend on the details of the quantum field theory, and can be extracted from [182–185]. At these loop orders, the system is universal for mass independent renormalisation schemes. The coefficients  $B$  and  $C$  are only sensitive to the non-abelian self-interaction and charged matter content, and read

$$\begin{aligned}B &= \frac{22}{3} C_2^G - \frac{4}{3} n_F S_2^F - \frac{1}{3} n_S S_2^S, \\ C &= -\frac{68}{3} (C_2^G)^2 + 4 n_F S_2^F (C_2^F + \frac{5}{3} C_2^G) + 4 n_S S_2^S (C_2^S + \frac{1}{6} C_2^G).\end{aligned}\tag{1.29}$$

The quantities  $S_2^R, C_2^R$  and  $d_R$ , are the Dynkin index, quadratic Casimir invariant and dimension of the gauge representations, while  $n_R$  are the field multiplicities of the fermions ( $R = F$ ), scalars ( $R = S$ ) and gauge bosons ( $R = G$ ). If more than one type of fermions and scalars are present, a sum over the indices  $F$  and  $S$  of matter interactions in (1.29) is implied. The group invariants are defined via

$$S_2^R \delta^{AB} = t_{ab}^A t_{ba}^B, \quad C_2^R{}_{ab} = t_{ac}^A t_{cb}^A, \quad d_R = \delta_{aa}, \tag{1.30}$$

where  $t_{ab}^A$  denotes the generator of representation  $R$ . For irreducible representations, one has  $C_2^R{}_{ab} = C_2^R \delta_{ab}$ . Moreover, this leads to the relation  $C_2^R d_R = S_2^R d_G$ .

As obvious from (1.29), the non-abelian self-interactions of the gauge bosons counteract influence of the charged matter sector. Scalars and fermions drive  $B$  negative and  $C$  positive, causing  $\beta_g$  to become more positive, but the pure gauge contribution have the opposite effect. While the coefficients  $B$  and  $C$  can take either sign, the Yukawa coefficients are manifestly positive for any quantum field theory  $D, F \geq 0$  and  $E > 0$ , where  $D = F = 0$  is only the case for uncharged fermions in the Yukawa interaction [182–185]. The signs of quartic coefficients  $H$  and  $J_{g,y}$  depend on the sign of the  $\alpha_i$ . However, for most scalar sectors, the choice of positive  $\alpha_i$  – corresponding to a potential bounded from below – also means  $H, J_{g,y}$  and  $J_{g,y}$  are positive. This implies that gauge and Yukawa interactions have a diametral effect in the quartic RGEs. Uncharged scalars lead to  $J_g = I_g = 0$ , while  $J_y = I_y = 0$  is symptomatic for scalars not involved in the Yukawa interactions. However, systems of several quartic interactions may also have some  $J_{g,y} = 0$  due to the choice of basis. Furthermore, the quartic sector is algebraically decoupled from the gauge-Yukawa system in (1.28):  $\alpha_i$  appear in  $\beta_g$  at first at three- or four-loop order, depending if the scalar is charged, and two-loop in the  $\beta_y$ . However, quartics are absent from this leading approximation, such that potential fixed point values  $\alpha_{g,y}^*$  can be extracted from  $\beta_g = \beta_y = 0$  first, and only then plugged into the quartic RGEs. However, unless  $J_{g,y} = 0$ , the quartic system is, unlike the gauge or Yukawa one, not technically natural, such that the  $\alpha_i$  cannot be switched off. The fixed point solutions  $\alpha_i^*$  extracted from  $\beta_i|_{\alpha_{g,y}=\alpha_{g,y}^*} = 0$  may then end up being complex or within a configuration where

FP	Type	$\alpha_g^*$	$\alpha_y^*$	$\vartheta_1$	$\vartheta_2$	Condition	Fig. 1.3
<b>G</b>	UV [IR]	0	0	0	0	$B > 0$ [ $B < 0$ ]	① ② ③ [④ ⑤]
<b>BZ</b>	IR	$\frac{B}{C}$	0	$\frac{B^2}{C}$	$-\frac{BF}{C}$	$B, C > 0$	② ③
<b>GY</b>	IR [UV]	$\frac{B}{C'}$	$\frac{BF}{C'E}$	eq. (1.39)	eq. (1.39)	$B, C' > 0$ [ $B, C' < 0$ ]	③ [④]

**Table 1.1:** Overview of gauge-Yukawa fixed points, critical exponents, conditions and phase diagrams in Fig. 1.3.

the scalar potential is unstable at the fixed point. In this case, the fixed point in the gauge-Yukawa system is invalidated, and referred to as pseudo-fixed point. Nevertheless, we will now turn to the potential fixed points in the gauge-Yukawa subsystem.

**Fixed points of the gauge-Yukawa system.** Now, we will review all possible fixed points of the gauge-Yukawa system [110], summarised in Tab. 1.1. We encounter the non-interacting Gaussian and interacting Banks-Zaks fixed points, which are well-known within non-abelian gauge theories in connection with the phenomena of asymptotic freedom and the IR conformal window, respectively. For this work, the novel gauge-Yukawa fixed point is crucial importance, as it doubles either as IR fixed point, or enable asymptotic safety beyond freedom. Without gauge interactions, it is easy to verify from (1.28) that no fixed point can arise: the Yukawa RG becomes  $\beta_y = E \alpha_y^2$  with  $E > 0$ , which only admits the trivial solution  $\alpha_y = 0$  at all scales.

The Gaussian fixed point **G** with  $\alpha_{g,y}^* = 0$  is an UV fixed point for  $B > 0$  in (1.28), in which case the theory is asymptotically free [84, 85]. According to (1.29), this is only achievable in non-abelian gauge theories  $C_2^G \neq 0$ , and with not too much charged matter content. Otherwise, we have  $B < 0$ , **G** is fully IR attractive and asymptotic freedom is lost.

Including the gauge two-loop order term in (1.28) with vanishing Yukawa interactions  $\beta_g = -B \alpha_g^2 + C \alpha_g^3 + \mathcal{O}(\alpha^4)$ , we find the infrared Banks-Zaks (**BZ**) [90, 91] fixed point, given that

$$B > 0, \quad C > 0 \quad \Rightarrow \quad \alpha_g^{\text{BZ}} = B/C, \quad \alpha_y^{\text{BZ}} = 0. \quad (1.31)$$

The critical exponents

$$\vartheta_1^{\text{BZ}} = B^2/C > 0, \quad \vartheta_2^{\text{BZ}} = -BF/C < 0, \quad (1.32)$$

indicate infrared attraction in the gauge, and UV attraction in the Yukawa direction. Hence, the **BZ** is only present in an asymptotic free regime. For  $B \approx 0$ , it exists within a perturbative regime  $0 < \alpha_g^{\text{BZ}} < \alpha_g^{\text{BZ},\text{max}}$ , bounded from above by the onset of strong-coupling effects. As argued before, starting from  $B \approx 0$  and decreasing matter content from the theory drives the coefficient  $B$  up while  $C$  decreases, pushing  $\alpha_g^{\text{BZ}}$  towards  $\alpha_g^{\text{BZ},\text{max}}$ . In QCD-like theories, this range of matter content that allows for **BZ** is often referred to as (IR) conformal window, see [90, 91, 109, 223] and references therein. Away from the asymptotic free regime, i.e.  $B < 0$ , the existence of an UV attractive version of the **BZ**, requiring  $C < 0$ , is excluded in any quantum field theory [110]. This can be inferred by rewriting (1.29)

$$C = -\frac{34}{11}BC_2^G + 4n_F S_2^F \left( C_2^F + \frac{7}{11} C_2^G \right) + 4n_S S_2^S \left( C_2^S - \frac{1}{11} C_2^G \right), \quad (1.33)$$

which for  $B \leq 0$  has only a negative contribution for charged scalars in a representation that

has,  $C_2^S < \frac{1}{11} C_2^G$ . However, the quadratic Casimir of any representation  $R$  fulfils, compared to the respective adjoint  $G$  of the group

$$C_2^R \geq \frac{3}{8} C_2^G \quad \Rightarrow \quad C > 0 \quad \text{for} \quad B \leq 0. \quad (1.34)$$

The argument can be extended to semi-simple gauge theories [110] and manifestly excludes weakly interacting UV fixed points in any pure gauge theory with matter.

The only recourse at the leading, non-trivial order is Yukawa interaction that is present at two-loop level in  $\beta_g$  (1.28). Borrowing a common index notation for the Yukawa interaction

$$\mathcal{L}_{\text{yuk}} = y h_{aij} \phi^a \psi^i \varepsilon \psi^j + \text{h.c.}, \quad \text{with normalisation} \quad h_{aij}^\dagger h_{aji} = h^2, \quad (1.35)$$

the new coefficients from (1.28) read

$$\begin{aligned} D &= d_G^{-1} \left[ C_{2ik}^F h_{aij} h_{ajk}^\dagger \right], \\ E &= h^{-2} h_{aij}^\dagger \left[ h_{bjk} h_{bkl}^\dagger h_{ali} + h_{ajk} h_{bkl}^\dagger h_{bli} + 4h_{bjk} h_{akl}^\dagger h_{bli} + h_{bji} \left( h_{akl}^\dagger h_{blk} + h_{bkl}^\dagger h_{alk} \right) \right], \\ F &= 6h^{-2} h_{aij}^\dagger \left[ C_{2jk}^F h_{aki} + h_{ajk} C_{2ki}^F \right]. \end{aligned} \quad (1.36)$$

Apart from the trivial solution,  $\beta_y = 0$  is also achieved for the *nullcline condition*  $\alpha_y = \frac{F}{E} \alpha_g$ , which effectively shifts the two-loop coefficient in  $\beta_g = -B \alpha_g^2 + C' \alpha_g^3 + \mathcal{O}(\alpha^4)$  via

$$C' = C - \frac{DF}{E} < C. \quad (1.37)$$

This allows for the gauge-Yukawa (**GY**) fixed point

$$B > 0, C' > 0 \quad \text{or} \quad B < 0, C' < 0 \quad \Rightarrow \quad \alpha_g^{\text{GY}} = B/C', \quad \alpha_y^{\text{GY}} = BF/EC', \quad (1.38)$$

and its critical exponents

$$\vartheta_{1,2}^{\text{GY}} = \frac{B}{2C'^2} \left[ BC + FC' \mp \sqrt{(BC + FC')^2 - 4BFC'^2} \right]. \quad (1.39)$$

While in the asymptotic free regime ( $B > 0, C' > 0$ ), both critical exponents are positive  $0 < \vartheta_1 < \vartheta_2$ , and **GY** is completely IR attractive. Due to the sign of the shift (1.37), the fixed point then coexists with the **BZ** with  $\alpha_g^{\text{GY}} > \alpha_g^{\text{BZ}}$  and the UV attractive Gaussian. Beyond asymptotic freedom, an interacting UV version of **GY** with  $B, C' < 0$  may exist in spite of  $C > 0$ , as  $\vartheta_1 < 0 < \vartheta_2$  admits an UV attractive direction. Hence, the theory exhibits asymptotic safety beyond freedom. At  $B \approx 0$ , the critical exponents are approximately

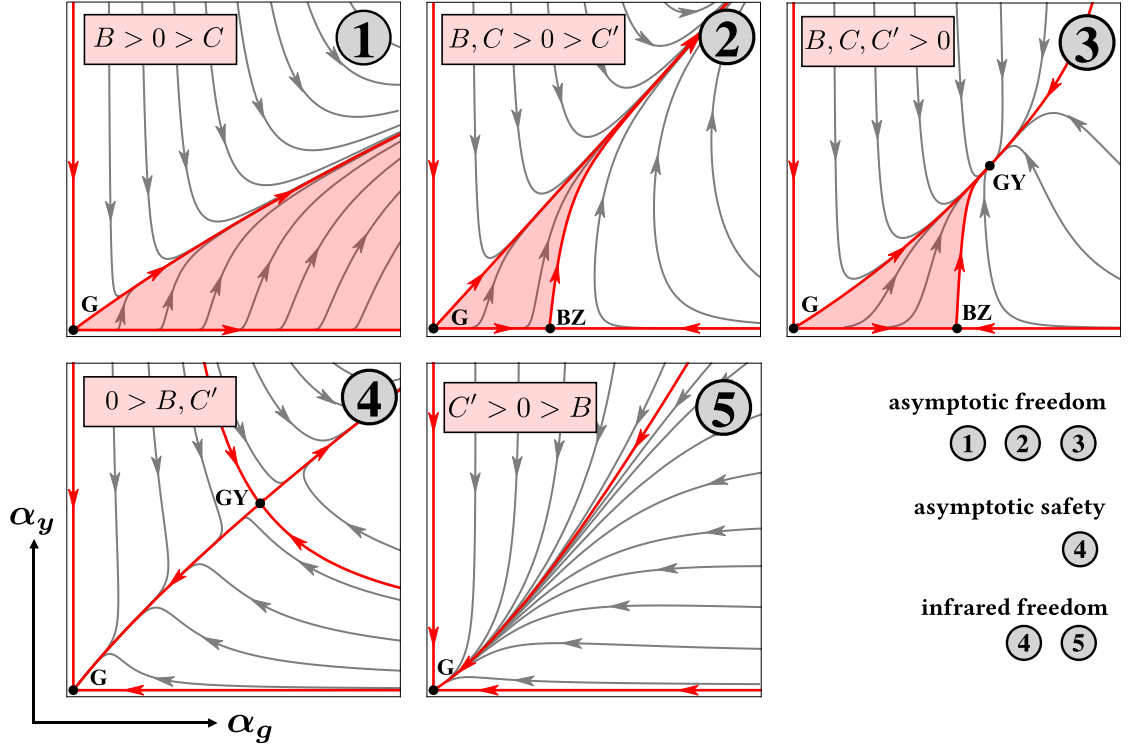
$$\vartheta_1^{\text{GY}} \approx B^2/C', \quad \vartheta_2^{\text{GY}} \approx BF/C', \quad (1.40)$$

which shows some similarity to (1.32). Hence, around the perturbative region  $B \approx 0$ , the **GY** fixed point is either UV or IR, with the sign of  $C'|_{B=0}$  determining either case. As it turns out, theories with interacting UV fixed points are relatively rare [224], with [112] being the first case ever

constructed. As the crucial mechanism for interacting UV fixed points is the Yukawa-induced shift (1.37) on the coefficient  $C$ , the ratio

$$\frac{\alpha_g^{\text{BZ}}}{\alpha_g^{\text{GY}}} = \frac{C'}{C} = 1 - \frac{DF}{CE} < 1 \quad (1.41)$$

is useful to quantify its relative size, with positive values indicating that the GY is IR, and the more negative the bigger - and hence the more robust - the shift.



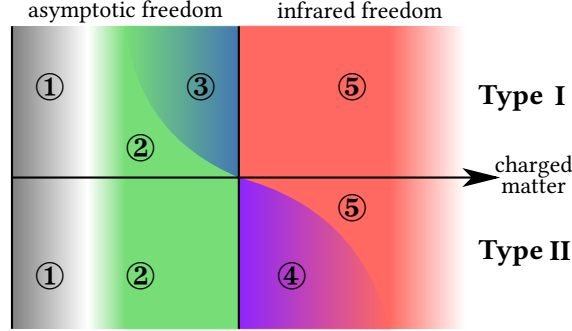
**Figure 1.3:** Phase diagrams of simple gauge-Yukawa theories in the  $\alpha_{g,y}$  plane, depending on the coefficients  $B$ ,  $C$  and  $C'$ . The arrows point from the UV to the IR. Gaussian (G), Banks-Zaks (BZ) and gauge-Yukawa (GY) fixed points are marked by black dots, separatrices as red lines. The red shaded area in ①, ② and ③ highlights asymptotic freedom.

**Phase diagrams.** Collecting all conditions on fixed points, each theory may exhibit the phase diagrams ①–⑤ of Fig. 1.3, projected in the gauge-Yukawa plane. These exhibit asymptotic freedom with any interacting fixed point ①, the Gaussian and BZ ②, or the  $G_{\text{UV}}$ , BZ as well as the infrared  $GY_{\text{IR}}$  fixed point ③. Beyond asymptotic freedom, the Gaussian is IR attractive, and the theory is either not UV complete ⑤ or asymptotically safe due to the  $GY_{\text{UV}}$  ④. In the latter, the critical surface is one-dimensional in the gauge-Yukawa plane, and is given by the separatrix connecting to the Gaussian, giving rise to a weakly coupled theory in the IR, or towards the strong coupling regime in the IR, governed by non-perturbative effects.

The scalar quartic sector may critically affect these diagrams: any of the interacting fixed points may be invalidated, and even asymptotic freedom could be lost if the Gaussian becomes disconnected from a physical region. On the other hand, there might also be multiple quartic solutions for each of the gauge-Yukawa fixed points.



**Representation dependence.** Phases ①–⑤ in a weakly coupled regime can be connected the observations made earlier about signs of matter and gauge boson contributions to (1.29). Fig. 1.4 illustrates the phase boundaries schematically depending on the number of charged matter fields. Two different kinds of quantum field theories exist, distinguished by containing  $\mathbf{GY}_{\text{IR}}$  (type I) or  $\mathbf{GY}_{\text{UV}}$  (type II) [224, 225].



**Figure 1.4:** Dependency of phases ①–⑤ on the matter multiplicities imply two different types I and II of quantum field theories.

Non-abelian gauge theories with no matter exhibit ①, with  $C \leq 0 \leq B$ . Continuously increasing the number of charged matter degrees of freedom,  $B$  as in (1.29) decreases but  $C$  grows. Due to (1.34),  $C$  turns positive before  $B$  becomes negative, leading to **BZ** emerge from infinity. The fixed point comes into a perturbative regime as  $B \rightarrow +0$ , leading to the phase ②. The parameter  $C' < C$  (1.37) increases likewise, and may become positive before  $B \rightarrow 0$  (type I) or thereafter (type II). In the first case, the  $\mathbf{GY}_{\text{IR}}$  fixed point emerges from infinity and becomes increasingly perturbative, eventually leading to phase ③. If  $C - C'$  is very small, the phase ② is very narrow. With  $B \rightarrow 0$ ,  $\mathbf{GY}_{\text{IR}}$  and **BZ** merge with the Gaussian, leading to phase ⑤ as asymptotic freedom is lost. For type II families,  $C' < 0$  and hence ② remains the case until  $B = 0$ . Barring the boundary case  $C'|_{B=0} = 0$  between I and II, the latter then exhibits asymptotic safety when freedom is lost via ④. As **BZ** merges into the Gaussian,  $\mathbf{GY}_{\text{UV}}$  emerges and is pushed towards higher values beyond freedom. This lasts until  $C'$  turns positive, leading to ⑤. However, the transition ④  $\rightarrow$  ⑤ is in a strongly coupled regime. Hence, it is not a priori clear how vast this UV conformal window is. Moreover, while  $B$  is linear in field dependencies but  $C'$  has a more complicated dependency, certain theories may have  $C'$  becoming positive and then negative again, giving rise to a second window. However, its non-perturbative nature casts these predictions unreliable within our approximation. Similarly, the lower end of the IR conformal windows, giving by the transitions ①  $\rightarrow$  ② and ②  $\rightarrow$  ③ cannot be determined with perturbative methods.

Of course, families of theories may possess several parameters counting matter fields, e.g. numbers of various fermions, scalars. Some changes may even result in a transition between I and II within one family. In a similar vein, this could happen for different gauge groups, dimensions and representations.

**Beyond simple gauge-Yukawa.** Theories with several gauge and Yukawa interactions exhibit a rich system of potential **BZ** and  $\mathbf{GY}$  fixed points, where a number of these couplings may be non-vanishing [114]. At leading order, for  $n_g$  gauge couplings and  $n_y$  Yukawas, up to  $(2^{n_g} - 1)$  **BZ**-type and  $(2^{n_g} - 1)(2^{n_y} - 1)$   $\mathbf{GY}$ -type solutions may exist, the actual number highly depending

on details of the theory. The generalised gauge  $\beta$ -function is

$$\beta_{g_i} = \alpha_{g_i}^2 \left[ -B_i + C_{ij} \alpha_{g_j} - D_{i\ell} \alpha_{y_\ell} \right], \quad (1.42)$$

with  $B_i$  and  $C_{ii}$  given by (1.29) with  $\{G, F, S\} \mapsto \{G_i, F_i, S_i\}$ , as well as manifestly positive coefficient

$$C_{ij}|_{j \neq i} = 4 \left[ n_{F_i} S_2^{F_i} C_2^{F_j} + n_{S_i} S_2^{S_i} C_2^{S_j} \right] \geq 0. \quad (1.43)$$

As a side note, this suggests a generalisation of (1.34), as  $C_{ij}|_{B_i \leq 0} > 0 \forall i, j$ . One gauge sector can effectively stabilise another via

$$B_i^{\text{eff}} = B_i - C_{ij} \alpha_{g_j}^* \Big|_{j \neq i} + D_{i\ell} \alpha_{y_\ell}^*, \quad (1.44)$$

which may reinstate asymptotic freedom even though it should be lost from the matter content alone ( $B_i < 0 < B_i^{\text{eff}}$ ), providing an alternative mechanism of UV completion, again relying on Yukawa contributions being large enough. This is a double-edged sword, as larger gauge contributions in (1.44) may even spoil effective asymptotic freedom. In supersymmetric theories, the asymptotically safe phase ④ does not exist [226, 227], however asymptotic safety can still be achieved for semi-simple gauge groups, when one of the gauge interactions is asymptotically free [115], due to the (1.44).

**Higher orders.** The perturbative ansatz (1.28) and any conclusions drawn from it are only valid in a regime of sufficiently small couplings. This is trivially the case for the Gaussian fixed point **G** and its vicinity. The interacting fixed points **BZ** and **GY** on the other hand require for the one-loop coefficient  $|B| \ll 1$  to lie within this region. In terms of Fig. 1.4, the domain of applicability of perturbation theory corresponds to a strip around both sides of the vertical middle axis separating asymptotic and infrared freedom.

The condition  $|B| \ll 1$  can always be achieved in the large- $N$  Veneziano limit [228], whereby fixed points arise as a systematic Taylor series in a small expansion parameter under increasing loop orders [2, 91]. This will be employed in the next section, as we continue to study simple gauge theories with matter where asymptotic safety is achieved through ④, but perturbativity of **GY**<sub>UV</sub> is guaranteed from the onset.

Beyond the Veneziano limit, a finite size of the **BZ** conformal window is obtained using various perturbative and non-perturbative techniques [92–109], and for the **GY** conformal window, see [2]. It is therefore reasonable to expect that conformal windows have a finite extensions even away from the Veneziano limit.

## 1.6 Exact asymptotic safety

Exact asymptotic safety means that the existence of the UV fixed point is protected by some mechanism. In particular, weakly coupled fixed points are guaranteed to be present starting from a minimal order to all higher ones in perturbation theory. Hence, the system is either exactly solvable, or all higher orders of the approximation scheme are controlled in the sense that they do not spoil the fixed point. For instance, asymptotic freedom in renormalisable QFTs is determined

at one-loop level in perturbation theory, as it is a series expansion around the potential fixed point itself. For asymptotic safety beyond freedom, rigorous proofs for the existence of interacting fixed points are rare, and usually require another ordering principle. One example are theories just above the critical dimension of asymptotic freedom. Consider for instance a theory with a single coupling  $G$ , canonically marginal in  $d_c$  dimensions, and  $g = \mu^{d-d_c} G$  its dimensionless version. The RG flow is given by

$$\beta_g = (d - d_c)g + \beta_{g,c}(g), \quad (1.45)$$

and if the flow at  $d = d_c$  is asymptotically free, i.e.  $\beta_{g,c} = -B g^2 + \mathcal{O}(g^3)$ , then slightly above this critical dimension  $d = d_c + \epsilon$  [229] an interacting UV fixed point  $g^* = \epsilon/B + \mathcal{O}(\epsilon^2)$  exists. Each additional order  $g^{n+2}$  in  $\beta_{g,c}$  only contributes via  $\epsilon^{n+1}$  to  $g^*$ . The theory is under perturbative control, and asymptotic safety is generated due to an interplay of classical scaling and quantum fluctuations. Notable examples of this principle include large- $N_f$  Gross-Neveu [68, 69] and large- $N$  non-linear  $\sigma$  models [75–78] both at  $d = 2 + \epsilon$ , Einstein-Hilbert gravity at  $d = 2 + \epsilon$  [32, 35, 60, 61], or Yang-Mills at  $d = 4 + \epsilon$  [65–67].

Alternatively, systematic expansions may be possible purely within quantum corrections, facilitated by large- $N$  limits. At  $d = 3$ , this is the case for large- $N$  scalar  $O(N)$  theories [72–74] and the large- $N_f$  Gross-Neveu models [70, 71]. In this work, the Veneziano limit with large  $N_f$  and  $N_c$  will be employed for gauge-Yukawa models in  $d = 4$ . In this setup has been utilised to rigorously proof the existence of the infrared Banks-Zaks fixed point [90, 91], and will be elaborated in the following sections. The distinct case of large- $N_f$  resummations in  $d = 4$  gauge theories has recently sparked discussions about the possible existence of a UV fixed point [126–136]. However, the potential fixed point is not exact as in the cases described above.

**Veneziano limit.** Now, we will demonstrate how strict perturbative control can be established in  $d = 4$  gauge theories in the limit of a large number of colours and flavours. The idea has first been formulated in [228] and is known as the Veneziano limit. The mechanism relies, much like the expansion around the critical dimension, on having the first coefficient in the perturbative gauge  $\beta$  function small and tunable. Indeed, the coefficient  $B$  in (1.28) controls all fixed point values and critical exponents in Tab. 1.1. Its definition (1.29) indicates that  $B$  can indeed be made small, but not continuously. For instance, in a  $SU(N_c)$  gauge theory with  $N_f$  Dirac fermions, one obtains

$$B = \frac{4}{3} \left[ \frac{11}{2} N_c - N_f \right], \quad (1.46)$$

which can only be made arbitrarily small and non-zero for both  $N_c, N_f \rightarrow \infty$ . In a perturbative expansion, the contributions with leading powers of  $N_{c,f}$  in each order stem from planar diagrams. The expansion coefficients can be rendered finite by absorbing these leading coefficients of  $N_{c,f}$  into coupling definitions [230]. We will refer to those as 't Hooft couplings, e.g.  $\alpha_g = N_c g^2/(4\pi)^2$  in the example above. Now, the Veneziano limit can be established by  $N_c, N_f \rightarrow \infty$  while keeping the ratio  $N_f/N_c$  finite and an open parameter. Rewriting (1.28) in terms of the 't Hooft couplings, some theories then allow for the coefficient  $B$  to be related to this ratio. For instance, introducing  $\epsilon = \frac{N_f}{N_c} + \frac{11}{2}$  and absorbing a factor  $N_c$  into the 't Hooft couplings  $\alpha_g$  turns (1.46) into  $B = -\frac{4}{3}\epsilon$ , with  $\epsilon$  being continuously tunable - its general defini-

tion depends on each theory. In fact, this property is the key to establish perturbative control, the cancellation of suppression of subleading terms in the large- $N_{c,f}$  is not a requirement, but a side-effect. This allows for a transition back to a finite- $N_{c,f}$  theory. Now, consider perturbative expansion at  $l$ ,  $m$  and  $n$  loop orders for the gauge, Yukawa and quartics  $\beta$  functions, subsequently referred to as  $(l, m, n)$ , in the Veneziano limit. Solving this system for fixed points, gives for the 't Hooft couplings  $\alpha_i^* = \sum_{n=1}^{\infty} a_i^{(n)} \epsilon^n$ . It turns out each coefficient  $a_i^{(n)} \forall i$  can be completely determined by solving the RGEs at  $(n+1, n, n)$ , with higher loop orders only contributing to higher order coefficients. Hence, the leading, non-trivial order is  $(2, 1, 1)$ . Besides being able to move interacting fixed points continuously close to the Gaussian, this stability of fixed point values and hence critical exponents against higher orders is another aspect of the Veneziano limit, which establishes an additional ordering principle on top of perturbation theory. Finally, perturbative control is of course established for  $0 < |\epsilon| \ll 1$ , and either sign of  $\epsilon$ . Hence, only two cases are possible regarding the phases of Fig. 1.3: the theory is either in ③ for  $\epsilon < 0$  and ⑤ for  $\epsilon > 0$ , or the theory exhibits the phases ② for  $\epsilon < 0$  and ④ for  $\epsilon > 0$ . This can be probed by computing

$$\Delta = \frac{C'}{C} \Big|_{B \rightarrow 0}, \quad (1.47)$$

which is reached at  $\epsilon \rightarrow 0$ . Due to (1.37) and (1.34), the quantity is bounded from above with  $1 \leq \Delta < 0$  implies ③, while  $\Delta < 0$  suggests the phase ④ instead. As we are interested in asymptotic safety, the latter case is the interesting one for us.

**Gauge sector.** We will now discuss strategies to construct perturbatively exact theories exhibiting weakly interacting UV fixed points in a simple gauge-Yukawa theory. The leading, non-trivial order of the Veneziano limit is  $(2, 1, 1)$ , and since the limit  $\epsilon \rightarrow 0$  needs to be possible, the system (1.28) must contain the solution, being of  $\mathbf{GY}_{UV}$  type. Hence, we require  $B < 0$  and  $C' < 0$ . As the second condition can only be achieved due to the Yukawa-induced shift in (1.37), matter degrees of freedom that are not involved in the Yukawa interaction are always counterproductive. Those spectator fields are either uncharged and hence completely decoupled, or only give a positive contribution to  $C$  and hence  $C'$  in (1.37). Moreover, in order to have  $B \propto \epsilon$ , we need to be able to balance both gauge and matter terms in (1.29) against each other in a continuous fashion while taking  $N_{c,f} \rightarrow \infty$ . Hence,  $U(1)$  gauge groups are excluded due to  $C_2^G = 0$ . Furthermore, none of the exceptional Lie groups  $G_2, F_4, E_6, E_7$  and  $E_8$  can be utilised either, since they do not provide a parameter  $N_c$ , and their Casimir  $C_2^G$  is just a constant. Only unitary, orthogonal and symplectic gauge groups are viable.

At large  $N_c$ , the adjoint Casimirs of  $SU(N_c)$  is  $C_2^G = N_c$ , or  $C_2^G = \frac{1}{2}N_c$  for  $SO(N_c)$  and  $Sp(N_c)$ . This has strict consequence for the possible choices of matter fields, as their Dynkin indices may at most scale  $S_2^R \propto N_c$ , but not higher. Otherwise, the matter term in (1.29) overpowers the non-abelian interaction at large- $N_{f,c}$ . These representation are collected in Tab. 1.2. More strictly, this means:

1. The theory needs to contain  $N_i \rightarrow \infty$  fermionic and/or scalar matter fields which transform under the fundamental representation of  $SU(N_c)$ ,  $SO(N_c)$  or  $Sp(N_c)$ , as these are the only choices with  $S_2^R = \frac{1}{2} \propto N_c^0$ .
2. The theory may contain a finite numbers  $n_j$  of matter fields in a two-index representation

Group	$R$	$d_R$	$S_2^R$	$C_2^R$
$SU(N)$	fun.	$N$	$\frac{1}{2}$	$\frac{N^2-1}{2N}$
	antisym.	$\frac{1}{2}N(N-1)$	$\frac{1}{2}(N-2)$	$\frac{(N+1)(N-2)}{N}$
	sym.	$\frac{1}{2}N(N+1)$	$\frac{1}{2}(N+2)$	$\frac{(N-1)(N+2)}{N}$
	adj.	$N^2-1$	$N$	$N$
$SO(N)$	fun.	$N$	$\frac{1}{2}$	$\frac{1}{4}(N-1)$
	adj.	$\frac{1}{2}N(N-1)$	$\frac{1}{2}(N-2)$	$\frac{1}{2}(N-2)$
	sym.	$\frac{1}{2}(N+2)(N-1)$	$\frac{1}{2}(N+2)$	$\frac{1}{2}N$
$Sp(N)$	fun.	$N$	$\frac{1}{2}$	$\frac{1}{4}(N+1)$
	antisym.	$\frac{1}{2}(N-2)(N+1)$	$\frac{1}{2}(N-2)$	$\frac{1}{2}N$
	adj.	$\frac{1}{2}N(N+1)$	$\frac{1}{2}(N+2)$	$\frac{1}{2}(N+2)$

**Table 1.2:** List of all representations in unitary, orthogonal and symplectic gauge groups, up to two indices, and their respective dimensions  $d_R$ , Dynkin indices  $S_2^R$  and quadratic Casimir  $C_2^R$ .

$S_2^R \propto N_c$  of the gauge group, which is bounded by the condition  $B(N_i, n_j)|_{N_i=0} > 0$ .<sup>2</sup>

3. The theory may contain an arbitrary amount of uncharged matter.

As the limit implies  $N_f \propto N_c$  (in the following, we may drop the indices wherever appropriate), it makes sense to visualise each field in a notation similar to 't Hooft's double lines [230] and birdtrack diagrams [231,232], with gauge- and flavour indices denoted by wiggly (~~~~) and straight lines (—). The one-loop coefficient then strictly requires double-lined fields  $B \propto \text{diagram}$ . At two-loop level, the coefficient then scales  $C \propto N^2$ , see (1.29).

**Yukawa sector.** The Yukawa coefficients  $D$ ,  $E$  and  $F$  in (1.28) are also sensitive to uncharged fields involved in the Yukawa interaction. Since at least two fields in the Yukawa interaction have to be charged and hence double-lined, two possible topologies of contractions arise:  $\text{diagram}$  and  $\text{diagram}$ . Here, the Yukawa vertex is depicted, with each external leg being either its scalar or one of its fermions. For the sake of the argument, it does not matter which leg corresponds to which field, nor what indices (solid lines) are gauge or global ones. Rather,  $\text{diagram}$  features three double-index fields ( $\text{diagram}$ ) while  $\text{diagram}$  has two double-index and one field without a large index ( $\text{diagram}$ ). We will now show that the case  $\text{diagram}$  is not useful at large  $N$ . Consider for each field  $i$  in the Yukawa interaction having overall  $v_i$  large lines, gauge and flavour, attached to them. The powers of  $N$  in the coefficients of (1.28) can then be inferred from simple counting of loops, and read

$$B \propto N, \quad C \propto N^2, \quad D \propto N^{\sum_i \frac{v_i}{2} - 1}, \quad E \propto N^{\sum_i \frac{v_i}{2} - v_{\min}}, \quad F \propto N, \quad (1.48)$$

where  $v_{\min}$  denotes the smallest of all  $v_i$ . This dependency enters because in the large- $N$  limit, only contributions from the field strength renormalisation of external legs survive in coefficient  $E$ , while proper vertex corrections are subleading. This can be easily understood on a diagrammatic level e.g. for the Yukawa vertex  $\text{diagram}$ , giving rise to a leg correction  $(\text{diagram} + \text{perm.}) \propto N$ , while the vertex one  $\text{diagram} \propto 1$  is indeed subleading. In general, the leg with the least

<sup>2</sup>In a purely two-index theory, it is possible to establish a similar limit where a non-continuous parameter  $\delta = \sum_j a_j n_j - c$  takes the place of the  $\epsilon$ .

external lines then sets the leading power of  $N$ . This means  $C - C' \propto N^{\nu_{\min}}$ , and in order to have the two-loop shift (1.37) compete with coefficient  $C$ , each field needs to be double-indexed.

**Yukawa taxonomy.** In summary, the families of theories with a simple gauge group and single Yukawa interaction, allowing for the Veneziano limit, can be categorised by their large index structure of their Yukawa interactions. We will denote these 5 classes as  $\text{---}\text{---}\text{---}$ ,  $\text{---}\text{---}\text{---}$ ,  $\text{---}\text{---}\text{---}$ ,  $\text{---}\text{---}\text{---}$  and  $\text{---}\text{---}\text{---}$ , which depicting the Yukawa vertex, while the left leg marks the scalar, and the right ones are fermionic. It will be proven in Ch. 4, that theories with uncharged fermions  $\text{---}\text{---}\text{---}$ , one scalar  $\text{---}\text{---}\text{---}$ , one fermion  $\text{---}\text{---}\text{---}$  or all fields  $\text{---}\text{---}\text{---}$  being in a two-index gauge representation have  $\Delta > 0$ , and do not allow for asymptotic safety, leaving  $\text{---}\text{---}\text{---}$  as the only viable choice. Indeed,  $\text{---}\text{---}\text{---}$  has been shown to contain a universality class of asymptotically safe theories [3, 112]. In this setup, the coefficients  $B$ ,  $C$  and  $F$  in (1.28) are only sensitive to the fermions, as scalars are uncharged. Hence, the scalars only affect  $D$  and  $E$  in the two-loop shift  $C' = C - DF/E$ . In consequence, while the fermion content is fixed by tuning  $B \approx -0$ , the more scalars can be embedded in the global symmetry, the stronger the shift towards  $C' < 0$ . It will be demonstrated in Ch. 6 that the number of real scalar degrees of freedom (DOF)  $N_S = \frac{11}{2} N_{\text{Weyl}}$  allows for asymptotic safety, while  $N_S = \frac{11}{4} N_{\text{Weyl}}$  does not, with  $N_{\text{Weyl}}$  being the number of Weyl fermions.

**Scalar sector.** Having established that scalar fields need to be double-indexed, this implies that at least two quartic interaction may be formulated:

$$u \text{tr} [\phi^\dagger \phi \phi^\dagger \phi] \propto \text{---}\text{---}\text{---}, \quad v (\text{tr} [\phi^\dagger \phi])^2 \propto \text{---}\text{---}\text{---}, \quad (1.49)$$

with the 't Hooft coupling  $\alpha_u \propto N u$  for the single trace, and  $\alpha_v \propto N^2 v$  for the double trace quartic interaction<sup>3</sup>. If the symmetry allows it, additional operators are present, which can be classified in the same fashion.

**Litim-Sannino model.** Putting everything together, we briefly introduce the model in [112] which has inspired the recent research of  $d = 4$  exact asymptotic safety beyond freedom, and will be the onset of investigations in this work:

$$\begin{aligned} \mathcal{L} = & -\frac{1}{4} F_A^{\mu\nu} F_{\mu\nu}^A + \overline{Q} i \not{D} Q + \text{tr} [\partial_\mu \phi^\dagger \partial^\mu \phi] + \mathcal{L}_{\text{gh}} + \mathcal{L}_{\text{gf}} \\ & - y [Q_i^{L\dagger} \phi_{ij} Q_j^R + Q_i^{R\dagger} \phi_{ij}^\dagger Q_j^L] - u \text{tr} [\phi^\dagger \phi \phi^\dagger \phi] - v \text{tr} [\phi^\dagger \phi] \text{tr} [\phi^\dagger \phi]. \end{aligned} \quad (1.50)$$

The theory features a  $SU(N_c)$  gauge group,  $N_f$  quark-like Dirac fermions  $Q$  in the fundamental representation (with chiral components  $Q_{L,R}$ ) as well as an uncharged meson-like scalar  $\phi$ , which is a complex  $N_f \times N_f$  matrix. The model has a chiral  $SU(N_f) \times SU(N_f)$  flavour symmetry and a single value Yukawa coupling  $y$ , as well as two scalar quartics  $u$  and  $v$  as discussed. It allows for the Veneziano limit to be taken, with the expansion parameter

$$\epsilon = \frac{N_f}{N_c} - \frac{11}{2}, \quad (1.51)$$

in the range  $(-\frac{11}{2}, \infty)$ . For  $\epsilon < 0$ , the theory is asymptotically free, and for  $0 < \epsilon < \epsilon_{\max}$ , asymptotic safety is realised by an interacting gauge-Yukawa fixed point. A more detailed analysis will follow

<sup>3</sup>This operator is compatible with the maximal  $O(N_S)$  symmetry of a scalar theory.

in Ch. 5.

Due to this novel property, the model has sparked lots of interests. Aspects of its vacuum stability have been explored in [113]. The RG analysis has been extended to higher loop order, mapping out the UV conformal window [2], which will be the subject Ch. 5. A large- $N$  triality of the model has been uncovered in [3], see Ch. 6. Extensions to semi-simple gauge groups [114], higher-order scalar operators [233, 234], as well as  $\mathcal{N} = 1$  supersymmetry has been studied [115]. Further works investigate the model away from  $d = 4$  dimensions [67], radiative symmetry breaking [116], the inclusion of gravity [117] and several more aspects [118–120]. Moreover, the theory has been embedded in SM extensions [4, 121, 122] and several phenomenological implication have been considered [4, 121], addressing issues such as anomalous magnetic moments of muon and electrons [123], dark matter [124] and inflation [125].

## 1.7 Outline

Now, as the motivation behind this work has been detailed, and all necessary terminology and supplementary material introduced, the main sections will be outlined, highlighting their importance. In summary, this thesis consists of three thematic parts, ranging from rather formal to practical topics: techniques of perturbative RG studies (Ch. 2 and Ch. 3), perturbatively exact asymptotic safety in toy models (Ch. 4, Ch. 5 and Ch. 6), as well as phenomenological applications in SM extensions (Ch. 7 and Ch. 8).

As for the first part, this works is concerned with the renormalisation group study of weakly coupled quantum field theories in  $d = 4$  in general. The main tool of investigation in this regime is perturbation theory, and the determination of  $\beta$  functions within this approximation is a central part of each of the studies presented.

**Techniques and tools.** Ch. 2 revisits the formal foundations of this methodology, by reviewing the template formulas for RGEs of arbitrary renormalisable QFTs. Several errors are identified and corrected within the most recent recomputation of these results [185], stemming from several main sources. For one, off-diagonal loop corrections to the field strength renormalisation have been neglected, leading to discrepancies in models with scalar mixing. Secondly, the dummy field method employed to obtain the running of masses and scalar cubics from the quartic and Yukawa  $\beta$  functions has been applied incorrectly, resulting in errors already at one-loop order. A numerical study of both improvements is undertaken, and the dummy field method is reviewed very thoroughly. Moreover, a careful cross-check is performed with the RGE templates of  $\mathcal{N} = 1$  supersymmetric theories, accommodating for the difference in renormalisation schemes. The results of this work have been factored into all major public tools for the automated determination of  $\beta$  functions. A third literature error in the Yukawa two-loop RGEs has been pointed out to us only recently. Overall, this work represents an important milestone in all perturbative RG studies and model building, and has superseded [185] as the state-of-the-art catalogue for template formulas of generic QFTs up to two-loop order.

However, due to the sheer complexity of using these formulas in any realistic theory, they are of little practical use without the computational tools to exploit them. Unfortunately, pre-existing

software solutions are scarce and all ill-equipped to process the models of interest in this work. In Ch. 3, the new public software package ARGES will be introduced, which stands out by its unique approach to the problem. The setup and functionality are detailed by example, and as its design is laid out, differences to other frameworks and how ARGES is superior in handling the tasks ahead are highlighted.

**Exact asymptotic safety.** Having provided the tools, the second part of this thesis focuses on the phenomenon of weakly coupled asymptotic safety in gauge-Yukawa theories, providing the building blocks for more realistic theories. The onset of this has been the seminal works [112, 113], which have identified a QCD-like theory exhibiting an interacting UV fixed point within a perturbatively exact framework in  $d = 4$ .

As a starting point, Ch. 4 picks up the trail of Sec. 1.6 for constructing theories with exact asymptotic safety. It is proven that theories with uncharged scalars, having a Yukawa contraction like  $\Rightarrow_{\text{Y}}$  are the only viable candidates for this property. Quantifying the degree of asymptotic safety via the quantity (1.47), a lower bound as well as a hierarchy of all possible models is unveiled. Arguments are brought forward that the theories in [3, 112] are indeed of special importance, as they represent the most asymptotically safe ones to be constructed.

In Ch. 5, missing two-loop contributions have been computed that extend these early findings up to a complete next-to-leading order in the  $\epsilon$ -expansion for the RG equations, fixed point couplings, critical exponents and anomalous dimensions. The extend of the UV conformal window is computed for the first time and with various methods and orders of approximation. This has allowed for a careful understanding of the mechanisms limiting the window, such as the instability of the scalar potential, fixed point mergers, as well as the onset of the strong coupling regime. This chapter remains the currently highest order analysis of the theory in [112, 113] and its implications are of utmost importance for UV safe model building.

After the discovery in [112, 113], the intriguing question had remained whether there are other theories with exact asymptotic safety, or if this model is unique. In Ch. 6, both answers are found to be yes. Two more models are identified that have a guaranteed interacting UV fixed point, featuring orthogonal or symplectic gauge groups. It is shown that these theories require Majorana fermions for asymptotic safety, while the one in [112, 113] only works with Diracs and a unitary gauge symmetry. In spite of their different symmetries and fermions, not only form these 3 families a universality class, but even a triality. The mechanisms behind this phenomenon are uncovered: negative dimensionality theorems and orbifolding in the large- $N$  limit protect not only this equivalence, but suggest the existence of many more duality webs.

**Particle Physics.** Part three of the thesis connects the knowledge obtained in the second one with real-world particle physics. In Ch. 7, directions and challenges for asymptotically safe BSM model building are highlighted. A new approach is introduced, where a BSM sector of colourless vector-like fermions and uncharged meson-like scalars is intertwined with the SM in a flavourful way. A set of six potential BSM extensions is obtained and the RG flow up to the Planck scale is studied in a novel bottom-up approach. Parameter spaces that provide safety and stability are mapped out, and phenomenological aspects are discussed.



In Ch. 8, a phenomenological study follows for a subset of these models that are safe until the Planck scale, stabilise the Higgs potential and can account for both discrepancies of muon and electron magnetic moments. Outstandingly, the latter is achieved without explicitly breaking lepton flavour universality. A parameter space is carved out from experimental bounds, and a prediction for the anomalous magnetic moment of the tauon is obtained.

In a final chapter, conclusions will be drawn and outlooks given.

## 2 Revisiting RGEs

### 2.1 Introduction

Renormalisation Group Equations (RGEs) are important as they provide the necessary link between the physics at different energy scales. The two-loop RGEs for all dimensionless parameters in general gauge theories have been derived already more than 30 years ago [179–184]. More recently, these results have been re-derived by Luo *et al.* [185] including the  $\beta$ -functions for dimensionful parameters. The latter results are based on the  $\beta$ -functions of dimensionless couplings by applying a so called “dummy field” method [195]. However, no independent direct calculation of the two-loop  $\beta$ -functions for scalar and fermion masses and scalar trilinear couplings exists so far in the literature. One of the aims of this paper is to provide a more detailed (pedagogical) discussion of the dummy field method and to critically examine the  $\beta$ -functions for the dimensionful parameters. As a result we will correct the  $\beta$ -functions for the fermion masses. We also find differences for the purely scalar couplings in certain models with respect to the literature. These differences arise from not always justified assumption about the properties of the wave-function renormalisation. We provide an independent cross-check using well tested supersymmetric RGEs which confirms our results. We believe that these corrections and validations are non-trivial and important in view of the wide use of the RGEs. Still, an independent direct calculation of the dimensionful  $\beta$ -functions would be useful.

The general equations have been implemented in the Mathematica package SARA [235–239] and in the Python package PyR@TE [240, 241]. More recent results which are (partially) included in these packages such as kinetic mixing [242] or running VEVs [191, 192] will not be discussed in this paper. The overarching purpose is to present the current state-of-the art of the two-loop  $\beta$ -functions and to collect the corrected expressions such that all the relevant information is at hand in one place.

### 2.2 The Lagrangian for a general gauge theory

In this section we review the Lagrangian for a general renormalisable field theory following [185]. The following particle content is considered:

- $V_\mu^A(x)$  ( $A = 1, \dots, d$ ) are gauge fields of a compact simple group  $G$  where  $d$  is the dimension of  $G$ .
- $\phi_a(x)$  ( $a = 1, \dots, N_\phi$ ) denote real scalar fields transforming under a (in general) reducible representation of  $G$ . The Hermitian generators of  $G$  in this representation will be denoted  $\Theta_{ab}^A$  ( $A = 1, \dots, d; a, b = 1, \dots, N_\phi$ ). Since the scalar fields are real, the generators  $\Theta^A$  are purely imaginary and antisymmetric.

- $\psi_j(x)$  ( $j = 1, \dots, N_\psi$ ) are left-handed complex two-component fermion fields transforming under a representation of  $G$  which is in general reducible as well. The Hermitian generators are denoted by  $t_{jk}^A$  ( $A = 1, \dots, d; j, k = 1, \dots, N_\psi$ ).

The most general renormalisable Lagrangian can be decomposed into three parts,

$$\mathcal{L} = \mathcal{L}_0 + \mathcal{L}_1 + (\text{gauge fixing} + \text{ghost terms}), \quad (2.1)$$

where  $\mathcal{L}_0$  is free of dimensional parameters and  $\mathcal{L}_1$  contains all terms with dimensional parameters. Here,  $\mathcal{L}_0$  reads

$$\begin{aligned} \mathcal{L}_0 = & -\frac{1}{4}F_{\mu\nu}^A F_{\mu\nu}^A + \frac{1}{2}D^\mu \phi_a D_\mu \phi_a + i\psi_j^\dagger \sigma^\mu D_\mu \psi_j \\ & - \frac{1}{2} \left( Y_{jk}^a \psi_j \zeta \psi_k \phi_a + Y_{jk}^{a*} \psi_j^\dagger \zeta \psi_k^\dagger \phi_a \right) - \frac{1}{4!} \lambda_{abcd} \phi_a \phi_b \phi_c \phi_d, \end{aligned} \quad (2.2)$$

where  $F_{\mu\nu}^A(x)$  is the gauge field strength tensor defined in the usual way in terms of the structure constants  $f^{ABC}$  of the gauge group and the gauge coupling constant  $g$ :

$$F_{\mu\nu}^A = \partial_\mu V_\nu^A - \partial_\nu V_\mu^A + g f^{ABC} V_\mu^B V_\nu^C. \quad (2.3)$$

The covariant derivatives of the scalar and fermion fields are given by

$$D_\mu \phi_a = \partial_\mu \phi_a - ig \Theta_{ab}^A V_\mu^A \phi_b, \quad (2.4)$$

$$D_\mu \psi_j = \partial_\mu \psi_j - ig t_{jk}^A V_\mu^A \psi_k. \quad (2.5)$$

Furthermore,  $Y_{jk}^a$  ( $a = 1, \dots, N_\phi; j, k = 1, \dots, N_\psi$ ) are complex Yukawa couplings and  $\zeta = i\sigma_2$  is the two-component spinor metric ( $\sigma_2$  is the second Pauli matrix). Finally,  $\lambda_{abcd}$  denotes quartic scalar couplings which are real and invariant under permutations of the set of indices  $\{a, b, c, d\}$ . The Lagrangian containing the dimensionful parameters is given by

$$\mathcal{L}_1 = -\frac{1}{2} \left[ (m_f)_{jk} \psi_j \zeta \psi_k + (m_f)_{jk}^* \psi_j^\dagger \zeta \psi_k^\dagger \right] - \frac{m_{ab}^2}{2!} \phi_a \phi_b - \frac{h_{abc}}{3!} \phi_a \phi_b \phi_c. \quad (2.6)$$

Here  $m_f$  is a complex matrix of fermion masses,  $m^2$  is a real matrix of scalar masses squared, and  $h_{abc}$  are real cubic scalar couplings. Our goal is to revisit the one- and two-loop  $\beta$ -functions for these dimensionful couplings which have been derived in Ref. [185], employing the so-called “dummy field” method which has been initially proposed in Ref. [195].

## 2.3 Renormalisation Group Equations

We are interested in the scale dependence of the Lagrangian parameters which, in general, is governed by RGEs. The RGEs can be calculated in different schemes. We are going to consider only dimensional regularisation with modified minimal subtraction, usually called  $\overline{\text{MS}}$ , for four dimensional field theories. In this scheme the  $\beta$ -functions, which describe the renormalisation

group running of the model parameters ( $\Theta_i$ ), are defined as

$$\beta_i = \mu \frac{d\Theta_i}{d\mu}, \quad (2.7)$$

where  $\mu$  is an arbitrary renormalisation scale.  $\beta_i$  can be expanded in a perturbative series:

$$\beta_i = \sum_n \frac{1}{(16\pi^2)^n} \beta_i^{(n)}, \quad (2.8)$$

where  $\beta_i^{(1)}$  and  $\beta_i^{(2)}$  are the one- and two-loop contributions to the running which we are interested in. Generic expressions of the one- and two-loop  $\beta$ -functions for dimensionless parameters in a general quantum field theory were derived in Refs. [182–184].

## 2.4 The dummy field method

In principle, one could calculate the renormalisation constants for the dimensionful couplings (the fermion masses  $(m_f)_{jk}$ , the squared scalar masses  $m_{ab}^2$ , and the cubic scalar couplings  $h_{abc}$ ) and derive the  $\beta$ -functions directly from them. However, this is tedious and has not been attempted so far in the literature. Instead, a “dummy field” method has been employed in Ref. [185] applying an idea, to our knowledge, first mentioned in Ref. [195]. Since a detailed description of this method is lacking in the literature we provide a careful discussion of it in this section. The idea is to introduce a scalar “dummy field”, i.e. a non-propagating real scalar field with no gauge interactions. The dummy field will be denoted by an index with a hat,  $\phi_{\hat{a}}$ , and satisfies the condition  $D_\mu \phi_{\hat{a}} = 0$ . As a consequence, expressions with two identical internal dummy indices (corresponding to a propagating dummy field) have to vanish. Furthermore, since  $D_\mu \phi_{\hat{a}} = 0$ , all gauge boson - dummy scalar vertices vanish as well:  $\Gamma_{V\phi_a\phi_{\hat{a}}} = \Gamma_{V\phi_{\hat{a}}\phi_{\hat{a}}} = \Gamma_{VV\phi_a\phi_{\hat{a}}} = \Gamma_{VV\phi_{\hat{a}}\phi_{\hat{a}}} = 0$ . Let us now consider the Lagrangian  $\mathcal{L}_0$  (2.2) in the presence of the same particle content plus one extra scalar dummy field ( $\phi_{\hat{a}}$ ) and separate the terms with the dummy field. Using  $D_\mu \phi_{\hat{a}} = 0$ ,  $\lambda_{ab\hat{d}\hat{d}} + \lambda_{a\hat{d}b\hat{d}} + \lambda_{\hat{d}ab\hat{d}} + \lambda_{\hat{d}\hat{d}ab} + \lambda_{\hat{d}a\hat{d}b} + \lambda_{\hat{d}\hat{d}ab} = 6\lambda_{ab\hat{d}\hat{d}}$ ,  $\lambda_{abc\hat{d}} + \lambda_{ab\hat{d}c} + \lambda_{a\hat{d}bc} + \lambda_{\hat{d}abc} = 4\lambda_{abc\hat{d}}$ , and  $\lambda_{a\hat{d}\hat{d}\hat{d}} + \lambda_{\hat{d}a\hat{d}\hat{d}} + \lambda_{\hat{d}\hat{d}a\hat{d}} + \lambda_{\hat{d}\hat{d}\hat{d}a} = 4\lambda_{a\hat{d}\hat{d}\hat{d}}$  one easily finds (writing the sums over the scalar indices explicitly):

$$\begin{aligned} \mathcal{L}_0 = & -\frac{1}{4}F_A^{\mu\nu}F_{\mu\nu}^A + \sum_{a=1}^{N_\phi} \frac{1}{2}D^\mu\phi_a D_\mu\phi_a + i\psi_j^\dagger \sigma^\mu D_\mu\psi_j \\ & - \frac{1}{2} \left( \sum_{a=1}^{N_\phi} Y_{jk}^a \psi_j \zeta \psi_k \phi_a + \text{h.c.} \right) - \sum_{a,b,c,d=1}^{N_\phi} \frac{1}{4!} \lambda_{abcd} \phi_a \phi_b \phi_c \phi_d \\ & - \frac{1}{2} \left( Y_{jk}^{\hat{d}} \psi_j \zeta \psi_k \phi_{\hat{d}} + \text{h.c.} \right) - 6 \sum_{a,b=1}^{N_\phi} \frac{1}{4!} \lambda_{ab\hat{d}\hat{d}} \phi_a \phi_b \phi_{\hat{d}} \phi_{\hat{d}} - 4 \sum_{a,b,c=1}^{N_\phi} \frac{1}{4!} \lambda_{abc\hat{d}} \phi_a \phi_b \phi_c \phi_{\hat{d}} \\ & - 4 \sum_{a=1}^{N_\phi} \frac{1}{4!} \lambda_{a\hat{d}\hat{d}\hat{d}} \phi_a \phi_{\hat{d}} \phi_{\hat{d}} \phi_{\hat{d}} - \frac{1}{4!} \lambda_{\hat{d}\hat{d}\hat{d}\hat{d}} \phi_{\hat{d}} \phi_{\hat{d}} \phi_{\hat{d}} \phi_{\hat{d}}. \end{aligned} \quad (2.9)$$

A few comments are in order:

- The first two lines reproduce the Lagrangian  $\mathcal{L}_0$  (2.2) with the original particle content

without the dummy field.

- The terms in the third line reproduce the Lagrangian  $\mathcal{L}_1$  (2.6) if one makes the following identifications:

$$Y_{jk}^{\hat{d}} \phi_{\hat{d}} = (m_f)_{jk}, \quad \lambda_{ab\hat{d}\hat{d}} \phi_{\hat{d}} \phi_{\hat{d}} = 2m_{ab}^2, \quad \lambda_{abc\hat{d}} \phi_{\hat{d}} = h_{abc}. \quad (2.10)$$

Note that these are the correct relations while the notation below Eq. (21) in [185] is rather sloppy:

$$Y_{jk}^{\hat{d}} = (m_f)_{jk}, \quad \lambda_{ab\hat{d}\hat{d}} = 2m_{ab}^2, \quad \lambda_{abc\hat{d}} = h_{abc}. \quad (2.11)$$

- The terms in the fourth line of Eq. (2.9) do not spoil the relations in Eq. (2.10) or (2.11). First of all, the second last term is only gauge invariant if  $\phi_a$  is a gauge singlet. Furthermore, it is an effective tadpole term which can be removed by a shift of the field  $\phi$ .<sup>4</sup> The last term is just a constant. In any case, contributions from the interactions in the fourth line to the  $\beta$ -functions of the other dimensionful parameters would involve at least one internal dummy line which gives a vanishing result.

The relations (2.11) have been used in Ref. [185] to derive the  $\beta$ -functions for the fermion masses from the known ones for the Yukawa interactions. Likewise, the  $\beta$ -functions for the scalar masses and the trilinear scalar couplings were obtained from the scalar quartic  $\beta$ -functions. This was achieved by removing contributions with a summation of  $\hat{d}$ -type indices and terms with  $\hat{d}$  indices appearing on the generators  $\Theta$ . However, a subtlety arises due to the wave-function renormalisation of external dummy scalar lines which leads to effective tadpole contributions. Such contributions should be removed from the  $\beta$ -functions for the Yukawa interactions and quartic couplings but are not necessarily eliminated by just suppressing the summation over  $\hat{d}$ -indices and associated gauge couplings. For this reason, we re-examine in the following sections all the  $\beta$ -functions for the dimensionful parameters by verifying the dummy method on a diagram by diagram basis.

## 2.5 Beta functions for dimensionful parameters

We now apply the dummy method to obtain the  $\beta$ -functions of the dimensionful parameters using the generic results for the dimensionless parameters given in Refs. [182–185]. In Sec. 2.5.1, we start with the fermion mass term. The trilinear scalar couplings will be discussed in Sec. 2.5.2 before we turn to the scalar mass terms in Sec. 2.5.3. First of all, it is necessary to introduce a number of group invariants and definitions for certain combinations of coupling constants. These definitions will be used to write the expressions for the  $\beta$ -functions in a more compact form.

**Group invariants**  $C_2(F)$  is the quadratic Casimir operator for the (in general) reducible fermion

---

<sup>4</sup>For the same reason such a term is not included in  $\mathcal{L}_1$  in Eq. (2.6).

representation:

$$C_2(F) := \sum_{A=1}^d t^A t^A, \quad \text{i.e. } [C_2(F)]_{ij} \equiv C_2^{ij}(F) = \sum_{A=1}^d \sum_{k=1}^{N_\psi} t_{ik}^A t_{kj}^A, \quad (2.12)$$

where  $i, j = 1, \dots, N_\psi$ . Due to Schur's lemma,  $C_2(F)$  is a diagonal  $N_\psi \times N_\psi$  matrix with the same eigenvalues for each irreducible representation. Similarly,  $C_2(S)$  is the quadratic Casimir operator for the (in general) reducible scalar representation:

$$C_2(S) := \sum_{A=1}^d \theta^A \theta^A, \quad \text{i.e. } [C_2(S)]_{ab} \equiv C_2^{ab}(S) = \sum_{A=1}^d \sum_{c=1}^{N_\phi} \theta_{ac}^A \theta_{cb}^A, \quad (2.13)$$

where  $a, b = 1, \dots, N_\phi$ . Again due to Schur's lemma,  $C_2(S)$  is a diagonal  $N_\phi \times N_\phi$  matrix. Furthermore,  $S_2(S)$  and  $S_2(F)$  denote the Dynkin index of the scalar and fermion representations, respectively,

$$\text{tr}[\theta^A \theta^B] =: S_2(S) \delta^{AB}, \quad \text{tr}[t^A t^B] =: S_2(F) \delta^{AB}, \quad (2.14)$$

and  $C_2(G)$  is the quadratic Casimir operator of the (irreducible) adjoint representation

$$C_2(G) \delta^{AB} := \sum_{C,D=1}^d f^{ACD} f^{BCD}. \quad (2.15)$$

**Coupling combinations** We start with two  $N_\psi \times N_\psi$  matrices formed out of the Yukawa matrices  $Y_{ij}^a$ :

$$Y_2(F) := \sum_{a=1}^{N_\phi} Y^{\dagger a} Y^a, \quad Y_2^\dagger(F) := \sum_{a=1}^{N_\phi} Y^a Y^{\dagger a}, \quad (2.16)$$

where the sum includes all ‘active’ (propagating) scalar indices but not the dummy index. It should be noted that  $Y_2^\dagger(F) \neq [Y_2(F)]^\dagger$ ; instead it represents the quantity  $Y_2(F)$  where the Yukawa coupling  $Y^a$  has been replaced by its conjugate  $Y^{\dagger a}$ . Furthermore, the following  $N_\phi \times N_\phi$  matrices are needed below:

$$Y_2^{ab}(S) := \frac{1}{2} \text{tr}[Y^{\dagger a} Y^b + Y^{\dagger b} Y^a], \quad (2.17)$$

$$H_{ab}^2(S) := \frac{1}{2} \sum_{c=1}^{N_\phi} \text{tr}[Y^a Y^{\dagger b} Y^c Y^{\dagger c} + Y^{\dagger a} Y^b Y^{\dagger c} Y^c], \quad (2.18)$$

$$\overline{H}_{ab}^2(S) := \frac{1}{2} \sum_{c=1}^{N_\phi} \text{tr}[Y^a Y^{\dagger c} Y^b Y^{\dagger c} + Y^{\dagger a} Y^c Y^{\dagger b} Y^c], \quad (2.19)$$

$$\Lambda_{ab}^2(S) := \frac{1}{6} \sum_{c,d,e=1}^{N_\phi} \lambda_{acde} \lambda_{bcde}, \quad (2.20)$$

$$Y_{ab}^{2F}(S) := \frac{1}{2} \text{tr}[C_2(F)(Y^a Y^{\dagger b} + Y^b Y^{\dagger a})]. \quad (2.21)$$

There is one crucial comment in order concerning the properties of these objects: in previous

works it is assumed that  $Y_2^{ab}(S) = Y_2(S)\delta_{ab}$  and  $\Lambda_{ab}^2(S) = \Lambda^2(S)\delta_{ab}$  holds. These properties are derived from group theoretical arguments. We agree with them as long as the considered model does not contain several scalar particles with identical quantum numbers. However, if this is the case than these relations are no longer valid. Or, in other words, the matrices  $Y_2^{ab}$  and  $\Lambda_{ab}^2$  are diagonal in the space of irreducible representations but not necessarily in the space of particles in the considered model. The consequence is that contributions from off-diagonal wave-function corrections may arise which are not included in Refs. [182–185]. This is one source for the discrepancies between our results and previous ones. This does not only affect the dimensionful parameters but also the quartic scalar couplings.

**RGEs for dimensionless parameters** The  $\beta$ -function for the dimensionful parameters are obtained from those of the dimensionless parameters using the dummy field method. The one- and two-loop expressions for the running of a Yukawa coupling are given by

$$\begin{aligned}
\beta_a^I &= \frac{1}{2} [Y_2^+(F)Y^a + Y^a Y_2(F)] + 2Y^b Y^{+a} Y^b + 2\kappa Y^b Y_2^{ab}(S) - 3g^2 \{C_2(F), Y^a\}, \\
\beta_a^{II} &= 2Y^c Y^{+b} Y^a (Y^{+c} Y^b - Y^{+b} Y^c) - Y^b [Y_2(F)Y^{+a} + Y^{+a} Y_2^+(F)] Y^b \\
&\quad - \frac{1}{8} [Y^b Y_2(F)Y^{+b} Y^a + Y^a Y^{+b} Y_2^+(F)Y^b] - \underline{4\kappa Y_2^{bc}(S)Y^b Y^{+a} Y^c} - 2\kappa Y^b \bar{H}_{ab}^2(S) \\
&\quad - \frac{3}{2} \kappa Y_2^{bc}(S)(Y^b Y^{+c} Y^a + Y^a Y^{+c} Y^b) - 3\kappa Y^b H_{ab}^2(S) - 2\lambda_{abcd} Y^b Y^{+c} Y^d \\
&\quad + \frac{1}{2} \Lambda_{ab}^2(S) Y^b + 3g^2 \{C_2(F), Y^b Y^{+a} Y^b\} + 5g^2 Y^b \{C_2(F), Y^{+a}\} Y^b \\
&\quad - \frac{7}{4} g^2 [C_2(F)Y_2^+(F)Y^a + Y^a Y_2(F)C_2(F)] \\
&\quad - \frac{1}{4} g^2 [Y^b C_2(F)Y^{+b} Y^a + Y^a Y^{+b} C_2(F)Y^b] + 6g^2 H_{2t}^a + 10\kappa g^2 Y^b Y_{ab}^{2F}(S) \\
&\quad + 6g^2 [C_2^{bc}(S)Y^b Y^{+a} Y^c - 2C_2^{ac}(S)Y^b Y^{+c} Y^b] + \frac{9}{2} g^2 C_2^{bc}(S)(Y^b Y^{+c} Y^a + Y^a Y^{+c} Y^b) \\
&\quad - \frac{3}{2} g^4 \{[C_2(F)]^2, Y^a\} + 6g^4 C_2^{ab}(S)\{C_2(F), Y^b\} \\
&\quad + g^4 \left[ -\frac{97}{6} C_2(G) + \frac{10}{3} \kappa S_2(F) + \frac{11}{12} S_2(S) \right] \{C_2(F), Y^a\} - \frac{21}{2} g^4 C_2^{ab}(S) C_2^{bc}(S) Y^c \\
&\quad + g^4 C_2^{ab}(S) \left[ \frac{49}{4} C_2(G) - 2\kappa S_2(F) - \frac{1}{4} S_2(S) \right] Y^b,
\end{aligned} \tag{2.22}$$

where the definition of  $H_{2t}^a$  can be found in App. 2.9.1 and the factor  $\kappa = 1/2$  for 2-component fermions and  $\kappa = 1$  for 4-component fermions. The underlined term differs from Refs. [183, 185] by a swapped index.

For the quartic coupling, we are going to use the following expressions:

$$\beta_{abcd}^I = \Lambda_{abcd}^2 - 8\kappa H_{abcd} + 2\kappa \underline{\Lambda_{abcd}^Y} - 3g^2 \Lambda_{abcd}^S + 3g^4 A_{abcd}, \quad (2.24)$$

$$\begin{aligned} \beta_{abcd}^{II} = & \frac{1}{12} \sum_{per} \Lambda_{af}^2 \lambda_{f bcd} - \bar{\Lambda}_{abcd}^3 - 4\kappa \bar{\Lambda}_{abcd}^{2Y} + \kappa \left[ 8\bar{H}_{abcd}^\lambda - \frac{1}{6} \sum_{per} [3H_{af}^2 + 2\bar{H}_{af}^2] \lambda_{f bcd} \right] \\ & + 4\kappa (H_{abcd}^Y + 2\bar{H}_{abcd}^Y + 2H_{abcd}^3) \\ & + g^2 \left[ 2\bar{\Lambda}_{abcd}^{2S} - 6\Lambda_{abcd}^{2g} + 4\kappa (H_{abcd}^S - H_{abcd}^F) + \frac{5}{3} \kappa \sum_{per} Y_{af}^{2F} \lambda_{f bcd} \right] \\ & - g^4 \left\{ \left[ \frac{35}{3} C_2(G) - \frac{10}{3} \kappa S_2(F) - \frac{11}{12} S_2(S) \right] \Lambda_{abcd}^S - \frac{3}{2} \Lambda_{abcd}^{SS} - \frac{5}{2} A_{abcd}^\lambda - \frac{1}{2} \bar{A}_{abcd}^\lambda \right. \\ & \quad \left. + 4\kappa (B_{abcd}^Y - 10\bar{B}_{abcd}^Y) \right\} \\ & + g^6 \left\{ \left[ \frac{161}{6} C_2(G) - \frac{32}{3} \kappa S_2(F) - \frac{7}{3} S_2(S) \right] A_{abcd} - \frac{15}{2} A_{abcd}^S + 27A_{abcd}^g \right\}, \quad (2.25) \end{aligned}$$

where the quantities  $\Lambda_{abcd}^2$ ,  $H_{abcd}$ ,  $\Lambda_{abcd}^Y$ ,  $\Lambda_{abcd}^S$ , and  $A_{abcd}$  in Eq. (2.24) are described in Sec. 2.5.2, while the definitions for the quantities  $\bar{\Lambda}_{abcd}^3, \dots, A_{abcd}^g$  in Eq. (2.25) can be found in App. 2.9.2. Here,  $\sum_{per}$  denotes a sum over all permutations of uncontracted scalar indices. Our equations (2.24) and (2.25) differ from the results in Refs. [184, 185] in the terms which are underlined. The reason is that only the possibility of diagonal wave-function renormalisation is included Refs. [184, 185] as discussed above.

Finally, to have all RGEs at one place, we give here also the  $\beta$ -functions for the gauge coupling although we will not use them in the following:

$$\beta_g^I = -g^3 \left[ \frac{11}{3} C_2(G) - \frac{4}{3} \kappa S_2(F) - \frac{1}{6} S_2(S) \right], \quad (2.26)$$

$$\begin{aligned} \beta_g^{II} = & -2\kappa g^3 Y_4(F) - g^5 \left[ \frac{34}{3} C_2(G)^2 - \kappa \left( 4C_2(F) + \frac{20}{3} C_2(G) \right) S_2(F) \right. \\ & \left. - \left( 2C_2(S) + \frac{1}{3} C_2(G) \right) S_2(S) \right]. \quad (2.27) \end{aligned}$$

### 2.5.1 Fermion mass

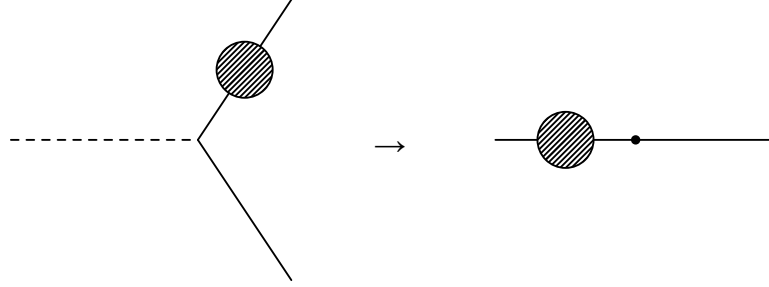
The  $\beta$ -function of the fermion mass term can be obtained from the expressions of the Yukawa coupling by considering the external scalar as dummy field. We follow a diagrammatic approach; for each class of diagrams we provide the coupling structure and show the resulting diagram together with its expression after applying the dummy field method. In accord with the discussion in Sec. 2.4, the following mappings are performed:

$$a \rightarrow \hat{d}, \quad Y^a \rightarrow Y^{\hat{d}} \rightarrow m_f, \quad Y^{\dagger a} \rightarrow Y^{\dagger \hat{d}} \rightarrow m_f^\dagger, \quad \lambda_{abcd} \rightarrow \lambda_{\hat{d}bcd} \rightarrow h_{bcd}.$$

The fermion mass insertions will be represented by black dots in the Feynman diagrams. We recall that dummy scalars do neither couple to gauge bosons nor propagate. There are two generically different wave function correction diagrams contributing to the running of the Yukawa



couplings: those stemming from either external fermions or scalars. For external fermions, the transition between the Yukawa coupling and fermion mass term looks as follows, where the grey blob depicts all loop corrections to the external line:



$$Y_2^\dagger(F)Y^a + Y^a Y_2(F) \rightarrow Y_2^\dagger(F)m_f + m_f Y_2(F) \quad (2.28)$$

$$\{C_2(F), Y^a\} \rightarrow \{C_2(F), m_f\} \quad (2.29)$$

$$Y^b Y_2(F) Y^{\dagger b} Y^a + Y^a Y^{\dagger b} Y_2^\dagger(F) Y^b \rightarrow Y^b Y_2(F) Y^{\dagger b} m_f + m_f Y^{\dagger b} Y_2^\dagger(F) Y^b \quad (2.30)$$

$$Y_2^{bc}(S)(Y^b Y^{\dagger c} Y^a + Y^a Y^{\dagger c} Y^b) \rightarrow Y_2^{bc}(S)(Y^b Y^{\dagger c} m_f + m_f Y^{\dagger c} Y^b) \quad (2.31)$$

$$g_2^2(C_2(F)Y_2^\dagger(F)Y^a + Y^a Y_2(F)C_2(F)) \rightarrow g_2^2(C_2(F)Y_2^\dagger(F)m_f + m_f Y_2(F)C_2(F)) \quad (2.32)$$

$$g_2^2(Y^b C_2(F)Y^{\dagger b} Y^a + Y^a Y^{\dagger b} C_2(F)Y^b) \rightarrow g_2^2(Y^b C_2(F)Y^{\dagger b} m_f + m_f Y^{\dagger b} C_2(F)Y^b) \quad (2.33)$$

$$g^2 C_2^{bc}(S)(Y^b Y^{\dagger c} Y^a + Y^a Y^{\dagger c} Y^b) \rightarrow g^2 C_2^{bc}(S)(Y^b Y^{\dagger c} m_f + m_f Y^{\dagger c} Y^b) \quad (2.34)$$

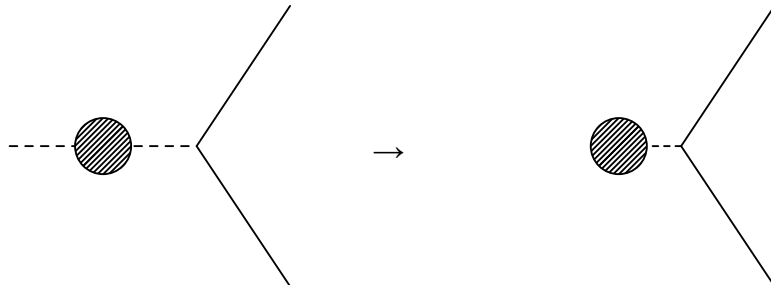
$$g^4 \{|C_2(F)|^2, Y^a\} \rightarrow g^4 \{|C_2(F)|^2, m_f\} \quad (2.35)$$

$$g^4 C_2(G)\{C_2(F), Y^a\} \rightarrow g^4 C_2(G)\{C_2(F), m_f\} \quad (2.36)$$

$$g^4(x_1 S_2(F) + x_2 S_2(S))\{C_2(F), Y^a\} \rightarrow g^4(x_1 S_2(F) + x_2 S_2(S))\{C_2(F), m_f\}. \quad (2.37)$$

Here,  $x_1$  and  $x_2$  are real numbers (cf. Eq. (2.23)).

Thus, we find counterparts for all contributions in both cases. The wave-function renormalisation part stemming from the external scalar is completely different: after applying the replacement with dummy fields, we find only tadpole contributions. However, those are usually absorbed into a re-definition of the vacuum, i.e., they don't contribute to the  $\beta$ -function of the fermion mass term, and the correct replacements are



$$Y^b Y_2^{ab}(S) \rightarrow 0 \quad (2.38)$$

$$Y^b \bar{H}_{ab}^2(S) \rightarrow 0 \quad (2.39)$$

$$Y^b H_{ab}^2(S) \rightarrow 0 \quad (2.40)$$

$$\Lambda_{ab}^2(S)Y^b \rightarrow 0 \quad (2.41)$$

$$g^2 Y^b Y_{ab}^{2F}(S) \rightarrow 0 \quad (2.42)$$

$$g^4 C_2^{ab}(S)\{C_2(F), Y^b\} \rightarrow 0 \quad (2.43)$$

$$g^4 C_2^{ab}(S)C_2^{bc}(S)Y^c \rightarrow 0 \quad (2.44)$$

$$g^4 C_2^{ab}(S)[x_1 C_2(G) + x_2 S_2(F) + x_3 S_2(S)]Y^b \rightarrow 0. \quad (2.45)$$

However, we find differences compared to the results of Ref. [185], where the following replacements have been made:

$$Y^b Y_2^{ab}(S) \rightarrow \frac{1}{2} Y^b \text{tr}[m_f^\dagger Y^b + Y^{\dagger b} m_f] \quad (2.46)$$

$$Y^b \bar{H}_{ab}^2(S) \rightarrow \frac{1}{2} Y^b \text{tr}[m_f Y^{\dagger c} Y^b Y^{\dagger c} + m_f^\dagger Y^c Y^{\dagger b} Y^c] \quad (2.47)$$

$$Y^b H_{ab}^2(S) \rightarrow \frac{1}{2} Y^b \text{tr}[m_f Y^{\dagger b} Y^b Y_2^\dagger(F) + m_f^\dagger Y^b Y_2(F)] \quad (2.48)$$

$$\Lambda_{ab}^2(S)Y^b \rightarrow \frac{1}{6} h_{cde} \lambda_{bcde} Y^b \quad (2.49)$$

$$g^2 Y^b Y_{ab}^{2F}(S) \rightarrow \frac{1}{2} g^2 Y^b \text{tr}[C_2(F)(m_f Y^{\dagger b} + Y^b m_f^\dagger)] \quad (2.50)$$

$$g^4 C_2^{ab}(S)\{C_2(F), Y^b\} \rightarrow 0 \quad (2.51)$$

$$g^4 C_2^{ab}(S)C_2^{bc}(S)Y^c \rightarrow 0 \quad (2.52)$$

$$g^4 C_2^{ab}(S)[...]Y^b \rightarrow 0. \quad (2.53)$$

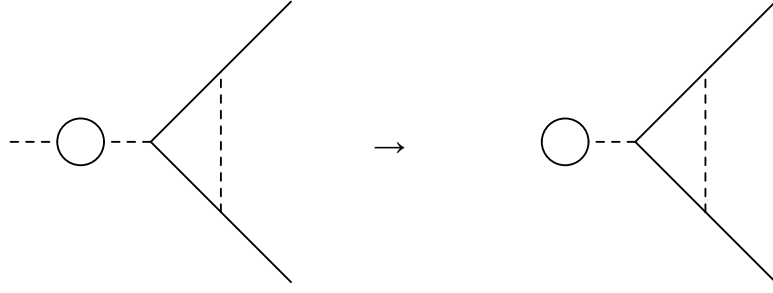
Thus, there is a disagreement between Eqs. (2.38) and (2.46) entering the one-loop beta-function for  $m_f$ . Furthermore, there are differences between Eqs. (2.39)–(2.42) and Eqs. (2.47)–(2.50) affecting the two-loop beta-function.

We now turn to the vertex corrections. At one-loop level, there is only one diagram which needs to be considered:

$$Y^b Y^{\dagger a} Y^b \rightarrow Y^b m_f^\dagger Y^b \quad (2.54)$$

At the two-loop level, there are many more contributions. The explicit diagrams are given in Appendix 2.9.1. While we completely agree with Ref. [185] for the one-loop vertex corrections, we also found differences at the two-loop level. Those stem from diagrams involving both, wave-function corrections of scalars as well as vertex corrections, as depicted in Fig. 2.1. According to our reasoning, these diagrams are also converted into tadpole diagrams which drop out.

Summarising our results, we find that the one-loop  $\beta$ -functions of fermion masses have one term



**Figure 2.1:** Two-loop diagram which does not contribute to the  $\beta$ -function of the fermion mass when replacing the external scalar by a dummy field as indicated here. The contribution depicted on the right hand side was included in Ref. [185].

less than the expression given in Ref. [185] and are given by the following form:

$$\beta_{m_f}^I = \frac{1}{2} \left[ Y_2^\dagger(F) m_f + m_f Y_2(F) \right] + 2Y^b m_f^\dagger Y^b - 3g^2 \{C_2(F), m_f\}. \quad (2.55)$$

At the two-loop level, we obtain

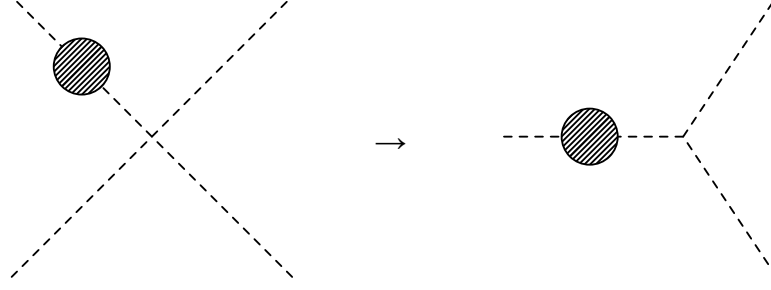
$$\begin{aligned} \beta_{m_f}^{II} = & 2Y^c Y^{\dagger b} m_f (Y^{\dagger c} Y^b - Y^{\dagger b} Y^c) - Y^b \left[ Y_2(F) m_f^\dagger + m_f^\dagger Y_2^\dagger(F) \right] Y^b \\ & - \frac{1}{8} \left[ Y^b Y_2(F) Y^{\dagger b} m_f + m_f Y^{\dagger b} Y_2^\dagger(F) Y^b \right] - 4\kappa Y_2^{bc}(S) Y^b m_f^\dagger Y^c \\ & - \frac{3}{2} \kappa Y_2^{bc}(S) (Y^b Y^{\dagger c} m_f + m_f Y^{\dagger c} Y^b) - 2h_{bcd} Y^b Y^{\dagger c} Y^d \\ & - 2h_{bcd} Y^b Y^{\dagger c} Y^d + 3g^2 \{C_2(F), Y^b m_f^\dagger Y^b\} + 5g^2 Y^b \{C_2(F), m_f^\dagger\} Y^b \\ & - \frac{7}{4} g^2 \left[ C_2(F) Y_2^\dagger(F) m_f + m_f Y_2(F) C_2(F) \right] \\ & - \frac{1}{4} g^2 \left[ Y^b C_2(F) Y^{\dagger b} m_f + m_f Y^{\dagger b} C_2(F) Y^b \right] \\ & + 6g^2 \left[ t^{A*} m_f Y^{\dagger b} t^{A*} Y^b + Y^b t^A Y^{\dagger b} m_f t^A \right] + 6g^2 C_2^{bc}(S) Y^b m_f^\dagger Y^c \\ & - \frac{3}{2} g^4 \{[C_2(F)]^2, m_f\} + \frac{9}{2} g^2 C_2^{bc}(S) (Y^b Y^{\dagger c} m_f + m_f Y^{\dagger c} Y^b) \\ & + g^4 \left[ -\frac{97}{6} C_2(G) + \frac{10}{3} \kappa S_2(F) + \frac{11}{12} S_2(S) \right] \{C_2(F), m_f\}. \end{aligned} \quad (2.56)$$

Here, we disagree in several terms as discussed above. The numerical impact of these differences compared to earlier results is briefly discussed at the example of a specific model in Sec. 2.7.

### 2.5.2 Trilinear coupling

We now turn to the purely scalar interactions. The  $\beta$ -functions of the cubic interactions are obtained from the expressions for the quartic couplings by replacing one external scalar by a dummy field. The translation of the wave-function contributions between both cases is straight-

forward and can be summarized as follows:



$$\Lambda_{abcd}^Y = \frac{1}{6} \sum_{per} Y_2^{af}(S) \lambda_{f bcd} \rightarrow \Lambda_{abc}^Y = \frac{1}{2} \sum_{per} Y_2^{af}(S) h_{f bc} \quad (2.57)$$

$$\Lambda_{abcd}^S = \sum_i C_2(i) \lambda_{abcd} \rightarrow \Lambda_{abc}^S = \sum_i C_2(i) h_{abc} \quad (2.58)$$

$$\frac{1}{6} \sum_{per} \Lambda_{af}^2(S) \lambda_{f bcd} \rightarrow \frac{1}{2} \sum_{per} \Lambda_{af}^2(S) h_{f bc} \quad (2.59)$$

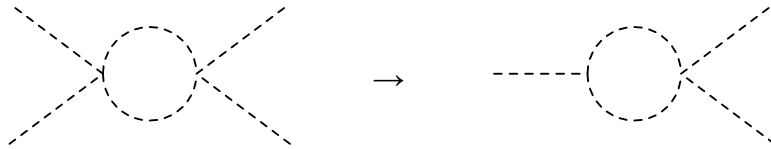
$$\frac{1}{6} \sum_{per} (3H_{af}^2(S) + 2\bar{H}_{af}^2(S)) \lambda_{f bcd} \rightarrow \frac{1}{2} \sum_{per} (3H_{af}^2(S) + 2\bar{H}_{af}^2(S)) h_{f bc} \quad (2.60)$$

$$\frac{1}{6} \sum_{per} Y_{af}^{2F}(S) \lambda_{f bcd} \rightarrow \frac{1}{2} \sum_{per} Y_{af}^{2F}(S) h_{f bc} \quad (2.61)$$

$$X \Lambda_{abcd}^S \rightarrow X \Lambda_{abc}^S \quad (2.62)$$

$$\Lambda_{abcd}^{SS} = \sum_i |C_2(i)|^2 \lambda_{abcd} \rightarrow \Lambda_{abc}^{SS} = \sum_i |C_2(i)|^2 h_{abc} \quad (2.63)$$

In this notation, the index  $i$  is summed over all uncontracted scalar indices. Furthermore, 'X' denotes the combination of group invariants multiplying  $\Lambda_{abcd}^S$  in Eq. (2.25). As discussed above, we have modified the parts which involve Yukawa or quartic couplings compared to Ref. [185]. The reason is that in these cases new contributions can be present due to off-diagonal wave-function renormalisation corrections. There are three generically different vertex corrections which contribute to the RGE of the quartic interaction. However, since the dummy field does not interact with the gauge sector, those kind of contributions do not appear in the case of the cubic interaction. Therefore, the translation at the one-loop level becomes:



$$\Lambda_{abcd}^2 = \frac{1}{8} \sum_{per} \lambda_{abef} \lambda_{efcd} \rightarrow \Lambda_{abc}^2 = \frac{1}{2} \sum_{per} \lambda_{abef} h_{efc} \quad (2.64)$$



$$H_{abcd} = \frac{1}{4} \sum_{per} \text{Tr}(Y^a Y^{\dagger b} Y^c Y^{\dagger d}) \quad H_{abc} = \frac{1}{2} \sum_{per} \text{Tr}(m_f Y^{\dagger a} Y^b Y^{\dagger c} + m_f^{\dagger} Y^a Y^{\dagger b} Y^c) \quad (2.65)$$



$$A_{abcd} = \frac{1}{8} \sum_{per} \{\theta^A, \theta^B\}_{ab} \{\theta^A, \theta^B\}_{cd} \quad 0 \quad (2.66)$$

The explicit form of the two-loop diagrams as well as their expressions in both cases are given in Appendix 2.9.2. We find agreement between our results and those of Ref. [185] at the one- and two-loop level up to the differences from off-diagonal wave-function renormalisations. Thus, the  $\beta$ -functions at the one- and two-loop levels are

$$\beta_{h_{abc}}^I = \Lambda_{abc}^2 - 8\kappa H_{abc} + 2\kappa \Lambda_{abc}^Y - 3g^2 \Lambda_{abc}^S, \quad (2.67)$$

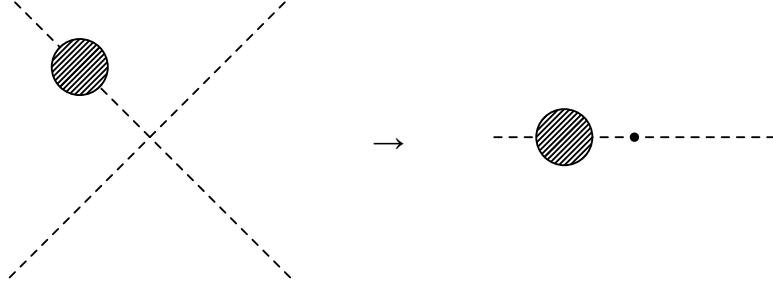
$$\begin{aligned} \beta_{h_{abc}}^{II} = & \frac{1}{4} \sum_{per} \Lambda_{af}^2(S) h_{fbc} - \bar{\Lambda}_{abc}^3 - 4\kappa \bar{\Lambda}_{abc}^{2Y} \\ & + \kappa \left[ 8\bar{H}_{abc}^{\lambda m} + 8\bar{H}_{abc}^h - \frac{1}{2} \sum_{per} [3H_{af}^2(S) + 2\bar{H}_{af}^2(S)] h_{fbc} \right] \\ & + 4\kappa (H_{abc}^Y + 2\bar{H}_{abc}^Y + 2H_{abc}^3) \\ & + g^2 \left[ 2\bar{\Lambda}_{abc}^{2S} - 6\Lambda_{abc}^{2g} + 4\kappa (H_{abc}^S - H_{abc}^F) + 5\kappa \sum_{per} Y_{af}^{2F}(S) h_{fbc} \right] \\ & - g^4 \left\{ \left[ \frac{35}{3} C_2(G) - \frac{10}{3} \kappa S_2(F) - \frac{11}{12} S_2(S) \right] \Lambda_{abc}^S \right. \\ & \quad \left. - \frac{3}{2} \Lambda_{abc}^{SS} - \frac{5}{2} A_{abc}^{\lambda} - \frac{1}{2} \bar{A}_{abc}^{\lambda} + 4\kappa (B_{abc}^Y - 10\bar{B}_{abc}^Y) \right\}, \quad (2.68) \end{aligned}$$

where the invariants are defined in Eqs. (2.64)–(2.65) and (2.221)–(2.237).

### 2.5.3 Scalar mass

Finally, we turn to the terms involving two scalar couplings. The procedure is very similar to the case of the cubic scalar coupling, and we find the following relations for the wave-function

corrections to the terms appearing for the quartic scalar coupling:



$$\Lambda_{abcd}^Y = \frac{1}{6} \sum_{per} Y_2^{ae}(S) \lambda_{ebcd} \rightarrow \Lambda_{ab}^Y = 2 \sum_{per} Y_2^{ae}(S) m_{eb}^2 \quad (2.69)$$

$$\Lambda_{abcd}^S = \sum_i C_2(i) \lambda_{abcd} \rightarrow \Lambda_{ab}^S = 2 \sum_i C_2(i) m_{ab}^2 \quad (2.70)$$

$$\frac{1}{6} \sum_{per} \Lambda_{ae}^2(S) \lambda_{ebcd} \rightarrow 2 \sum_{per} \Lambda_{ae}^2(S) m_{eb}^2 \quad (2.71)$$

$$\frac{1}{6} \sum_{per} (3H_{af}^2(S) + 2\bar{H}_{af}^2(S)) \lambda_{fbcd} \rightarrow 2 \sum_{per} (3H_{af}^2(S) + 2\bar{H}_{af}^2(S)) m_{fb}^2 \quad (2.72)$$

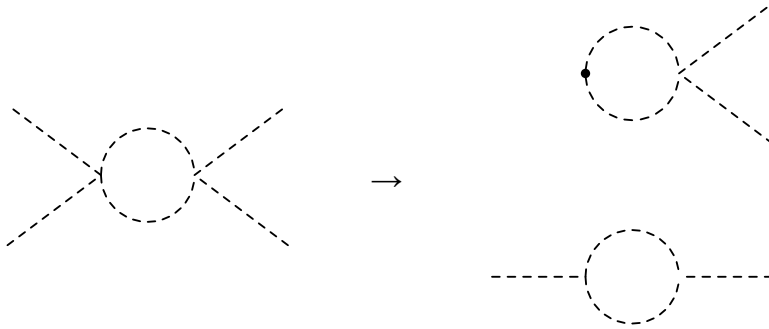
$$\frac{1}{6} \sum_{per} Y_{af}^{2F}(S) \lambda_{fbcd} \rightarrow 2 \sum_{per} Y_{af}^{2F}(S) m_{fb}^2 \quad (2.73)$$

$$X \Lambda_{abcd}^S \rightarrow X \Lambda_{ab}^S \quad (2.74)$$

$$\Lambda_{abcd}^{SS} = \sum_i |C_2(i)|^2 \lambda_{abcd} \rightarrow \Lambda_{ab}^{SS} = 2 \sum_i |C_2(i)|^2 m_{ab}^2. \quad (2.75)$$

Again, 'X' denotes the combination of group invariants multiplying  $\Lambda_{abcd}^S$  in Eq. (2.25).

Again, we need to consider the three generically different diagrams which contribute to the running of the quartic functions. The one with vector bosons in the loop vanishes due to inserting dummy fields, while for the other two diagrams additional terms arise.



$$\Lambda_{abcd}^2 = \frac{1}{8} \sum_{per} \lambda_{abef} \lambda_{efcd} \quad 2m_{ef}^2 \lambda_{abef} + 2h_{aef} h_{bef} \quad (2.76)$$



$$H_{abcd} = \frac{1}{4} \sum_{per} \text{Tr}(Y^a Y^{\dagger b} Y^c Y^{\dagger d}) \quad H_{ab} = \sum_{per} \text{Tr}(Y^a Y^{\dagger b} m_f m_f^{\dagger} + Y^{\dagger a} Y^b m_f^{\dagger} m_f + \frac{1}{2} Y^{\dagger a} m_f Y^b m_f^{\dagger} + \frac{1}{2} Y^a m_f^{\dagger} Y^b m_f) \quad (2.77)$$



$$A_{abcd} = \frac{1}{8} \sum_{per} \{\theta^A, \theta^B\}_{ab} \{\theta^A, \theta^B\}_{cd} \quad 0 \quad (2.78)$$

The two-loop diagrams are given in Appendix 2.9.3. We also find agreement between our results here and the ones given in Ref. [185] up to the wave-function renormalisation. One needs to be careful about some factor of  $\frac{1}{2}$  due to  $\beta_{m_{ab}^2} = \frac{1}{2} \beta_{\lambda_{ab\dot{a}\dot{b}}}$ , which we have included here explicitly into the definition of the  $\beta$ -function for  $m_{ab}^2$ , while it has been partially absorbed into other definitions in Ref. [185]. Thus, with our conventions the one- and two-loop  $\beta$ -functions read

$$\beta_{m_{ab}^2}^I = m_{ef}^2 \lambda_{abef} + h_{aef} h_{bef} - 4\kappa H_{ab} + \kappa \Lambda_{ab}^Y - \frac{3}{2} g^2 \Lambda_{ab}^S, \quad (2.79)$$

$$\begin{aligned} \beta_{m_{ab}^2}^{II} = & \frac{1}{2} \sum_{per} \Lambda_{af}^2(S) m_{fb}^2 - \frac{1}{2} \bar{\Lambda}_{ab}^3 - 2\kappa \bar{\Lambda}_{ab}^{2Y} \\ & + \kappa \left[ 4\bar{H}_{ab}^{\lambda} - \sum_{per} [3H_{af}^2(S) + 2\bar{H}_{af}^2(S)] m_{fb}^2 \right] \\ & + 2\kappa (H_{ab}^Y + 2\bar{H}_{ab}^Y + 2H_{ab}^3) \\ & + g^2 \left[ \bar{\Lambda}_{ab}^{2S} - 3\Lambda_{ab}^{2g} + 2\kappa (H_{ab}^S - H_{ab}^F) + 10\kappa \sum_{per} Y_{af}^{2F}(S) m_{fb}^2 \right] \\ & - g^4 \left\{ \left[ \frac{35}{6} C_2(G) - \frac{5}{3} \kappa S_2(F) - \frac{11}{24} S_2(S) \right] \Lambda_{ab}^S \right. \\ & \left. - \frac{3}{4} \Lambda_{ab}^{SS} - \frac{5}{4} A_{ab}^{\lambda} - \frac{1}{4} \bar{A}_{ab}^{\lambda} + 2\kappa (B_{ab}^Y - 10\bar{B}_{ab}^Y) \right\}, \quad (2.80) \end{aligned}$$

where we used the objects defined in Eqs. (2.76)–(2.77) and (2.238)–(2.254).

## 2.6 Comparison with supersymmetric RGEs

We have now re-derived the full one- and two-loop RGEs for the dimensionful parameters. While we agree with Ref. [185] concerning the bilinear and cubic scalar interactions (up to wave-function renormalisation), we find differences in the fermion mass terms. Therefore, we

want to double-check our results by comparing to those obtained using supersymmetric (SUSY) RGEs. The general RGEs for a softly broken SUSY model have been independently calculated in Refs. [195–197] and the general agreement between all results has been discussed in Ref. [198]. Thus, there is hardly any doubt that these RGEs are absolutely correct. Therefore, we want to test our results with a model in which we enforce SUSY relations among parameters. After a translation from the  $\overline{\text{MS}}$  to the  $\overline{\text{DR}}$  scheme one should recover the SUSY results.

Since a supersymmetric extension of the SM yields many couplings which are generically all of the same form, we opt for a more compact theory. We consider a toy model with one vector superfield  $\hat{B}$  and three chiral superfields

$$\hat{H}_d : Q = -\frac{1}{2}, \quad (2.81)$$

$$\hat{H}_u : Q = \frac{1}{2}, \quad (2.82)$$

$$\hat{S} : Q = 0, \quad (2.83)$$

where  $Q$  denotes the electric charge. The superpotential consists of two terms<sup>5</sup>

$$W = \lambda \hat{H}_u \hat{H}_d \hat{S} + \mu \hat{H}_u \hat{H}_d \quad (2.84)$$

and the soft-breaking terms are

$$\begin{aligned} -L_{SB} = & \left( B_\mu H_d H_u + T_\lambda H_d H_u S + \frac{1}{2} M_B \tilde{B}^2 + \text{h.c.} \right) + \\ & m_{H_d}^2 |H_d|^2 + m_{H_u}^2 |H_u|^2 + m_S^2 |S|^2. \end{aligned} \quad (2.85)$$

This model contains all of the relevant generic structure we need to test. Making use of the results of Ref. [195], which are also implemented in the package SARAH, we find the following expressions for the one- and two-loop RGEs for the different parts of the model:

### 1. Gauge Couplings

$$\beta_g^{(1)} = \frac{1}{2} g^3 \quad (2.86)$$

$$\beta_g^{(2)} = \frac{1}{2} g^3 \left( -2|\lambda|^2 + g^2 \right) \quad (2.87)$$

### 2. Gaugino Mass Parameters

$$\beta_{M_B}^{(1)} = g^2 M_B \quad (2.88)$$

$$\beta_{M_B}^{(2)} = 2g^2 \left( g^2 M_B + \lambda^* \left( -M_B \lambda + T_\lambda \right) \right) \quad (2.89)$$

### 3. Trilinear Superpotential Parameters

$$\beta_\lambda^{(1)} = \lambda \left( 3|\lambda|^2 - g^2 \right) \quad (2.90)$$

---

<sup>5</sup>We neglect terms  $\propto \hat{S}^2, \hat{S}^3$  which are not essential for our argument.



$$\beta_\lambda^{(2)} = \lambda \left( -6|\lambda|^4 + g^2|\lambda|^2 + g^4 \right) \quad (2.91)$$

## 4. Bilinear Superpotential Parameters

$$\beta_\mu^{(1)} = -\mu \left( -2|\lambda|^2 + g^2 \right) \quad (2.92)$$

$$\beta_\mu^{(2)} = \mu \left( -4|\lambda|^4 + g^4 \right) \quad (2.93)$$

## 5. Trilinear Soft-Breaking Parameters

$$\beta_{T_\lambda}^{(1)} = 2g^2 M_B \lambda - \left( -9|\lambda|^2 + g^2 \right) T_\lambda \quad (2.94)$$

$$\beta_{T_\lambda}^{(2)} = -30|\lambda|^4 T_\lambda + g^2|\lambda|^2 \left( -2M_B \lambda + 3T_\lambda \right) + g^4 \left( -4M_B \lambda + T_\lambda \right) \quad (2.95)$$

## 6. Bilinear Soft-Breaking Parameters

$$\beta_{B_\mu}^{(1)} = 2g^2 M_B \mu + 4|\lambda|^2 B_\mu + 4\mu \lambda^* T_\lambda - g^2 B_\mu \quad (2.96)$$

$$\beta_{B_\mu}^{(2)} = \left( 2g^2|\lambda|^2 - 8|\lambda|^4 + g^4 \right) B_\mu - 2\mu \left( 10|\lambda|^2 \lambda^* T_\lambda + 2g^4 M_B + g^2 M_B |\lambda|^2 \right) \quad (2.97)$$

## 7. Soft-Breaking Scalar Masses

$$\beta_{m_{H_d}^2}^{(1)} = -2g^2 |M_B|^2 + 2 \left( m_{H_d}^2 + m_{H_u}^2 + m_S^2 \right) |\lambda|^2 + 2|T_\lambda|^2 - \frac{1}{2}g^2 \left( -m_{H_d}^2 + m_{H_u}^2 \right) \quad (2.98)$$

$$\begin{aligned} \beta_{m_{H_d}^2}^{(2)} &= 6g^4 |M_B|^2 - 8 \left( m_{H_d}^2 + m_{H_u}^2 + m_S^2 \right) |\lambda|^4 - 16|\lambda|^2 |T_\lambda|^2 \\ &\quad + g^4 m_{H_d}^2 + g^2 |\lambda|^2 \left( m_{H_u}^2 - m_{H_d}^2 \right) \end{aligned} \quad (2.99)$$

$$\beta_{m_{H_u}^2}^{(1)} = -2g^2 |M_B|^2 + 2 \left( m_{H_d}^2 + m_{H_u}^2 + m_S^2 \right) |\lambda|^2 + 2|T_\lambda|^2 + \frac{1}{2}g^2 \left( -m_{H_d}^2 + m_{H_u}^2 \right) \quad (2.100)$$

$$\begin{aligned} \beta_{m_{H_u}^2}^{(2)} &= 6g^4 |M_B|^2 - 8 \left( m_{H_d}^2 + m_{H_u}^2 + m_S^2 \right) |\lambda|^4 - 16|\lambda|^2 |T_\lambda|^2 \\ &\quad + g^4 m_{H_u}^2 + g^2 |\lambda|^2 \left( -m_{H_u}^2 + m_{H_d}^2 \right) \end{aligned} \quad (2.101)$$

$$\beta_{m_S^2}^{(1)} = 2 \left( \left( m_{H_d}^2 + m_{H_u}^2 + m_S^2 \right) |\lambda|^2 + |T_\lambda|^2 \right) \quad (2.102)$$

$$\begin{aligned} \beta_{m_S^2}^{(2)} &= 2 \left( -4 \left( m_{H_d}^2 + m_{H_u}^2 + m_S^2 \right) |\lambda|^4 + \lambda^* \left( g^2 M_B^* \left( 2M_B \lambda - T_\lambda \right) + \right. \right. \\ &\quad \left. \left. \lambda \left( -8|T_\lambda|^2 + g^2 \left( m_{H_d}^2 + m_{H_u}^2 + m_S^2 \right) \right) \right) + g^2 T_\lambda^* \left( -M_B \lambda + T_\lambda \right) \right) \end{aligned} \quad (2.103)$$

As before, we have suppressed the pre-factors  $\frac{1}{16\pi^2}$  and  $\frac{1}{(16\pi^2)^2}$  for the one- and two-loop  $\beta$ -functions. With these functions, the running of all parameters at the one- and two-loop level is fixed. However, for later comparison, it will be convenient to know the  $\beta$ -functions for some products of parameters as well. That is done by applying the chain rule:

$$\beta_{\frac{1}{8}g^2}^{(1)} = \frac{1}{4}g\beta_g^{(1)} = \frac{1}{8}g^4, \quad (2.104)$$

$$\beta_{\frac{1}{8}g^2}^{(2)} = \frac{1}{4}g\beta_g^{(2)} = -\frac{1}{4}|\lambda|^2 g^4 + \frac{1}{8}g^6, \quad (2.105)$$

$$\beta_{|\lambda|^2}^{(1)} = \lambda(\beta_\lambda^{(1)})^* + \lambda^* \beta_\lambda^{(1)} = 2|\lambda|^2(3|\lambda|^2 - g^2), \quad (2.106)$$

$$\beta_{|\lambda|^2}^{(2)} = \lambda(\beta_\lambda^{(2)})^* + \lambda^* \beta_\lambda^{(2)} = 2|\lambda|^2(-6|\lambda|^4 + g^2|\lambda|^2 + g^4), \quad (2.107)$$

$$\beta_{|\lambda|^2 - \frac{1}{4}g^2}^{(1)} = 2\lambda\beta_\lambda^{(1)} - \frac{1}{2}g\beta_g^{(1)} = -2|\lambda|^2g^2 + 6|\lambda|^4 - \frac{1}{4}g^4, \quad (2.108)$$

$$\beta_{|\lambda|^2 - \frac{1}{4}g^2}^{(2)} = 2\lambda\beta_\lambda^{(2)} - \frac{1}{2}g\beta_g^{(2)} = -12|\lambda|^6 - \frac{1}{4}g^6 + \frac{5}{2}g^4|\lambda|^2 + 2g^2|\lambda|^4, \quad (2.109)$$

$$\beta_{\lambda\mu^*}^{(1)} = \lambda(\beta_\mu^{(1)})^* + \mu^* \beta_\lambda^{(1)} = \mu^* \lambda(-2g^2 + 5|\lambda|^2), \quad (2.110)$$

$$\beta_{\lambda\mu^*}^{(2)} = \lambda(\beta_\mu^{(2)})^* + \mu^* \beta_\lambda^{(2)} = \mu^* \lambda(-10|\lambda|^4 + 2g^4 + g^2|\lambda|^2), \quad (2.111)$$

$$\beta_{|\mu|^2}^{(1)} = \mu(\beta_\mu^{(1)})^* + \mu^* \beta_\mu^{(1)} = -2|\mu|^2(-2|\lambda|^2 + g^2), \quad (2.112)$$

$$\beta_{|\mu|^2}^{(2)} = \mu(\beta_\mu^{(2)})^* + \mu^* \beta_\mu^{(2)} = 2|\mu|^2(-4|\lambda|^4 + g^4). \quad (2.113)$$

We now consider the same model written as a non-supersymmetric version. In this case, we have one gauge boson  $B$ , four fermions

$$\tilde{H}_d : Q = -\frac{1}{2}, \quad (2.114)$$

$$\tilde{H}_u : Q = \frac{1}{2}, \quad (2.115)$$

$$\tilde{S} : Q = 0, \quad (2.116)$$

$$\tilde{B} : Q = 0, \quad (2.117)$$

and three scalars

$$H_d : Q = -\frac{1}{2}, \quad (2.118)$$

$$H_u : Q = \frac{1}{2}, \quad (2.119)$$

$$S : Q = 0. \quad (2.120)$$

The full potential for this models involves a substantial amount of different couplings

$$\begin{aligned} V = & (T_1 S |H_d|^2 + T_2 S |H_u|^2 + T_3 H_d H_u S + \text{h.c.}) \\ & + m_1^2 |H_d|^2 + m_2^2 |H_u|^2 + m_3^2 |S|^2 \\ & + \lambda_1 |S|^2 |H_d|^2 + \lambda_2 |S|^2 |H_u|^2 + \lambda_3 |H_d|^2 |H_u|^2 + \lambda_4 |H_d|^4 + \lambda_5 |H_u|^4 \\ & + (M_1 \tilde{B} \tilde{B} + M_2 \tilde{H}_d \tilde{H}_u + B H_d H_u + \text{h.c.}) \\ & + \left( Y_1 S \tilde{H}_d \tilde{H}_u + Y_2 \tilde{S} H_d \tilde{H}_u + Y_3 \tilde{S} \tilde{H}_d H_u - \frac{1}{\sqrt{2}} g_d \tilde{B} \tilde{H}_d H_d^* + \frac{1}{\sqrt{2}} g_u \tilde{B} \tilde{H}_u H_u^* + \text{h.c.} \right). \end{aligned} \quad (2.121)$$

We think that this rather lengthy form justifies our approach to consider only a toy model, but not a realistic SUSY theory. We have neglected couplings that would be allowed by the symmetry of this theory, but vanish as we match to the SUSY model. In particular, CP even and odd part of the complex field  $S$  will run differently unless specific (SUSY) relations among the

parameters exist. Therefore, one would need to decompose  $S$  into its real components and write down all possible potential terms involving these fields. However, we are only interested in the  $\beta$  functions in the SUSY limit where no splitting between these fields is introduced. Therefore, we retain the more compact notation in (2.121). We can now make use of our revised expressions to calculate the RGEs up to two-loop. For this purpose, we modified the packages SARAH and PyR@TE accordingly. The lengthy expressions in the general case are given in Appendix 2.10. In order to make connection to the SUSY case, we can make the following associations between parameters of these models:

$$g_d = g_u = g, \quad (2.122)$$

$$Y_1 = Y_2 = Y_3 = \lambda, \quad (2.123)$$

$$\lambda_1 = \lambda_2 = |\lambda|^2, \quad (2.124)$$

$$\lambda_3 = |\lambda|^2 - \frac{1}{4}g^2, \quad (2.125)$$

$$\lambda_4 = \lambda_5 = \frac{1}{8}g^2, \quad (2.126)$$

$$T_1 = T_2 = \mu^* \lambda, \quad (2.127)$$

$$T_3 = T_\lambda, \quad (2.128)$$

$$M_1 = \frac{1}{2}M_B, \quad (2.129)$$

$$M_2 = \mu, \quad (2.130)$$

$$m_1^2 = m_{H_d}^2 + |\mu|^2, \quad (2.131)$$

$$m_2^2 = m_{H_u}^2 + |\mu|^2, \quad (2.132)$$

$$m_3^2 = m_S^2, \quad (2.133)$$

$$B = B_\mu. \quad (2.134)$$

By doing that, we obtain the following RGEs:

### 1. Gauge Couplings

$$\beta_g^{(1)} = \frac{1}{2}g^3 \quad (2.135)$$

$$\beta_g^{(2)} = \frac{1}{2}g^3 \left( -2|\lambda|^2 + g^2 \right) \quad (2.136)$$

### 2. Quartic scalar couplings

$$\beta_{\lambda_1}^{(1)} = \beta_{\lambda_2}^{(1)} = 2|\lambda|^2 \left( 3|\lambda|^2 - g^2 \right) \quad (2.137)$$

$$\beta_{\lambda_1}^{(2)} = \beta_{\lambda_2}^{(2)} = 2|\lambda|^2 \left( -6|\lambda|^4 + \frac{5}{4}g^2|\lambda|^2 + \frac{17}{8}g^4 \right) \quad (2.138)$$

$$\beta_{\lambda_3}^{(1)} = -2g^2|\lambda|^2 + 6|\lambda|^4 - \frac{1}{4}g^4 \quad (2.139)$$

$$\beta_{\lambda_3}^{(2)} = -12|\lambda|^6 - \frac{17}{8}g^6 + \frac{31}{4}g^4|\lambda|^2 + g^2|\lambda|^4 \quad (2.140)$$

$$\beta_{\lambda_4}^{(1)} = \beta_{\lambda_5}^{(1)} = \frac{1}{8}g^4 \quad (2.141)$$

$$\beta_{\lambda_4}^{(2)} = \beta_{\lambda_5}^{(2)} = \frac{7}{8}g^4|\lambda|^2 - g^2|\lambda|^4 + \frac{1}{16}g^6 \quad (2.142)$$

$$(2.143)$$

### 3. Yukawa Couplings

$$\beta_{g_d}^{(1)} = \beta_{g_u}^{(1)} = \frac{1}{2}g^3 \quad (2.144)$$

$$\beta_{g_d}^{(2)} = \beta_{g_u}^{(2)} = \frac{1}{2}g^3 \left( -\frac{22}{8}|\lambda|^2 + \frac{11}{8}g^2 \right) \quad (2.145)$$

$$\beta_{Y_1}^{(1)} = \lambda \left( 3|\lambda|^2 - g^2 \right) \quad (2.146)$$

$$\beta_{Y_1}^{(2)} = \lambda \left( -6|\lambda|^4 + \frac{1}{4}g^2|\lambda|^2 + \frac{11}{8}g^4 \right) \quad (2.147)$$

$$\beta_{Y_2}^{(1)} = \beta_{Y_3}^{(1)} = \lambda \left( 3|\lambda|^2 - g^2 \right) \quad (2.148)$$

$$\beta_{Y_2}^{(2)} = \beta_{Y_3}^{(2)} = \lambda \left( -6|\lambda|^4 + \frac{11}{8}g^2|\lambda|^2 + \frac{13}{16}g^4 \right) \quad (2.149)$$

### 4. Fermion Mass Terms

$$\beta_{M_1}^{(1)} = \frac{1}{2}g^2M_B \quad (2.150)$$

$$\beta_{M_1}^{(2)} = g^2 \left( \frac{9}{8}g^2M_B + \lambda^* \left( -M_B\lambda + T_\lambda \right) \right) \quad (2.151)$$

$$\beta_{M_2}^{(1)} = -\mu \left( -2|\lambda|^2 + g^2 \right) \quad (2.152)$$

$$\beta_{M_2}^{(2)} = \mu \left( -4|\lambda|^4 + \frac{11}{8}g^4 - \frac{1}{4}g^2|\lambda|^2 \right) \quad (2.153)$$

### 5. Trilinear Scalar couplings

$$\beta_{T_1}^{(1)} = \beta_{T_2}^{(1)} = \lambda\mu^* \left( -2g^2 + 5|\lambda|^2 \right) \quad (2.154)$$

$$\beta_{T_1}^{(2)} = \beta_{T_2}^{(2)} = \lambda\mu^* \left( -10|\lambda|^4 + \frac{17}{4}g^4 + 2g^2|\lambda|^2 \right) \quad (2.155)$$

$$\beta_{T_3}^{(1)} = 2g^2M_B\lambda - \left( -9|\lambda|^2 + g^2 \right) T_\lambda \quad (2.156)$$

$$\beta_{T_3}^{(2)} = -30|\lambda|^4T_\lambda + g^2|\lambda|^2 \left( -2M_B\lambda + 3T_\lambda \right) + g^4 \left( -4M_B\lambda + \frac{7}{4}T_\lambda \right) \quad (2.157)$$

### 6. Scalar Mass Terms

$$\beta_B^{(1)} = 2g^2M_B\mu + 4B_\mu|\lambda|^2 + 4\mu\lambda^*T_\lambda - B_\mu g^2 \quad (2.158)$$

$$\beta_B^{(2)} = \left( -8|\lambda|^4 + \frac{5}{2}g^2|\lambda|^2 + \frac{7}{4}g^4 \right) B_\mu - 2\mu \left( 10|\lambda|^2\lambda^*T_\lambda + 2g^4M_B + g^2|\lambda|^2M_B \right) \quad (2.159)$$

$$\begin{aligned} \beta_{m_i^2}^{(1)} = & -2g^2|M_B|^2 + 2|\lambda|^2 \left( m_{H_d}^2 + m_{H_u}^2 + m_S^2 \right) + 2|T_\lambda|^2 + \frac{1}{2}g^2 \left( m_{H_d}^2 - m_{H_u}^2 \right) \\ & + \left( 4|\lambda|^2 - 2g^2 \right) |\mu|^2 \end{aligned} \quad (2.160)$$

$$\begin{aligned}
\beta_{m_1^2}^{(2)} = & \frac{11}{2} g^4 |M_B|^2 - 8 \left( m_{H_d}^2 + m_{H_u}^2 + m_S^2 \right) |\lambda|^4 - 16 |T_\lambda|^2 |\lambda|^2 \\
& + \frac{1}{2} |\lambda|^2 g^2 \left( 2 m_{H_u}^2 - m_{H_d}^2 \right) + \frac{1}{4} g^4 \left( + 2 m_{H_u}^2 + 9 m_{H_d}^2 \right) \\
& + |\mu|^2 \left( \frac{3}{2} |\lambda|^2 g^2 - 8 |\lambda|^4 + \frac{17}{4} g^4 \right)
\end{aligned} \tag{2.161}$$

$$\begin{aligned}
\beta_{m_2^2}^{(1)} = & - 2 g^2 |M_B|^2 + 2 |\lambda|^2 \left( m_{H_d}^2 + m_{H_u}^2 + m_S^2 \right) + 2 |T_\lambda|^2 + \frac{1}{2} g^2 \left( m_{H_u}^2 - m_{H_d}^2 \right) \\
& + \left( 4 |\lambda|^2 - 2 g^2 \right) |\mu|^2
\end{aligned} \tag{2.162}$$

$$\begin{aligned}
\beta_{m_2^2}^{(2)} = & \frac{11}{2} g^4 |M_B|^2 - 8 \left( m_{H_d}^2 + m_{H_u}^2 + m_S^2 \right) |\lambda|^4 - 16 |T_\lambda|^2 |\lambda|^2 \\
& + \frac{1}{2} |\lambda|^2 g^2 \left( 2 m_{H_d}^2 - m_{H_u}^2 \right) + \frac{1}{4} g^4 \left( + 2 m_{H_d}^2 + 9 m_{H_u}^2 \right) \\
& + |\mu|^2 \left( \frac{3}{2} |\lambda|^2 g^2 - 8 |\lambda|^4 + \frac{17}{4} g^4 \right)
\end{aligned} \tag{2.163}$$

$$\beta_{m_3^2}^{(1)} = 2 \left( \left( m_{H_d}^2 + m_{H_u}^2 + m_S^2 \right) |\lambda|^2 + |T_\lambda|^2 \right) \tag{2.164}$$

$$\begin{aligned}
\beta_{m_3^2}^{(2)} = & - 2 \left( 4 \left( m_{H_d}^2 + m_{H_u}^2 + m_S^2 \right) \lambda^2 + g^2 \mu^2 \right) \lambda^{*2} - 2 g^2 \left( \lambda^2 \mu^{*2} + T_\lambda^* \left( M_B \lambda - T_\lambda \right) \right) \\
& + \lambda^* \left( g^2 \lambda \left( 2 m_{H_d}^2 + 2 m_{H_u}^2 + 4 |M_B|^2 + 8 |\mu|^2 + m_S^2 \right) - 2 \left( 8 \lambda T_\lambda^* + g^2 M_B^* \right) T_\lambda \right)
\end{aligned} \tag{2.165}$$

We see that all one-loop expressions as well as the two-loop  $\beta$ -function of the gauge coupling agree with the SUSY expressions. The remaining discrepancies at two-loop are due to the differences between  $\overline{\text{MS}}$  and  $\overline{\text{DR}}$  scheme. In order to translate the non-SUSY expressions to the  $\overline{\text{DR}}$ -scheme, we need to apply the following shifts [243]

$$g_{d,u} \rightarrow g_{d,u} \left( 1 - \frac{1}{16\pi^2} \cdot \frac{1}{8} g^2 \right), \tag{2.166}$$

$$Y_1 \rightarrow Y_1 \left( 1 + \frac{1}{16\pi^2} \cdot \frac{1}{4} g^2 \right), \tag{2.167}$$

$$Y_{2,3} \rightarrow Y_{2,3} \left( 1 - \frac{1}{16\pi^2} \cdot \frac{1}{8} g^2 \right), \tag{2.168}$$

$$\lambda_3 \rightarrow \lambda_3 - \frac{1}{16\pi^2} \cdot \frac{1}{4} g^4, \tag{2.169}$$

$$\lambda_{4,5} \rightarrow \lambda_{4,5} - \frac{1}{16\pi^2} \cdot \frac{1}{8} g^4, \tag{2.170}$$

$$M_2 \rightarrow M_2 \left( 1 + \frac{1}{16\pi^2} \cdot \frac{1}{4} g^2 \right), \tag{2.171}$$

which have to be applied to the expressions of the one-loop  $\beta$  functions to obtain the corresponding two-loop shifts. In addition, one must take into account that for the quartic couplings and the Yukawa couplings an additional shift appears ‘on the left hand side’ of the expression, e.g.

$$\beta_Y^{\overline{\text{DR}}} = \frac{d}{dt} Y^{\overline{\text{DR}}} = \frac{d}{dt} \left( Y^{\overline{\text{MS}}} \left( 1 + \frac{c}{16\pi^2} g^2 \right) \right) = \beta_Y^{\overline{\text{MS}}} \left( 1 + \frac{c}{16\pi^2} g^2 \right) + 2 g Y^{\overline{\text{MS}}} \frac{c}{16\pi^2} \beta_g \tag{2.172}$$

with some coefficient  $c$  depending on the charges of the involved fields.

We find the following shifts for the different couplings:

$$\Delta \lambda_1 = -\frac{1}{2} g^2 |\lambda|^4 - \frac{9}{4} g^4 |\lambda|^2 \tag{2.173}$$

$$\Delta\lambda_3 = \frac{15}{8}g^6 - \frac{21}{4}g^4|\lambda|^2 + g^2|\lambda|^4 \quad (2.174)$$

$$\Delta\lambda_4 = \frac{1}{16}g^6 - \frac{9}{8}g^4|\lambda|^2 + g^2|\lambda|^4 \quad (2.175)$$

$$\Delta g_d = -\frac{3}{16}g^5 + \frac{3}{8}g^3|\lambda|^2 \quad (2.176)$$

$$\Delta Y_1 = \frac{3}{4}g^2\lambda|\lambda|^2 - \frac{3}{8}g^4\lambda \quad (2.177)$$

$$\Delta Y_2 = \frac{3}{16}g^4\lambda - \frac{3}{8}g^2\lambda|\lambda|^2 \quad (2.178)$$

$$\Delta M_1 = -\frac{1}{8}g^4 M_B \quad (2.179)$$

$$\Delta M_2 = \frac{1}{4}g^2\mu|\lambda|^2 - \frac{3}{8}g^4\mu \quad (2.180)$$

$$\Delta T_1 = -\frac{1}{4}g^2\lambda\left(4|\lambda|^2 + 9g^2\right)\mu^* \quad (2.181)$$

$$\Delta T_3 = -\frac{3}{4}g^4 T_\lambda \quad (2.182)$$

$$\Delta B = -\frac{1}{4}Bg^2\left(2|\lambda|^2 + 3g^2\right) \quad (2.183)$$

$$\Delta m_1^2 = -\frac{1}{4}g^2\left(-2g^2|M_B|^2 + 2|\lambda|^2\left(3|\mu|^2 + m_{H_d}^2\right) + g^2\left(2m_{H_u}^2 + 5m_{H_d}^2 + 9|\mu|^2\right)\right) \quad (2.184)$$

$$\Delta m_2^2 = -\frac{1}{4}g^2\left(-2g^2|M_B|^2 + 2|\lambda|^2\left(3|\mu|^2 + m_{H_u}^2\right) + g^2\left(2m_{H_d}^2 + 5m_{H_u}^2 + 9|\mu|^2\right)\right) \quad (2.185)$$

$$\Delta m_3^2 = g^2\left(2\lambda^2\mu^{*2} + 2\mu^2(\lambda^*)^2 + |\lambda|^2\left(-8|\mu|^2 + m_S^2\right)\right) \quad (2.186)$$

This gives a complete agreement between the two-loop  $\beta$ -functions of both calculations. Thus, our revised results for the RGEs of a general quantum field theory are confirmed.

## 2.7 Numerical impact

### 2.7.1 Running of fermion mass terms

We briefly want to discuss the numerical impact on the changes in the  $\beta$ -function for the fermion mass term. Differences in the running will only appear in models in which the Lagrangian contains fermionic terms

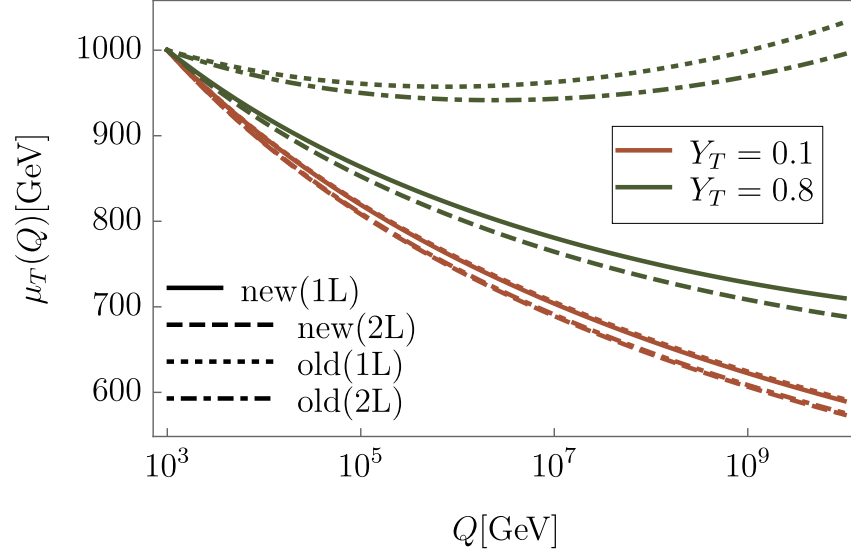
$$\mathcal{L} \supset Y S f_1 f_2 + \mu f_1 f_2 + \text{h.c.} \quad (2.187)$$

with a Yukawa-like coupling  $Y$  between two Weyl fermions  $f_1, f_2$  and a scalar  $S$  as well as a fermion mass term  $\mu$ . Both terms can only be present if  $S$  is a gauge singlet and if  $f_1, f_2$  form a vector-like fermion pair. As concrete example, we consider the case of heavy top-like states and a real singlet, i.e.

$$T' : (\mathbf{3}, \mathbf{1})_{-\frac{1}{3}}, \quad (2.188)$$

$$\bar{T}' : (\bar{\mathbf{3}}, \mathbf{1})_{\frac{1}{3}}, \quad (2.189)$$

$$S : (\mathbf{1}, \mathbf{1})_0, \quad (2.190)$$



**Figure 2.2:** The running mass  $\mu_T$  of the vector-like top partners at one- and two-loop level for two different choices of the Yukawa coupling  $Y_T$ . Here, we show the results using the incorrect ('old') expressions in literature as well as our derived expressions ('new'). The other parameters are set to  $\lambda_{HS} = 0$ ,  $\lambda_S = 1$ ,  $\kappa_{HS} = \kappa = 1$  TeV.

and the potential reads

$$V = V_{SM} + \frac{1}{4}\lambda_S S^4 + \frac{1}{2}\lambda_{SH}|H|^2 S^2 + \kappa_{SH}|H|^2 S + \frac{1}{3}\kappa S^3 + \frac{1}{2}m_S^2 S^2 + (Y_T S \bar{T}' T' + \mu_T \bar{T}' T' + \text{h.c.}) . \quad (2.191)$$

The one- and two-loop  $\beta$ -functions are computed using our corrected expression and read

$$\beta_{\mu_T}^{(1)} = 2Y_T^2 \mu_T^* - \frac{2}{5}(20g_3^2 + g_1^2)\mu_T + \mu_T |Y_T|^2 , \quad (2.192)$$

$$\begin{aligned} \beta_{\mu_T}^{(2)} = & \frac{1}{450}(667g_1^4 - 240g_1^2 g_3^2 - 46600g_3^4)\mu_T + \frac{4}{15}(2g_1^2 \mu_T + 40g_3^2 \mu_T - 15\kappa Y_T)|Y_T|^2 \\ & - \frac{37}{4}\mu_T |Y_T|^4 + \frac{2}{15}Y_T^2 \left( -105|Y_T|^2 + 8(20g_3^2 + g_1^2) \right) \mu_T^* , \end{aligned} \quad (2.193)$$

while the differences compared to the old results are

$$\Delta\beta_{\mu_T}^{(1)} = -6\mu_T Y_T^2 , \quad (2.194)$$

$$\Delta\beta_{\mu_T}^{(2)} = Y_T(-2\kappa_{HS}\lambda_{HS} - \kappa_S\lambda_S + \mu_T Y_T(27Y_T^2 - 2g_1^2 - 40g_3^2) - 12\mu_T^* Y_T |Y_T|^2) . \quad (2.195)$$

The numerical impact of this difference is depicted in Fig. 2.2 where we assumed a value of 1 TeV for  $\mu_T$  at the scale  $Q = 1$  TeV and used different values  $Y_T$ . As expected from Eq. (2.194), the discrepancy between the old and new results rapidly grows with increasing  $Y_T$ . Thus, the correction in the RGEs is crucial for instance to study grand unified theories which also predict additional vector-like fermions with large Yukawa couplings to a gauge singlet.

### 2.7.2 Off-diagonal wave-function renormalisation

We now turn to the numerical impact of the off-diagonal wave-function renormalisation which is not included in the previous works. For this purpose, we consider the general Two-Higgs-Doublet-Model type-III with the following scalar potential:

$$V = m_1^2 |H_1|^2 + m_2^2 |H_2|^2 + \lambda_1 |H_1|^4 + \lambda_2 |H_2|^4 + \lambda_3 |H_1|^2 |H_2|^2 + \lambda_4 |H_2^\dagger H_1|^2 + \left( \frac{1}{2} \lambda_5 (H_2^\dagger H_1) + \lambda_6 |H_1|^2 (H_1^\dagger H_2) + \lambda_7 |H_2|^2 (H_1^\dagger H_2) - M_{12} H_1^\dagger H_2 + \text{h.c.} \right) \quad (2.196)$$

and the Yukawa interactions

$$\mathcal{L}_Y = - \left( Y_d H_1^\dagger d q + Y_e H_1^\dagger e l - Y_u H_2 u q + \epsilon_d H_2^\dagger d q + \epsilon_e H_2^\dagger e l - \epsilon_u H_1 u q + \text{h.c.} \right). \quad (2.197)$$

Due to the presence of all Yukawa interactions allowed by gauge invariance, the anomalous dimensions of the Higgs doublets  $H_1$  and  $H_2$  are no longer diagonal, but a mixing is induced proportional to  $\text{Tr}(Y_i \epsilon_i)$  with  $i = e, d, u$ . If we neglect for the moment all terms involving either the electroweak gauge couplings ( $g_1, g_2$ ), a lepton or down-quark Yukawa coupling ( $Y_d, Y_e, \epsilon_d, \epsilon_e$ ), the one-loop  $\beta$ -functions for the quartic coupling read

$$\beta_{\lambda_1}^{(1)} = 24\lambda_1^2 + 2\lambda_3^2 + 2\lambda_3\lambda_4 + \lambda_4^2 + |\lambda_5|^2 + 12|\lambda_6|^2 + 12\lambda_1 \text{Tr}(\epsilon_u \epsilon_u^\dagger) + \underline{6\text{Re}(\lambda_6)\text{Tr}(\epsilon_u Y_u^\dagger)} - 6\text{Tr}(\epsilon_u \epsilon_u^\dagger \epsilon_u \epsilon_u^\dagger), \quad (2.198)$$

$$\beta_{\lambda_2}^{(1)} = 24\lambda_2^2 + 2\lambda_3^2 + 2\lambda_3\lambda_4 + \lambda_4^2 + |\lambda_5|^2 + 12|\lambda_7|^2 + 12\lambda_2 \text{Tr}(Y_u Y_u^\dagger) + \underline{6\text{Re}(\lambda_7)\text{Tr}(\epsilon_u Y_u^\dagger)} - 6\text{Tr}(Y_u Y_u^\dagger Y_u Y_u^\dagger), \quad (2.199)$$

$$\beta_{\lambda_3}^{(1)} = 2|\lambda_5|^2 + 2\lambda_4^2 + 4\lambda_3^2 + \underline{6\text{Re}(\lambda_6 + \lambda_7)\text{Tr}(\epsilon_u Y_u^\dagger)} + 4|\lambda_7|^2 + 4|\lambda_6|^2 + 16\text{Re}(\lambda_6 \lambda_7^*) + 6\lambda_3 \text{Tr}(\epsilon_u \epsilon_u^\dagger + Y_u Y_u^\dagger) + 4(\lambda_1 + \lambda_2)(3\lambda_3 + \lambda_4) - 12\text{Tr}(\epsilon_u \epsilon_u^\dagger Y_u Y_u^\dagger), \quad (2.200)$$

$$\beta_{\lambda_4}^{(1)} = 4\lambda_4(2\lambda_3 + \lambda_1 + \lambda_2 + \lambda_4) + 8|\lambda_5|^2 + \underline{6\text{Re}(\lambda_6 + \lambda_7)\text{Tr}(\epsilon_u Y_u^\dagger)} + 2\lambda_6^*(5\lambda_6 + \lambda_7) + 2\lambda_7^*(5\lambda_7 + \lambda_6) + 6\lambda_4 \text{Tr}(\epsilon_u \epsilon_u^\dagger + Y_u Y_u^\dagger) - 12\text{Tr}(\epsilon_u Y_u^\dagger Y_u \epsilon_u^\dagger), \quad (2.201)$$

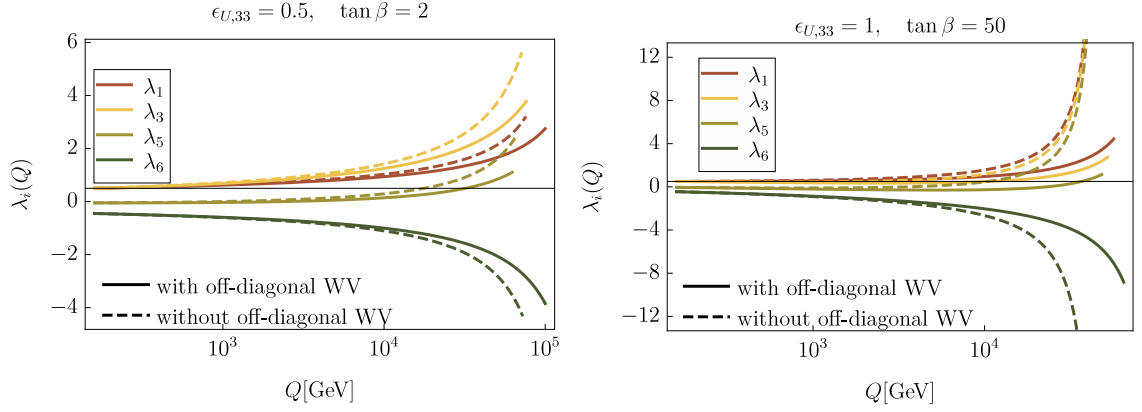
$$\beta_{\lambda_5}^{(1)} = 2\left(2(2\lambda_3 + 3\lambda_4 + \lambda_1 + \lambda_2)\lambda_5 + 5\lambda_6^{*2} + 2\lambda_6^* \lambda_7^* + 5\lambda_7^{*2} + 3(\lambda_6^* + \lambda_7^*)\text{Tr}(\epsilon_u Y_u^\dagger) + 3\lambda_5(\text{Tr}(\epsilon_u \epsilon_u^\dagger) + \text{Tr}(Y_u Y_u^\dagger)) - 6\text{Tr}(\epsilon_u Y_u^\dagger \epsilon_u Y_u^\dagger)\right), \quad (2.202)$$

$$\beta_{\lambda_6}^{(1)} = 24\lambda_1 \lambda_6 + 6\lambda_3(\lambda_6 + \lambda_7) + 4\lambda_4(2\lambda_6 + \lambda_7) + \lambda_5^*(10\lambda_6^* + 2\lambda_7^*) + 3\lambda_5^* \text{Tr}(\epsilon_u Y_u^\dagger) + \underline{3(2\lambda_1 + \lambda_3 + \lambda_4)\text{Tr}(Y_u \epsilon_u^\dagger)} + 3\lambda_6 \text{Tr}(3\epsilon_u \epsilon_u^\dagger + Y_u Y_u^\dagger) - 12\text{Tr}(\epsilon_u \epsilon_u^\dagger Y_u \epsilon_u^\dagger), \quad (2.203)$$

$$\beta_{\lambda_7}^{(1)} = 4\lambda_4 \lambda_6 + 8(3\lambda_2 + \lambda_4)\lambda_7 + 6\lambda_3(\lambda_6 + \lambda_7) + \lambda_5^*(10\lambda_7^* + 2\lambda_6^*) + 3\lambda_5^* \text{Tr}(\epsilon_u Y_u^\dagger) + \underline{3(2\lambda_2 + \lambda_3 + \lambda_4)\text{Tr}(Y_u \epsilon_u^\dagger)} + 3\lambda_7 \text{Tr}(3Y_u Y_u^\dagger + \epsilon_u \epsilon_u^\dagger) - 12\text{Tr}(Y_u \epsilon_u^\dagger Y_u Y_u^\dagger). \quad (2.204)$$

The underlined terms stem from the off-diagonal wave-function renormalisation and are missing in the results of Refs. [182–185]. In Fig. 2.3 we show the numerical impact of the additional one-loop contributions on the running of the quartic couplings for two different points. The





**Figure 2.3:** The running of different quartic couplings in the THDM-III with and without the contributions of off-diagonal wave-function renormalisation to the  $\beta$ -functions of the quartic couplings. Here, we have used the input parameters  $\lambda_1 = \lambda_3 = \lambda_4 = 0.5$ ,  $\lambda_5 = -0.05$ ,  $\lambda_6 = \lambda_7 = -0.45$ ,  $\tan \beta = 2$  and  $M_{12} = 500^2 \text{ GeV}^2$  at  $Q = m_t$ . On the left, we have used  $\epsilon_{U,33} = 0.5$ ,  $\lambda_2 = 0.5$ ,  $\tan \beta = 2$ , and on the right  $\epsilon_{U,33} = 1$ ,  $\lambda_2 = 0.15$ ,  $\tan \beta = 50$ . All other  $\epsilon_i$  are zero.

chosen sets of the quartic couplings,  $\tan \beta$  and  $M_{12}$  result in a tree-level Higgs mass of 125 GeV.<sup>6</sup> We see that the additional terms can lead to sizeable differences already for  $\epsilon_{u,33} = 0.5$  and small  $\tan \beta = 2$ . This is due to  $\text{Tr}(\epsilon_u Y_u^\dagger)$ . When increasing  $\epsilon_{u,33}$  to 1 and  $\tan \beta = 50$ , one obtains  $\text{Tr}(\epsilon_u Y_u^\dagger) \simeq 1$  and the impact on the running couplings is tremendous.

Of course, there are also differences at the two-loop level. Those read within the same approximation:

$$\begin{aligned} \Delta\beta_{\lambda_1}^{(2)} = & \frac{1}{4}(6\lambda_5^*\lambda_6^{*2} + 6\lambda_6((2\lambda_2 + \lambda_3 + \lambda_4)\lambda_7^* + \lambda_5(\lambda_6 + \lambda_7)) \\ & + \lambda_6\epsilon_t Y_t(-27\epsilon_u^2 - 27Y_u^2 + 80g_3^2) + \lambda_6^*(12\lambda_2\lambda_7 + 24\lambda_1\lambda_6 - 27\epsilon_u^3 Y_t - 27\epsilon_t Y_u^3 \\ & + 6(\lambda_3 + \lambda_4)(2\lambda_6 + \lambda_7) + 6\lambda_5^*\lambda_7^* + 80\epsilon_t g_3^2 Y_t)), \end{aligned} \quad (2.205)$$

$$\begin{aligned} \Delta\beta_{\lambda_2}^{(2)} = & \frac{1}{4}(\lambda_7(6\lambda_5(\lambda_6 + \lambda_7) + \epsilon_t Y_t(-27\epsilon_u^2 - 27Y_u^2 + 80g_3^2)) \\ & + 6\lambda_6^*((2\lambda_1 + \lambda_3 + \lambda_4)\lambda_7 + \lambda_5^*\lambda_7^*) + \lambda_7^*(12\lambda_1\lambda_6 + 24\lambda_2\lambda_7 - 27\epsilon_u^3 Y_t - 27\epsilon_t Y_u^3 \\ & + 6(\lambda_3 + \lambda_4)(2\lambda_7 + \lambda_6) + 6\lambda_5^*\lambda_7^* + 80\epsilon_t g_3^2 Y_t)), \end{aligned} \quad (2.206)$$

$$\begin{aligned} \Delta\beta_{\lambda_3}^{(2)} = & \frac{1}{4}((\lambda_6 + \lambda_7)(6\lambda_5(\lambda_6 + \lambda_7) + \epsilon_t Y_t(-27\epsilon_u^2 - 27Y_u^2 + 80g_3^2)) + 6\lambda_5^*\lambda_6^{*2} + 6\lambda_5^*\lambda_7^{*2} \\ & + 12(\lambda_5^*\lambda_6^*\lambda_7^* + (2\lambda_2 + \lambda_3 + \lambda_4)(|\lambda_7|^2 + |\lambda_6|^2) + 2(\lambda_1 + \lambda_2 + \lambda_3 + \lambda_4)\text{Re}(\lambda_7^*\lambda_6)) \\ & + (\lambda_7^* + \lambda_6^*)(-27\epsilon_u^3 Y_t - 27\epsilon_t Y_u^3 + 80\epsilon_t g_3^2 Y_t)), \end{aligned} \quad (2.207)$$

$$\begin{aligned} \Delta\beta_{\lambda_4}^{(2)} = & \frac{1}{4}((\lambda_6 + \lambda_7)(6\lambda_5(\lambda_6 + \lambda_7) + \epsilon_t Y_t(-27\epsilon_u^2 - 27Y_u^2 + 80g_3^2)) + 6\lambda_5^*\lambda_6^{*2} + 6\lambda_5^*\lambda_7^{*2} \\ & + 12(\lambda_5^*\lambda_6^*\lambda_7^* + (2\lambda_2 + \lambda_3 + \lambda_4)(|\lambda_7|^2 + |\lambda_6|^2) + 2(\lambda_1 + \lambda_2 + \lambda_3 + \lambda_4)\text{Re}(\lambda_7^*\lambda_6)) \\ & + (\lambda_7^* + \lambda_6^*)(-27\epsilon_u^3 Y_t - 27\epsilon_t Y_u^3 + 80\epsilon_t g_3^2 Y_t)), \end{aligned} \quad (2.208)$$

<sup>6</sup>While it is in principle possible to renormalise the Higgs sector of the THDM-III on-shell, large radiative corrections can occur when extracting the  $\overline{\text{MS}}$  parameters which enter the RGEs [244]. Therefore, the given example is meant as an illustration on the difference in the running, but the input parameters in the running will change when including those corrections.

$$\Delta\beta_{\lambda_5}^{(2)} = \frac{1}{2}(\lambda_6^* + \lambda_7^*)(6(2\lambda_1 + \lambda_3 + \lambda_4)\lambda_6^* + 6(2\lambda_2 + \lambda_3 + \lambda_4)\lambda_7^* + 6\lambda_5(\lambda_6 + \lambda_7) + \epsilon_t Y_t(-27\epsilon_u^2 - 27Y_u^2 + 80g_3^2)), \quad (2.209)$$

$$\Delta\beta_{\lambda_6}^{(2)} = \frac{1}{4}((2\lambda_1 + \lambda_3 + \lambda_4)(12(\lambda_1\lambda_6 + \lambda_2\lambda_7) - 27(\epsilon_u^3 Y_t + \epsilon_t Y_u^3) + 6(\lambda_3 + \lambda_4)(\lambda_6 + \lambda_7) + 80\epsilon_t g_3^2 Y_t) + \lambda_5^*(12(2\lambda_1 + \lambda_3 + \lambda_4)\lambda_6^* + 12(\lambda_1 + \lambda_2 + \lambda_3 + \lambda_4)\lambda_7^* + 6\lambda_5(\lambda_6 + \lambda_7) + \epsilon_t Y_t(-27(\epsilon_u^2 + Y_u^2) + 80g_3^2))), \quad (2.210)$$

$$\Delta\beta_{\lambda_7}^{(2)} = \frac{1}{4}(6\lambda_5^*\lambda_6^{*,2} + \lambda_6(6(2\lambda_2 + \lambda_3 + \lambda_4)\lambda_7^* + 6\lambda_5(\lambda_6 + \lambda_7) + \epsilon_t Y_t(-27(\epsilon_u^2 + Y_u^2) + 80g_3^2)) + \lambda_6^*(12\lambda_2\lambda_7 + 24\lambda_1\lambda_6 - 27(\epsilon_u^3 Y_t + \epsilon_t Y_u^3) + 6(\lambda_3 + \lambda_4)(2\lambda_6 + \lambda_7) + 6\lambda_5^*\lambda_7^* + 80\epsilon_t g_3^2 Y_t)). \quad (2.211)$$

## 2.8 Conclusions

In this paper, we have revisited the general RGEs with the goal to present the current state-of-the-art and to correct some mistakes in the literature. In particular, the known expressions for the scalar quartic couplings [184,185] assume a diagonal wave-function renormalisation which is not appropriate for models with mixing in the scalar sector. We therefore have corrected/generalized the expressions for the  $\beta$ -functions of the quartic couplings in (2.24) and (2.25). While finalizing this work, a related paper appeared on the arxiv [245] which confirms our findings concerning the couplings in the scalar sector. Furthermore, we have carefully re-examined the dummy field method and have provided a detailed description of it, which has so far been missing in the literature. We then have used this method to re-derive the  $\beta$ -functions for the dimensionful parameters (fermion masses, scalar masses, and the cubic scalar couplings). For cubic scalar couplings and scalar masses, the only differences to Ref. [185] are due to the aforementioned off-diagonal wave-function renormalisation. However, discrepancies for the fermion mass  $\beta$ -functions in [185] have been found and reconciled in (2.55) and (2.56). We have also performed an independent cross-check of our results using well-tested supersymmetric RGEs and we find complete agreement.

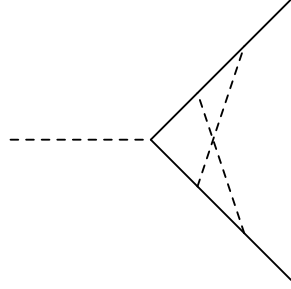
We have illustrated the numerical impact on the changes in the  $\beta$ -function for the fermion mass terms using a toy model with a heavy vector-like fermion pair coupled to a scalar gauge singlet. Unsurprisingly, the correction to the running of the fermion mass rapidly grows with increasing Yukawa coupling. Thus it is crucial to use the corrected RGEs if one wants to study for instance grand unified theories which predict additional vector-like fermions with large Yukawa couplings to a gauge singlet. In addition, we have demonstrated the importance of the correction to the  $\beta$ -functions of the scalar quartic couplings using a general type-III Two-Higgs-Doublet-Model. As can be seen in Fig. 2.3 the corrections to the running couplings are non-negligible and can become very large in certain regions of the parameter space.

All the corrected expressions have been implemented in updated versions of the Mathematica package SARAH and the Python package PyR@TE. We hope that this paper will be a useful resource in which all the relevant information on the two-loop  $\beta$ -functions is at hand in one place.

## 2.9 Appendix: Dummy field method at two-loop

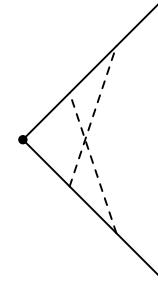
In this appendix, we list all two-loop vertex corrections which are needed to obtain the  $\beta$  functions for dimensionful parameters.

### 2.9.1 Fermion mass

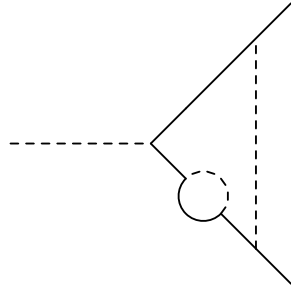


$$Y^c Y^{\dagger b} Y^a (Y^{\dagger c} Y^b - Y^{\dagger b} Y^c)$$

→

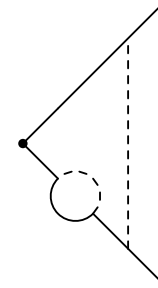


$$Y^c Y^{\dagger b} m_f (Y^{\dagger c} Y^b - Y^{\dagger b} Y^c) \quad (2.212)$$

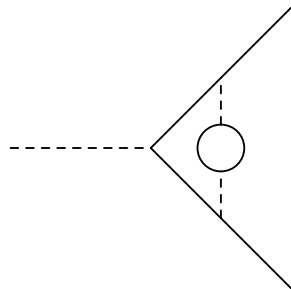


$$Y^b (Y_2(F) Y^{\dagger a} + Y^{\dagger a} Y_2^{\dagger}(F)) Y^b$$

→

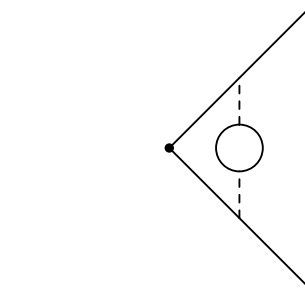


$$Y^b (Y_2(F) m_f^{\dagger} + m_f^{\dagger} Y_2^{\dagger}(F)) Y^b \quad (2.213)$$



$$Y_2^{bc}(S) Y^b Y^{\dagger a} Y^c$$

→



$$Y_2^{bc}(S) Y^b m_f^{\dagger} Y^c \quad (2.214)$$

Diagrammatic equation (2.215) showing the replacement of a vertex with a triangle loop by a vertex with a triangle loop and a horizontal dashed line.

$$\lambda_{abcd} Y^b Y^{\dagger c} Y^d \quad \rightarrow \quad h_{abc} Y^a Y^{\dagger b} Y^c \quad (2.215)$$

Diagrammatic equation (2.216) showing the replacement of a vertex with a triangle loop and a wavy line by a vertex with a triangle loop and a wavy line, with a black dot at the vertex.

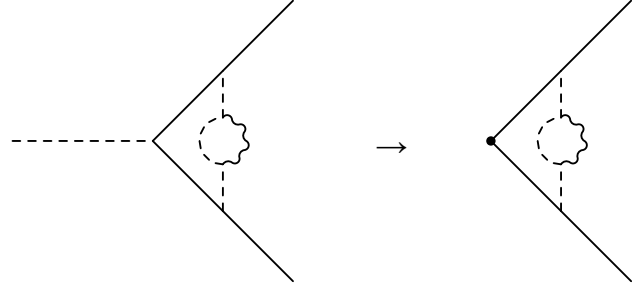
$$g^2 \{C_2(F), Y^b Y^{\dagger a} Y^b\} \quad \rightarrow \quad g^2 \{C_2(F), Y^b m_f Y^b\} \quad (2.216)$$

Diagrammatic equation (2.217) showing the replacement of a vertex with a triangle loop and a wavy line by a vertex with a triangle loop and a wavy line, with a black dot at the vertex.

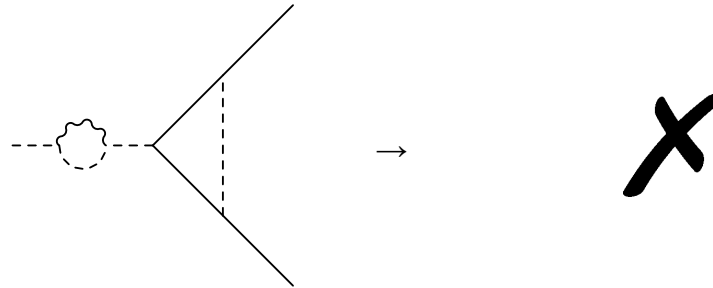
$$g^2 Y^b \{C_2(F), Y^{\dagger a}\} Y^b \quad \rightarrow \quad g^2 Y^b \{C_2(F), m_f^{\dagger}\} Y^b \quad (2.217)$$

Diagrammatic equation (2.218) showing the replacement of a vertex with a triangle loop and a wavy line by a vertex with a triangle loop and a wavy line, with a black dot at the vertex.

$$g^2 H_{2t}^a = g^2 (t^{A*} Y^a Y^{\dagger b} t^{A*} Y^b + Y^b t^A Y^{\dagger b} Y^a t^A) \quad \rightarrow \quad g^2 (t^{A*} m_f Y^{\dagger b} t^{A*} Y^b + Y^b t^A Y^{\dagger b} m_f t^A) \quad (2.218)$$



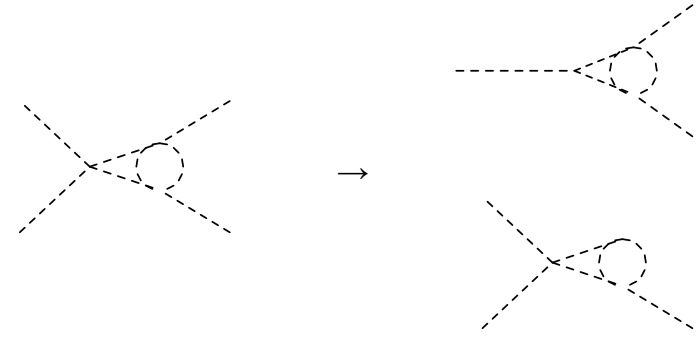
$$g^2 C_2^{bc}(S) Y^b Y^{\dagger a} Y^c \quad \rightarrow \quad g^2 C_2^{bc}(S) Y^b m_f^{\dagger} Y^c \quad (2.219)$$



$$g^2 C_2^{ac} Y^b Y^{\dagger c} Y^b \quad \rightarrow \quad 0 \quad (2.220)$$

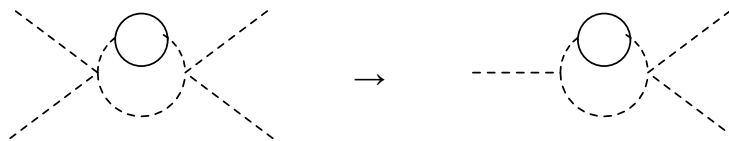
### 2.9.2 Cubic scalar coupling

#### 1. Scalar-only contributions:



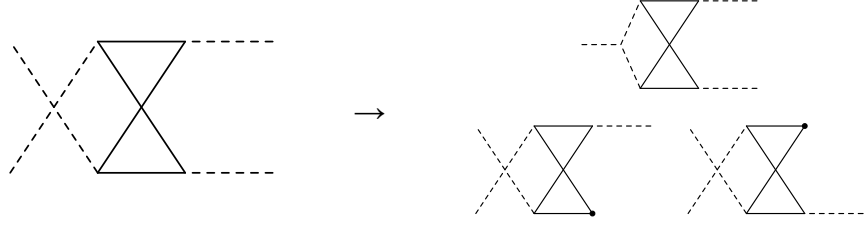
$$\bar{\Lambda}_{abcd}^3 = \frac{1}{4} \sum_{per} \lambda_{abef} \lambda_{cegh} \lambda_{dfgh} \quad \bar{\Lambda}_{abc}^3 = \frac{1}{2} \sum_{per} [h_{aef} \lambda_{begh} \lambda_{cfgh} + \lambda_{abef} \lambda_{cegh} h_{fgh}] \quad (2.221)$$

#### 2. Scalar-Fermion contributions:



$$\bar{\Lambda}_{abcd}^{2Y} = \frac{1}{8} \sum_{per} Y_2^{fg}(S) \lambda_{abef} \lambda_{cdeg}$$

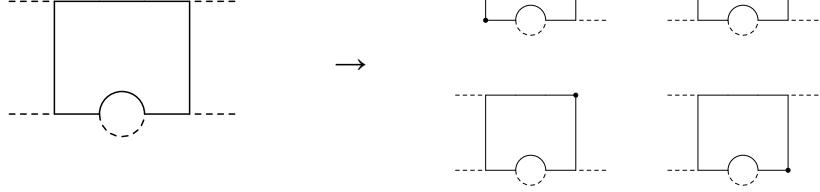
$$\bar{\Lambda}_{abc}^{2Y} = \frac{1}{2} \sum_{per} Y_2^{fg}(S) \lambda_{abef} h_{ceg} \quad (2.222)$$



$$\bar{H}_{abcd}^{\lambda} = \frac{1}{8} \sum_{per} \lambda_{abef} \text{Tr}(Y^c Y^{\dagger e} Y^d Y^{\dagger f} + Y^{\dagger c} Y^e Y^{\dagger d} Y^f)$$

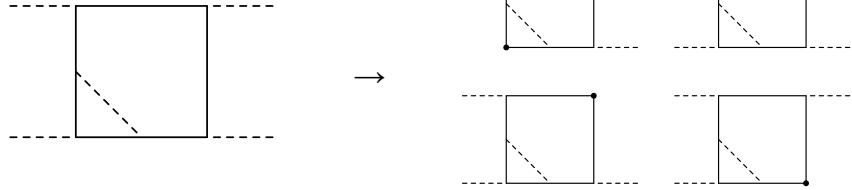
$$\begin{aligned} \bar{H}_{abc}^h + \bar{H}_{abc}^{\lambda m} = & \frac{1}{4} \sum_{per} h_{aef} \text{Tr}(Y^b Y^{\dagger e} Y^c Y^{\dagger f} \\ & + Y^{\dagger b} Y^e Y^{\dagger c} Y^f) + \\ & \frac{1}{4} \sum_{per} \lambda_{abef} \text{Tr}(m_f Y^{\dagger e} Y^c Y^{\dagger f} \\ & + Y^{\dagger c} Y^e m_f^{\dagger} Y^f) \end{aligned}$$

(2.223)



$$H_{abcd}^Y = \sum_{per} \text{Tr}(Y_2(F) Y^{\dagger a} Y^b Y^{\dagger c} Y^d)$$

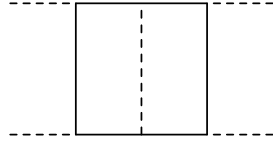
$$\begin{aligned} H_{abc}^Y = \sum_{per} \text{Tr} \Big( & Y_2(F) [m_f^{\dagger} Y^a Y^{\dagger b} Y^c \\ & + Y^{\dagger a} m_f Y^{\dagger b} Y^c + Y^{\dagger a} Y^b m_f^{\dagger} Y^c \\ & + Y^{\dagger a} Y^b Y^{\dagger c} m_f] \Big) \end{aligned} \quad (2.224)$$



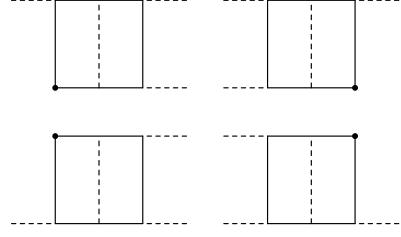
$$\bar{H}_{abcd}^Y = \sum_{per} \frac{1}{2} \text{Tr}(Y^e Y^{\dagger a} Y^e Y^{\dagger b} Y^c Y^{\dagger d} + Y^{\dagger e} Y^a Y^{\dagger e} Y^{\dagger b} Y^{\dagger c} Y^d)$$

$$\begin{aligned} \bar{H}_{abc}^Y = & \frac{1}{2} \sum_{per} \text{Tr}(Y^e m_f^{\dagger} Y^e Y^{\dagger a} Y^b Y^{\dagger c} + \\ & Y^e Y^{\dagger a} Y^e m_f^{\dagger} Y^b Y^{\dagger c} \\ & + Y^e Y^{\dagger a} Y^e Y^{\dagger b} m_f^{\dagger} Y^{\dagger c} + \\ & Y^e Y^{\dagger a} Y^e Y^{\dagger b} Y^c m_f^{\dagger} + \text{h.c.}) \end{aligned}$$

(2.225)



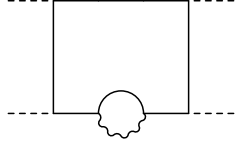
→



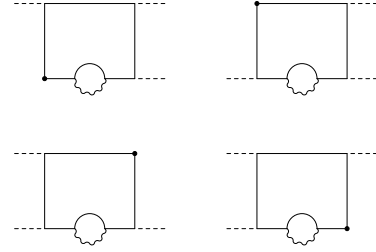
$$H_{abcd}^3 = \frac{1}{2} \sum_{per} \text{Tr}(Y^a Y^{\dagger b} Y^e Y^{\dagger c} Y^d Y^{\dagger e})$$

$$H_{abc}^a = \frac{1}{2} \sum_{per} \text{Tr}(m_f Y^{a\dagger} Y^e Y^{\dagger b} Y^c Y^{\dagger e} + Y^a m_f^{\dagger} Y^e Y^{\dagger b} Y^c Y^{\dagger e} + Y^a Y^{\dagger b} Y^e m_f^{\dagger} Y^c Y^{\dagger e} + Y^a Y^{\dagger b} Y^e Y^{\dagger c} m_f Y^{\dagger e})$$

(2.226)



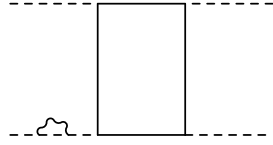
→



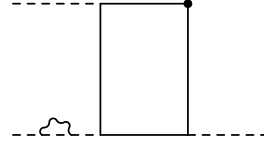
$$H_{abcd}^F = \sum_{per} \text{Tr}(\{C_2(F), Y^a\} Y^{\dagger b} Y^c Y^{\dagger d})$$

$$H_{abc}^F = \sum_{per} \text{Tr}(\{C_2(F), m_f\} Y^{a\dagger} Y^b Y^{\dagger c} + \{C_2(F), Y^a\} m_f^{\dagger} Y^b Y^{\dagger c} + \{C_2(F), Y^a\} Y^{\dagger b} m_f Y^{\dagger c} + \{C_2(F), Y^a\} Y^{\dagger b} Y^c m_f^{\dagger})$$

(2.227)



→

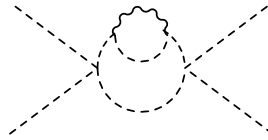


$$H_{abcd}^S = \sum_i C_2(i) H_{abcd}$$

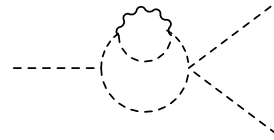
$$H_{abc}^S = \sum_i C_2(i) H_{abc}$$

(2.228)

### 3. Scalar-Vector contributions



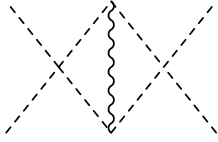
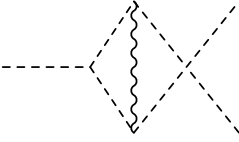
→



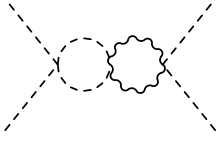
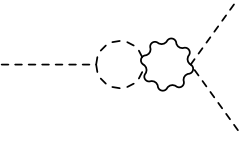
$$\bar{\Lambda}_{abcd}^{2S} = \frac{1}{8} \sum_{per} C_2^{fg}(S) \lambda_{abef} \lambda_{cdeg}$$

$$\bar{\Lambda}_{abc}^{2S} = \frac{1}{2} \sum_{per} C_2^{fg}(S) h_{aef} \lambda_{bceg}$$

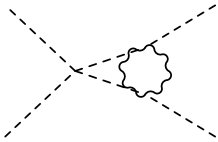
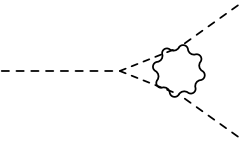
(2.229)


→


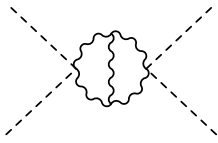

$$\bar{\Lambda}_{abcd}^{2g} = \frac{1}{8} \sum_{per} \lambda_{abef} \lambda_{cdgh} \theta_{eg}^A \theta_{fh}^A \quad \bar{\Lambda}_{abc}^{2g} = \frac{1}{2} \sum_{per} h_{aef} \lambda_{bcgh} \theta_{eg}^A \theta_{fh}^A \quad (2.230)$$


→


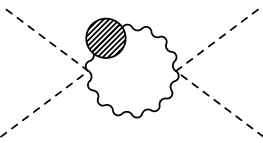

$$A_{abcd}^{\lambda} = \frac{1}{4} \sum_{per} \lambda_{abef} \{\theta^A, \theta^B\}_{ef} \{\theta^A, \theta^B\}_{cd} \quad A_{abc}^{\lambda} = \frac{1}{2} \sum_{per} h_{aef} \{\theta^A, \theta^B\}_{ef} \{\theta^A, \theta^B\}_{bc} \quad (2.231)$$


→


$$\bar{A}_{abcd}^{\lambda} = \frac{1}{4} \sum_{per} \lambda_{abef} \{\theta^A, \theta^B\}_{ce} \{\theta^A, \theta^B\}_{df} \quad \bar{A}_{abc}^{\lambda} = \frac{1}{2} \sum_{per} h_{aef} \{\theta^A, \theta^B\}_{be} \{\theta^A, \theta^B\}_{cf} \quad (2.232)$$

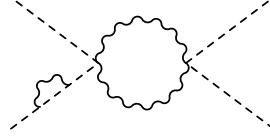

→


$$A_{abcd}^g = \frac{1}{8} f^{ACE} f^{BDE} \sum_{per} \{\theta^A, \theta^B\}_{ab} \{\theta^C, \theta^D\}_{cd} \quad 0 \quad (2.233)$$


→


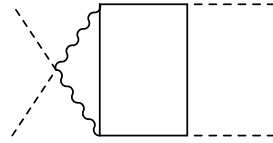
$$XA_{abcd} = X \{\theta^A, \theta^B\}_{ab} \{\theta^A, \theta^B\}_{cd} \quad 0 \quad (2.234)$$





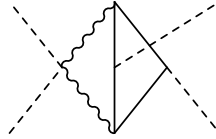
$$A_{abcd}^S = \sum_i C_2(i) \{\theta^A, \theta^B\}_{ab} \{\theta^A, \theta^B\}_{cd} = 0 \quad (2.235)$$

#### 4. Scalar-Fermion-Vector contributions



$$B_{abcd}^Y = \frac{1}{4} \sum_{per} \{\theta^A, \theta^B\}_{ab} \text{Tr}(t^{A*} t^{B*} Y^c Y^{\dagger d} + Y^c t^A t^B Y^{\dagger d})$$

$$B_{abc}^Y = \frac{1}{4} \sum_{per} \{\theta^A, \theta^B\}_{ab} \text{Tr}(t^{A*} t^{B*} m_f Y^{\dagger c} + m_f t^A t^B Y^{\dagger c} + t^{A*} t^{B*} Y^c m_f^{\dagger} + Y^c t^A t^B m_f^{\dagger}) \quad (2.236)$$

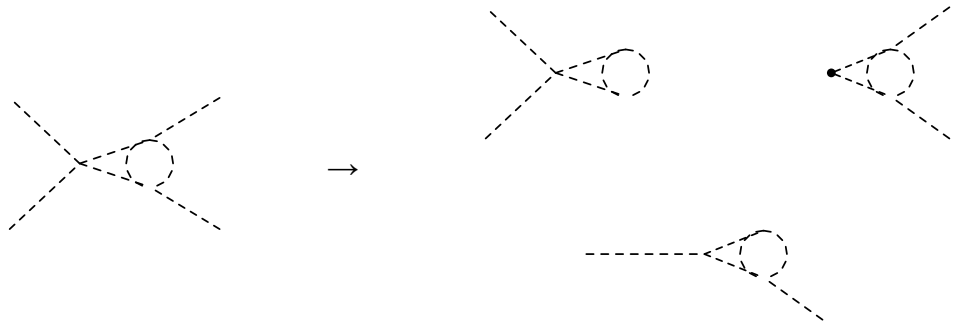


$$\bar{B}_{abcd}^Y = \frac{1}{4} \sum_{per} \{\theta^A, \theta^B\}_{ab} \text{Tr}(t^{A*} Y^c t^B Y^{\dagger d})$$

$$\bar{B}_{abc}^Y = \frac{1}{4} \sum_{per} \{\theta^A, \theta^B\}_{ab} \text{Tr}(t^{A*} m_f t^B Y^{\dagger c} + t^{A*} Y^c t^B m_f^{\dagger}) \quad (2.237)$$

### 2.9.3 Bilinear scalar

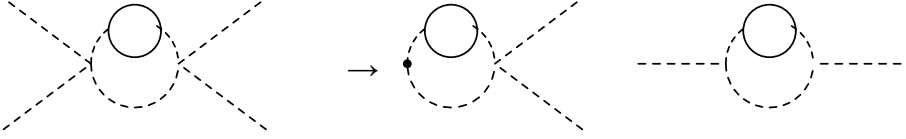
#### 1. Scalar-only contributions:



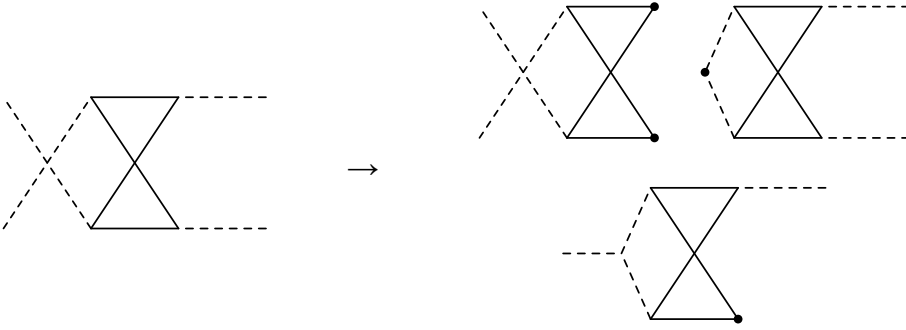
$$\bar{\Lambda}_{abcd}^3 = \frac{1}{4} \sum_{per} \lambda_{abef} \lambda_{cegh} \lambda_{dfgh}$$

$$\bar{\Lambda}_{ab}^3 = \lambda_{abef} h_{egl} h_{fgl} + 2m_{ef}^2 \lambda_{aegl} \lambda_{bfgl} + 2 \sum_{per} h_{aef} h_{fgl} \lambda_{begl} \quad (2.238)$$

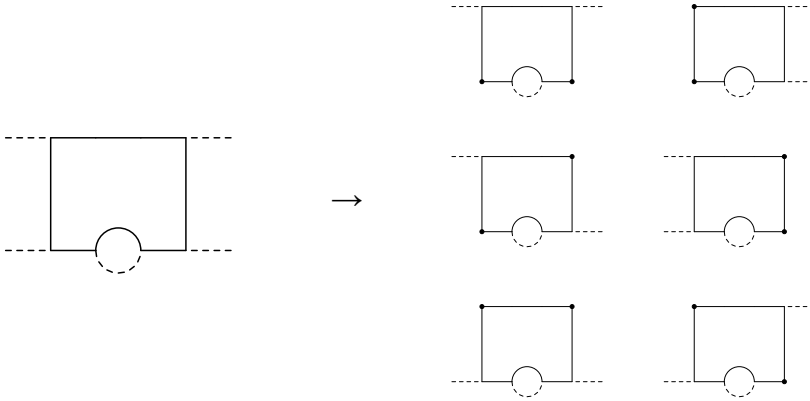
## 2. Scalar-Fermion contributions:



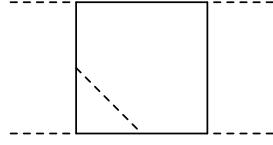
$$\bar{\Lambda}_{abcd}^{2Y} = \frac{1}{8} \sum_{per} Y_2^{fg}(S) \lambda_{abef} \lambda_{cdeg} \quad \bar{\Lambda}_{ab}^{2Y} = 2Y_2^{fg}(S)(m_{eg}^2 \lambda_{abef} + h_{aef} h_{beg}) \quad (2.239)$$



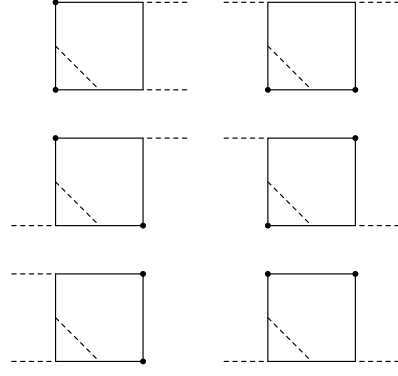
$$\bar{H}_{abcd}^{\lambda} = \frac{1}{8} \sum_{per} \lambda_{abef} \text{Tr}(Y^c Y^{\dagger e} Y^d Y^{\dagger f} + Y^{\dagger c} Y^e Y^{\dagger d} Y^f) \quad \bar{H}_{ab}^{\lambda} = \frac{1}{2} \lambda_{abef} \text{Tr}(m_f Y^{\dagger e} m_f Y^{\dagger f} + \text{h.c.}) + m_{ef}^2 \text{Tr}(Y^a Y^{\dagger e} Y^b Y^{\dagger f} + \text{h.c.}) + \sum_{per} h_{aef} \text{Tr}(Y^b Y^{\dagger e} m_f Y^{\dagger f} + \text{h.c.}) \quad (2.240)$$



$$H_{abcd}^Y = \sum_{per} \text{Tr}(Y_2(F) Y^{\dagger a} Y^b Y^{\dagger c} Y^d) \quad H_{ab}^Y = 2 \sum_{per} \left[ \text{Tr}(\{Y_2(F), m_f^{\dagger} m_f\} Y^{\dagger a} Y^b) + \text{Tr}(Y_2(F) Y^{\dagger a} m_f (Y^{\dagger b} m_f + m_f^{\dagger} Y^b) + Y_2(F) m_f^{\dagger} Y^a (Y^{\dagger b} m_f + m_f^{\dagger} Y^b)) \right] \quad (2.241)$$



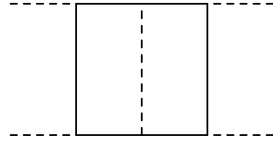
→



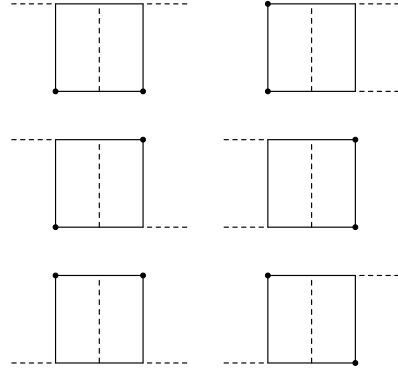
$$\begin{aligned} \bar{H}_{abcd}^Y = & \sum_{per} \frac{1}{2} \text{Tr}(Y^e Y^{\dagger a} Y^e Y^{\dagger b} Y^c Y^{\dagger d} \\ & + Y^{\dagger e} Y^a Y^{\dagger e} Y^b Y^{\dagger c} Y^d) \end{aligned}$$

$$\begin{aligned} \bar{H}_{ab}^Y = \sum_{per} \left[ \text{Tr} \left( Y^e Y^{\dagger a} Y^e Y^{\dagger b} m_f^{\dagger} m_f^{\dagger} + \right. \right. \\ \left. \left. Y^e m_f^{\dagger} Y^e m_f^{\dagger} Y^a Y^{\dagger b} + \right. \right. \\ \left. \left. (Y^e Y^{\dagger a} Y^e m_f^{\dagger} + Y^e m_f^{\dagger} Y^e Y^{\dagger a}) \times \right. \right. \\ \left. \left. (Y^b m_f^{\dagger} + m_f^{\dagger} Y^{\dagger b}) + \text{h.c.} \right) \right] \end{aligned}$$

(2.242)



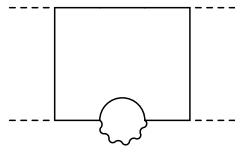
→



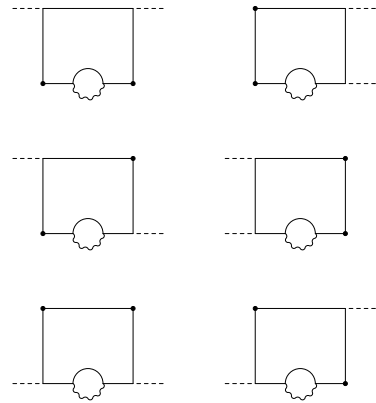
$$H_{abcd}^3 = \frac{1}{2} \sum_{per} \text{Tr}(Y^a Y^{\dagger b} Y^e Y^{\dagger c} Y^d Y^{\dagger e})$$

$$\begin{aligned} H_{ab}^3 = \sum_{per} \left[ \text{Tr} \left( Y^a Y^{\dagger b} Y^e m_f^{\dagger} m_f^{\dagger} Y^{\dagger e} \right. \right. \\ \left. \left. + m_f^{\dagger} m_f^{\dagger} Y^e Y^{\dagger a} Y^b Y^{\dagger e} \right. \right. \\ \left. \left. Y^a m_f^{\dagger} Y^e (Y^{\dagger b} m_f^{\dagger} + m_f^{\dagger} Y^b) Y^{\dagger e} \right. \right. \\ \left. \left. + m_f^{\dagger} Y^{\dagger a} Y^e (Y^{\dagger b} m_f^{\dagger} + m_f^{\dagger} Y^b) Y^{\dagger e} \right) \right] \end{aligned}$$

(2.243)

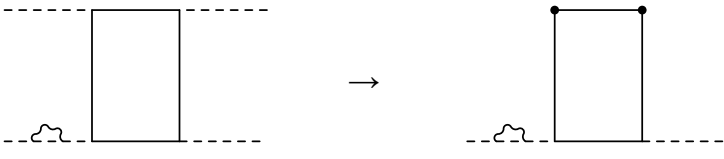


→



$$\begin{aligned}
H_{abcd}^F &= \sum_{per} \text{Tr}(\{C_2(F), Y^a\} Y^{\dagger b} Y^c Y^{\dagger d}) \\
H_{ab}^F &= 2 \sum_{per} \text{Tr} \left[ \{C_2(F), m_f\} Y^{a\dagger} (Y^b m_f^\dagger + \text{h.c.}) \right. \\
&\quad + \{C_2(F), Y^a\} m_f^\dagger (Y^b m_f^\dagger + \text{h.c.}) \\
&\quad + \{C_2(F), Y^a\} Y^{\dagger b} m_f m_f^\dagger \\
&\quad \left. + \{C_2(F), m_f\} m_f^\dagger Y^a Y^{\dagger b} \right]
\end{aligned} \tag{2.244}$$

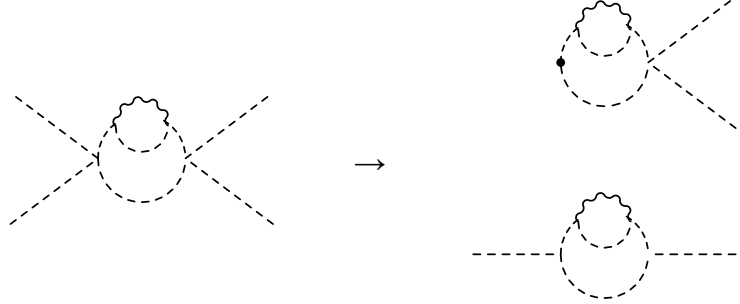
---



$$H_{abcd}^S = \sum_i C_2(i) H_{abcd} \qquad H_{ab}^S = \sum_i C_2(i) H_{ab} \tag{2.245}$$

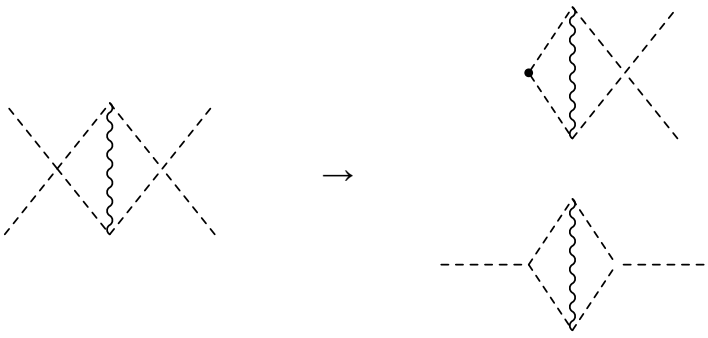

---

### 3. Scalar-Vector contributions



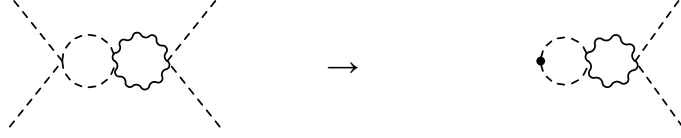
$$\begin{aligned}
\bar{\Lambda}_{abcd}^{2S} &= \frac{1}{8} \sum_{per} C_2^{fg}(S) \lambda_{abef} \lambda_{cdeg} \\
\bar{\Lambda}_{ab}^{2S} &= 2 C_2^{fg}(S) (\lambda_{abef} m_{eg}^2 + h_{aef} h_{beg})
\end{aligned} \tag{2.246}$$


---



$$\begin{aligned}
\bar{\Lambda}_{abcd}^{2g} &= \frac{1}{8} \sum_{per} \lambda_{abef} \lambda_{cdgh} \theta_{eg}^A \theta_{fh}^A \\
\bar{\Lambda}_{ab}^{2g} &= 2 (\lambda_{abef} m_{gh}^2 + h_{aef} h_{bgh}) \theta_{eg}^A \theta_{fh}^A
\end{aligned} \tag{2.247}$$

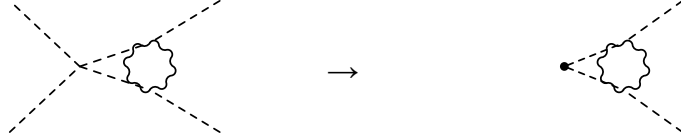

---



$$A_{abcd}^{\lambda} = \frac{1}{4} \sum_{per} \lambda_{abef} \{ \theta^A, \theta^B \}_{ef} \{ \theta^A, \theta^B \}_{cd}$$

$$A_{ab}^{\lambda} = 2m_{ef}^2 \{ \theta^A, \theta^B \}_{ef} \{ \theta^A, \theta^B \}_{ab}$$

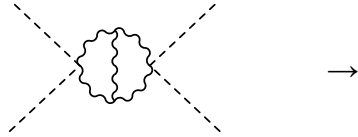
(2.248)



$$\bar{A}_{abcd}^{\lambda} = \frac{1}{4} \sum_{per} \lambda_{abef} \{ \theta^A, \theta^B \}_{ce} \{ \theta^A, \theta^B \}_{df}$$

$$\bar{A}_{ab}^{\lambda} = 2m_{ef}^2 \{ \theta^A, \theta^B \}_{ae} \{ \theta^A, \theta^B \}_{bf}$$

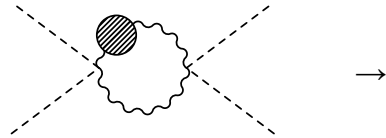
(2.249)



$$A_{abcd}^g = \frac{1}{8} f^{ACE} f^{BDE} \sum_{per} \{ \theta^A, \theta^B \}_{ab} \{ \theta^C, \theta^D \}_{cd}$$

0

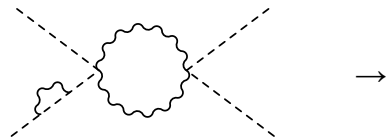
(2.250)



$$XA_{abcd} = X \{ \theta^A, \theta^B \}_{ab} \{ \theta^A, \theta^B \}_{cd}$$

0

(2.251)

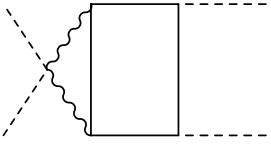


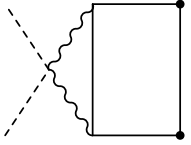
$$A_{abcd}^S = \sum_i C_2(i) \{ \theta^A, \theta^B \}_{ab} \{ \theta^A, \theta^B \}_{cd}$$

0

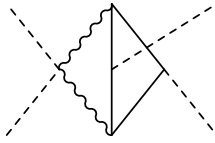
(2.252)

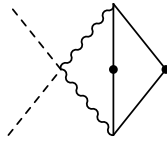
## 4. Scalar-Fermion-Vector contributions



$$B_{abcd}^Y = \frac{1}{4} \sum_{per} \{ \theta^A, \theta^B \}_{ab} \text{Tr}(t^{A*} t^{B*} Y^c Y^{\dagger d} + Y^c t^A t^B Y^{\dagger d})$$


$$B_{ab}^Y = \{ \theta^A, \theta^B \}_{ab} \text{Tr}(t^{A*} t^{B*} m_f m_f^{\dagger} + m_f t^A t^B m_f^{\dagger})$$
(2.253)



$$\bar{B}_{abcd}^Y = \frac{1}{4} \sum_{per} \{ \theta^A, \theta^B \}_{ab} \text{Tr}(t^{A*} Y^c t^B Y^{\dagger d})$$


$$\bar{B}_{abc}^Y = \{ \theta^A, \theta^B \}_{ab} \text{Tr}(t^{A*} m_f t^B m_f^{\dagger})$$
(2.254)

## 2.10 Appendix: Full two-loop RGEs

In this appendix, the full  $\beta$ -functions for all parameters of the non-supersymmetric toy model in Sec. 2.6 are listed up to two-loop order.

## 2.10.1 Gauge couplings

$$\beta_g^{(1)} = \frac{1}{2} g^3 \quad (2.255)$$

$$\beta_g^{(2)} = \frac{1}{8} g^3 \left( -2|Y_2|^2 - 2|Y_3|^2 - 4|Y_1|^2 + 6g^2 - |g_d|^2 - |g_u|^2 \right) \quad (2.256)$$

## 2.10.2 Quartic scalar couplings

$$\beta_{\lambda_4}^{(1)} = 20\lambda_4^2 + 2\lambda_4|g_d|^2 - 2|Y_2|^4 - 3g^2\lambda_4 + 4\lambda_4|Y_2|^2 - \frac{1}{2}|g_d|^4 + \frac{3}{8}g^4 + \lambda_1^2 + \lambda_3^2 \quad (2.257)$$

$$\begin{aligned} \beta_{\lambda_4}^{(2)} = & -\frac{25}{16}g^6 - 4\lambda_1^3 + \frac{5}{4}g^4\lambda_3 + 2g^2\lambda_3^2 - 4\lambda_3^3 + \frac{63}{8}g^4\lambda_4 - 10\lambda_1^2\lambda_4 - 10\lambda_3^2\lambda_4 + 28g^2\lambda_4^2 \\ & - 240\lambda_4^3 - 2\lambda_1^2|Y_1|^2 - \frac{1}{4}g^4|Y_2|^2 + \frac{5}{2}g^2\lambda_4|Y_2|^2 - 40\lambda_4^2|Y_2|^2 - 2\lambda_3^2|Y_3|^2 + 2\lambda_4|Y_2|^4 \\ & + 2|Y_1|^2|Y_2|^4 + 2|Y_3|^2|Y_2|^4 + g_d^3g_d^{*3} - 3\lambda_4Y_2|Y_1|^2Y_2^* + 8Y_2^3Y_2^{*3} \\ & + \frac{1}{4}g_dg_d^{*2} \left( 2 \left( -2g_uY_3Y_2^* + g_d\lambda_4 + g_d|Y_1|^2 + g_d|Y_3|^2 \right) + g_d|g_u|^2 \right) - 3\lambda_4Y_3|Y_2|^2Y_3^* \\ & - \frac{1}{2}g_u^* \left( 2g_u\lambda_3^2 - 2g_u|Y_2|^4 + 4g_d \left( -\lambda_4 + \lambda_3 \right) Y_2Y_3^* + |Y_2|^2 \left( 3g_u\lambda_4 + 4g_dY_2Y_3^* \right) \right) \end{aligned}$$

$$\begin{aligned}
& -\frac{1}{8}g_d^* \left( g^4 g_d - 10g^2 g_d \lambda_4 + 160g_d \lambda_4^2 + 12g_d \lambda_4 |Y_3|^2 + 16g_u \lambda_3 Y_3 Y_2^* - 16g_u \lambda_4 Y_3 Y_2^* \right. \\
& + 16g_u Y_2 Y_3 Y_2^{*2} + 4g_d |Y_1|^2 \left( 3\lambda_4 - 4Y_2 Y_2^* \right) - 16g_d Y_3 |Y_2|^2 Y_3^* \\
& \left. + 2g_d g_u^* \left( 3g_u \lambda_4 + 4g_d Y_2 Y_3^* - 4g_u |Y_2|^2 \right) \right) \quad (2.258)
\end{aligned}$$

$$\begin{aligned}
\beta_{\lambda_3}^{(1)} = & +\frac{3}{4}g^4 + 2\lambda_1 \lambda_2 - 3g^2 \lambda_3 + 4\lambda_3^2 + 8\lambda_3 \lambda_4 + 8\lambda_3 \lambda_5 + 2\lambda_3 |Y_2|^2 + 2\lambda_3 |Y_3|^2 \\
& + g_d^* \left( -2g_d |Y_3|^2 + 2g_u Y_3 Y_2^* - g_d |g_u|^2 + g_d \lambda_3 \right) - 4Y_3 |Y_2|^2 Y_3^* \\
& + g_u^* \left( 2g_d Y_2 Y_3^* - 2g_u |Y_2|^2 + g_u \lambda_3 \right) \quad (2.259)
\end{aligned}$$

$$\begin{aligned}
\beta_{\lambda_3}^{(2)} = & -\frac{25}{8}g^6 - 4\lambda_1^2 \lambda_2 - 4\lambda_1 \lambda_2^2 + \frac{43}{8}g^4 \lambda_3 - \lambda_1^2 \lambda_3 - 8\lambda_1 \lambda_2 \lambda_3 - \lambda_2^2 \lambda_3 + 2g^2 \lambda_3^2 - 10\lambda_3^3 \\
& + 5g^4 \lambda_4 + 16g^2 \lambda_3 \lambda_4 - 48\lambda_3^2 \lambda_4 - 40\lambda_3 \lambda_4^2 + 5g^4 \lambda_5 + 16g^2 \lambda_3 \lambda_5 - 48\lambda_3^2 \lambda_5 - 40\lambda_3 \lambda_5^2 \\
& - 4\lambda_1 \lambda_2 |Y_1|^2 - \frac{1}{4}g^4 |Y_2|^2 + \frac{5}{4}g^2 \lambda_3 |Y_2|^2 - 4\lambda_3^2 |Y_2|^2 - 16\lambda_3 \lambda_4 |Y_2|^2 - \frac{1}{4}g^4 |Y_3|^2 \\
& + \frac{5}{4}g^2 \lambda_3 |Y_3|^2 - 4\lambda_3^2 |Y_3|^2 - 16\lambda_3 \lambda_5 |Y_3|^2 - 3\lambda_3 |Y_2|^4 + 10|Y_3|^2 |Y_2|^4 - 3\lambda_3 |Y_3|^4 \\
& + 10|Y_2|^2 |Y_3|^4 - \frac{3}{2}\lambda_3 Y_2 |Y_1|^2 Y_2^* - \frac{1}{4}g_d^2 g_d^{*2} \left( 3\lambda_3 - 10|Y_3|^2 - 5|g_u|^2 \right) \\
& - 3g_u g_d g_d^{*2} Y_3 Y_2^* - \frac{3}{2}\lambda_3 Y_3 |Y_1|^2 Y_3^* + 5\lambda_3 Y_3 |Y_2|^2 Y_3^* + 12Y_2 Y_3 |Y_1|^2 Y_2^* Y_3^* \\
& - \frac{1}{4}g_u g_u^{*2} \left( -10g_u |Y_2|^2 + 12g_d Y_2 Y_3^* + 3g_u \lambda_3 \right) \\
& + g_d^* \left( -\frac{1}{8}g^4 g_d + \frac{5}{8}g^2 g_d \lambda_3 - 2g_d \lambda_3^2 - 8g_d \lambda_3 \lambda_4 + \frac{5}{2}g_d \lambda_3 |Y_3|^2 + \frac{5}{4}g_d |g_u|^4 + 5g_d |Y_3|^4 \right. \\
& + 2g_u \lambda_3 Y_3 Y_2^* - 8g_u \lambda_4 Y_3 Y_2^* - 8g_u \lambda_5 Y_3 Y_2^* - 6g_u Y_2 Y_3 Y_2^{*2} \\
& + Y_1^* \left( 2g_d Y_1 |Y_3|^2 - 4g_u Y_1 Y_3 Y_2^* - \frac{3}{4}g_d \lambda_3 Y_1 \right) + 6g_d Y_3 |Y_2|^2 Y_3^* - 6g_u Y_3^2 Y_2^* Y_3^* \\
& + g_u^* \left( 3g_d g_u |Y_1|^2 - 3g_d^2 Y_2 Y_3^* + 3g_d g_u |Y_3|^2 + 3g_u \left( g_d Y_2 - g_u Y_3 \right) Y_2^* + \frac{5}{4}g_d g_u \lambda_3 \right) \left. \right) \\
& - \frac{1}{8}g_u^* \left( g^4 g_u - 5g^2 g_u \lambda_3 + 16g_u \lambda_3^2 + 64g_u \lambda_3 \lambda_5 - 40g_u |Y_2|^4 - 16g_d \lambda_3 Y_2 Y_3^* \right. \\
& + 64g_d (\lambda_4 Y_2 Y_3^* + \lambda_5 Y_2 Y_3^*) + 48g_d Y_2 Y_3 Y_3^{*2} + 16|Y_1|^2 \left( 2g_d Y_2 Y_3^* + \frac{3}{8}g_u \lambda_3 \right. \\
& \left. \left. - g_u Y_2 Y_2^* \right) + 4|Y_2|^2 \left( 12 \left( g_d Y_2 - g_u Y_3 \right) Y_3^* - 5g_u \lambda_3 \right) \right) \quad (2.260)
\end{aligned}$$

$$\begin{aligned}
\beta_{\lambda_1}^{(1)} = & 2\lambda_1 |Y_2|^2 + 2\lambda_2 \lambda_3 + 2|Y_1|^2 \left( \lambda_1 - 2Y_2 Y_2^* \right) + 4\lambda_1^2 + 8\lambda_1 \lambda_4 - \frac{3}{2}g^2 \lambda_1 \\
& + |g_d|^2 \left( \lambda_1 - 2Y_1 Y_1^* \right) \quad (2.261)
\end{aligned}$$

$$\begin{aligned}
\beta_{\lambda_1}^{(2)} = & \frac{39}{16}g^4 \lambda_1 + g^2 \lambda_1^2 - 10\lambda_1^3 + \frac{5}{4}g^4 \lambda_2 - \lambda_1 \lambda_2^2 + 4g^2 \lambda_2 \lambda_3 - 8\lambda_1 \lambda_2 \lambda_3 - 4\lambda_2^2 \lambda_3 - \lambda_1 \lambda_3^2 \\
& - 4\lambda_2 \lambda_3^2 + 16g^2 \lambda_1 \lambda_4 - 48\lambda_1^2 \lambda_4 - 40\lambda_1 \lambda_4^2 - 3g^4 |Y_1|^2 + \frac{5}{2}g^2 \lambda_1 |Y_1|^2 - 4\lambda_1^2 |Y_1|^2 \\
& + \frac{5}{4}g^2 \lambda_1 |Y_2|^2 - 4\lambda_1^2 |Y_2|^2 - 16\lambda_1 \lambda_4 |Y_2|^2 - 4\lambda_2 \lambda_3 |Y_3|^2 - \frac{1}{4} \left( -10|Y_1|^2 + 3\lambda_1 \right) |g_d|^4 \\
& - 3\lambda_1 |Y_1|^4 + 10|Y_2|^2 |Y_1|^4 - 3\lambda_1 |Y_2|^4 + 10|Y_1|^2 |Y_2|^4 - 2g^2 Y_2 |Y_1|^2 Y_2^* \\
& + 5\lambda_1 Y_2 |Y_1|^2 Y_2^* - \frac{3}{2}\lambda_1 Y_3 |Y_1|^2 Y_3^* - \frac{3}{2}\lambda_1 Y_3 |Y_2|^2 Y_3^* + 12Y_2 Y_3 |Y_1|^2 Y_2^* Y_3^* \\
& - \frac{1}{4}g_u^* \left( 8g_u \lambda_2 \lambda_3 + 3g_u \lambda_1 |Y_2|^2 - 4g_d \lambda_1 Y_2 Y_3^* + 8g_d \lambda_2 Y_2 Y_3^* \right)
\end{aligned}$$

$$\begin{aligned}
& + |Y_1|^2 \left( 24g_d Y_2 Y_3^* + 3g_u \lambda_1 - 8g_u Y_2 Y_2^* \right) \\
& + \frac{1}{8} g_d^* \left( 5g^2 g_d \lambda_1 - 16g_d \lambda_1^2 - 64g_d \lambda_1 \lambda_4 - 6g_d \lambda_1 |Y_3|^2 + 40g_d |Y_1|^4 \right. \\
& - 3g_d |g_u|^2 \left( \lambda_1 - 8Y_1 Y_1^* \right) + 8g_u \lambda_1 Y_3 Y_2^* - 16g_u \lambda_2 Y_3 Y_2^* \\
& \left. + 4|Y_1|^2 \left( 12 \left( g_d Y_2 - g_u Y_3 \right) Y_2^* + g_d \left( -2g^2 + 4Y_3 Y_3^* + 5\lambda_1 \right) \right) \right) \quad (2.262)
\end{aligned}$$

$$\beta_{\lambda_5}^{(1)} = 20\lambda_5^2 + 2\lambda_5 |g_u|^2 - 2|Y_3|^4 - 3g^2 \lambda_5 + 4\lambda_5 |Y_3|^2 - \frac{1}{2} |g_u|^4 + \frac{3}{8} g^4 + \lambda_2^2 + \lambda_3^2 \quad (2.263)$$

$$\begin{aligned}
\beta_{\lambda_5}^{(2)} = & -\frac{25}{16} g^6 - 4\lambda_2^3 + \frac{5}{4} g^4 \lambda_3 + 2g^2 \lambda_3^2 - 4\lambda_3^3 + \frac{63}{8} g^4 \lambda_5 - 10\lambda_2^2 \lambda_5 - 10\lambda_3^2 \lambda_5 + 28g^2 \lambda_5^2 \\
& - 240\lambda_5^3 - 2\lambda_2^2 |Y_1|^2 - 2\lambda_3^2 |Y_2|^2 - \frac{1}{4} g^4 |Y_3|^2 + \frac{5}{2} g^2 \lambda_5 |Y_3|^2 - 40\lambda_5^2 |Y_3|^2 + 2\lambda_5 |Y_3|^4 \\
& + 2|Y_1|^2 |Y_3|^4 + 2|Y_2|^2 |Y_3|^4 + g_u^3 g_u^{*3} - 3\lambda_5 Y_3 |Y_1|^2 Y_3^* - 3\lambda_5 Y_3 |Y_2|^2 Y_3^* + 8Y_3^3 Y_3^{*3} \\
& + \frac{1}{2} g_u g_u^{*2} \left( -2g_d Y_2 Y_3^* + g_u \lambda_5 + g_u |Y_1|^2 + g_u |Y_2|^2 \right) \\
& - \frac{1}{8} g_u^* \left( g^4 g_u - 10g^2 g_u \lambda_5 + 160g_u \lambda_5^2 + 16g_d \lambda_3 Y_2 Y_3^* - 16g_d \lambda_5 Y_2 Y_3^* + 16g_d Y_2 Y_3 Y_3^{*2} \right. \\
& + 4g_u |Y_1|^2 \left( 3\lambda_5 - 4Y_3 Y_3^* \right) + 4g_u |Y_2|^2 \left( 3\lambda_5 - 4Y_3 Y_3^* \right) \left. \right) \\
& - \frac{1}{4} g_d^* \left( 2g_d \left( 2\lambda_3^2 - 2|Y_3|^4 + 3\lambda_5 |Y_3|^2 \right) - g_d |g_u|^4 + 8g_u Y_3 \left( -\lambda_5 + \lambda_3 + |Y_3|^2 \right) Y_2^* \right. \\
& \left. + |g_u|^2 \left( 3g_d \lambda_5 - 4g_d Y_3 Y_3^* + 4g_u Y_3 Y_2^* \right) \right) \quad (2.264)
\end{aligned}$$

$$\begin{aligned}
\beta_{\lambda_2}^{(1)} = & 2\lambda_1 \lambda_3 + 2\lambda_2 |Y_3|^2 + 2|Y_1|^2 \left( -2Y_3 Y_3^* + \lambda_2 \right) + 4\lambda_2^2 + 8\lambda_2 \lambda_5 - \frac{3}{2} g^2 \lambda_2 \\
& + |g_u|^2 \left( -2Y_1 Y_1^* + \lambda_2 \right) \quad (2.265)
\end{aligned}$$

$$\begin{aligned}
\beta_{\lambda_2}^{(2)} = & g^4 \left( \frac{5}{4} \lambda_1 + \frac{39}{16} \lambda_2 \right) - \lambda_1^2 \lambda_2 + g^2 \lambda_2^2 - 10\lambda_2^3 - 4 \left( \lambda_1 \lambda_3^2 + \lambda_1^2 \lambda_3 - g^2 \lambda_1 \lambda_3 \right) - 8\lambda_1 \lambda_2 \lambda_3 \\
& - \lambda_2 \lambda_3^2 + 16g^2 \lambda_2 \lambda_5 - 48\lambda_2^2 \lambda_5 - 40\lambda_2 \lambda_5^2 - 3g^4 |Y_1|^2 + \frac{5}{2} g^2 \lambda_2 |Y_1|^2 - 4\lambda_2^2 |Y_1|^2 \\
& - 4\lambda_1 \lambda_3 |Y_2|^2 + \frac{5}{4} g^2 \lambda_2 |Y_3|^2 - 4\lambda_2^2 |Y_3|^2 - 16\lambda_2 \lambda_5 |Y_3|^2 - \frac{1}{4} \left( 3\lambda_2 - 10|Y_1|^2 \right) |g_u|^4 \\
& - 3\lambda_2 |Y_1|^4 + 10|Y_3|^2 |Y_1|^4 - 3\lambda_2 |Y_3|^4 + 10|Y_1|^2 |Y_3|^4 - \frac{3}{2} \lambda_2 Y_2 |Y_1|^2 Y_2^* \\
& - 2g^2 Y_3 |Y_1|^2 Y_3^* + 5\lambda_2 Y_3 |Y_1|^2 Y_3^* - \frac{3}{2} \lambda_2 Y_3 |Y_2|^2 Y_3^* + 12Y_2 Y_3 |Y_1|^2 Y_2^* Y_3^* \\
& + \frac{1}{8} g_u^* \left( 5g^2 g_u \lambda_2 - 16g_u \lambda_2^2 - 64g_u \lambda_2 \lambda_5 - 6g_u \lambda_2 |Y_2|^2 + 40g_u |Y_1|^4 - 16g_d \lambda_1 Y_2 Y_3^* \right. \\
& + 8g_d \lambda_2 Y_2 Y_3^* + 4|Y_1|^2 \left( -12g_d Y_2 Y_3^* + 12g_u Y_3 Y_3^* - 2g^2 g_u + 4g_u Y_2 Y_2^* + 5g_u \lambda_2 \right) \left. \right) \\
& - \frac{1}{8} g_d^* \left( 3g_d |g_u|^2 \left( -8Y_1 Y_1^* + \lambda_2 \right) \right. \\
& + 2 \left( 8g_d \lambda_1 \lambda_3 + 3g_d \lambda_2 |Y_3|^2 + 8g_u \lambda_1 Y_3 Y_2^* - 4g_u \lambda_2 Y_3 Y_2^* \right. \\
& \left. \left. + |Y_1|^2 \left( 24g_u Y_3 Y_2^* + 3g_d \lambda_2 - 8g_d Y_3 Y_3^* \right) \right) \right) \quad (2.266)
\end{aligned}$$



## 2.10.3 Yukawa couplings

$$\beta_{g_d}^{(1)} = \frac{1}{4} \left( 2g_d |Y_1|^2 + 2g_d |Y_3|^2 - 3g^2 g_d + 4g_d^2 g_d^* + 4g_d |Y_2|^2 - 8g_u Y_3 Y_2^* + g_d |g_u|^2 \right) \quad (2.267)$$

$$\begin{aligned} \beta_{g_d}^{(2)} = & \frac{1}{32} \left( -7g_d |g_u|^4 - 10g_d^3 g_d^{*2} + g_u^* \left( 28g_d g_u |Y_1|^2 + 2g_u \left( -7g_d Y_2 + 24g_u Y_3 \right) Y_2^* \right. \right. \\ & + g_d \left( 16g_d Y_2 Y_3^* - 32g_u \lambda_3 - 56g_u |Y_3|^2 - 7g^2 g_u \right) \left. \right) - |g_d|^2 \left( 2 \left( 12g_d Y_2 Y_2^* \right. \right. \\ & - 8g_u Y_3 Y_2^* - 31g^2 g_d + 64g_d \lambda_4 + 7g_d Y_1 Y_1^* + 7g_d Y_3 Y_3^* \left. \right) + 7g_d g_u g_u^* \left. \right) \\ & - 2 \left( 14g_d |Y_1|^4 - 2 \left( 16g_u \lambda_3 Y_3 + \left( 24g_u Y_3 - 7g_d Y_2 \right) |Y_3|^2 + g^2 \left( 5g_d Y_2 - 4g_u Y_3 \right) \right) Y_2^* \right. \\ & + 8Y_2 \left( 3g_d Y_2 - 4g_u Y_3 \right) Y_2^{*2} + 2|Y_1|^2 \left( 4g_d \left( 4\lambda_1 + g^2 \right) + \left( 7g_d Y_2 - 8g_u Y_3 \right) Y_2^* \right) \\ & \left. \left. + g_d \left( \left( -11g^2 Y_3 + 32\lambda_3 Y_3 \right) Y_3^* + 14|Y_3|^4 + 2 \left( -4 \left( 8\lambda_4^2 + \lambda_1^2 + \lambda_3^2 \right) + g^4 \right) \right) \right) \right) \end{aligned} \quad (2.268)$$

$$\beta_{g_u}^{(1)} = \frac{1}{4} \left( 2g_u |Y_1|^2 + 2g_u |Y_2|^2 - 3g^2 g_u + 4g_u^2 g_u^* + 4g_u |Y_3|^2 - 8g_d Y_2 Y_3^* + g_u |g_d|^2 \right) \quad (2.269)$$

$$\begin{aligned} \beta_{g_u}^{(2)} = & \frac{1}{32} \left( -7g_u |g_d|^4 \right. \\ & - g_d^* \left( 7g^2 g_d g_u + 32g_d g_u \lambda_3 - 28g_d g_u |Y_1|^2 + 56g_d g_u |Y_2|^2 + 14g_d g_u |Y_3|^2 + 7g_d g_u^2 g_u^* \right. \\ & - 16g_u^2 Y_3 Y_2^* - 48g_d^2 Y_2 Y_3^* \left. \right) \\ & - 2 \left( 2g^4 g_u - 8g_u \lambda_2^2 - 8g_u \lambda_3^2 - 64g_u \lambda_5^2 - 11g^2 g_u |Y_2|^2 + 32g_u \lambda_3 |Y_2|^2 - 10g^2 g_u |Y_3|^2 \right. \\ & + 14g_u |Y_1|^4 + 14g_u |Y_2|^4 + 24g_u |Y_3|^4 + 5g_u^3 g_u^{*2} + 8g^2 g_d Y_2 Y_3^* - 32g_d \lambda_3 Y_2 Y_3^* \\ & + 14g_u Y_3 |Y_2|^2 Y_3^* - 48g_d Y_2^2 Y_2^* Y_3^* - 32g_d Y_2 Y_3 Y_3^{*2} \\ & + |g_u|^2 \left( 12g_u Y_3 Y_3^* - 8g_d Y_2 Y_3^* - 31g^2 g_u + 64g_u \lambda_5 + 7g_u Y_1 Y_1^* + 7g_u Y_2 Y_2^* \right) \\ & \left. \left. + 2|Y_1|^2 \left( 4g_u \left( 4\lambda_2 + g^2 \right) + \left( 7g_u Y_3 - 8g_d Y_2 \right) Y_3^* \right) \right) \right) \end{aligned} \quad (2.270)$$

$$\beta_{Y_3}^{(1)} = \frac{1}{4} \left( \left( 2g_u Y_3 - 4g_d Y_2 \right) g_u^* + Y_3 \left( 2|Y_1|^2 + 2|Y_2|^2 - 3g^2 + 8|Y_3|^2 \right) + Y_3 |g_d|^2 \right) \quad (2.271)$$

$$\begin{aligned} \beta_{Y_3}^{(2)} = & \frac{1}{32} \left( -7Y_3 |g_d|^4 + g_d^* \left( g_d \left( -7g_u Y_3 + 24g_d Y_2 \right) g_u^* + Y_3 \left( -8 \left( -2g_u Y_3 \right. \right. \right. \right. \\ & + 7g_d Y_2 \left. \right) Y_2^* + g_d \left( 11g^2 - 14|Y_3|^2 - 32\lambda_3 \right) \left. \right) \left. \right) - 2 \left( 2g_u \left( 3g_u Y_3 - 4g_d Y_2 \right) g_u^{*2} \right. \\ & + g_u^* \left( 4g^2 g_d Y_2 - 16g_d \lambda_3 Y_2 - 5g^2 g_u Y_3 + \left( 7g_u Y_3 - 24g_d Y_2 \right) |Y_2|^2 - 8g_d Y_2 |Y_3|^2 \right. \\ & + \left( 7g_u Y_1 Y_3 - 8g_d Y_1 Y_2 \right) Y_1^* + 12g_u Y_3^2 Y_3^* \left. \right) + Y_3 \left( 14|Y_1|^4 + 14|Y_2|^4 \right. \\ & + 2|Y_1|^2 \left( -14Y_2 Y_2^* + 4 \left( 4\lambda_2 + g^2 \right) + 7Y_3 Y_3^* \right) + |Y_2|^2 \left( 14Y_3 Y_3^* + 32\lambda_3 + 7g^2 \right) \\ & \left. \left. + 2 \left( 10|Y_3|^4 + \left( -31g^2 Y_3 + 64\lambda_5 Y_3 \right) Y_3^* - 4 \left( 8\lambda_5^2 + \lambda_2^2 + \lambda_3^2 \right) + g^4 \right) \right) \right) \end{aligned} \quad (2.272)$$

$$\beta_{Y_2}^{(1)} = \frac{1}{4} \left( 2 \left( -2g_u Y_3 + g_d Y_2 \right) g_d^* + Y_2 \left( 2|Y_1|^2 + 2|Y_3|^2 - 3g^2 + 8|Y_2|^2 + |g_u|^2 \right) \right) \quad (2.273)$$

$$\begin{aligned} \beta_{Y_2}^{(2)} = & \frac{1}{32} \left( -4g_d \left( 3g_d Y_2 - 4g_u Y_3 \right) g_d^{*2} + g_d^* \left( \left( -7g_d Y_2 + 24g_u Y_3 \right) |g_u|^2 \right. \right. \\ & + 2 \left( 5g^2 g_d Y_2 - 4g^2 g_u Y_3 + 16g_u \lambda_3 Y_3 - 12 \left( -\frac{2}{3} g_u Y_3 + g_d Y_2 \right) |Y_2|^2 - 7g_d Y_2 |Y_3|^2 \right. \\ & \left. \left. + \left( 8g_u Y_1 Y_3 - 7g_d Y_1 Y_2 \right) Y_1^* + 24g_u Y_3^2 Y_3^* \right) \right) \end{aligned}$$

$$\begin{aligned}
& -Y_2 \left( 7|g_u|^4 + g_u^* \left( -11g^2 g_u + 14g_u |Y_2|^2 + 32g_u \lambda_3 - 8 \left( 2g_d Y_2 - 7g_u Y_3 \right) Y_3^* \right) \right. \\
& + 2 \left( 2g^4 - 8\lambda_1^2 - 8\lambda_3^2 - 64\lambda_4^2 + 7g^2 |Y_3|^2 + 32\lambda_3 |Y_3|^2 + 14|Y_1|^4 + 20|Y_2|^4 + 14|Y_3|^4 \right. \\
& \left. \left. + 2|Y_1|^2 \left( 16\lambda_1 - 14Y_3 Y_3^* + 4g^2 + 7Y_2 Y_2^* \right) + 2|Y_2|^2 \left( 64\lambda_4 - 31g^2 + 7Y_3 Y_3^* \right) \right) \right) \quad (2.274)
\end{aligned}$$

$$\beta_{Y_1}^{(1)} = \frac{1}{4} Y_1 \left( 2|Y_2|^2 + 2|Y_3|^2 - 6g^2 + 8|Y_1|^2 + |g_d|^2 + |g_u|^2 \right) \quad (2.275)$$

$$\begin{aligned}
\beta_{Y_1}^{(2)} = & -\frac{1}{32} Y_1 \left( 7|g_d|^4 + 7|g_u|^4 + g_d^* \left( 32g_d \lambda_1 - 11g^2 g_d - 14g_d |g_u|^2 + 14g_d |Y_1|^2 \right. \right. \\
& - 32g_u Y_3 Y_2^* + 56g_d |Y_2|^2 \left. \right) + g_u^* \left( 14g_u |Y_1|^2 + (32\lambda_2 - 11g^2) g_u - 8 \left( 4g_d Y_2 \right. \right. \\
& - 7g_u Y_3 \left. \right) Y_3^* \left. \right) + 2 \left( 20|Y_1|^4 + 14(|Y_2|^4 + |Y_3|^4) - 8(\lambda_1^2 + \lambda_2^2) - 11g^2(g^2 + |Y_3|^2) \right. \\
& \left. + 32\lambda_2 |Y_3|^2 + |Y_2|^2 \left( 32\lambda_1 - 11g^2 - 28Y_3 Y_3^* \right) + 14|Y_1|^2 \left( Y_2 Y_2^* + Y_3 Y_3^* - \frac{26}{7} g^2 \right) \right) \quad (2.276)
\end{aligned}$$

#### 2.10.4 Fermion mass terms

$$\beta_{M_1}^{(1)} = \frac{1}{2} M_1 \left( |g_d|^2 + |g_u|^2 \right) \quad (2.277)$$

$$\begin{aligned}
\beta_{M_1}^{(2)} = & \frac{1}{16} \left( M_1 |g_d|^4 + g_u \left( 16g_d T_3 Y_1^* + g_u M_1 g_u^{*2} + M_1 \left( -12|Y_3|^2 + 17g^2 \right. \right. \right. \\
& \left. \left. - 2|Y_1|^2 - 2|Y_2|^2 \right) g_u^* \right) + M_1 |g_d|^2 \left( -12Y_2 Y_2^* + 17g^2 - 2Y_1 Y_1^* - 2Y_3 Y_3^* \right) \quad (2.278)
\end{aligned}$$

$$\beta_{M_2}^{(1)} = \frac{1}{4} M_2 \left( 2|Y_2|^2 + 2|Y_3|^2 + 4|Y_1|^2 - 6g^2 + |g_d|^2 + |g_u|^2 \right) \quad (2.279)$$

$$\begin{aligned}
\beta_{M_2}^{(2)} = & \frac{1}{32} \left( 22g^4 M_2 + 64g^2 M_2 |Y_1|^2 + 22g^2 M_2 |Y_2|^2 + 22g^2 M_2 |Y_3|^2 - 7M_2 |g_d|^4 \right. \\
& - 7M_2 |g_u|^4 + 8M_2 |Y_1|^4 - 28M_2 |Y_2|^4 - 28M_2 |Y_3|^4 - 64Y_1 |Y_2|^2 T_1^* - 64Y_1 |Y_3|^2 T_2^* \\
& + g_d^* \left( 14g_d M_2 |g_u|^2 - 32g_d Y_1 T_1^* + M_2 \left( 11g^2 g_d - 2g_d |Y_1|^2 + 32g_u Y_3 Y_2^* \right. \right. \\
& \left. \left. - 56g_d |Y_2|^2 \right) \right) - 4M_2 Y_2 |Y_1|^2 Y_2^* - 4M_2 Y_3 |Y_1|^2 Y_3^* + 56M_2 Y_3 |Y_2|^2 Y_3^* \\
& \left. + g_u^* \left( -32g_u Y_1 T_2^* + M_2 \left( 11g^2 g_u - 2g_u |Y_1|^2 + 8 \left( 4g_d Y_2 - 7g_u Y_3 \right) Y_3^* \right) \right) \right) \quad (2.280)
\end{aligned}$$

#### 2.10.5 Trilinear scalar couplings

$$\begin{aligned}
\beta_{T_3}^{(1)} = & \frac{1}{2} \left( g_d^* \left( 8M_1 Y_1 g_u^* + g_d T_3 \right) \right. \\
& \left. + T_3 \left( 2|Y_1|^2 + 2|Y_2|^2 + 2|Y_3|^2 - 3g^2 + 4\lambda_1 + 4\lambda_2 + 4\lambda_3 + |g_u|^2 \right) \right) \quad (2.281)
\end{aligned}$$

$$\begin{aligned}
\beta_{T_3}^{(2)} = & \frac{1}{16} \left( -2g_d^{*2} \left( 3g_d^2 T_3 + 40g_d M_1 Y_1 g_u^* - 64M_1 Y_1 Y_3 Y_2^* \right) \right. \\
& + g_d^* \left( -80g_u M_1 Y_1 g_u^{*2} + 2g_u^* \left( -32\lambda_3 M_1 Y_1 \right. \right. \\
& \left. \left. - 32M_1 Y_1^2 Y_1^* - 48M_1 Y_1 |Y_2|^2 - 48M_1 Y_1 |Y_3|^2 + 5g_d g_u T_3 + 8g^2 M_1 Y_1 \right) \right)
\end{aligned}$$

$$\begin{aligned}
& + T_3 \left( -12g_d|Y_1|^2 + 16g_u Y_3 Y_2^* + g_d \left( -12|Y_3|^2 - 16(\lambda_1 + \lambda_3) + 5g^2 \right) \right) \\
& + T_3 g_u^* \left( -12g_u|Y_1|^2 - 12g_u|Y_2|^2 + 16g_d Y_2 Y_3^* - 16g_u \lambda_2 - 16g_u \lambda_3 + 5g^2 g_u \right) \\
& + g_u^{*2} \left( 128M_1 Y_1 Y_2 Y_3^* - 6g_u^2 T_3 \right) + T_3 \left( 19g^4 + 8g^2 \lambda_1 \right. \\
& - 16\lambda_1^2 + 8g^2 \lambda_2 - 96\lambda_1 \lambda_2 - 16\lambda_2^2 + 64g^2 \lambda_3 - 96\lambda_1 \lambda_3 - 96\lambda_2 \lambda_3 - 16\lambda_3^2 \\
& - 64(2\lambda_1 \lambda_4 + 2\lambda_3 \lambda_4 - \lambda_4^2 + 2\lambda_2 \lambda_5 + 2\lambda_3 \lambda_5 - \lambda_5^2) + 10g^2|Y_3|^2 - 32\lambda_2|Y_3|^2 \\
& - 32\lambda_3|Y_3|^2 - 24(|Y_1|^4 + |Y_2|^4 + |Y_3|^4) + 4|Y_1|^2 \left( 10(Y_2 Y_2^* + Y_3 Y_3^*) + 5g^2 \right. \\
& \left. \left. - 8(\lambda_1 + \lambda_2) \right) + 2|Y_2|^2 \left( -16(\lambda_1 + \lambda_3) + 20Y_3 Y_3^* + 5g^2 \right) \right) \quad (2.282)
\end{aligned}$$

$$\begin{aligned}
\beta_{T_1}^{(1)} &= 2\lambda_3 T_2 + 2T_1|Y_2|^2 + 4\lambda_1 T_1 - 4Y_1|Y_2|^2 M_2^* + 8\lambda_4 T_1 - \frac{3}{2}g^2 T_1 \\
&+ |g_d|^2 \left( -2Y_1 M_2^* + T_1 \right) + T_1|Y_1|^2 \quad (2.283)
\end{aligned}$$

$$\begin{aligned}
\beta_{T_1}^{(2)} &= \frac{39}{16}g^4 T_1 + g^2 \lambda_1 T_1 - \frac{21}{2}\lambda_1^2 T_1 + \frac{1}{2}\lambda_2^2 T_1 - 4\lambda_2 \lambda_3 T_1 - \lambda_3^2 T_1 + 16g^2 \lambda_4 T_1 \\
&- 48\lambda_1 \lambda_4 T_1 - 40\lambda_4^2 T_1 + \frac{5}{4}g^4 T_2 - 2\lambda_1 \lambda_2 T_2 + 4g^2 \lambda_3 T_2 - 4\lambda_1 \lambda_3 T_2 - 4\lambda_2 \lambda_3 T_2 \\
&- 4\lambda_3^2 T_2 + \frac{5}{4}g^2 T_1|Y_1|^2 - 4\lambda_1 T_1|Y_1|^2 + \frac{5}{4}g^2 T_1|Y_2|^2 - 4\lambda_1 T_1|Y_2|^2 - 16\lambda_4 T_1|Y_2|^2 \\
&- 4\lambda_3 T_2|Y_3|^2 - \frac{3}{2}T_1|Y_1|^4 - 3T_1|Y_2|^4 - 3g^4 Y_1 M_2^* - 2g^2 Y_1|Y_2|^2 M_2^* + 4\lambda_1 Y_1|Y_2|^2 M_2^* \\
&+ 10Y_1|Y_2|^4 M_2^* - \frac{1}{4}|g_d|^4 \left( -10Y_1 M_2^* + 3T_1 \right) + 10Y_1^2|Y_2|^2 M_2^* Y_1^* + \frac{7}{4}T_1 Y_2|Y_1|^2 Y_2^* \\
&+ \frac{1}{8}g_d^* \left( 5g^2 g_d T_1 - 16g_d \lambda_1 T_1 - 64g_d \lambda_4 T_1 + 7g_d T_1|Y_1|^2 - 6g_d T_1|Y_3|^2 \right. \\
&- 3g_d|g_u|^2 \left( -8Y_1 M_2^* + T_1 \right) + 8g_u T_1 Y_3 Y_2^* - 16g_u T_2 Y_3 Y_2^* \\
&+ 8Y_1 M_2^* \left( 2g_d \lambda_1 + 2g_d|Y_3|^2 + 5g_d|Y_1|^2 + 6g_d|Y_2|^2 - 6g_u Y_3 Y_2^* - g^2 g_d \right) \\
&- \frac{3}{4}T_1 Y_3|Y_1|^2 Y_3^* - \frac{3}{2}T_1 Y_3|Y_2|^2 Y_3^* + 12Y_1 Y_3|Y_2|^2 M_2^* Y_3^* - \frac{3}{8}g_u^* g_u T_1|Y_1|^2 \\
&- \frac{1}{8}g_u^* \left( 2 \left( 4g_d Y_2 \left( 2T_2 + 6Y_1 M_2^* - T_1 \right) Y_3^* + 8g_u \lambda_3 T_2 + g_u|Y_2|^2 \left( 3T_1 - 8Y_1 M_2^* \right) \right) \right) \quad (2.284)
\end{aligned}$$

$$\begin{aligned}
\beta_{T_2}^{(1)} &= 2\lambda_3 T_1 + 2T_2|Y_3|^2 + 4\lambda_2 T_2 - 4Y_1|Y_3|^2 M_2^* + 8\lambda_5 T_2 - \frac{3}{2}g^2 T_2 \\
&+ |g_u|^2 \left( -2Y_1 M_2^* + T_2 \right) + T_2|Y_1|^2 \quad (2.285)
\end{aligned}$$

$$\begin{aligned}
\beta_{T_2}^{(2)} &= \frac{5}{4}g^4 T_1 - 2\lambda_1 \lambda_2 T_1 + 4g^2 \lambda_3 T_1 - 4\lambda_1 \lambda_3 T_1 - 4\lambda_2 \lambda_3 T_1 - 4\lambda_3^2 T_1 + \frac{39}{16}g^4 T_2 + \frac{1}{2}\lambda_1^2 T_2 \\
&+ g^2 \lambda_2 T_2 - \frac{21}{2}\lambda_2^2 T_2 - 4\lambda_1 \lambda_3 T_2 - \lambda_3^2 T_2 + 16g^2 \lambda_5 T_2 - 48\lambda_2 \lambda_5 T_2 - 40\lambda_5^2 T_2 \\
&+ \frac{5}{4}g^2 T_2|Y_1|^2 - 4\lambda_2 T_2|Y_1|^2 - 4\lambda_3 T_1|Y_2|^2 + \frac{5}{4}g^2 T_2|Y_3|^2 - 4\lambda_2 T_2|Y_3|^2 \\
&- 16\lambda_5 T_2|Y_3|^2 - \frac{3}{2}T_2|Y_1|^4 - 3T_2|Y_3|^4 - 3g^4 Y_1 M_2^* - 2g^2 Y_1|Y_3|^2 M_2^* \\
&+ 4\lambda_2 Y_1|Y_3|^2 M_2^* + 10Y_1|Y_3|^4 M_2^* - \frac{1}{4}|g_u|^4 \left( -10Y_1 M_2^* + 3T_2 \right) + 10Y_1^2|Y_3|^2 M_2^* Y_1^* \\
&- \frac{3}{4}T_2 Y_2|Y_1|^2 Y_2^* - \frac{1}{8}g_d^* \left( 3g_d T_2|Y_1|^2 + 3g_d|g_u|^2 \left( -8Y_1 M_2^* + T_2 \right) \right. \\
&+ 2 \left( 4g_u Y_3 \left( 2T_1 + 6Y_1 M_2^* - T_2 \right) Y_2^* + g_d \left( 8\lambda_3 T_1 + |Y_3|^2 \left( 3T_2 - 8Y_1 M_2^* \right) \right) \right) \quad (2.286)
\end{aligned}$$

$$\begin{aligned}
& + \frac{7}{4} T_2 Y_3 |Y_1|^2 Y_3^* - \frac{3}{2} T_2 Y_3 |Y_2|^2 Y_3^* + 12 Y_1 Y_3 |Y_2|^2 M_2^* Y_3^* + \frac{1}{8} g_u^* \left( 5 g^2 g_u T_2 \right. \\
& - 16 g_u \lambda_2 T_2 - 64 g_u \lambda_5 T_2 + 7 g_u T_2 |Y_1|^2 - 6 g_u T_2 |Y_2|^2 - 16 g_d T_1 Y_2 Y_3^* + 8 g_d T_2 Y_2 Y_3^* \\
& \left. + 8 Y_1 M_2^* \left( 2 g_u \lambda_2 + 2 g_u |Y_2|^2 + 5 g_u |Y_1|^2 - 6 g_d Y_2 Y_3^* + 6 g_u |Y_3|^2 - g^2 g_u \right) \right) \quad (2.286)
\end{aligned}$$

### 2.10.6 Scalar mass terms

$$\begin{aligned}
\beta_B^{(1)} &= \frac{1}{2} \left( 2B |Y_2|^2 + 2B |Y_3|^2 - 3B g^2 + 4B \lambda_3 + 4T_3 T_1^* + 4T_3 T_2^* + B |g_u|^2 \right. \\
& \left. + g_d^* \left( 8M_1 M_2 g_u^* + B g_d \right) \right) \quad (2.287)
\end{aligned}$$

$$\begin{aligned}
\beta_B^{(2)} &= + \frac{19}{16} B g^4 + \frac{1}{2} B \lambda_1^2 - 2B \lambda_1 \lambda_2 + \frac{1}{2} B \lambda_2^2 + 4B g^2 \lambda_3 - B \lambda_3^2 - 8B \lambda_3 \lambda_4 + 4B \lambda_4^2 \\
& - 8B \lambda_3 \lambda_5 + 4B \lambda_5^2 + \frac{5}{8} B g^2 |Y_2|^2 - 2B \lambda_3 |Y_2|^2 + \frac{5}{8} B g^2 |Y_3|^2 - 2B \lambda_3 |Y_3|^2 - \frac{3}{2} B |Y_2|^4 \\
& - \frac{3}{2} B |Y_3|^4 + \frac{1}{2} g^2 T_3 T_1^* - 2\lambda_1 T_3 T_1^* - 2\lambda_2 T_3 T_1^* - 6\lambda_3 T_3 T_1^* - 8\lambda_4 T_3 T_1^* - 2T_3 |Y_1|^2 T_1^* \\
& - 2T_3 |Y_2|^2 T_1^* + \frac{1}{2} g^2 T_3 T_2^* - 2\lambda_1 T_3 T_2^* - 2\lambda_2 T_3 T_2^* - 6\lambda_3 T_3 T_2^* - 8\lambda_5 T_3 T_2^* \\
& - 2T_3 |Y_1|^2 T_2^* - 2T_3 |Y_3|^2 T_2^* + 4M_2 T_3 |Y_2|^2 Y_1^* + 4M_2 T_3 |Y_3|^2 Y_1^* - \frac{3}{4} B Y_2 |Y_1|^2 Y_2^* \\
& + g_d^* \left( -5 g_d M_1 M_2 g_u^* + 8M_1 M_2 Y_3 Y_2^* - \frac{3}{8} B g_d^2 \right) \\
& - \frac{1}{16} g_d^* \left( \left( 64\lambda_3 M_1 M_2 + 64M_1 M_2 |Y_1|^2 + 96M_1 M_2 (|Y_2|^2 + |Y_3|^2) - 10B g_d g_u \right. \right. \\
& \left. - 16g^2 M_1 M_2 \right) g_u^* + 80g_u M_1 M_2 g_u^{*2} + 16g_d T_3 T_1^* + B \left( 12g_d |Y_3|^2 + 16(g_d \lambda_3 - g_u Y_3 Y_2^*) \right. \\
& \left. - 5g^2 g_d + 6g_d |Y_1|^2 \right) \left. \right) - B Y_3 \left( \frac{3}{4} |Y_1|^2 - \frac{5}{2} |Y_2|^2 \right) Y_3^* + g_u^{*2} \left( 8M_1 M_2 Y_2 Y_3^* - \frac{3}{8} B g_u^2 \right) \\
& + g_u^* \left( \frac{1}{16} B \left( 16g_d Y_2 Y_3^* - 12g_u |Y_2|^2 - 16g_u \lambda_3 + 5g^2 g_u - 6g_u |Y_1|^2 \right) - g_u T_3 T_2^* \right) \quad (2.288)
\end{aligned}$$

$$\begin{aligned}
\beta_{m_1^2}^{(1)} &= -\frac{3}{2} g^2 m_1^2 + 8\lambda_4 m_1^2 + 2\lambda_3 m_2^2 + 2\lambda_1 m_3^2 + 4|T_1|^2 + 2|T_3|^2 + 2m_1^2 |Y_2|^2 \\
& + |g_d|^2 \left( -2M_2 M_2^* - 8M_1 M_1^* + m_1^2 \right) - 4Y_2 |M_2|^2 Y_2^* \quad (2.289)
\end{aligned}$$

$$\begin{aligned}
\beta_{m_1^2}^{(2)} &= \left( \frac{39}{16} g^4 - \lambda_1^2 - \lambda_3^2 + 16g^2 \lambda_4 - 40\lambda_4^2 \right) m_1^2 + \left( \frac{5}{4} g^4 + 4g^2 \lambda_3 - 4\lambda_3^2 \right) m_2^2 - 4\lambda_1^2 m_3^2 \\
& - 3g^4 |M_2|^2 + g^2 |T_1|^2 - 10\lambda_1 |T_1|^2 - 48\lambda_4 |T_1|^2 - 2\lambda_1 |T_2|^2 - 4\lambda_3 |T_2|^2 \\
& + \frac{1}{2} g^2 |T_3|^2 - 6\lambda_1 |T_3|^2 - 6\lambda_3 |T_3|^2 - 8\lambda_4 |T_3|^2 - 4\lambda_1 m_3^2 |Y_1|^2 + \frac{5}{4} g^2 m_1^2 |Y_2|^2 \\
& - 16\lambda_4 m_1^2 |Y_2|^2 - 4\lambda_3 m_2^2 |Y_3|^2 - \frac{1}{4} \left( 3m_1^2 - 10|M_2|^2 - 64|M_1|^2 \right) |g_d|^4 - 3m_1^2 |Y_2|^4 \\
& + 10|M_2|^2 |Y_2|^4 - 4\lambda_3 T_2 T_1^* + 4Y_1 |Y_2|^2 M_2^* T_1^* - 4\lambda_3 T_1 T_2^* - 4Y_1 |T_1|^2 Y_1^* \\
& - 2Y_1 |T_3|^2 Y_1^* + 4M_2 T_1 |Y_2|^2 Y_1^* - 2g^2 Y_2 |M_2|^2 Y_2^* - 4Y_2 |T_1|^2 Y_2^* - \frac{3}{2} m_1^2 Y_2 |Y_1|^2 Y_2^* \\
& + 10Y_1 Y_2 |M_2|^2 Y_1^* Y_2^* - 2Y_3 |T_3|^2 Y_3^* - \frac{3}{2} m_1^2 Y_3 |Y_2|^2 Y_3^* + 12Y_2 Y_3 |M_2|^2 Y_2^* Y_3^* \\
& + \frac{1}{8} g_d^* \left( 5g^2 g_d m_1^2 - 64g_d \lambda_4 m_1^2 - 16g_d |T_1|^2 - 6g_d m_1^2 |Y_1|^2 - 6g_d m_1^2 |Y_3|^2 \right)
\end{aligned}$$

$$\begin{aligned}
& -3g_d|g_u|^2 \left( -16M_1M_1^* - 8M_2M_2^* + m_1^2 \right) + 16g_dM_2T_1Y_1^* + 32g_dY_1|M_1|^2Y_1^* \\
& + 8g_um_1^2Y_3Y_2^* - 16g_um_2^2Y_3Y_2^* - 64g_uY_3|M_1|^2Y_2^* \\
& + 8M_2^2 \left( 2g_dY_1T_1^* + M_2 \left( 2g_d|Y_3|^2 + 5g_d|Y_1|^2 + 6g_d|Y_2|^2 - 6g_uY_3Y_2^* - g^2g_d \right) \right) \\
& + 32g_dY_3|M_1|^2Y_3^* \Big) - \frac{1}{4}g_u^* \left( 4g_u|T_3|^2 + g_u|Y_2|^2 \left( 3m_1^2 - 32M_1M_1^* - 8M_2M_2^* \right) \right. \\
& \left. + 4 \left( 2g_u\lambda_3m_2^2 + g_dY_2 \left( 2m_2^2 + 6|M_2|^2 + 8|M_1|^2 - m_1^2 \right) Y_3^* \right) \right) \quad (2.290)
\end{aligned}$$

$$\begin{aligned}
\beta_{m_2^2}^{(1)} &= 2\lambda_3m_1^2 - \frac{3}{2}g^2m_2^2 + 8\lambda_5m_2^2 + 2\lambda_2m_3^2 + 4|T_2|^2 + 2|T_3|^2 + 2m_2^2|Y_3|^2 \\
& + |g_u|^2 \left( -2M_2M_2^* - 8M_1M_1^* + m_2^2 \right) - 4Y_3|M_2|^2Y_3^* \quad (2.291)
\end{aligned}$$

$$\begin{aligned}
\beta_{m_2^2}^{(2)} &= \left( \frac{5}{4}g^4 + 4g^2\lambda_3 - 4\lambda_3^2 \right) m_1^2 + \left( \frac{39}{16}g^4 - \lambda_2^2 - \lambda_3^2 + 16g^2\lambda_5 - 40\lambda_5^2 \right) m_2^2 \\
& - 4\lambda_2^2m_3^2 - 3g^4|M_2|^2 - 2\lambda_2|T_1|^2 - 4\lambda_3|T_1|^2 + g^2|T_2|^2 - 10\lambda_2|T_2|^2 - 48\lambda_5|T_2|^2 \\
& + \frac{1}{2}g^2|T_3|^2 - 6\lambda_2|T_3|^2 - 6\lambda_3|T_3|^2 - 8\lambda_5|T_3|^2 - 4\lambda_2m_3^2|Y_1|^2 - 4\lambda_3m_1^2|Y_2|^2 \\
& + \frac{5}{4}g^2m_2^2|Y_3|^2 - 16\lambda_5m_2^2|Y_3|^2 - \frac{1}{4} \left( -10|M_2|^2 + 3m_2^2 - 64|M_1|^2 \right) |g_u|^4 \\
& - 3m_2^2|Y_3|^4 + 10|M_2|^2|Y_3|^4 - 4\lambda_3T_2T_1^* - 4\lambda_3T_1T_2^* + 4Y_1|Y_3|^2M_2^*T_2^* \\
& - 4Y_1|T_2|^2Y_1^* - 2Y_1|T_3|^2Y_1^* + 4M_2T_2|Y_3|^2Y_1^* - 2Y_2|T_3|^2Y_2^* \\
& - \frac{1}{8}g_d^* \left( 3g_d|g_u|^2 \left( m_2^2 - 16M_1M_1^* - 8M_2M_2^* \right) + 2 \left( 4g_d|T_3|^2 \right. \right. \\
& \left. \left. + g_d \left( 8\lambda_3m_1^2 + |Y_3|^2 \left( 3m_2^2 - 32M_1M_1^* - 8M_2M_2^* \right) \right) \right) \right. \\
& \left. + 4g_uY_3 \left( 2m_1^2 + 6|M_2|^2 + 8|M_1|^2 - m_2^2 \right) Y_2^* \right) - 2g^2Y_3|M_2|^2Y_3^* - 4Y_3|T_2|^2Y_3^* \\
& - \frac{3}{2}m_2^2Y_3|Y_1|^2Y_3^* - \frac{3}{2}m_2^2Y_3|Y_2|^2Y_3^* + 10Y_1Y_3|M_2|^2Y_1^*Y_3^* + 12Y_2Y_3|M_2|^2Y_2^*Y_3^* \\
& + \frac{1}{8}g_u^* \left( 5g^2g_um_2^2 - g_u \left( 64\lambda_5m_2^2 + 16|T_2|^2 + 6m_2^2|Y_1|^2 + 6m_2^2|Y_2|^2 - 16M_2T_2Y_1^* \right) \right. \\
& \left. + 32g_u \left( Y_1|M_1|^2Y_1^* + Y_2|M_1|^2Y_2^* \right) - g_d \left( 16m_1^2Y_2Y_3^* - 8m_2^2Y_2Y_3^* + 64Y_2|M_1|^2Y_3^* \right) \right. \\
& \left. + 8M_2^2 \left( 2g_uY_1T_2^* + M_2 \left( 2g_u|Y_2|^2 + 5g_u|Y_1|^2 - 6g_dY_2Y_3^* + 6g_u|Y_3|^2 - g^2g_u \right) \right) \right) \quad (2.292)
\end{aligned}$$

$$\begin{aligned}
\beta_{m_3^2}^{(1)} &= 2\lambda_1m_1^2 + 2\lambda_2m_2^2 - T_1^2 - T_2^2 + 2|T_1|^2 + 2|T_2|^2 + 2|T_3|^2 + 2m_3^2|Y_1|^2 + 2Y_1^2M_2^{*2} \\
& - T_1^{*2} - T_2^{*2} - 8Y_1|M_2|^2Y_1^* + 2M_2^2Y_1^{*2} \quad (2.293)
\end{aligned}$$

$$\begin{aligned}
\beta_{m_3^2}^{(2)} &= 4g^2\lambda_1m_1^2 - 4\lambda_1^2m_1^2 + 4g^2\lambda_2m_2^2 - 4\lambda_2^2m_2^2 - \lambda_1^2m_3^2 - \lambda_2^2m_3^2 - 2g^2T_1^2 + 4\lambda_1T_1^2 \\
& - 2g^2T_2^2 + 4\lambda_2T_2^2 + 4g^2|T_1|^2 - 12\lambda_1|T_1|^2 + 4g^2|T_2|^2 - 12\lambda_2|T_2|^2 + 4g^2|T_3|^2 \\
& - 6\lambda_1|T_3|^2 - 6\lambda_2|T_3|^2 + \frac{5}{2}g^2m_3^2|Y_1|^2 - 4\lambda_1m_1^2|Y_2|^2 + 2T_1^2|Y_2|^2 - 4\lambda_2m_2^2|Y_3|^2 \\
& + 2T_2^2|Y_3|^2 - 3m_3^2|Y_1|^4 + 32|M_2|^2|Y_1|^4 + 2g^2Y_1^2M_2^{*2} - 2Y_1^2 \left( |Y_2|^2 + |Y_3|^2 \right) M_2^{*2} \\
& - 2g^2T_1^{*2} + 4\lambda_1T_1^{*2} + 2|Y_2|^2T_1^{*2} - 2g^2T_2^{*2} + 4\lambda_2T_2^{*2} + 2|Y_3|^2T_2^{*2} \\
& - 8g^2Y_1|M_2|^2Y_1^* - 4g_dg_uT_3M_1^*Y_1^* - 8Y_1^3M_2^{*2}Y_1^* + 2g^2M_2^2Y_1^{*2} - 2M_2^2|Y_2|^2Y_1^{*2} \\
& - 2M_2^2|Y_3|^2Y_1^{*2} - 8M_2^2Y_1Y_1^{*3} \\
& - \frac{1}{4}|g_u|^2 \left( 8\lambda_2m_2^2 - 4T_2^2 + 4Y_1^2M_2^{*2} + 8T_2T_2^* - 4T_2^{*2} + 4T_3T_3^* + 3m_3^2Y_1Y_1^* \right.
\end{aligned}$$

$$\begin{aligned}
& - 32M_1 Y_1 M_1^* Y_1^* - 16M_2 Y_1 M_2^* Y_1^* + 4M_2^2 Y_1^{*2} \Big) \\
& + g_d^* \Big( - 2g_d \lambda_1 m_1^2 + g_d T_1^2 - 2g_d |T_1|^2 - g_d |T_3|^2 - \frac{3}{4} g_d m_3^2 |Y_1|^2 - g_d Y_1^2 M_2^{*2} + g_d T_1^{*2} \\
& - 4M_1 Y_1 g_u^* T_3^* + 8g_d Y_1 |M_1|^2 Y_1^* + 4g_d Y_1 |M_2|^2 Y_1^* - g_d M_2^2 Y_1^{*2} \Big) \\
& - 4Y_2 |T_1|^2 Y_2^* - 2Y_2 |T_3|^2 Y_2^* - \frac{3}{2} m_3^2 Y_2 |Y_1|^2 Y_2^* + 8Y_1 Y_2 |M_2|^2 Y_1^* Y_2^* - 4Y_3 |T_2|^2 Y_3^* \\
& - 2Y_3 |T_3|^2 Y_3^* - \frac{3}{2} m_3^2 Y_3 |Y_1|^2 Y_3^* + 8Y_1 Y_3 |M_2|^2 Y_1^* Y_3^*
\end{aligned} \tag{2.294}$$

## 3 ARGES

### 3.1 Overview

In ancient greek mythology, Argos is the name of a cyclops who, after being exiled by the Titans was eventually freed by Zeus to forge lightning bolts for his battle against their former masters. In this tradition of being a helping hand in times of struggle, we introduce the computational tool ARGES — Advanced Renormalisation Group Equation Simplifier. Written in the *Wolfram Language*, it was tested for Mathematica versions 8.0 – 12.0 [246] and is available via [247] under *GNU General Public License* [248]. As the name suggests, ARGES is a framework to calculate perturbative  $\overline{\text{MS}}$  renormalisation group flows of renormalisable QFTs in  $d = 4$ . To that end, it requires information about the input QFT in terms of its gauge group, matter content and other interaction terms.

The framework profits from the ansatz for a general QFT (1.26), which acts as a template in which any renormalisable QFT can be embedded. This allows the computation to be broken down into two steps.

In a first step, momentum integrals and spinor traces are resolved, and all RGEs expressed in terms of generalised couplings. These can be mapped back onto the desired QFT in the second step. However, resolving the remaining contraction of indices running over field species, generations, flavours, and gauge components is a highly complicated task. Moreover, the embedding is non-trivial, as fermions need to be decomposed into Weyl components, scalars into real and imaginary parts, and indices of Yukawa couplings, masses and scalar interactions have to be symmetrised. In fact, with increasing features of the QFT, such as more field content and interactions, this second step becomes more involved than the first one. At higher loop orders, the complexity increases even further.

ARGES utilises known literature results for the template RGEs up to the highest available loop order and automatises the second step of mapping those results back onto the input theory. The framework provides  $\beta$ -functions of the gauge coupling up the three-loop order [182, 185–190], as well as RG equations for Yukawa interactions [1, 183, 185], scalar quartics [1, 184, 185] and cubics [1, 184, 185], fermion and scalar masses [1, 183–185], vacuum expectation values [191, 192] as well as scalar and fermion anomalous dimensions [183–185] at two-loop order.

### 3.2 Design & comparison with other frameworks

The design goals of ARGES are complementary to the two other software packages available with the same scope, namely SARAH 4 [235–239] and PyR@TE 2 [240, 241].<sup>7</sup> Both are quite different in

---

<sup>7</sup>At the time of writing, PyR@TE 3 is still in development.

their implementation – PyR@TE is a highly specialised *python* package accepting a single input file and command line parameters. It allows for theories ranging from simplest toy models to complicated SM extensions. SARAH on the other hand is a large *Mathematica* package and in fact a wider framework with many more capabilities. Geared towards realistic theories, it requires complex inputs, and is the backend of various scientific software. However, the inner workings of PyR@TE and SARAH are conceptually quite similar, while ARGES takes a slightly different approach. The key differences in ARGES functionality will be highlighted in the following.

**Index contractions are user input.** With the exception of interaction terms involving gauge bosons, contractions of gauge and global indices over each interaction vertex have to be specified as input. ARGES knows only very little about the Lie algebras, and shifts the responsibility of formulating a gauge invariant action, consistent with the desired symmetries, to the user. The advantage however is that the user has full control over the shape of the action, eliminating any uncertainty e.g. about coupling normalisations. In comparison, SARAH and PyR@TE link to external packages Susyno [249] and its *python* clone PyLie [250] that automatise the search for index contractions, providing a much less fine-grained control, especially in cases where more than one contraction is possible. Although the automatisisation avoids explicit violations of gauge invariance, all three codes may give inconsistent results if not all interactions allowed by the symmetries of the QFT are manually included.

**Groups, representation and multiplicities can be variables.** As opposed to PyR@TE and SARAH, ARGES allows for gauge groups to be either completely undetermined, formulating the results in terms of general gauge invariants (1.30), or to be an entire family of like  $SU(N)$ , without specifying  $N$ . More so, the representations for each field can be kept a variable as well, and so does the number of generations. This ties in with the previous point: ARGES is agnostic to symmetries and algebras, and treats everything as an index. That allows for a systematic study of a large ranges of models, and represents a main advantage over existing codes.

**Gauge invariants are not resolved by default.** ARGES does not resolve gauge invariants as in (1.30) by default. In general, they are also considered user input, but for simple representations of  $U(1)$ ,  $SU(N)$ ,  $SO(N)$  and  $Sp(2N)$  gauge groups, invariants can be computed automatically and are available as substitution rules.

**Scalars can carry flavour, non-matrix Yukawas are allowed.** In SARAH and PyR@TE, only fermions carry a single flavour index, while scalars do not. This constrains Yukawa couplings to be of matrix form  $y_{ij} \bar{\psi}_i \phi \psi'_j + \text{h.c.}$  In ARGES, scalars carry two such indices instead which can be contracted freely, also allowing for Yukawa vertices with a single coupling, but a matrix multiplication in the fields  $y \bar{\psi}_i \phi_{ij} \psi'_j + \text{h.c.}$  This expands the space of possible input models with respect to SARAH and PyR@TE.

**Disentanglement of RGEs by the user.** Due to the RG template formulas being computed for generalised couplings  $\alpha_{abc\dots}$ , a single  $\beta$ -function  $\partial \alpha_{abc\dots} / \partial \ln \mu = \beta(\alpha)_{abc\dots}$  can be extracted for each choice of external fields, which depends on the gauge- and flavour indices ( $a, b, c \dots$ ) of the latter. At tree level, this may correspond to linear combination of several couplings in the input theory  $\alpha_{abc\dots} = \sum_i h^i_{abc\dots} \alpha_i$ . Hence, several choices of external indices have to be computed, each coupling disentangled by solving the system at tree level, and matched up with the correspond-



ing linear combinations of  $\beta$ -functions at loop level. Even for a single coupling, this might be necessary to fix the correct normalisation.

PyR@TE and SARA<sup>H</sup> automatise this procedure, however, these attempts can be unsuccessful and causes the applications to hang or crash. This may occur in valid models, but is bound to happen if couplings specified simply cannot be disentangled. In ARGES, the disentanglement is up to the user, which bears two more advantages other than stability of the program: for one, there are several choices of external indices, and the user is free to chose the one minimising the computation efforts for the RGEs, e.g. with the most symmetries of external legs. Secondly, the mechanism provided allows the user to input external indices as variables as well, and reconcile tree- with loop-level contractions, thus identifying if couplings allowed by the symmetry have been omitted, but are switched on by the renormalisation group running.

**Efficient handling of unknown interactions.** In fact, ARGES allows index contraction to be merely defined by a number of relations, providing a mechanism to insert such information and allow for an efficient computation of RGEs. An example will be given later in this work.

At the time of writing, ARGES is limited to irreducible representations, while reducible ones can be handled by SARA<sup>H</sup> and PyR@TE. Moreover, it does not allow for kinetic mixing of  $U(1)$  gauge groups, implemented in SARA<sup>H</sup>. All three packages assume an  $R_\xi$  gauge fixing.

### 3.3 Setup

ARGES is designed to be easily distributable, the code has no external dependencies and is located in a single file `ARGES.m`. Moreover, another design goal is that ARGES does neither require nor encourage a notebook, or any graphical user interface in general, access to a Mathematica kernel is sufficient. The source code can be acquired from [247], e.g. by cloning the git repository.

```
git clone https://github.com/TomSteu/ARGES
```

The relevant file can be loaded by the kernel directly via

```
Get["~/path/to/ARGES.m", ARGES];
```

or alternatively, moved into a location contained in `$Path` manually, using `Install[...]` or the graphical user interface and included via:

```
<<ARGES
```

If no output is produced by whatever the method of choice, then the installation was successful. Next, we will proceed with an example on how to define a valid input model.

## 3.4 ARGES by example

Now, we will demonstrate the basic and advanced functionality of ARGES by application, in good faith that a generalisation is obvious.

### 3.4.1 Defining a model

The input required by ARGES can either be provided by a model file or in an interactive session. ARGES is very well capable of competing with SARA<sup>H</sup> and PyR@TE in processing realistic models

like SM-extensions, but we will proceed with the model in [112], and the Lagrangian (1.50) to demonstrate the strength of ARGES, as this theory cannot be implemented in neither SARAH nor PyR@TE. The reasons for that are in fact manifold: neither the general  $SU(N_c)$  gauge group can be handled by these packages, nor the multiplicity of  $N_f$  Dirac fermions. The  $N_f \times N_f$  two-index scalar cannot be used as input, and specifying the correct contractions of the Yukawa vertex and quartics is problematic, and so is disentangling both quartic RGEs.<sup>8</sup> For ARGES, no such limitations apply, and we start by loading the code.

```
1 <<ARGES `
2 Reset [] ;
```

ARGES is stateful, and `Reset []` wipes any previous input without affecting the kernel memory. It is not necessary to invoke for the first run, but recommended in notebooks as cells may be re-evaluated. Next, the gauge sector will be specified, starting with the number of gauge groups.

```
3 NumberOfSubgroups = 1;
4 Gauge[g, SU[Nc], {Nc^2 - 1}];
```

Then, the functions `Gauge[...]` are called once for each gauge group, which implies the ordering of gauge indices. The first argument is the symbol of the gauge coupling, followed by the group, or any place holder for an unknown unspecified one thereof. Finally a list of length `NumberOfSubgroups` denotes the multiplicity of the gauge bosons<sup>9</sup> under each gauge group, in the implied ordering. Next, the matter content can be specified. We will start with registering the fermions in terms of their Weyl components.

```
5 WeylFermion[QL, Nf, {Nc}];
6 WeylFermion[QR, Nf, {Nc}];
```

Hereby, the first argument is the name of the fermion, the second the number of flavours and the third a list of its gauge multiplicities in the same order as before. For  $U(1)$  gauge groups, the charge of the field is to be inserted here. Scalar matter can be inserted with

```
7 ComplexScalar[H, {Nf, Nf}, {1}];
```

which will add two real components `Re[H]` and `Im[H]`. Whenever the complex field is specified somewhere, the decomposition  $H = (\text{Re}[H] + i\text{Im}[H])/\sqrt{2}$  is then automatically inserted. Alternatively, one may add the components manually via `RealScalar[_,_,_]` with the same calling conventions. The syntax is similar to the fermionic case, only the second argument is now a list of two elements, as scalars always carry two flavour indices. We are now in the position to add interactions. A Yukawa term with a single coupling  $y$  is inserted via

```
8 Yukawa[y, H, adj[QL], QR, {KroneckerDelta[#2,#3]&}, (KroneckerDelta
  [#1,#3] KroneckerDelta[#2,#4]&) ];
```

The second to fourth argument represent the scalar and fermionic fields involved. The fifth argument is a list of `NumberOfSubgroups` elements, each being a function of three arguments representing the contractions of gauge indices of the scalar and two fermionic fields involved, in the order of appearance at this vertex. To optimise the simplification, `Mathematica`'s built-in

<sup>8</sup>As long as only the intact  $SU(N_f) \times SU(N_f)$  flavour symmetry is considered, there is a trick to promote these to two gauge symmetries with vanishing couplings which should in principle allow model input.

<sup>9</sup>In the  $U(1)$  case, it marks the charge instead.

function `KroneckerDelta[_,_]` should be used for each contraction. The final argument is the contraction function of flavour indices and expects four arguments, the first two being indices of the scalar, and the second two for each of the fermions, again in the order of appearance. Obviously, we have used Mathematica's capability to define anonymous functions as `(_)&`, with the  $n$ th argument denoted by `#n`. In the same manner, quartics can now be added, keeping in mind that scalars have two flavour indices each.

```

9  ScalarQuartic[u, adj[H], H, adj[H], H, {1&}, (KroneckerDelta[#2,#3]
      KroneckerDelta[#4,#5] KroneckerDelta[#6,#7] KroneckerDelta
      [#8,#1])& ];
10 ScalarQuartic[v, adj[H], H, adj[H], H, {1&}, (KroneckerDelta[#2,#3]
      KroneckerDelta[#4,#1] KroneckerDelta[#6,#7] KroneckerDelta
      [#8,#5])& ];

```

Similarly, the functions `ScalarCubic[___]`, `ScalarMass[___]` and `FermionMass[___]` exist. In addition, `YukawaMat[___]` and `FermionMassMat[___]` define couplings as matrices in the fermion flavours and assume the last argument to be simply a normalisation constant. The model is now defined, and we can already compute all the gauge invariants available via

```

11 ComputeInvariants[];

```

which will be stored as a substitution rule in `subInvariants`.

### 3.4.2 Obtaining output

Now, the model from the previous section

```

1  <<ARGES '
2  Reset[];
3  NumberOfSubgroups = 1;
4  Gauge[g, SU[Nc], {Nc^2 - 1}];
5  WeylFermion[QL, Nf, {Nc}];
6  WeylFermion[QR, Nf, {Nc}];
7  ComplexScalar[H, {Nf, Nf}, {1}];
8  Yukawa[y, H, adj[QL], QR, {KroneckerDelta[#2,#3]&}, (KroneckerDelta
      [#1,#3] KroneckerDelta[#2,#4])& ];
9  ScalarQuartic[u, adj[H], H, adj[H], H, {1&}, (KroneckerDelta[#2,#3]
      KroneckerDelta[#4,#5] KroneckerDelta[#6,#7] KroneckerDelta
      [#8,#1])& ];
10 ScalarQuartic[v, adj[H], H, adj[H], H, {1&}, (KroneckerDelta[#2,#3]
      KroneckerDelta[#4,#1] KroneckerDelta[#6,#7] KroneckerDelta
      [#8,#5])& ];
11 ComputeInvariants[];

```

will be analysed.  $\beta$ -functions for the gauge coupling  $g$  can be obtained via

```

In[1]:= (4  $\pi$ )^2  $\beta$ [g, 1] //. subInvariants // Expand
Out[1]= -11/3 Nc g^3 + 2/3 Nf g^3

```

where the second argument indicates the loop order. For any other couplings, RG equations are extracted by specifying external fields and their indices. In order to properly normalise and disentangle the system of couplings, this has to be done at tree level first. For the Yukawa interaction, the syntax is

```
In[2]:=  $\beta[\text{Re}[H], \text{adj}[QL], QR, \{i1, i2, 1\}, \{j1, a\}, \{j2, b\}, 0]$ 
Out[2]=  $y \delta_{i1,j1} \delta_{i2,j2} \delta_{a,b} / \text{Sqrt}[2]$ 
```

where the first three arguments specify the scalar and fermions at the vertex of interest, followed by lists of the quantum numbers of each field, in that order. The leading elements of that list are flavour (one for fermions, two for scalars), and the remaining components gauge indices.<sup>10</sup> Finally the last argument is again the loop order, with 0 indicating tree-level. From this output, the desirable normalisation and index structure can be read off. Now, the one-loop  $\beta$ -function of  $y$  is extracted by changing the last argument, and taking the correct normalisation into account.

```
In[3]:= (4  $\pi$ )^2 Sqrt[2]  $\beta[\text{Re}[H], \text{adj}[QL], QR, \{1,1,1\}, \{1,1\}, \{1,1\}, 1]$ 
//. subInvariants // Expand
Out[3]=  $3/N_c g^2 y - 3 N_c g^2 y + N_c y^2 \text{conj}[y] + N_f y^2 \text{conj}[y]$ 
```

For the scalar quartics, syntax and procedure is very similar.

```
In[4]:=  $\beta[\text{adj}[H], H, H, H, \{1,1,1\}, \{1,1,1\}, \{1,1,1\}, \{1,1,1\}, 0]$  //
Expand
Out[4]=  $u + v$ 
In[5]:=  $\beta[\text{adj}[H], H, H, H, \{2,2,1\}, \{2,2,1\}, \{1,1,1\}, \{1,1,1\}, 0]$  //
Expand
Out[5]=  $v/3$ 
In[6]:=  $bv = 3 (4 \pi)^2 \beta[\text{adj}[H], H, H, H, \{2,2,1\}, \{2,2,1\}, \{1,1,1\},$ 
 $\{1,1,1\}, 1]$  //. subInvariants // Expand
Out[6]=  $12 u^2 + 16 N_f u v + 16 v^2 + 4 N_f^2 v^2 + 4 N_c v y \text{conj}[y]$ 
In[7]:=  $bu = - bv + (4 \pi)^2 \beta[\text{adj}[H], H, H, H, \{1,1,1\}, \{2,2,1\}, \{1,1,1\},$ 
 $\{1,1,1\}, 1]$  //. subInvariants // Expand
Out[7]=  $8 N_f u^2 + 24 u v + 4 N_c u y \text{conj}[y] - 2 N_c y^2 \text{conj}[y]^2$ 
```

In fact, this syntax  $\beta[\_]$ , followed by the fields and then respective lists of indices, is universal for all couplings apart from gauge interactions. Finally, field anomalous dimensions can simply be obtained as follows.

```
In[8]:= (4  $\pi$ )^2  $\gamma[\text{adj}[H], H, \{1,1,1\}, \{1,1,1\}, 1]$  //. subInvariants //
Expand
Out[8]=  $N_c y \text{conj}[y]$ 
In[9]:= (4  $\pi$ )^2  $\gamma[\text{adj}[QL], QL, \{1,1,1\}, \{1,1,1\}, 1]$  //. subInvariants //
Expand
Out[9]=  $-\xi g^2 / (2 N_c) + N_c \xi / 2 g^2 + N_f / 2 y \text{conj}[y]$ 
```

This concludes the presentation of ARGES basic input and output functionality, which should be sufficient for a first instruction. In the next section we will turn towards a more advanced example, demonstrating a more specialised use of ARGES.

### 3.4.3 Advanced capabilities

Under the hood, ARGES optimises index summations by employing simplification rules like resolving KroneckerDelta contractions directly instead of brute-forcing  $\text{Sum}[\_\_\_]$ . This is critical for ARGES' performance, as such contraction sums are typically very long. Internally, they are simplified as expressions of the shape  $\text{SimplifySum}[\_\_\_]$ , and only in the last step converted

<sup>10</sup>In case of a  $U(1)$  gauge group, a dummy index 1 has to be provided.

back to Mathematica's built-in function `Sum[...]` (the syntax is compatible), if required.<sup>11</sup> This simplification can be enforced on any expression using `SimplifyProduct[...]`.

The user may inject custom simplification rules into this mechanism by adding them to the list `subSimplifySum`. This will be demonstrated by example of a theory with a  $SU(n)$  global symmetry and real scalars in the adjoint. The action of interest is

$$\mathcal{L} = \frac{1}{2} \partial_\mu \phi^A \partial^\mu \phi^A - \frac{1}{2} m^2 \phi^A \phi^A - \frac{1}{4} \lambda_1 (\phi^A \phi^A)^2 - \frac{1}{2} \lambda_2 \phi^A \phi^B \phi^C \phi^D (T^{ABCD} + T^{DCBA}), \quad (3.1)$$

where the the object

$$T^{ABC\dots} = \text{tr} [t^A t^B t^C \dots]. \quad (3.2)$$

are traces of  $t^A$ , the generator of the fundamental representation of  $SU(n)$ . These structures are difficult to resolve in general, but due to the completeness relation

$$t_{ab}^A t_{cd}^A = \frac{1}{2} (\delta_{ad} \delta_{bc} - \frac{1}{n} \delta_{ab} \delta_{cd}), \quad (3.3)$$

the Dynkin index definition, and the tracelessness of the generators, the following relations can be inferred

$$\begin{aligned} T &= \text{tr} [\mathbb{1}] = n, \\ T^A &= 0, \\ T^{AB} &= \frac{1}{2} \delta^{AB}, \\ \sum_A T^{B_1 \dots B_i A C_1 \dots C_j A D_1 \dots D_k} &= \frac{1}{2} (T^{B_1 \dots B_i D_1 \dots D_k} T^{C_1 \dots C_j} - \frac{1}{n} T^{B_1 \dots B_i C_1 \dots C_j} D_1 \dots D_k) \\ \sum_A T^{B_1 \dots B_i A C_1 \dots C_j T^{D_1 \dots D_k A E_1 \dots E_l}} &= \frac{1}{2} (T^{B_1 \dots B_i E_1 \dots E_l} D_1 \dots D_k C_1 \dots C_j - \frac{1}{n} T^{B_1 \dots B_i C_1 \dots C_j} T^{D_1 \dots D_k E_1 \dots E_l}). \end{aligned} \quad (3.4)$$

This also holds when index ranges like  $B_1 \dots B_i$  are empty. Using ARGES, the model (3.1) can be analysed by entering (3.4) into `subSimplifySum` using patterns. It can be assumed that sums over gauge and flavour indices are expanded and each term contained in `SimplifySum[...]` expression which is not nested.

```

1  <<ARGES '
2  Reset[];
3
4  NumberOfSubgroups=0;
5  RealScalar[phi, {n^2-1,1}, {}];
6  ScalarMass[m2, phi, phi, {}, KroneckerDelta[#1,#3]/2&];
7  ScalarQuartic[λ1, phi, phi, phi, phi, {}, KroneckerDelta[#1,#3]
   KroneckerDelta[#5,#7]/4&];
8  ScalarQuartic[λ2, phi, phi, phi, phi, {}, (T[#1,#3,#5,#7] + T
   [#7,#5,#3,#1])/2&];
9
10 subSimplifySum = {
11
12   T[] -> n,
13   T[_] :> 0,

```

<sup>11</sup>Disabling this last step with `DisableNativeSums[]` may in fact give a performance boost.

```

14      T[A_, B_] :=> 1/2 KroneckerDelta[A,B],
15
16      SimplifySum[c_ T[B___, A_, C___, A_, D___], sum1___, {A_, __},
          sum2___] :=> SimplifySum[c/2 (T[B, D] T[C] - T[B C D]/n ), sum1,
          sum2],
17      SimplifySum[T[B___, A_, C___, A_, D___], sum1___, {A_, __}, sum2___]
          :=> SimplifySum[1/2 (T[B, D] T[C] - T[B C D]/n ), sum1, sum2],
18
19      SimplifySum[c_ T[B___, A_, C___] T[D___, A_, E___], sum1___, {A_, __},
          sum2___] :=> SimplifySum[c/2 (T[B, E, D, C] - T[B C] T[D, E]/
          n ), sum1, sum2],
20      SimplifySum[T[B___, A_, C___] T[D___, A_, E___], sum1___, {A_, __},
          sum2___] :=> SimplifySum[1/2 (T[B, E, D, C] - T[B C] T[D, E]/n )
          , sum1, sum2],
21      SimplifySum[c_ T[B___, A_, C___]^2, sum1___, {A_, __}, sum2___] :=>
          SimplifySum[c/2 (T[B, C, B, C] - T[B C]^2/n ), sum1, sum2],
22      SimplifySum[T[B___, A_, C___]^2, sum1___, {A_, __}, sum2___] :=>
          SimplifySum[1/2 (T[B, C, B, C] - T[B C]^2/n ), sum1, sum2]
23  };

```

While the first three lines in `subSimplifySum` are the same as in (3.4), the second and third block cover the last two lines in (3.4) respectively, and account for complications due to possible prefactors and squares in the expression. Commencing with the evaluation, mass anomalous dimensions can be obtained in the usual way.

```

In[1]:=  $\beta[\text{phi}, \text{phi}, \{1,1\}, \{1,1\}, 0]$ 
Out[1]=  $m^2/24$ 
In[2]:=  $(4 \pi)^2 24/m^2 \beta[\text{phi}, \text{phi}, \{1,1\}, \{1,1\}, 1]$  // Expand
Out[2]=  $2 \lambda_1 + 2 n^2 \lambda_1 + 4 n \lambda_2$ 
In[3]:=  $(4 \pi)^4 24/m^2 \beta[\text{phi}, \text{phi}, \{1,1\}, \{1,1\}, 2]$  // Expand
Out[3]=  $-10 \lambda_1^2 - 10 n^2 \lambda_1^2 - 40 \lambda_1 \lambda_2 - 15 \lambda^2 - 5 n^2 \lambda_2^2$ 

```

In the quartic sector, the structures  $T[___]$  will reappear at both tree and loop level, and  $\beta$ -functions can be extracted from their prefactors. Alternatively, the  $T[___]$  may be completely removed by contracting external indices. In fact, we can even enforce the evaluation of the algebra as defined above by calling `SimplifyProduct[_]` on the contraction defined in terms of `SimplifySum[_]` instead of `Sum[_]`. At tree level, one possibility is for instance

```

In[4]:= c1 = SimplifyProduct[
          SimplifySum[
            12  $\beta[\text{phi}, \text{phi}, \text{phi}, \text{phi}, \{a,1\}, \{a,1\}, \{1,1\}, \{1,1\}, 0]$ ,
            {a, 1, n^2-1}
          ]
        ]
Out[4]=  $\lambda_1 + n^2 \lambda_1 + 2 n \lambda_2$ 
In[5]:= c2 = SimplifyProduct[
          SimplifySum[
            96 T[a, b, c, d]  $\beta[\text{phi}, \text{phi}, \text{phi}, \text{phi}, \{a,1\}, \{b,1\}, \{c,1\}, \{c,1\}, 0]$ ,
            {a, 1, n^2-1}, {b, 1, n^2-1}, {c, 1, n^2-1}, {d, 1, n^2-1}
          ]
        ]
Out[5]=  $2 n \lambda_1 + 4 n^3 \lambda - 4 \lambda_2 + 5 n^2 \lambda_2 + n^4 \lambda_2$ 

```

which is indeed free of the trace. This has to be matched up with the loop-level expressions

```
In[6]:= b1 = SimplifyProduct[
  SimplifySum[
    12 (4  $\pi$ )^2  $\beta$ [phi, phi, phi, phi, {a,1}, {a,1}, {1,1}, {1,1},
    1],
    {a, 1, n^2-1}
  ]
] // Simplify
Out[6]= 2 (7 + 8 n^2 + n^4)  $\lambda_1^2$  + 8 n (7 + n^2)  $\lambda_1 \lambda_2$ 
+ (95 + 24 n - 95 n^2 + 56 n^3)/(4 n)  $\lambda_2^2$ 

In[7]:= b2 = SimplifyProduct[
  SimplifySum[
    96 (4  $\pi$ )^2 T[a, b, c, d]  $\beta$ [phi, phi, phi, phi, {a,1}, {b,1},
    {c,1}, {c,1}, 1],
    {a, 1, n^2-1}, {b, 1, n^2-1}, {c, 1, n^2-1}, {d, 1, n^2-1}
  ]
] // Simplify
Out[7]= 4 n (7 + 15 n^2 + 2 n^4)  $\lambda_1^2$  - 8 (12 - 17 n^2 - 7 n^4)  $\lambda_1 \lambda_2$ 
+ 4 n (1 - 11 n^2 - n^4)  $\lambda_2^2$ 
```

which is left as a trivial exercise to the reader.

### 3.5 Conclusion

We have introduced ARGES, a new framework for the computation of renormalisation group equations. A comparison with existing software has detailed that ARGES is different by design, following a more algebraic than numerical approach to resolve index contractions. Setup, input and output are very straightforward, and yet the code is highly specialised and powerful, offering a maximum of user control. ARGES can be applied for simple toy models to most complex BSM theories – its interactive API invites a quick and dynamic working style. Moreover, ARGES handles models no existing framework is able to process, including theories with general gauge groups and representations, matrix scalars, highly complex potentials and even unknown vertex contractions. Its unique capability to insert information into the simplification process allows to adapt for computational challenges.

The sheer increase of complexity in computing RGE for complicated theories and high loop orders spells out the requirement for automation tools, and ARGES complementary design underpins its claim for niche among existing software, without undermining them.

In fact, ARGES has been utilised for every single chapter of this thesis. Due to the shortcomings of SARAH and PyR@TE when dealing with models like the one in [112], which are of special interest in this work, ARGES has played a key role in computing RGEs for [2–4] in particular, as well as the content of Ch. 4. Moreover, it was critically tested against the other tools, and employed in [1].

## 4 Theorems for exact asymptotic safety

### 4.1 Introduction

In this chapter, we will connect to [110], which has provided theorems outlining the field content and interactions of theories exhibiting weakly coupled asymptotic safety in  $d = 4$ . The objective is to refine the results of [110] to perturbatively exact QFTs, and constrain the structure and parameter space of models where asymptotic safety can be guaranteed. This is by no means a vain aspiration, as such models may represent a very functional building block to construct asymptotically safe QFTs.

As a prerequisite, the reader is strongly recommended to revisit Sec. 1.5 and Sec. 1.6, as it explains all the necessary technicalities required in sufficient detail. Nevertheless, we will reiterate the points most important.

It has been shown in [110, 111] that the existence of a weakly interacting UV fixed point requires a non-abelian gauge sector as well as a Yukawa interaction. This implies both fermionic and scalar matter fields. For this study, we restrict ourselves to simple gauge groups and a single Yukawa interaction, but will highlight some aspects of a generalisation. In order to establish a strict perturbative control, the Veneziano limit [228] is employed, suggesting that each field has a number of large indices running from  $1..N_i \rightarrow \infty$ , besides small ones from  $1..n_j$  that remain finite. The key mechanism is that after introducing 't Hooft couplings, the one-loop coefficient  $B$  of the gauge  $\beta$ -function (1.28) is controlled by a continuously tunable expansion parameter  $B \propto -\epsilon$ , which is given by  $\epsilon = \sum_i c_i N_i/N_j$ . Near the limit  $\epsilon \rightarrow +0$ , all quantities controlled by  $\epsilon$  become perturbatively exact.

In this setting, the existence of asymptotic safety is determined by coefficients of 2-loop gauge and 1-loop Yukawa  $\beta$ -functions (1.28), see (1.29), (1.36) and (1.37). The quantity  $\Delta$  as in (1.47) is indicative if the corresponding **GY** fixed point is indeed UV with  $\Delta < 0$  or IR with  $1 \geq \Delta \geq 0$ , in which case asymptotic safety is absent.

### 4.2 Classification

It has been argued in Sec. 1.6 that due to the large- $N$  limit, balancing powers of  $N$  in order to have the coefficient  $B$  in (1.28) tunable, and  $\Delta \neq 1$  requires  $SU(N_c)$ ,  $SO(N_c)$  or  $Sp(N_c)$  gauge groups, as well as that each field has exactly two large indices in the range  $1..N_i \rightarrow \infty$ , irrespective of whether these belong to the gauge or flavour symmetries. All relevant representations are collected in Tab. 6.1. The large index contraction at the Yukawa vertex is then schematically depicted as  $\asymp$ . Here, the left leg corresponds to the scalar, while the right ones are the fermions at the Yukawa vertex, while solid lines denote large indices. If we distinguish gauge indices as wiggly ( $\sim$ ) and flavour indices by straight lines ( $-$ ), depicting 2-index representations



(symmetric, antisymmetric, adjoint) as double lines, we find five classes of Yukawa contractions that can be illustrated as  $\begin{array}{c} \text{---} \text{---} \\ \text{---} \end{array}$ ,  $\begin{array}{c} \text{---} \text{---} \\ \text{---} \end{array}$ ,  $\begin{array}{c} \text{---} \text{---} \\ \text{---} \end{array}$ ,  $\begin{array}{c} \text{---} \text{---} \\ \text{---} \end{array}$  and  $\begin{array}{c} \text{---} \text{---} \\ \text{---} \end{array}$ . The case  $\begin{array}{c} \text{---} \text{---} \\ \text{---} \end{array}$  is invalid, as suitable gauge sector is either decoupled or missing completely. The contraction  $\begin{array}{c} \text{---} \text{---} \\ \text{---} \end{array}$  on the other hand is special because all large indices belong to the gauge sector. Its group dimension provides the only large parameter  $N$ . Without a second such quantity  $N'$  from a global symmetry, no tunable ratio  $N'/N$  exists, which is problematic for establishing perturbative control. We will investigate the case  $\begin{array}{c} \text{---} \text{---} \\ \text{---} \end{array}$  nevertheless.

The 5 classes  $\begin{array}{c} \text{---} \text{---} \\ \text{---} \end{array}$ ,  $\begin{array}{c} \text{---} \text{---} \\ \text{---} \end{array}$ ,  $\begin{array}{c} \text{---} \text{---} \\ \text{---} \end{array}$ ,  $\begin{array}{c} \text{---} \text{---} \\ \text{---} \end{array}$  and  $\begin{array}{c} \text{---} \text{---} \\ \text{---} \end{array}$  leave out certain details about the actual QFTs involved, which may however be decisive for asymptotic safety. These details are:

- (a) The gauge groups and representations.
- (b) Symmetrisations/antisymmetrisations in any of the indices.
- (c) Possible spectator fields.
- (d) If scalars real or complex.
- (e) If fermions are Majorana or Dirac.
- (f) The contractions of the small indices  $1..n_j$ .

Accounting for each of those intricacies make a extensive study very tedious. In the following, a careful analysis will be conducted taking these details into consideration, computing the coefficients  $B - F$  in the large- $N$  limit. Since we are mostly interested in the minimal reachable value of  $\Delta_{\min}$ , spectator fields not involved in the Yukawa interaction will be neglected, as they only increase  $\Delta$ . In detail, we will compute the coefficients  $B - F$  in (1.28), using  $\alpha_g = g^2/(4\pi)^2$  and  $\alpha_y = y^2/(4\pi)^2$ .

#### 4.2.1 Uncharged scalars

First, we will consider the class  $\begin{array}{c} \text{---} \text{---} \\ \text{---} \end{array}$ , where the scalar is uncharged. In this general discussion, we will consider  $N_{L,R}$  Weyl fermions  $\psi^{L,R}$  in the fundamental of a unitary, orthogonal or symplectic gauge group, bearing  $N_c$  gauge indices. Moreover,  $N_s$  uncharged real scalars  $\phi$  are included. The Yukawa coupling is given by

$$\mathcal{L}_{\text{yuk}} = -y_{ijk} \phi_i \psi_{aj}^{L\dagger} \psi_{ak}^R + \text{h.c.}, \quad (4.1)$$

where  $y_{ijk}$  is a general contraction of the global indices. This ansatz with  $N_s$  real degrees of freedom allows to account for the scalar to be either real or complex, and many global symmetries to be implemented. In fact, even a scalar singlet would be covered by this approach. The case of charged spectators is not considered here, as discussed earlier. As only the large- $N$  results are relevant, it is sufficient to define the contraction in terms of the following trace relations

$$y_{ikl}^* y_{jkl} = y^2 \delta_{ij}, \quad y_{ijl}^* y_{ikl} = y^2 \frac{N_s}{N_L} \delta_{jk}, \quad y_{ijl}^* y_{ijm} = y^2 \frac{N_s}{N_R} \delta_{lm}, \quad (4.2)$$

which are consistent with  $y_{ijk}^* y_{ijk} = y^2 N_s$ . Here, the single coupling  $y$  is the Yukawa interaction. A normalisation alternative to  $y^2$  could have been chosen, but the difference washes out in any physical observable, such as (1.47), which we are interested in. Due to leaving out further details of  $y_{ijk}$ , index contractions cannot be fully resolved in vertex corrections to coefficient  $E$  of (1.28).

However, these terms are subleading in the large- $N$  limit. The coefficients  $B$ – $F$  (1.28) read

$$\begin{aligned} B &= \frac{2}{3} \left[ 11 C_2^G - N_L - N_R \right], \\ C &= \frac{2}{3} \left[ -34 \left( C_2^G \right)^2 + \left( 5 C_2^G + 3 C_2^F \right) (N_L + N_R) \right], \\ D &= 2 N_s, \quad E = 4 N_c + \frac{N_s}{N_L} + \frac{N_s}{N_R}, \quad F = 12 C_2^F, \end{aligned} \quad (4.3)$$

where  $C_2^{G,F}$  are quadratic Casimirs invariants of the adjoint and fundamental representations in either of the  $SU(N_c)$ ,  $SO(N_c)$  or  $Sp(N_c)$ , using  $S_2^F = \frac{1}{2}$ ,  $d_F = N_c$  and  $d_G = 2 C_2^F N_c$ . The condition  $B = 0$  can be established via the replacement  $C_2^G = \frac{1}{11} (N_L + N_R)$ , which yields

$$\Delta = 1 - \frac{8 C_2^F N_s N_L N_R}{\left[ C_2^F + \frac{7}{121} (N_L + N_R) \right] [N_L + N_R] [4 N_c N_L N_R + N_s (N_L + N_R)]}. \quad (4.4)$$

Further analysis now requires to specify the gauge group. In the  $SU(N_c)$  case, anomaly cancellation requires  $N_L = N_R = N_f$ , and one obtains  $N_c = \frac{2}{11} N_f$ . For both  $SO(N_c)$  and  $Sp(N_c)$ , no triangle anomalies arise, but it turns out the the expression (4.4) is minimised for  $N_R = N_L = N_f$ , and one obtains  $N_c = \frac{4}{11} N_f$ .

In the case of  $N_f$  Majorana fermions  $\psi$ , the  $SU(N_c)$  gauge group is excluded as no invariant gauge contraction can be written down. The Yukawa interaction is replaced by

$$\mathcal{L}_{\text{yuk}} = -\frac{1}{2} y_{ijk} f^{ab} \phi_i \psi_{ja}^\dagger \varepsilon \psi_{bk} + \text{h.c.}, \quad (4.5)$$

with  $f$  being the gauge contractions of fundamental indices in  $SO(N_c)$  or  $Sp(N_c)$ . This results in the parameters

$$\begin{aligned} B &= \frac{2}{3} \left[ \frac{11}{2} N_c - N_f \right], \quad C = \frac{1}{6} N_c \left[ 13 N_f - 34 N_c \right], \\ D &= N_s, \quad E = 2 N_c + \frac{2 N_s}{N_f}, \quad F = 3 N_c. \end{aligned} \quad (4.6)$$

Finally, we parametrise the content of real scalar degrees of freedom via  $N_s = s N_f^2$ , collecting the results

$$\Delta = \begin{cases} \frac{100-88s}{100+275s} & \text{for } SU(N_c) \quad \text{Dirac} \\ \frac{50-88s}{50+275s} & \text{for } SO(N_c), Sp(N_c) \quad \text{Majorana} \\ \frac{200-88s}{200+275s} & \text{for } SO(N_c), Sp(N_c) \quad \text{Dirac.} \end{cases} \quad (4.7)$$

In any case, more scalar matter with the same fermion content improves the asymptotic safety of the gauge-Yukawa fixed point, with an universal asymptotic value for  $s \rightarrow \infty$

$$\Delta_{\min} = -\frac{8}{25}. \quad (4.8)$$

For complex scalars and  $SU(N_c)$  Dirac fermions ( $s = 2$ ) as well as  $SO(N_c)$  or  $Sp(N_c)$  Majoranas ( $s = 1$ ), a triality of asymptotically safe theories [3] exist with

$$\Delta_3 = -\frac{38}{325}. \quad (4.9)$$

The same models with real scalars ( $s \mapsto s/2$ ) or Dirac fermions with orthogonal or symplectic

$s = 2$  gauge groups and complex ones, belong to a larger equivalence class  $\Delta = 4/125$  without asymptotic safety. If the scalars are real in the latter case, the class is  $\Delta = 112/475$  instead. Many more example theories exist, in fact the spectrum of  $\Delta_3 \leq \Delta < 1$  is continuous. For instance, we may define a projection  $\mathcal{P}$  on any matrix scalar  $\phi_{ij}$  which just sets an arbitrary number of its components to zero. As the scalar is uncharged, replacing it with  $\phi_{ij} \mapsto (\mathcal{P} \phi)_{ij}$  everywhere in the Yukawa and scalar potential completely decouples the components projected out. This renders the parameter  $s$  continuously tunable in the large- $N$  limit.

The question remains if theories with  $\Delta_3 > \Delta > \Delta_{\min}$  exist. Their construction is non-trivial, introducing for instance a double copy of the scalar with an otherwise identical Yukawa contraction does not change the value of  $\Delta$ . This is because the change can be reabsorbed into field and coupling redefinitions, but  $\Delta$  is an independent physical quantity. The case is different when building a complex scalar out of two real components, as the global symmetry is modified. This indicates that symmetries may play a key role constructing asymptotically safe theories. The maximal flavour symmetry is  $SU(N_L + N_R) [SU(N_f)]$  for theories with Dirac [Majorana] fermions. In the Dirac case, the fermion bilinear in the Yukawa interaction breaks it down  $SU(N_L) \times SU(N_R)$ . The triality with  $\Delta = \Delta_3$  corresponds to the choices of models respecting the highest symmetry and hence the biggest global representation, guaranteeing the largest number of scalars. This, in turn, suggest that  $\Delta$  is maximised in these cases.

#### 4.2.2 Uncharged fermion

The class  $\rightsquigarrow$  is comparatively uncomplicated as the option for Majorana fermions is excluded. Instead,  $N_s$  real scalars  $\phi$  and  $N_f$  Weyl fermions  $\psi$ , both with  $N_c$  gauge indices as well as  $N_n$  uncharged fermions  $\chi$  are coupled together via the Yukawa interaction

$$\mathcal{L}_{yuk} = -y_{ijk} \phi_{ia} \psi_{ja}^\dagger \chi_k + \text{h.c.}, \quad (4.10)$$

following the relations

$$y_{ikl}^* y_{jkl} = y^2 \frac{N_n}{N_s} \delta_{ij}, \quad y_{ijl}^* y_{ikl} = y^2 \frac{N_n}{N_f} \delta_{jk}, \quad y_{ijl}^* y_{ijm} = y^2 \delta_{lm}. \quad (4.11)$$

The requirement for  $\phi$  to be complex in some cases is here transferred to the choice of  $N_s$  and detail of the contraction. Once more, small global symmetries are then absorbed into the choice of  $N_{s,f,n}$ . For a unitary gauge group, charged spectator fermions are required for anomaly cancellation. We will ignore this for the sake of discussion, computing only a lower bound for the actual  $\Delta$ . The the loop coefficients read

$$\begin{aligned} B &= \frac{2}{3} \left[ 11C_2^G - N_f - \frac{1}{4}N_s \right], \\ C &= \frac{2}{3} \left[ -34 \left( C_2^G \right)^2 + C_2^G \left( 5N_f + \frac{1}{2}N_s \right) + 3C_2^F \left( N_f + N_s \right) \right], \\ D &= N_n, \quad E = N_c + \frac{N_n}{N_f} + \frac{4N_n}{N_s}, \quad F = 6 C_2^F. \end{aligned} \quad (4.12)$$

This leads to the quantity

$$\Delta = \frac{N'_n \left( 100N_f^2 + 28N_fN_s + 9N_s^2 \right) + N_fN_s \left( 10N_f + 3N_s \right)^2 + N_f^2N_s^2}{(4N_f + N_s) (25N_f + 9N_s) (N'_n + N_fN_s)}, \quad (4.13)$$

with  $N'_n = 44N_n$  for an  $SU(N_c)$  or  $N'_n = 22N_n$  for  $SO(N_c)$ ,  $Sp(N_c)$  gauge groups. Choosing  $N'_n = nN_f^2$  and  $N_s = sN_f$ , the expression simplifies and gives a lower bound

$$\Delta = 1 - \frac{33ns}{(1+n)(4+s)(25+9s)} > \frac{8}{11}, \quad (4.14)$$

which is reached in the limit of infinitely many neutral fermions with  $n \rightarrow \infty$  and  $s = \frac{10}{3}$ . As  $\Delta > 0$ , asymptotic safety cannot be achieved within this class.

### 4.2.3 Two-index fermion

Turning towards the case  $\rightsquigarrow^{\text{ff}}$ , we have once more a topology that does not allow for Majorana fermions. With the scalar  $\phi$  and fermion  $\psi$  as in the case  $\rightsquigarrow^{\text{ff}}$ , the only difference are now  $n$  Weyl fermions  $\rho$  in a two-index representation  $R$  of the gauge group. The multiplicity  $n$  is integer-valued and remains finite in the Veneziano limit. In the Yukawa sector, the interaction

$$\mathcal{L}_{\text{yuk}} = -y_{ijk} h_{abI} \phi_{ia} \psi_{jb}^\dagger \rho_{Ik} + \text{h.c.} \quad (4.15)$$

now contains two generalised contractions, the global one with

$$y_{ikl}^* y_{jkl} = y^2 \delta_{ij}, \quad y_{ijl}^* y_{ikl} = y^2 \frac{N_s}{N_f} \delta_{jk}, \quad y_{ijl}^* y_{ijm} = y^2 \frac{N_s}{n} \delta_{lm}, \quad (4.16)$$

as well as a gauge index contraction

$$h_{abI}^* h_{dbI} = \frac{d_R}{N_c} \delta_{ad}, \quad h_{abI}^* h_{adI} = \frac{d_R}{N_c} \delta_{bd}, \quad h_{abI}^* h_{abJ} = \delta_{IJ}. \quad (4.17)$$

Computing the coefficients of (1.28), one obtains:

$$\begin{aligned} B &= \frac{2}{3} \left[ 11C_2^G - 2nS_2^R - N_f - \frac{1}{4}N_s \right], \\ C &= \frac{2}{3} \left[ -34 \left( C_2^G \right)^2 + 5C_2^G \left( N_f + 2nS_2^R \right) + 3C_2^F \left( N_s + N_f + \frac{4nN_c}{d_R} \left( S_2^R \right)^2 \right) \right], \\ D &= N_s \left[ \frac{d_R}{N_c} + 2S_2^R \right], \quad E = \frac{d_R}{N_c} \left[ 4 + \frac{N_s}{N_f} \right] + \frac{N_s}{n}, \quad F = 6C_2^F \left[ 1 + \frac{2N_c}{d_R} S_2^R \right]. \end{aligned} \quad (4.18)$$

Besides the usual relations, the Casimir of the two-index fermion has been replaced by the equivalent expression  $C_2^R = \frac{2N_c}{d_R} C_2^F S_2^R$ . This leads to a long expression for  $\Delta$ , which simplifies when considering all possibilities for the representation  $R$ . While the global symmetry can be very complicated, only three distinct cases for the gauge symmetry exist according to Tab. 6.1:

- (a) The gauge group is  $SU(N_c)$  and the 2-index fermion is in the adjoint representation  $R = G$ . In this case,  $n < 6$  is required for the limit  $B \rightarrow 0$ .
- (b) The gauge group is  $SU(N_c)$  and  $R$  is the 2-index symmetric or antisymmetric representation. This suggests  $n < 12$  is required for the perturbative exactness.

- (c) The gauge group is  $SO(N_c)$  or  $Sp(N_c)$  and the representation  $R$  is the symmetric or anti-symmetric one. This also requires  $n < 6$ .

Using again the parametrisation  $N_s = s N_f$ , one obtains:

$$\Delta = \begin{cases} 1 - \frac{27n(11-2n)s(4+s)}{(25+2n+9s)(44s+n(s^2+16))} & \text{for (a) and (c)} \\ 1 - \frac{27n(11-n)s(4+s)}{(25+n+9s)(88s+n(s^2+16))} & \text{for (b)} \end{cases}, \quad (4.19)$$

which are positive and reach the minimum

$$\Delta_{\min} \approx 0.2204 \quad \text{at} \quad s \approx 3.269 \quad \text{and} \quad \begin{cases} n = 2 & \text{for (a) and (c)} \\ n = 4 & \text{for (b)} \end{cases}, \quad (4.20)$$

thus excluding asymptotic safety. It is curious that for  $n \mapsto 2n$  in (b), (4.19) and the requirement  $n < 6$  becomes universal. Moreover, this implies (a) and (b) to have the same count of degrees of freedom in the large- $N$  limit. Hence, we suspect that all cases are related by orbifold projections and negative dimensionality theorems [3].

#### 4.2.4 Two-index scalar

The case  $\text{---}\text{---}\text{---}$  requires to combine the strategies of the previous cases. We will assume  $n$  real scalars  $\phi$  in a 2-index representation  $R$  of the gauge group, where  $n$  remains a finite integer. Both fundamental Majorana or Dirac fermions may be employed. We will first assume the latter with chiral components  $\psi^{L,R}$  and flavour multiplicity  $N_{L,R}$ , as well as a Yukawa interaction

$$\mathcal{L}_{\text{yuk}} = -y_{ijk} h_{Iab} \phi_{Ii} \psi_{ja}^{L\dagger} \psi_{kb}^R + \text{h.c.} \quad (4.21)$$

The flavour and gauge contractions are then given by

$$y_{ikl}^* y_{jkl} = y^2 \delta_{ij}, \quad y_{ijl}^* y_{ikl} = y^2 \frac{n}{N_L} \delta_{jk}, \quad y_{ijl}^* y_{ijm} = y^2 \frac{n}{N_R} \delta_{lm}, \quad (4.22)$$

as well as

$$h_{Iab}^* h_{Jab} = \delta_{IJ}, \quad h_{Iab}^* h_{Idb} = \frac{d_R}{N_c} \delta_{ad}, \quad h_{Iab}^* h_{Iad} = \frac{d_R}{N_c} \delta_{bd}. \quad (4.23)$$

Moreover, the parametrisation  $N_f^2 = N_L N_R$  and  $k = (N_L + N_R)/N_f \geq 2$  is introduced for convenience, leading to the coefficients

$$\begin{aligned} B &= \frac{2}{3} \left[ 11 C_2^G - \frac{1}{2} n S_2^R - k N_f \right], \\ C &= \frac{2}{3} \left[ -34 \left( C_2^G \right)^2 + 5 C_2^G \left( k N_f + \frac{n}{5} S_2^R \right) + 3 C_2^F \left( k N_f + \frac{8 n N_c}{3 d_R} \left( S_2^R \right)^2 \right) \right], \\ D &= \frac{2 n d_R}{N_c}, \quad E = 4 + \frac{k n d_R}{N_f N_c}, \quad F = 12 C_2^F. \end{aligned} \quad (4.24)$$

For  $N_f$  Majorana fermions, the same coefficients  $B$ ,  $C$  and  $F$  are obtained with  $k = 1$  and  $d_R = \frac{1}{2} N_c^2$ , the others are

$$D = \frac{n d_R}{N_c}, \quad E = 2 + 2 \frac{n d_R}{N_f N_c}. \quad (4.25)$$

Once again, this leads to several distinct cases for the gauge representation:

- (a) The gauge group is  $SU(N_c)$ , which is only viable with Dirac fermions and  $k = 2$ , and the scalar is in the adjoint representation. This requires  $n < 22$ .
- (b) The gauge group is  $SU(N_c)$ , which is only viable with Dirac fermions and  $k = 2$ , and the scalar is in the symmetric or antisymmetric representation. This requires  $n < 44$ .
- (c) The gauge group is  $SO(N_c)$  or  $Sp(N_c)$ ,  $R$  is either the symmetric or antisymmetric representation, the fermions are of Dirac-type with  $k \geq 2$ , requiring  $n < 22$ .
- (d) The gauge group is  $SO(N_c)$  or  $Sp(N_c)$ ,  $R$  is either the symmetric or antisymmetric representation, the fermions are of Majorana-type with  $k = 1$ , requiring  $n < 22$ .

Hence, only case (c) allows for a variable parameter  $k$ , as it is fixed in the other cases by either the Majorana nature or anomaly cancellation. Computing the quantity  $\Delta$  in (c) yields

$$\Delta^{(c)} = 1 - \frac{12n(22 - n)}{5(10 + n)(44 + n(k^2 - 2))}, \quad (4.26)$$

which is minimised by the choice  $k = 2$ , meaning  $N_L = N_R$ . Collecting all cases, one obtains

$$\Delta \geq \begin{cases} \frac{11}{5} + \frac{32}{10+n} - \frac{484}{5(22+n)} & \text{for (a), (c) and (d)} \\ \frac{11}{5} + \frac{64}{20+n} - \frac{968}{5(44+n)} & \text{for (b)} \end{cases}, \quad (4.27)$$

which leads to a minimal coefficient  $\Delta_{\min} = \frac{26}{35}$ , reachable in all cases with  $n = 6$  [ $n = 12$  for (b)], excluding asymptotic safety. We observe the same phenomenon regarding the redefinition  $n \mapsto 2n$  in case (b) as already for  $\mathcal{N} = 4$ , and we draw the same conclusions.

#### 4.2.5 All fields 2-index gauged

For completeness, we will briefly consider the case  $\mathcal{N} = 4$ , although a smooth limit  $B \rightarrow 0$  is not possible, as the fermions and scalars have finite integer multiplicities  $n_{L,R}$  and  $n_S$ . Allowing for these multiplicities to be continuous, there are four distinct cases of gauge groups and representations to consider

- (a) The gauge group is  $SO(N_c)$  or  $Sp(N_c)$ , the fermions are of Dirac-type and each field is either in the symmetric or antisymmetric representation. No triangle anomalies arise. The quantity  $\Delta$  is minimised for  $n_L = n_R$  and  $n_L + n_R = n_f$ .
- (b) The gauge group is  $SO(N_c)$  or  $Sp(N_c)$ , the  $n_f$  fermions are Majoranas.
- (c) The gauge group is  $SU(N_c)$  and the fermions are of Dirac-type. For each field  $i = \{L, R, S\}$  a variable  $c_i$  can be introduced, depending on whether the representation is the adjoint ( $c_i = 1$ ) or the symmetric/antisymmetric one ( $c_i = 1/2$ ). They give rise to different Dynkin indices  $S_2^i = c_i N_c$  and dimensions  $d_i = c_i N_c^2$  of the representations. Rewriting  $d_i = N_c S_2^i$ , a redefinition of multiplicities  $n_i \mapsto n_i/c_i$  absorbs these distinctions. As before the quantity  $\Delta$  is minimised for  $n_L = n_R = \frac{1}{2} n_f$ . This case also cancels all anomalies.
- (d) The case of  $n_f$   $SU(N_c)$  Majorana fermions is only viable with adjoint representations for all fields in order to avoid anomalies and retain gauge invariance for the contraction over the Yukawa vertex.

Universally for all cases, the shape of the gauge coefficient

$$B \propto N_c (22 - 4n_f - n_S) \quad (4.28)$$

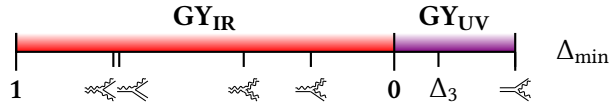
allows to substitute for  $n_s$  as long as  $n_f < \frac{11}{2}$ . As this class is an edge case, we will refrain from giving coefficients in (1.28) for each of the cases in detail. Instead, we will provide the quantity

$$\Delta \geq 1 - \frac{6 n_f \left( \frac{11}{2} - n_f \right)}{220 - 52 n_f + 3 n_f^2} \gtrsim 0.398 \text{ at } n_f \approx 4.12, \quad (4.29)$$

which is universal. The smallest  $\Delta$  for  $n$  being integers have  $\Delta_{\min} = \frac{2}{5}$  at  $n_f = 4$  and  $n_s = 6$ , for which  $B = 0$ .

### 4.3 Discussion

**Summary.** We have computed  $\Delta_{\min}$  for each of the perturbatively exact classes  $\Rightarrow$ ,  $\Leftarrow$ ,  $\Leftarrow$ ,  $\Leftarrow$  and  $\Leftarrow$ , summarised in Fig. 4.1.



**Figure 4.1:** Minimal values of  $\Delta$  (1.47) for each Yukawa topology. The value  $\Delta_3$  is given by (4.9).

This proves that merely the class  $\Leftarrow$  may exhibit perturbatively exact asymptotic safety beyond freedom. Moreover, a lower bound for the spectrum of  $\Delta$  was discovered:  $1 \geq \Delta \geq -8/25$ . It is clear that  $\Leftarrow$  has a densely populated spectrum  $1 \geq \Delta \geq \Delta_3$ , and we have conjectured that  $\Delta_3 > \Delta > -8/25$  is not realised by any consistent QFT. This would mark the theories [3, 112] as the most asymptotically safe ones.

In the following, we will give an outlook on how these results generalise beyond the limitations of our analysis. We will start with loosening the restrictions of the gauge group.

**Semi-simple gauge groups.** The advocated notion of perturbative exactness is in fact compatible with having several gauge interactions, as long as the restriction of exactly two large indices per field is honoured. Up to two-loop order, the gauge  $\beta$ -function is then given by

$$\begin{aligned} \beta_{g_i} &= \alpha_{g_i}^2 \left[ -B_i + C_{ij} \alpha_{g_j} - D_i \alpha_y \right], \\ \beta_y &= \alpha_y \left[ E \alpha_y - F_i \alpha_{g_i} \right]. \end{aligned} \quad (4.30)$$

The usual coefficients  $B_i$  and  $C_{ii}$  (1.29) experience the gauge subgroups  $j \neq i$  as global symmetries, i.e. their matter representations are just global multiplicities. However, the new coefficient  $C_{ij}$  as in (1.43) interweaves the gauge sectors. Inserting the nullcline condition  $E \alpha_y = F_i \alpha_{g_i}$  into (4.30), gives  $\beta_{g_i} = \alpha_{g_i}^2 \left[ -B_i + C'_{ij} \alpha_{g_j} \right]$  where

$$C'_{ij} = C_{ij} - \frac{D_i F_j}{E}. \quad (4.31)$$

Due to the technical naturalness of each gauge symmetry, several **GY** solutions exist at this loop order, where each gauge coupling is either interacting or vanishing. Cases with one Yukawa coupling and a single gauge group interacting at the fixed point then fall back onto the 5 classes above.

**Free sectors.** As already observed earlier, several gauge groups in (4.30) introduce an effective one-loop coefficient

$$B_i^{\text{eff}} = B_i - C_{ij \neq i} \alpha_{g_j} + D_i \alpha_y, \quad (4.32)$$

for a vanishing coupling  $\alpha_{g_i}$ . Hence, asymptotic freedom might be enabled although it should be lost, if  $B_i < 0 < B_i^{\text{eff}}$ . This requires at least one non-vanishing coupling  $g_j$ , admitting a **GY** fixed point. A consequence are fixed points like **G**<sub>UV</sub>  $\times$  **GY**<sub>IR</sub>: asymptotic freedom in a non-free coupling  $g_1$  may be established, even though the fixed point is of infrared gauge-Yukawa-type in the  $g_2$ -direction [114, 115]. In particular, this mechanism is relevant for small-index gauge sectors, for instance  $U(1)$  gauge groups. The violation of our requirements for two large indices for the gauge field is without consequence, as it is decoupled at the fixed point. Being unaffected by the Veneziano limit, such gauge sectors are matter dominated. Considering the example with a small gauge sector with coupling  $g_1$ , and a large one with  $g_2$ , large- $N$  scalings read

$$B_{1,2} \propto N^{2,1}, \quad C_{11,22} \propto N^2, \quad C_{12} \propto N^3, \quad D_{1,2} \propto N^{3,2}, \quad E \propto N, \quad F_2 \propto N. \quad (4.33)$$

At the fixed point, we have  $\alpha_{g_1}^* = 0$  and  $\alpha_y^* = \frac{F_2}{E} \alpha_{g_2}^*$ . Hence, in the vicinity of the **G**  $\times$  **GY**, the effective coefficient reads

$$B_1^{\text{eff}} = B_1 - C_{12} \alpha_{g_2}^* + D_1 \alpha_y^* = B_1 - \left[ C_{12} - \frac{D_1 F_2}{E} \right] \alpha_{g_2}^* = B_1 - B_2 \left[ \frac{C'_{12}}{C'_{22}} \right]. \quad (4.34)$$

Keeping in mind that  $\alpha_{g_2}^* \propto N^{-1}$  since we have not employed 't Hooft couplings, yields  $B_1^{\text{eff}} \propto N^2$ , which is indeed the same scaling as for the unshifted coefficient  $B_1$ .

**Interacting subgroups.** In order to retain perturbative control, the condition  $B_i \approx \mp 0$  is mandatory for all groups with  $\alpha_{g_i}^* \neq 0$ . In practice, this is non-trivial to achieve, especially when additional conditions for anomaly cancellation are required. Moreover, a Yukawa interaction is necessary, as the matrix  $C_{ij}$  in (4.30) only has positive components in this case. For each non-vanishing gauge coupling, the values  $\alpha_{g_i}^* \neq 0$  can be determined via  $0 = -B_i + C'_{ij} \alpha_{g_j}^*$ . Therefore the eigenvalues of  $C'$  are decisive for the UV attractiveness of these **GY**-type fixed points. In our case of a single Yukawa coupling, the system is parametrised by (4.30), and the matrix  $C'$  computed via (4.31). If  $C'$  was diagonal, the case of semi-simple gauge groups would just decouple into independent discussions of each simple subgroup. The question is how off-diagonal elements  $C'_{ij}$  compare to diagonal ones like  $C'_{ii}$ . If they have negative signs, the mechanism for asymptotic safety is strengthened by these elements, while it is weakened in the positive case. Let us now accommodate two gauge couplings  $g_1$  ( $\sim$ ) and  $g_2$  ( $\dashv$ ). This is not possible in  $\mathcal{N}=4$  SYM, and we will drop this case. Inserting the nullcline condition  $E \alpha_y^* = F_i \alpha_{g_i}^*$  as well as using the definitions (4.31), (1.43) and (1.36), one can parametrise

$$C'_{ij \neq i} = G_i C_2^{\text{fun}_j}. \quad (4.35)$$

Here,  $C_2^{\text{fun}_j}$  denotes the quadratic Casimir of the fundamental representation. This factorises the influence of both gauge groups on the off-diagonal elements of  $C'$ .



Borrowing the notation from the case  $\text{---}\text{---}\text{---}$ , we obtain

$$\text{---}\text{---}\text{---} : \quad G_1 = 2N_s - 6DE^{-1} = 2N_s \frac{N_n (N_f + N_s) + N_c N_f N_s}{N_n (4N_f + N_s) + N_c N_f N_s} > 0, \quad (4.36)$$

The first two terms stem from (1.43) and denote Dynkin indices of fields charged under both subgroups. In the last term the prefactor is determined by  $F_2$ , see (1.36). The result also suggests that  $G_2 > 0$  when  $(\text{---}\text{---}\text{---}) \leftrightarrow (\text{---}\text{---}\text{---})$ . This means  $\text{---}\text{---}\text{---}$  does not allow for an interacting UV fixed point beyond asymptotic freedom of both subgroups. In a similar vein,

$$\begin{aligned} \text{---}\text{---}\text{---} : \quad G_1 &= 2N_f + 2N_s - 6DE^{-1} = \frac{N_s}{n} + \frac{2(2N_f - N_s)^2}{4N_f + N_s} > 0, \\ \text{---}\text{---}\text{---} : \quad G_1 &= 2N_s + 2N_f - 18DE^{-1} = 2 \frac{N_n (2N_f - N_s)^2 + N_c N_f N_s (N_f + N_s)}{N_n (4N_f + N_s) + N_c N_f N_s} > 0, \end{aligned} \quad (4.37)$$

where the first and second line use the results of  $\text{---}\text{---}\text{---}$  and  $\text{---}\text{---}\text{---}$  respectively. Moreover, the expression of  $G_1$  for  $\text{---}\text{---}\text{---}$  is universal for all choices of viable gauge groups and representations. Hence  $\text{---}\text{---}\text{---}$  or equivalently  $\text{---}\text{---}\text{---}$  are excluded from developing an interacting UV fixed point beyond freedom, for any parameter choices. The same guarantees cannot be given for  $\text{---}\text{---}\text{---}$ ,  $\text{---}\text{---}\text{---}$  and the respective cases with  $(\text{---}\text{---}\text{---}) \leftrightarrow (\text{---}\text{---}\text{---})$ . Here,  $G_{1,2}$  are negative for some parameter regions. In all of those cases one of the subgroups is in the  $\text{---}\text{---}\text{---}$  class, which is already unique for enabling  $\mathbf{GY}_{UV}$  with a simple gauge setting. We conclude that within our setup, a  $\text{---}\text{---}\text{---}$  subsector is a necessary requirement for asymptotic safety beyond freedom, but will not pursue a more detailed analysis within this work.

**Multiple Yukawa couplings.** Considering several Yukawa couplings  $y_n$  which are non-overlapping, i.e. they do not share any attached fields, the system becomes

$$\begin{aligned} \beta_{g_i} &= \alpha_{g_i}^2 \left[ -B_i + C_{ij} \alpha_{g_j} - D_{in} \alpha_{y_n} \right], \\ \beta_{y_n} &= \alpha_{y_n} \left[ E_n \alpha_{y_n} - F_{ni} \alpha_{g_i} \right]. \end{aligned} \quad (4.38)$$

It is obvious from (1.29) that matter contributions are linear in coefficients  $B_i$  and  $C_{ij}$ . Hence, they can be split up into matter belonging to the non-overlapping Yukawa sectors as well as an offset  $B_i^0$ ,  $C_{ij}^0$  from gauge-boson self-interactions. Assuming there are no leftover spectator fields, this means  $B_i = B_i^0 + \sum_n B_i^n$ ,  $C_{ij} = C_{ij}^0 + \sum_n C_{ij}^n$ . Coefficients  $D_{in}$ ,  $E_n$  and  $F_{in}$  on the other hand are properties of the Yukawa couplings (1.36) and do not decompose further like  $B_i$  and  $C_{ij}$ . Inserting the nullcline condition, we obtain

$$C_{ij}'^n = C_{ij}^n - \frac{D_{in} F_{nj}}{E_n}, \quad C_{ij}' = C_{ij}^0 + \sum_n C_{ij}'^n. \quad (4.39)$$

Overall, the conditions  $B_i \approx 0$  implies that in spite of the theory gaining more diversity, there is not more charged matter admitted than before. Moreover,  $C_{ij}|_{B=0} > 0$  remains true. The question arises if multiple Yukawas improve the situation for a  $\mathbf{GY}_{UV}$  fixed point. Consider a single gauge group, but with many non-overlapping Yukawas. While the gauge group remains fixed, the matter multiplicities are scaled back by  $\xi_n$  for each Yukawa sector with  $\sum_n \xi_n = 1$  and  $0 < \xi_n \leq 1$ .

In particular, this means  $B^n \propto \xi_n$  and  $C^n \propto \xi_n$  for each model, ensuring  $B = 0 = B^0 + \sum_n B^n$ . Furthermore,  $B^0$ ,  $C^0$  and each  $F_n$  are independent of all  $\xi_m$ . We have seen that





$$\begin{aligned} \text{---}\diagdown\diagup\text{---}, \quad \text{---}\diagdown\diagup\text{---} & : D_n \propto \xi_n^2, \quad E_n > \xi_n(E_n|_{\xi_n=1}), \\ \text{---}\diagdown\diagup\text{---}, \quad \text{---}\diagdown\diagup\text{---} & : D_n \propto \xi_n, \quad E_n \propto \xi_n, \end{aligned} \tag{4.40}$$

while the scaling of the small multiplicities in  $\mathcal{M}_{\text{small}}$  is not clear. For the other cases, the inequalities

$$\left| \xi_n C^0 + C^n - \frac{D_n F_n}{E_n} \right| \leq \xi_n \left| C^0 + C'^n \right|_{\xi_{n=1}} \Rightarrow C - C' \leq \max_n \left[ \frac{D_n F_n}{E_n} \right]_{\xi_{n=1}} \quad (4.41)$$

hold. This scaling behaviour shows that at  $B = 0$ , two-loop shifts  $C - C'$  of a theory with a single Yukawa interaction cannot be improved by having several non-overlapping Yukawa sectors. Therefore,  $\Rightarrow$  remains a crucial requirement for **GY**<sub>UV</sub>. If the fields are overlapping, additional contributions to  $D_n$  and  $E_n$  arise. However, a complete analysis is complicated and beyond the scope of this discussion.

**Scalar quartic sector.** Inserting potential fixed point solutions of the gauge-Yukawa system into the scalar quartic RGEs provides an additional set of constraints. In particular, fixed points might be invalidated by becoming complex (merger) or result have an unstable scalar potential. The general shape of the RG system has been introduced in (1.28). The exact number of quartics varies even within each class, and not many statements can be made without descending into more details of the theory. In this sense, it is not possible to make general remarks, in particular about the stability of the scalar potential. However, some observations can be made from the shape of the  $\beta$ -functions.

Due to all fields being matrix-like, quartics are either single ( $u_i$ ) or double traced ( $v_i$ ) in the large indices, see (1.49). In the large- $N$  limit, leading contributions of each type then scale  $\propto N u_i$  and  $\propto N^2 v_i$  respectively. At one-loop order, scalar self-interactions  decompose into   $\propto N u_i u_j$ ,   $\propto N u_i v_j$  and   $\propto N^2 v_i v_j$ . Both points together imply that single-trace quartics form another algebraically decoupled system at this order, given by

$$\beta_{u_i} = (4\pi)^{-2} N \left[ H^{ijk} u_j u_k - I_g^{ij} g^2 u_j + I_y^{ij} y^2 u_j + J_g^i g^4 - J_y^i y^4 \right]. \quad (4.42)$$

Signs of the coefficients depend on coupling definitions, but in most cases they can all be chosen non-negative. Evaluating  $\beta_{u_i} = 0$  means solving a set of quadratic equations. The main sources of complex solutions are the inhomogeneity terms  $J_g^i$  of the gauge interaction. Within the Yukawa classes, once again only  $\mathbb{E}_6$  stands out by having all  $J_g = I_g = 0$  due to the scalar being uncharged. This improves the resilience of the quartic sector against complex solutions, while inviting negative ones. For example, consider a theory with only one gauge, Yukawa and single-trace quartic coupling each. The solutions are

$$u^* = \frac{g^{*2}}{2H} \left[ I_g - \frac{F}{E} I_y \pm \sqrt{\left( I_g - \frac{F}{E} I_y \right)^2 + 2H \left( \frac{F^2}{E^2} J_y - J_g \right)} \right] \quad (4.43)$$

over the **GY** fixed point, and the same expression with  $I_y, J_y \mapsto 0$  over a **BZ** one. In both cases, complex values are indeed absent for  $J_g = 0$ .

The only inhomogeneities in the double-trace quartic system stem from subleading single-trace self-interactions:

$$\beta_{v_i} = (4\pi)^{-2} \left[ \tilde{H}_{uu}^{ijk} u_j u_k + N \tilde{H}_{uv}^{ijk} u_j v_k + N^2 \tilde{H}_{vv}^{ijk} v_j v_k - N \tilde{I}_g^{ij} g^2 v_j + N \tilde{I}_y^{ij} y^2 v_j \right]. \quad (4.44)$$

Once again, we have  $\tilde{I}_g = 0$  for  $\Rightarrow_{\text{IR}}$ . This suggests that some of the  $v_i$  may need to be negative to achieve  $\beta_{v_i} = 0$ , which endangers vacuum stability.

**Equivalences.** Each class investigated here contains several universality classes of conformal field theories at the **GY** fixed point, irrespective of whether it is **GY<sub>UV</sub>** or **GY<sub>IR</sub>**. These theories may even be equivalent away from the fixed point in the weakly coupled regime, due to a generalised orbifold equivalence and negative dimensionality theorems [3]. Indications of this have been spotted within our analysis, and the topic will be elaborated in Ch. 6.

## 5 UV conformal window for asymptotic safety

### 5.1 Introduction

In recent years the asymptotic safety conjecture [32] has grown into a powerful paradigm of its own, with many applications ranging from quantum gravitation to particle physics and critical phenomena [57]. It states that quantum field theories remain well-defined and predictive up to highest energies provided they are governed by an interacting UV fixed point under their renormalisation group evolution of couplings [171]. Asymptotic safety generalises the notion of asymptotic freedom [84, 85]. The most striking new effects are residual interactions in the UV which modify canonical power counting and the dynamics of theories at shortest distances [41]. Asymptotic safety has originally been proposed to cure the high energy behaviour of  $4d$  quantum gravity by means of an interacting UV fixed point [32]. A lot of progress has been made over the past decades to substantiate the feasibility for an asymptotically safe version of quantum gravity [35, 37, 41, 54, 56, 57, 251–253]. In  $3d$  settings, asymptotic safety is known to arise in models with scalars, or fermions, or both. In suitable large- $N$  limits, exact results at weak coupling are available from the renormalisation group [68, 69, 71, 74], including models with supersymmetry or spontaneously broken scale invariance [254–256]. Lattice results are available for non-linear sigma models [257]. More recently, it has been discovered that asymptotic safety is operative in  $4d$  gauge theories with matter [112]. For this to happen at weak coupling, all three types of elementary fields – gauge fields, fermions, and scalars – are required, together with suitable Yukawa couplings [110]. By now, necessary and sufficient conditions alongside strict no-go theorems for asymptotic safety of general gauge theories are known [110, 258]. Explicit proofs for asymptotic safety have been given for simple [112], semi-simple [114] and supersymmetric gauge theories coupled to matter [115]. Coleman-Weinberg resummations [113], the impact of interactions with negative canonical mass dimensions [233] and fixed points for models away from  $4d$  [67] have also been investigated. Asymptotically safe extensions of the Standard Model and their signatures at colliders have first been put forward in [121].

An important open question relates to the size of the conformal window for asymptotically safe gauge theories, meaning the range in parameter space where a viable interacting UV fixed point persists. While interacting UV fixed points are under good control at weak coupling, much less is known about asymptotic safety at strong coupling [41]. On the other hand, IR conformal windows of QCD-like theories have been studied more extensively. There, conformal windows are known to extend into the domain of strong coupling [96, 259–261]. Similar insights into UV conformal windows would be most useful, both conceptually, and from the viewpoint of phenomenology and model building.

In this paper, we access the conformal window with the help of perturbation theory. It is shown how fixed points, scaling exponents, and anomalous dimensions are obtained as a systematic power series in a small parameter (Sect. 5.2). We analyse the systematics of perturbative approximations for general theories with weakly interacting fixed points and compare the ordering principle with conventional perturbation theory and Weyl consistency condition. The work of [112] is extended to derive the requisite beta functions, fixed points, anomalous dimensions, and scaling exponents at the complete next-to-next-to-leading order (Sect. 5.3). A consistent picture for the conformal window is uncovered by comparing various levels of approximation, with vacuum stability offering the tightest constraints (Sect. 5.4). Implications for model building and cosmology are indicated as well. We close with a brief discussion (Sect. 5.5). Some technicalities are summarised in an Appendix (App. 5.5).

## 5.2 Asymptotic safety

In this section, we recall the model of [112] in the Veneziano limit, and provide its beta function for all canonically massless couplings up to 3-loop (2-loop) order in the gauge (Yukawa, scalar) beta functions, and all anomalous dimensions up to 2-loop. We also discuss the underlying systematics for expansions in perturbation theory.

### 5.2.1 The model

We consider  $4d$  massless quantum field theories with  $SU(N_C)$  gauge fields  $A_\mu^a$  with field strength  $F_{\mu\nu}^a$ , coupled to  $N_F$  flavors of fermions  $Q_i$  in the fundamental representation. The theory also contains a scalar singlet “meson” field  $H$ , a  $N_F \times N_F$  complex matrix uncharged under the gauge group, which interacts with the fermions via a Yukawa term. The theory has a global  $SU(N_F) \times SU(N_F)$  flavor symmetry. The action is taken to be the sum of the Yang-Mills action, the fermion and scalar kinetic terms, the Yukawa term, and the scalar self-interaction Lagrangean

$$L = L_{\text{YM}} + L_{\text{kin.}} + L_{\text{Yuk.}} + L_{\text{pot.}} \quad (5.1)$$

where

$$\begin{aligned} L_{\text{YM}} &= -\frac{1}{2} \text{tr} F^{\mu\nu} F_{\mu\nu} \\ L_{\text{kin.}} &= \text{tr} (\bar{Q} i \not{D} Q) + \text{tr} (\partial_\mu H^\dagger \partial^\mu H) \\ L_{\text{Yuk.}} &= -y \text{tr} (\bar{Q}_L H Q_R) + \text{h.c.} \\ L_{\text{pot.}} &= -u \text{tr} (H^\dagger H H^\dagger H) - v (\text{tr} H^\dagger H)^2. \end{aligned} \quad (5.2)$$

$\text{tr}$  is the trace over both color and flavor indices, and the decomposition  $Q = Q_L + Q_R$  with  $Q_{L/R} = \frac{1}{2}(1 \pm \gamma_5)Q$  is understood. The theory has four canonically marginal couplings given by the gauge coupling  $g$ , the Yukawa  $y$  and two quartic scalar couplings  $u$  and  $v$ . The theory is renormalisable in perturbation theory.

### 5.2.2 Veneziano limit

To prepare for the Veneziano (large- $N$ ) limit with finite couplings [228], we rescale the four canonically dimensionless couplings with suitable powers of field multiplicities,

$$\alpha_g = \frac{g^2 N_C}{(4\pi)^2}, \quad \alpha_y = \frac{y^2 N_C}{(4\pi)^2}, \quad \alpha_u = \frac{u N_F}{(4\pi)^2}, \quad \alpha_v = \frac{v N_F^2}{(4\pi)^2}. \quad (5.3)$$

The theory is then characterised by two free parameters  $N_C$  and  $N_F$ , related to the field multiplicities. In the Veneziano limit, these are sent to infinity while the ratio is kept fixed. This procedure reduces the set of free parameters down to one, which we chose to be

$$\epsilon = \frac{N_F}{N_C} - \frac{11}{2}. \quad (5.4)$$

In the Veneziano limit,  $\epsilon$  is a continuous parameter taking values within  $[-11/2, \infty]$ . For  $\epsilon < 0$ , the theory is asymptotically free in all couplings. Trajectories running out of the Gaussian fixed point are trivially “UV complete”. For  $\epsilon > 0$ , asymptotic freedom of the gauge sector is lost. In this regime, and for sufficiently small  $\epsilon$ , the theory develops an interacting UV fixed point. Strict perturbative control for an asymptotically safe UV fixed point is guaranteed as long as

$$0 \leq \epsilon \ll 1, \quad (5.5)$$

which is the regime of interest for the rest of this work.

### 5.2.3 Renormalisation group

Quantum effects and the energy-dependence of couplings are encoded in the RG beta functions, which are obtained in the  $\overline{\text{MS}}$  renormalisation scheme [182–185, 187]. For small coupling, the perturbative loop expansion is reliable, and we write

$$\beta = \beta^{(1)} + \beta^{(2)} + \beta^{(3)} + \dots \quad (5.6)$$

for any of the beta functions  $\beta \equiv d\alpha/d \ln \mu$ . Here, we denote with  $\beta^{(n)}$  the  $n^{\text{th}}$  loop contribution. Some technicalities in the derivation of beta functions from general expressions are summarised in App. 5.5.

In concrete terms, the gauge beta function  $\beta_g$  up to three loops is given by

$$\begin{aligned} \beta_g^{(1)} &= \frac{4}{3} \epsilon \alpha_g^2, \\ \beta_g^{(2)} &= \left(25 + \frac{26}{3} \epsilon\right) \alpha_g^3 - 2 \left(\frac{11}{2} + \epsilon\right)^2 \alpha_y \alpha_g^2, \\ \beta_g^{(3)} &= \left(\frac{701}{6} + \frac{53}{3} \epsilon - \frac{112}{27} \epsilon^2\right) \alpha_g^4 \\ &\quad - \frac{27}{8} (11 + 2\epsilon)^2 \alpha_g^3 \alpha_y + \left(\frac{11}{2} + \epsilon\right)^2 (20 + 3\epsilon) \alpha_y^2 \alpha_g^2. \end{aligned} \quad (5.7)$$

Up to three loop, the running of the gauge coupling is only sensitive to the gauge and Yukawa coupling. Subleading terms of the order  $\sim 1/N_F$  and  $\sim 1/N_C$  do not contribute in the Veneziano limit and have been suppressed.

Couplings	Orders in perturbation theory							Scheme
$\beta_{\text{gauge}}$	1	1	2	2	2	3	3	
$\beta_{\text{Yukawas}}$	0	1	1	1	2	2	2	3
$\beta_{\text{quartics}}$	0	1	0	1	2	1	2	3
	LO		NLO		2NLO		PT	
	LO'		NLO'		2NLO'		FP	
	LO''		NLO''		2NLO''		Weyl	

**Table 5.1:** Approximation schemes sorted according to the loop orders retained in the various beta functions, comparing perturbation theory (PT), fixed point consistency conditions (FP) [112, 113], and Weyl consistency conditions (Weyl), each to leading (LO), next-to-leading (NLO) and next-to-next-to-leading (2NLO) order.

The Yukawa beta function  $\beta_y$  up to two loops is given by

$$\begin{aligned}
\beta_y^{(1)} &= (13 + 2\epsilon) \alpha_y^2 - 6 \alpha_y \alpha_g, \\
\beta_y^{(2)} &= \frac{20\epsilon - 93}{6} \alpha_g^2 \alpha_y + (49 + 8\epsilon) \alpha_g \alpha_y^2 \\
&\quad - 4 \left[ (11 + 2\epsilon) \alpha_y - \alpha_u \right] \alpha_u \alpha_y - \left( \frac{385}{8} + \frac{23\epsilon}{2} + \frac{\epsilon^2}{2} \right) \alpha_y^3.
\end{aligned} \tag{5.8}$$

The Yukawa beta function depends on the gauge and Yukawa couplings, at any loop order. From two loop level onwards, it also depends on the scalar coupling  $\alpha_u$ . In the Veneziano limit, neither (5.7) nor (5.8) depends on the double-trace scalar coupling  $\alpha_v$ , at any loop order.

The beta function for the single trace scalar quartic coupling  $\beta_u$  up to two loops is given by

$$\begin{aligned}
\beta_u^{(1)} &= -(11 + 2\epsilon) \alpha_y^2 + 4 \alpha_u (\alpha_y + 2 \alpha_u), \\
\beta_u^{(2)} &= \alpha_u \alpha_y \left[ 10 \alpha_g - 16 \alpha_u - 3(11 + 2\epsilon) \alpha_y \right] \\
&\quad + (11 + 2\epsilon) \left[ (11 + 2\epsilon) \alpha_y - 2 \alpha_g \right] \alpha_y^2 - 24 \alpha_u^3.
\end{aligned} \tag{5.9}$$

The beta function  $\beta_v$  for the double trace quartic scalar coupling is given by

$$\begin{aligned}
\beta_v^{(1)} &= 12 \alpha_u^2 + 4 \alpha_v (\alpha_v + 4 \alpha_u + \alpha_y), \\
\beta_v^{(2)} &= 8 \alpha_v \alpha_y \left[ \frac{5}{4} \alpha_g - 4 \alpha_u - \alpha_v - \left( \frac{33}{8} + \frac{3}{4} \epsilon \right) \alpha_y \right] \\
&\quad + (11 + 2\epsilon) \left[ (11 + 2\epsilon) \alpha_y + 4 \alpha_u \right] \alpha_y^2 - 8 \alpha_u^2 \left[ 12 \alpha_u + 5 \alpha_v + 3 \alpha_y \right].
\end{aligned} \tag{5.10}$$

Starting from the two loop level, both scalar beta function additionally depend on the gauge coupling. Our result is also in accord with the findings of [262] which state that  $\beta_v$  is quadratic in  $\alpha_v$  to all loop orders in the Veneziano limit.

Some of the expressions have previously been given in [112]. The main new additions here are the 2-loop scalar terms in (5.9) and (5.10). In the Veneziano limit, the subsystem  $(\beta_g, \beta_y)$  is independent of  $(\alpha_u, \alpha_v)$  at the leading non-trivial order which is two (one) loop in the gauge (Yukawa, scalar) couplings. Beyond this order, the subsystem  $(\beta_g, \beta_y, \beta_u)$  remains independent of  $\alpha_v$ .

### 5.2.4 Anomalous dimensions

We also provide results for the anomalous dimensions associated to the fermions and scalars [182, 185]. If mass terms are present, their renormalisation group flow is induced through the RG flow of the gauge, Yukawa, and scalar couplings. Following [114], we define the scalar anomalous dimensions as  $\Delta_H = 1 + \gamma_H$ , where  $\gamma_H \equiv \frac{1}{2} d \ln Z_H / d \ln \mu$ , and the fermion anomalous dimension as  $\gamma_Q \equiv d \ln Z_Q / d \ln \mu$ . Within perturbation theory, the one and two loop contributions read

$$\begin{aligned}\gamma_H &= \alpha_y - \frac{3}{2} \left( \frac{11}{2} - \epsilon \right) \alpha_y^2 + \frac{5}{2} \alpha_y \alpha_g + 2\alpha_u^2, \\ \gamma_Q &= \left( \frac{11}{2} + \epsilon \right) \alpha_y + \xi \alpha_g - \left( \epsilon - 2\xi - \frac{1}{4}\xi^2 \right) \alpha_g^2 \\ &\quad - (11 + 2\epsilon) \alpha_g \alpha_y - \left( \frac{253}{16} + \frac{17}{4}\epsilon + \frac{1}{4}\epsilon^2 \right) \alpha_y^2,\end{aligned}\tag{5.11}$$

up to corrections of order  $\mathcal{O}(\alpha^3)$ . Here,  $\xi$  denotes the  $R_\xi$  gauge fixing parameter. The anomalous dimension for the scalar mass term follows from the composite operator  $\sim M^2 \text{tr } H^\dagger H$  with  $\gamma_M = d \ln M^2 / d \ln \mu$ . The anomalous dimension for the fermion mass operator is defined as  $\Delta_Q = 3 + \gamma_{M_Q}$  with  $\gamma_{M_Q} \equiv d \ln M_Q / d \ln \mu$ . Within perturbation theory, we find

$$\begin{aligned}\gamma_M &= 8\alpha_u + 4\alpha_v + 2\alpha_y - \left( \frac{33}{2} + 3\epsilon \right) \alpha_y^2 - \left( 16\alpha_u + 8\alpha_v - 5\alpha_g \right) \alpha_y - 20\alpha_u^2, \\ \gamma_{M_Q} &= \left( \frac{11}{2} + \epsilon \right) \alpha_y - 3\alpha_g + (22 + 4\epsilon) \alpha_g \alpha_y - \left( \frac{31}{4} - \frac{5}{3}\epsilon \right) \alpha_g^2 - \left( \frac{253}{16} + \frac{17}{4}\epsilon + \frac{\epsilon^2}{4} \right) \alpha_y^2\end{aligned}\tag{5.12}$$

up to terms of order  $\mathcal{O}(\alpha^3)$ . We note that  $\gamma_M$  is manifestly positive at leading order. For  $\gamma_{M_Q}$  we observe that the gauge and Yukawa contributions arise with manifestly opposite signs at leading order. Hence these may take either sign respectively, depending on whether the gauge or Yukawa contributions dominate. Utilizing (5.12), mass terms then evolve according to

$$\begin{aligned}\beta_{M^2} &= \gamma_M M^2 - 8\alpha_y M_Q^2 + \mathcal{O}(\alpha^3), \\ \beta_{M_Q} &= \gamma_{M_Q} M_Q + \mathcal{O}(\alpha^3).\end{aligned}\tag{5.13}$$

The flow of mass terms already mixes to leading order in the couplings, even in the Veneziano limit. Additional mixing contributions are present as soon as  $N_C$  and  $N_F$  take finite values.

### 5.2.5 Systematics

Next, we discuss the systematics of fixed point searches in perturbation theory, Tab. 5.1. Our considerations in this section apply to any 4d theory with weakly-coupled fixed points, and are more general as such than the concrete asymptotically safe model introduced above.

Theories in 4d without gauge interactions cannot develop weakly coupled fixed points [110, 258]. Hence, gauge interactions must invariably be present to generate fixed points at weak coupling. Scalar or Yukawa couplings may also be present, depending on the particulars of the matter content. If so, scalar quartic and Yukawa couplings and their beta functions arise alongside those for the gauge couplings. We then denote the approximations which retain terms up to order  $k$ ,  $n$ , and  $m$  in the loop expansion of the gauge, Yukawa, and scalar beta functions by

$$(k, m, n).\tag{5.14}$$



Whenever unambiguous, we drop the commas inbetween. Evidently, without scalars, we have  $n = m = 0$  throughout. One might wonder which approximation orders lead to self-consistent fixed points.

Within perturbation theory, and without any other a priori information about the theory, it seems natural to retain beta functions up to the same loop order for all couplings, corresponding to the sequence

$$\text{PT: } (n, n, n). \quad (5.15)$$

The first few approximations are the leading order (111), the next-to-leading order (222), and the next-to-next-to-leading order (333), as indicated in Tab. 5.1.

In theories with weakly interacting fixed points, however, further information is available. In fact, close to fixed points the naive perturbative ordering is upset owing to interactions. It has been established in [110, 258] that any weakly interacting fixed point requires the one loop gauge coefficient to be parametrically small.<sup>12</sup> If we denote the small parameter which controls the smallness of the gauge one loop coefficient by  $\epsilon$  (in the model (5.7), the one-loop coefficient reads  $-\frac{4}{3}\epsilon$ ), this structure implies that  $\beta_g^{(1)} \sim \epsilon \alpha_g^2 \ll \alpha_g^2$ . In such settings, the leading order approximation is (100) rather than (111) owing to the parametric slowing-down of the gauge coupling as opposed to the other sectors. Barring exceptional cancellations, this structure also implies that the one and two loop gauge contributions are of the same order of magnitude  $\beta_g^{(1)} \sim \beta_g^{(2)} \sim \epsilon^3$ , close to interacting fixed points  $\alpha^* \sim \epsilon$ , see (5.6). On the other hand, Yukawa and scalar beta functions at one loop cannot be made parametrically small. Consequently, the approximation which provides the first order at which a consistent fixed point  $\alpha^* = \mathcal{O}(\epsilon)$  for all couplings arises is (211): in the gauge sector the fixed point materialises due to cancellations between the one and two loop terms, and in the Yukawa and scalar sectors through cancellations at one loop [110, 258]. All higher loop contributions are parametrically smaller and obey  $\beta^{(n)} \sim \epsilon^{n+1}$  for the gauge beta function once  $n \geq 2$  as well as  $\beta^{(n)} \sim \epsilon^{n+1}$  for the Yukawa and the scalar beta functions for all  $n \geq 1$ . This pattern proceeds systematically to higher order [114]. It follows that the sequence of approximations with consistent interacting fixed point (FP) solutions is given by

$$\text{FP: } (n + 1, n, n). \quad (5.16)$$

We denote this approximation as  $n\text{NLO}'$ . It determines the fixed point  $\alpha^*(\epsilon) = \alpha^*|_{n\text{NLO}'} + \mathcal{O}(\epsilon^{n+1})$  for all couplings, with  $\alpha^*|_{n\text{NLO}'}$  an exact polynomial in  $\epsilon$  up to including terms of order  $\epsilon^n$ . The first few approximations are the leading (100), the next-to-leading (211), and the next-to-next-to-leading (322) order, see Tab. 5.1.

Finally, a third sequence of approximations exploits information related to Weyl consistency conditions [150, 153]. Weyl consistency conditions have formally been derived for weakly coupled theories on classical gravitational backgrounds. On the level of the path integral they state that two independent Weyl rescalings commute with each other. In terms of the couplings  $\{g_i\} \equiv \{g, y, u, v\}$  with  $\beta$  functions  $\beta_i = dg_i/d\ln\mu$ , the Weyl consistency conditions take the form of integrability conditions  $\partial\beta^j/\partial g_i = \partial\beta^i/\partial g_j$  in that they relate partial derivatives of the

<sup>12</sup>Strictly speaking, it is required that the ratio of the one-loop and the two-loop gauge coefficient is a perturbatively small number. If so, it can then always be achieved that the gauge one loop coefficient is small by a suitable reparametrisation of the gauge coupling.

various  $\beta$  functions to each other, and  $\beta^i \equiv \chi^{ij} \beta_j$ . The functions  $\chi^{ij}$  play the role of a metric in the space of couplings. Weyl consistency conditions are expected to hold in the full theory, and hence it might seem desirable to satisfy them even within finite perturbative approximations. Note that the metric  $\chi^{ij}$  itself is a function of the couplings which is why Weyl-consistent solutions relate different orders of perturbation theory. For the gauge-Yukawa theory studied here, a perturbative expression for the metric  $\chi$  has been given in [263]. Accordingly, Weyl-consistent approximations are given by the sequence

$$\text{Weyl: } (n+1, n, n-1). \quad (5.17)$$

We denote this approximation as  $n\text{NLO}''$ . The first few approximations are the leading (100), the next-to-leading (210), and the next-to-next-to-leading (321) order, see Tab. 5.1. Notice that the FP (5.16) and Weyl (5.17) approximations only differ in the scalar sector, where the former retains an additional loop order. However, in any QFT, scalar couplings only enter the Yukawa beta functions starting at two loop order, and the gauge sector at even higher loop level. For this reason, the higher loop term in the scalar sector only generates subleading corrections for the gauge and Yukawa fixed point. This pattern implies that power series expansions of fixed points at  $n\text{NLO}'$  or  $n\text{NLO}''$  accuracy coincide for the gauge, Yukawa (scalar) couplings, modulo subleading terms of order  $\sim \epsilon^{n+1}$  ( $\sim \epsilon^n$ ), for all  $n$ .

The PT and Weyl schemes up to 2NLO and 2NLO'' have recently been used to investigate the vacuum stability of the Standard Model [23, 264]. For the model at hand (5.1), (5.2), the approximations  $\text{NLO}''$ ,  $\text{NLO}'$ , and  $2\text{NLO}''$  have been investigated in [112, 113]. Below, we extend approximations to the complete 2NLO' order (322) in the spirit of (5.16), and compare the PT, FP, and Weyl approximation schemes quantitatively.

### 5.2.6 Away from four dimensions

As an aside, we note that the power counting detailed in Tab. 5.1 applies uniquely to weakly interacting QFTs in  $4d$ . Away from four dimensions, the gauge, Yukawa and quartic self-interactions have a non-vanishing canonical mass dimension, and their  $\beta$ -functions receive a tree level contribution which alters the power counting in Tab. 5.1. Specifically, in  $d = 4 - \delta$  dimensions, the tree level parameter  $|\delta| \ll 1$  now controls the perturbative expansion and the existence of fixed points. Barring exceptional cancellations, the leading non-trivial order with a consistent interacting fixed point  $\alpha_i^* = \mathcal{O}(\delta)$  is one-loop (111), where quantum fluctuations cancel the tree level terms for some or all couplings (see [67] for a recent example). This pattern proceeds to higher order, as is well-known from, e.g., the Wilson-Fisher fixed point [229].

## 5.3 Results at 2NLO'

In this section, we summarise our results for fixed points, anomalous dimensions, vacuum stability, and scaling exponents at the complete 2NLO' order.

### 5.3.1 Fixed points

It is straightforward if tedious to identify the weakly interacting fixed points at order  $\epsilon^2$  of the system (5.7), (5.8), (5.9) and (5.10). Given the polynomial nature of the beta function, however, a large variety of (potentially spurious) fixed points arises. Those fixed points which are proportional to  $\epsilon$  in the leading order are under strict perturbative control and can be viewed as “exact”. Using the beta functions at (322) accuracy, and performing a systematic expansion (5.16) up to subleading corrections of order  $\epsilon^3$ , we find

$$\begin{aligned}
\alpha_g^* &= \frac{26}{57} \epsilon + 23 \frac{75245 - 13068\sqrt{23}}{370386} \epsilon^2, \\
\alpha_y^* &= \frac{4}{19} \epsilon + \frac{43549 - 6900\sqrt{23}}{20577} \epsilon^2, \\
\alpha_u^* &= \frac{\sqrt{23} - 1}{19} \epsilon + \frac{365825\sqrt{23} - 1476577}{631028} \epsilon^2, \\
\alpha_v^* &= -\frac{1}{19} \left( 2\sqrt{23} - \sqrt{20 + 6\sqrt{23}} \right) \epsilon - \left( \frac{321665}{13718\sqrt{23}} - \frac{27248}{6859} + \frac{\frac{33533}{6859} - \frac{452563}{13718\sqrt{23}}}{\sqrt{20 + 6\sqrt{23}}} \right) \epsilon^2.
\end{aligned} \tag{5.18}$$

Results are accurate at the cited order, meaning that higher loop corrections will only generate subleading terms of order  $\epsilon^3$ . Results agree with the (321) approximation adopted previously [112] in all but the  $\epsilon^2$ -terms of the scalar quartic couplings. The reason for this is that the scalar couplings interfere with the Yukawa and gauge beta functions starting at the second and fourth loop level, respectively, see (5.8). In consequence, at (322), only the  $O(\epsilon)$  coefficient of the scalar couplings contribute to the  $O(\epsilon^2)$  value of the Yukawa coupling, whence agreement with (321). Quantitatively, we have

$$\begin{aligned}
\alpha_g^* &= 0.4561\epsilon + 0.7808\epsilon^2 + 3.8922\epsilon^3, \\
\alpha_y^* &= 0.2105\epsilon + 0.5082\epsilon^2 + 2.4222\epsilon^3, \\
\alpha_u^* &= 0.1998\epsilon + 0.4403\epsilon^2 + 1.8780\epsilon^3, \\
\alpha_v^* &= -0.1373\epsilon - 0.6318\epsilon^2 - 3.6685\epsilon^3.
\end{aligned} \tag{5.19}$$

All terms have coefficients of order unity. We have also indicated the  $\epsilon^3$  terms which originate from subleading contributions in  $\epsilon$  at 2NLO' accuracy; they are only indicative as further higher loop corrections beyond (322) will modify them. Also note that all terms at order  $\epsilon^2$  arise with the same sign as those at order  $\epsilon$ . This implies that the  $\alpha_g$  and  $\alpha_y$  remain positive for all  $\epsilon$ , as they must, offering no limitations on the domain of validity. It would be very useful to know whether the radius of convergence (in  $\epsilon$ ) comes out finite, or not. Same sign correction terms hint at a slow rate of convergence in  $\epsilon$  and the presence of complex conjugate poles in the complexified field plane [265, 266].

### 5.3.2 Vacuum stability

We now turn our attention to the stability of the vacuum. It is well-known that the scalar couplings control the stability of the ground state. The stability for scalar potentials as in (5.1) has

first been investigated in [267]. In the Veneziano limit, and in terms of the couplings used here, it is required that [112, 113]

$$\alpha_u^* > 0 \quad \text{and} \quad \alpha_u^* + \alpha_v^* > 0. \quad (5.20)$$

The first approximation with non-trivial scalar couplings is NLO' (211). At one loop, the fixed point in the scalar sector is fuelled by the Yukawa fixed point. Most importantly, vacuum stability has been established quantitatively [112], with

$$\alpha_u^* + \alpha_v^* \Big|_{(211)} = 0.0625\epsilon + O(\epsilon^2). \quad (5.21)$$

Notice the smallness of the leading coefficient. It arises through the cancellation of the leading order fixed point values of the single and double trace couplings, which by themselves are twice or thrice as large as their sum, (5.18). It has also been shown that the Coleman-Weinberg-type resummation of leading logarithmic corrections does not alter the conclusion [113]. A first step beyond the leading order (211) has been performed in [112] by using the Weyl-consistent (321) approximation. The result

$$\alpha_u^* + \alpha_v^* \Big|_{(321)} = 0.0625\epsilon + 0.1535\epsilon^2 \quad (5.22)$$

shows that the induced subleading, higher loop effects from the gauge-Yukawa sector are supportive of vacuum stability, for all  $\epsilon$ . This can also be understood from observing that the scalar quartic couplings are at one loop proportional to the Yukawa coupling; and since the latter grows with subleading corrections, so does (5.22) over (5.21). At (322) accuracy, however, we find the complete  $\epsilon^2$ -correction from (5.18). Quantitatively, we have

$$\alpha_u^* + \alpha_v^* \Big|_{(322)} = 0.0625\epsilon - 0.1915\epsilon^2 + O(\epsilon^3). \quad (5.23)$$

Notice that the leading and the subleading terms now arise with opposite signs. At order  $\epsilon^2$ , this comes about because the double-trace scalar coupling receives larger (and negative) corrections than the single trace coupling. We also observe that the two loop terms in the scalar beta function outweigh the gauge-Yukawa corrections in (5.22).

### 5.3.3 Anomalous dimensions

For the field and mass anomalous dimensions, using (5.11) and (5.12) in conjunction with (5.18), we find

$$\begin{aligned} \gamma_H \Big|_{(322)} &= 0.211\epsilon + 0.462\epsilon^2, \\ \gamma_Q \Big|_{(322)} &= (1.158 + 0.456\xi)\epsilon + (1.249 + 1.197\xi + 0.052\xi^2)\epsilon^2, \\ \gamma_M \Big|_{(322)} &= 1.470\epsilon + 0.521\epsilon^2, \\ \gamma_{M_Q} \Big|_{(322)} &= -0.421\epsilon + 0.926\epsilon^2, \end{aligned} \quad (5.24)$$

up to terms of order  $\mathcal{O}(\epsilon^3)$ , and where  $\xi$  denotes the gauge fixing parameter in  $R_\xi$  gauge. We observe that the subleading corrections have the same sign as the leading order ones, except for the mass anomalous dimension  $\gamma_{M_Q}$ . Results are compatible with unitarity bounds. With increasing  $\epsilon$ , the anomalous dimension  $\gamma_M$  exceeds the classical dimension starting at about  $\epsilon = 1.36$  at (211) or  $\epsilon = 1.00$  at (322). For the fermion mass anomalous dimension, this happens

at  $\epsilon = 1.29$  at (322). This implies that mass terms become irrelevant operators in the UV for sufficiently large  $\epsilon$ . We interpret this phenomenon as the onset of strong coupling where the validity of perturbation theory becomes questionable.

### 5.3.4 Scaling exponents

Next we discuss universal exponents which are obtained as eigenvalues of the stability matrix  $\partial\beta_i/\partial\alpha_j|_*$ . We order the eigenvalues according to magnitude,  $\vartheta_1 < 0 < \vartheta_2 < \vartheta_3 < \vartheta_4$ .<sup>13</sup> Scaling exponents have been known at (211) and (321) accuracy previously [112]. Our results for the scaling exponents at 2NLO' are

$$\begin{aligned}\vartheta_1 &= -\frac{104}{171}\epsilon^2 + \frac{2296}{3249}\epsilon^3, \\ \vartheta_2 &= \frac{52}{19}\epsilon + \frac{136601719 - 22783308\sqrt{23}}{4094823}\epsilon^2, \\ \vartheta_3 &= \frac{8}{19}\sqrt{20 + 6\sqrt{23}}\epsilon + \frac{2\sqrt{2}(50059110978 + 10720198219\sqrt{23})}{157757(10 + 3\sqrt{23})^{9/2}}\epsilon^2, \\ \vartheta_4 &= \frac{16}{19}\sqrt{23}\epsilon + \frac{4(68248487\sqrt{23} - 255832864)}{31393643}\epsilon^2.\end{aligned}\tag{5.25}$$

The new coefficients are  $\epsilon^2$ -corrections to the irrelevant eigenvalues  $\vartheta_3$  and  $\vartheta_4$ , which are the only terms sensitive to the two-loop scalar beta functions; the  $\sim \epsilon^2$  contribution to  $\vartheta_2$  is only dependent on the scalar couplings to one-loop. Note that the rational coefficients in  $\vartheta_1$  and  $\vartheta_2$  arise from the gauge-Yukawa subsector, whereas all irrational coefficients arise with contributions from the scalar subsector. It is interesting to note that the relevant scaling exponent  $\vartheta_1$  is completely determined to  $O(\epsilon^3)$  already at (210) order, as noted in [112]. However, in contrast to the other exponents, and expectation, increasing our approximation to (322) does not fix any further coefficients, as the  $\sim \epsilon^4$  coefficient is sensitive to four-loop (three-loop) contributions to the gauge (Yukawa) beta functions. Numerically, we have

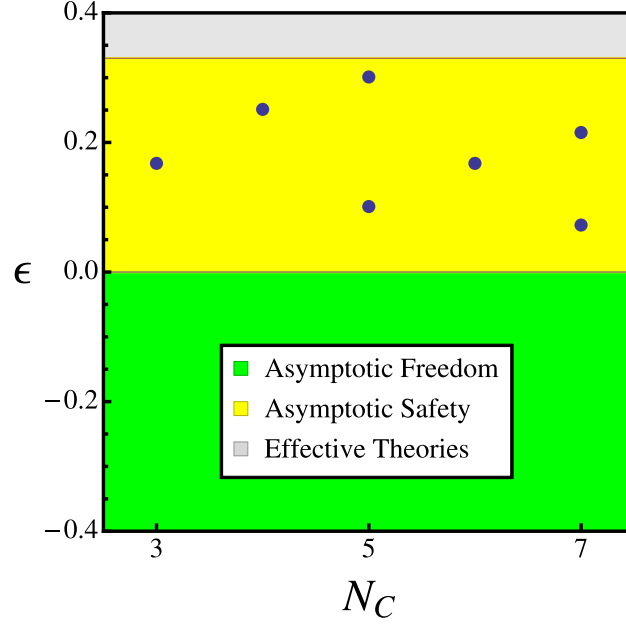
$$\begin{aligned}\vartheta_1 &= -0.6082\epsilon^2 + 0.7067\epsilon^3 + 3.322\epsilon^4, \\ \vartheta_2 &= 2.737\epsilon + 6.676\epsilon^2 + 18.44\epsilon^3, \\ \vartheta_3 &= 2.941\epsilon + 1.041\epsilon^2 - 2.986\epsilon^3, \\ \vartheta_4 &= 4.039\epsilon + 9.107\epsilon^2 + 44.43\epsilon^3,\end{aligned}\tag{5.26}$$

where we additionally show the next subleading coefficient in each case (e.g. the  $\epsilon^4$ -term in  $\vartheta_1$  and the  $\epsilon^3$ -terms for the other exponents). The latter terms are subject to corrections from the next loop level, and quantify subleading effects already present within the (322) approximation.

## 5.4 UV conformal window

We are now in a position to investigate the size of the UV conformal window for asymptotic safety for theories with action (5.1) using perturbation theory.

<sup>13</sup>This relates to the convention used in [112] under the exchange  $\vartheta_3 \leftrightarrow \vartheta_4$ .



**Figure 5.1:** The UV conformal window with asymptotic safety (yellow band) from fixed points and scaling exponents, (5.27), also showing regimes with asymptotic freedom (green) and effective theories (grey). Dots indicate the first few integer solutions (5.33).

#### 5.4.1 Limits for interacting fixed points

The results of the previous sections have established a UV fixed point to second order in  $\epsilon \ll 1$ . With increasing  $\epsilon$ , the conformal window for the UV fixed point is limited through one of several mechanisms:

- Strong coupling. With increasing  $\epsilon$ , regimes with parametrically strong coupling in  $\epsilon$  can arise either through algebraic poles of fixed point couplings  $\alpha(\epsilon)$  at finite  $\epsilon$ , or in the limit  $\epsilon \rightarrow \infty$ . In the latter case, we impose  $\alpha^* < 1$  to delimit the range of validity.
- Fixed point mergers. Fixed point conditions for approximations beyond (211) are at least quadratic (or higher) order in one of the couplings. Consequently, additional strongly coupled IR fixed point solutions may arise. With increasing  $\epsilon$ , these may collide with the asymptotically safe UV fixed point, and then disappear in the complex plane, setting an upper limit on  $\epsilon$ . Equivalently, this is signalled by the vanishing of the relevant scaling exponent.
- Vacuum instability. The signs and size of the scalar couplings are solely constrained by the requirement of vacuum stability (5.20). Consequently, the change of sign for the linear combination (5.20) with increasing  $\epsilon$  indicates the onset of instabilities.
- Negative coupling. Regions with parametrically weak gauge or Yukawa coupling  $\alpha(\epsilon) \rightarrow 0$  for increasing  $\epsilon > 0$  offer upper limits due to a change of sign of these couplings and the subsequent disappearance of fixed points into the unphysical regime.

From the point of view of practical applications, it is crucial to understand up to which finite maximal value  $\epsilon < \epsilon_{\text{max}}$  the conformal window is going to persist, and which mechanism is responsible for generating an upper bound, if any.

Couplings		Orders in perturbation theory							
$\beta_{\text{gauge}}$	2	2	2	2	2	3	3	3	3
$\beta_{\text{Yukawas}}$	1	1	1	2	2	1	1	2	2
$\beta_{\text{quartics}}$	0	1	2	1	2	1	2	1	2
$\epsilon_{\text{strict}}$	2.192 <sup>a</sup>	2.192 <sup>a</sup>	0.135 <sup>c</sup>	16.16 <sup>a</sup>	0.222 <sup>c</sup>	0.029 <sup>b</sup>	0.029 <sup>b</sup>	0.145 <sup>b</sup>	0.095 <sup>c</sup>
$\epsilon_{\text{subl.}}$	1.048 <sup>a</sup>	1.048 <sup>a</sup>	0.116 <sup>c</sup>	3.112 <sup>b</sup>	0.208 <sup>c</sup>	0.027 <sup>b</sup>	0.027 <sup>b</sup>	0.117 <sup>b</sup>	0.087 <sup>c</sup>

**Table 5.2:** Maximal values  $\epsilon_{\text{strict}}$  and  $\epsilon_{\text{subl.}}$  for the parameter  $\epsilon$  up until which asymptotic safety is realised. Limits arise due to *a*) strong coupling, *b*) fixed point mergers, or *c*) vacuum instability.

### 5.4.2 Bounds from fixed points and exponents

A first estimate for an upper bound follows from the complete results at (211) and (322) order for the couplings (up to second order in  $\epsilon$ ), and the scaling exponents (up to fourth order in  $\epsilon$ ). Since all couplings receive same-sign corrections at (322), (5.18), the scenario *d*) cannot arise. Requiring  $\alpha^* < 1$  leads to  $\epsilon < 2$  approximately. However, vacuum stability offers tighter constraints. We conclude from (5.23) that the two loop scalar corrections impose an upper bound for the conformal window through the onset of vacuum instability, approximately given by  $\epsilon_{\text{max}} \approx 0.326$ .

Let us see whether some of the incomplete higher order corrections offer a similar, or even tighter bound. From the relevant eigenvalue (5.25), an upper limit  $\epsilon_{\text{max}} \approx 0.861$  arises from sign change of  $\vartheta_1$  through the incomplete  $\epsilon^3$  term, indicating a fixed point merger [112]. Considering incomplete  $\epsilon^4$  contributions from (322), the upper bound is reduced to  $\epsilon_{\text{max}} \approx 0.335$ . A sign change in  $\vartheta_3$  would arise at even larger  $\epsilon$  and can be ignored. No constraints arise from anomalous dimensions. Based on the explicit power series expressions for couplings and exponents at 2NLO', we conclude that the conformal window is limited through the onset of vacuum instability (5.23) and the vanishing of the relevant eigenvalue (5.25),

$$\epsilon_{\text{max}} \approx 0.326 \dots 0.335, \quad (5.27)$$

see Fig. 5.1. It is interesting to observe that the tightest bound from incomplete higher order terms comes out very close to (yet, larger than) the vacuum stability bound. In this light, we view (5.27) as indicative for the range of validity at this order. Constraints through parametrically strong or weak coupling do not play any role. As we will see next, the UV conformal window becomes more strongly constrained once bounds from beta functions are taken into consideration.

### 5.4.3 Stabilising vs destabilising fluctuations

Next, we investigate constraints arising directly from the beta functions rather than their power series solutions. We will see that this leads to tighter constraints yet. As a first step, it is interesting to ask into which direction the higher loop corrections are going to shift the beta functions. Inserting the order  $\epsilon$  fixed point results from [112] into the higher loop terms, we find the leading shifts

$$\beta_g^{(3)} \Big|_{(211)} = 2.48 \epsilon^4, \quad \beta_y^{(2)} \Big|_{(211)} = -0.49 \epsilon^3, \quad \beta_u^{(2)} \Big|_{(211)} = 0.26 \epsilon^3, \quad \beta_v^{(2)} \Big|_{(211)} = 0.99 \epsilon^3. \quad (5.28)$$

Higher loop contributions to the gauge (Yukawa, scalar) sectors do not appear until order  $\epsilon^4$  ( $\epsilon^3$ ), as is necessarily the case. At the leading non-trivial order in  $\epsilon$ , the fixed point at the leading order (211) shifts the subleading gauge and scalar beta functions upwards, but the Yukawa beta function downwards, see (5.28). In general, upward shifts  $\Delta\beta > 0$  at some finite couplings potentially destabilise UV fixed points, simply because beta functions might no longer be able to generate a non-trivial zero once upward shifts become too large. For the same reason, downward shifts  $\Delta\beta < 0$  always stabilise interacting UV fixed points, simply because  $\beta > 0$  for sufficiently small couplings, which guarantees that a solution to  $\beta = 0$  can still be found for finite positive couplings. Altogether this means that higher loop corrections (5.28) to the running of the Yukawa (gauge, scalar) coupling stabilise (de-stabilise) the fixed point. It remains to be seen how this “competition of fluctuations” balances out quantitatively across the various beta functions and loop orders.

#### 5.4.4 Bounds from beta functions

Next, we determine bounds from beta functions quantitatively [268]. We adopt two strategies to determine  $\epsilon_{\max}$  from beta functions, for each set of loop orders. The first “strict” strategy, whose bounds we call  $\epsilon < \epsilon_{\text{strict}}$ , uses the loop orders as indicated in Tab. 5.2. In addition, all terms in the beta functions (5.6) which are parametrically larger than  $\epsilon^{n+1}$  at the  $n$ -th loop order are suppressed (couplings count as  $\alpha \sim \epsilon$ ). The rationale for this strict approach is that the approximate beta functions are now stripped of those higher order contributions (in  $\epsilon$ ), which are not (yet) accurately determined due to the absence of higher loop terms. As such, the scheme primarily acknowledges the power counting  $\alpha \sim \epsilon$ , as dictated by the fixed point. The bounds  $\epsilon_{\text{strict}}$  are sensitive to the competition between the stabilising Yukawa and the destabilising gauge and scalar loop contributions at higher order (5.28).

The second strategy is agnostic to these finer considerations and employs the plain loop level approximation as discussed in Tab. 5.2, without touching the explicit  $\epsilon$  dependence within loop coefficients. This strategy retains subleading terms in  $\epsilon$  and we refer to its bounds as  $\epsilon_{\text{subl.}}$ . With the result (5.18) at hand, we can estimate what the effect of these subleading terms is going to be by inserting the fixed point solutions to order  $\epsilon^2$  back into the beta functions at (322), finding

$$\beta_g|_{(322)} = 10.24 \epsilon^5, \quad \beta_y|_{(322)} = -1.71 \epsilon^4, \quad \beta_u|_{(322)} = 1.70 \epsilon^4, \quad \beta_v|_{(322)} = 7.24 \epsilon^4. \quad (5.29)$$

Subleading terms contribute starting at order  $\epsilon^5$  ( $\epsilon^4$ ) in the gauge (Yukawa, scalar) sectors, as expected from (5.18). Most notably, we find that the subleading terms shift the gauge and scalar beta functions upwards and the Yukawa beta function downwards. This is the exact same pattern as observed in (5.28), albeit smaller by a power in  $\epsilon$ . Moreover, once  $\epsilon \approx 0.14$  (0.25), the scalar (gauge, Yukawa) shifts (5.29) are of the same size as (5.28). Since the bounds  $\epsilon_{\text{subl.}}$  are sensitive to the combined effect of (5.28) and (5.29), our line of reasoning suggests that the bounds  $\epsilon_{\text{subl.}}$  must follow the same pattern as  $\epsilon_{\text{strict}}$  albeit being slightly tighter due to the additional shift (5.29).

In Tab. 5.2 we summarise results for  $\epsilon_{\text{strict}}$  and  $\epsilon_{\text{subl.}}$ , also indicating which mechanism is limiting the domain of validity for each case.<sup>14</sup> At the lowest orders (210), (211) and (221), we observe

<sup>14</sup>In cases where  $\epsilon_{\text{strict}}$  and  $\epsilon_{\text{subl.}}$  are constrained by the same mechanism,  $|\epsilon_{\text{strict}} - \epsilon_{\text{subl.}}|$  gives a reasonable estimate for the error of the expansion.



that  $\epsilon_{\text{strict}}$  is constrained via  $\alpha^* < 1$ . At (221), mergers in the Yukawa sector could have arisen. However, the growth of the coupling with  $\epsilon$  is much slower due to a large negative quadratic correction,  $\alpha_g = 0.456\epsilon - 3.061\epsilon^2 + O(\epsilon^3)$ , leading to a wider UV conformal window and the avoidance of mergers. In (210) and (211) bounds for  $\epsilon_{\text{subl.}}$  arise from the onset of strong coupling through a pole at finite  $\epsilon$ . In these cases, the effective gauge two loop coefficient changes sign and findings can no longer be trusted in perturbation theory. At (221), instead, the bound for  $\epsilon_{\text{subl.}}$  arises through a proper fixed point merger. As soon as two-loop effects in the scalar sector are retained, such as in (212) and (222), we find that the onset of vacuum instability dominates the upper limit. Quantitatively, the bounds are weaker in (222) than in (212). Hence, two loop Yukawa (scalar) terms increase (decrease) the domain of validity and the conformal window.

Turning to three loop effects, we observe that (311) is limited by fixed point mergers through fluctuations in the gauge sector. The new effect is triggered by a large positive quadratic correction  $\alpha_g = 0.456\epsilon + 3.841\epsilon^2 + O(\epsilon^3)$  which accelerates the growth of the gauge coupling, the exact opposite of what happens in (221). The effect clearly dominates over the bounds found at the preceding orders (210), (211) and (221). This continues to be true at (312), where gauge fluctuations offer a tighter constraint than vacuum stability. Including two loop Yukawa contributions, however, we find that the domain of validity is substantially enhanced — by a factor of four in (321) and a factor of about three in (322). While in (321) the upper limit arises due to mergers, in (322) it comes about through vacuum instability.

We now return to the induced shifts (5.28) and (5.29). From Tab. 5.2, and for all settings considered, it is evident that the bound  $\epsilon_{\text{subl.}}$  is systematically tighter than the bound  $\epsilon_{\text{strict}}$ ,

$$\epsilon_{\text{subl.}} \leq \epsilon_{\text{strict}}. \quad (5.30)$$

The result thus validates our semi-quantitative considerations based on induced shifts of beta functions, see (5.28) and (5.29). We will now discuss our results from the viewpoint of perturbation theory (5.15) vs. fixed point (5.16) vs. Weyl (5.17) consistency conditions (see Tab. 5.1). The highest systematic perturbative approximation is NLO, or (222), where bounds in the range of  $\epsilon_{\text{max}} \approx 0.21$  arise through vacuum instability. In the Weyl consistency scheme 2NLO'', or (321), the bound is pushed towards  $\epsilon_{\text{max}} \approx 0.13$  due to mergers. In this work, we have argued that the consistent fixed point approximation 2NLO', or (322), should be favoured. Its bound  $\epsilon_{\text{max}} \approx 0.09$  is even lower than the one in the Weyl scheme, and, as in the PT scheme, dominated by vacuum instability rather than mergers. Taking the most advanced approximations as benchmarks, we conclude that the UV conformal window extends up to

$$\epsilon_{\text{max}} \approx 0.09 \dots 0.13, \quad (5.31)$$

see Fig. 5.2. The bounds (5.31) from beta functions are stronger than the bounds from their perturbative solutions (5.27). Also, all couplings and anomalous mass dimensions are still small (below 0.06 and 0.15, respectively) and in the range (5.31) where perturbation theory is viable.

In summary, competing effects due to higher loop contributions in the gauge, scalar and Yukawa sector constrain the size of the UV conformal window. While higher loop terms in the Yukawa sector continue to stabilise the fixed point, those in the gauge and scalar sector destabilise it.

The combined effect is such that vacuum stability comes out as the most constraining factor. Subleading terms in  $\epsilon$  in all beta function coefficients always lead to tighter constraints (5.30). The fact that the constraints for  $\epsilon_{\text{subl.}}$  and  $\epsilon_{\text{strict}}$  are quantitatively close to each other is a strong sign for the intrinsic consistency of results.

#### 5.4.5 Bounds from strong coupling

We briefly comment on the prospect for asymptotic safety when  $\epsilon$  becomes large [112]. Increasing  $\epsilon$  implies that the one-loop term (5.7) is no longer small and perturbative control is lost. For an interacting fixed point to exist, cancellations between different loop orders must take place. For  $N_F \rightarrow \infty$  and at finite  $N_C$ , corresponding to the limit  $1/\epsilon \rightarrow 0$ , the running of couplings is fully dominated by fermion loops, and gluon loops can be neglected. An infinite order resummation for the  $U(1)$  [127] and  $SU(N)$  [128] beta functions can be achieved, showing a non-perturbative UV fixed point in the gauge sector with  $\epsilon \alpha_g^*$  of order unity (5.3). However, subleading corrections in  $1/N_F$  may spoil the result and must be investigated before definite conclusions can be taken [129]. Also, the Yukawa and scalar couplings do not play a role and can be omitted ( $\alpha_y = \alpha_u = \alpha_v = 0$ ). Based on continuity in  $(N_F, N_C)$  it has been argued that a fingerprint of the fixed point should be visible at loop level [112]. Then, *assuming* that the UV fixed point exists non-perturbatively for sufficiently large and finite  $N_F, N_C$ , we may use the loop expansion to estimate a lower bound for its conformal window. Specifically, for large  $\epsilon$ , the leading  $n$ -loop contribution scales as  $c_n \epsilon^{n-1} \alpha_g^{n+1}$  ( $n > 1$ ) where  $c_n$  is of order unity and independent of  $\epsilon$ . Cancellation with the one loop term gives the estimate  $\alpha_g^* \sim \epsilon^{(2-n)/(n-1)}$  from the  $n$ th loop order ( $c_n < 0$ ) [269, 270]. Quantitatively, the three loop beta function (5.7) indicates that a strongly coupled fixed point obeys  $\epsilon > \epsilon_{\text{min}}$ , with

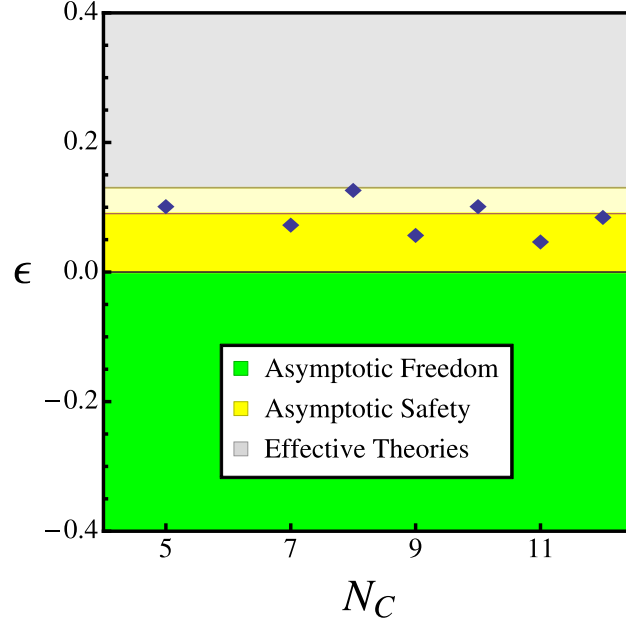
$$\epsilon_{\text{min}} = \frac{3}{224}(159 + 19\sqrt{505}) \approx 7.49. \quad (5.32)$$

The bound arises from strong coupling with  $\alpha_g \rightarrow \infty$  for  $\epsilon \rightarrow \epsilon_{\text{min}}$ . Technically, it is due to a competition between subleading three loop terms and the two loop term. In the domain  $\epsilon > \epsilon_{\text{min}}$  the effective gauge coupling  $\sqrt{\epsilon} \alpha_g^*$  is of order unity. The fixed point has one relevant eigendirection and the scaling exponent is large and bounded from above,  $\vartheta(\epsilon) \leq -20.69$ , with  $\epsilon \approx 44.6$  at the maximum. Moreover, the scaling exponent diverges ( $\vartheta \rightarrow -\infty$ ) at the bound (5.32), and in the limit  $\epsilon \rightarrow \infty$  [112]. Hence, the expected characteristics of the fixed point at strong coupling are quite different from those at small  $\epsilon$  where couplings and exponents are both parametrically small.

#### 5.4.6 Implications for model building and cosmology

Finally, we discuss a few implications of our results for model building and cosmology [57]. It has already been shown that asymptotic safety offers novel opportunities for model building, including explicit BSM scenarios and phenomenological signatures with the Standard Model gauge group  $SU(3)_C \times SU(2)_W \times U(1)_Y$  [121]. Moreover, estimates for the UV conformal window in terms of matter field multiplicities and representations have equally been derived [121].

For the model at hand, and using the bound (5.27) from fixed points and scaling exponents at



**Figure 5.2:** The UV conformal window with asymptotic safety (yellow bands) from beta functions, also showing regimes with asymptotic freedom (green) and effective theories (grey). The lower yellow band corresponds to the full 2NLO' result, the upper yellow band covers the range (5.31), and symbols indicate the first few integer solutions (5.34) and (5.35).

2NLO', we obtain the smallest pair of integer values for  $(N_C, N_F)$  compatible with asymptotic safety. The first few integer solutions within (5.27) are

$$(N_C, N_F) = (3, 17), (4, 23), (5, 28), (5, 29), (6, 34), (7, 39), (7, 40), \dots \quad (5.33)$$

as indicated in the yellow band of Fig. 5.1. Solutions cover all special unitary gauge groups with  $N_C > 2$ . Starting from  $N_C = 5$  onwards, multiple solutions for the corresponding fermion flavour multiplicities  $N_F$  become available. Bounds for the conformal window from beta functions (5.31) are tighter. Considering the bound from (321), Tab. 5.2, the first few integer solutions are

$$(N_C, N_F) = (5, 28), (7, 39), (8, 45), (9, 50), (10, 56), (11, 61), (12, 67), \dots \quad (5.34)$$

corresponding to the entire yellow band in Fig. 5.2. For the few leading values for  $(N_C, N_F)$ , the bound (5.34) is the same irrespective of whether one uses the limit  $\epsilon_{\text{subl.}}$  (as has been done in [112]), or the limit  $\epsilon_{\text{strict.}}$  Moreover, solutions for  $SU(3)$ ,  $SU(4)$  and  $SU(6)$  are no longer available. The asymptotically safe solution with the smallest number of fields corresponds to  $SU(5)$  with 28 flavours of fermions in the fundamental representation. This is quite close to the  $SU(5)$  GUT candidate [271], which, with  $N_F = 24$  flavours of fermions, remains marginally asymptotically free. Hence, (5.34) suggests that asymptotic safety can already be achieved in a GUT-like scenario, with just a few more flavours of fermions (to destabilise asymptotic freedom), plus additional elementary mesons and Yukawa couplings (to generate asymptotic safety). Extending approximations to the complete (322) level, the bounds are shifted and the UV conformal window

narrows down, starting with

$$(N_C, N_F) = (7, 39), (9, 50), (11, 61), (12, 67), \dots \quad (5.35)$$

corresponding to the lower yellow band in Fig. 5.2. Once again, the few leading integer solutions in (5.35) do not depend on having used either  $\epsilon_{\text{strict}}$  or  $\epsilon_{\text{subl.}}$  to fix the conformal window. In particular, the cases  $(N_C, N_F) = (5, 28), (8, 45)$  and  $(10, 56)$  have dropped out due to the onset of vacuum instability in the fundamental meson sector, turning the first viable candidate into  $SU(7)$ . Asymptotic safety has also been considered as a mechanism for inflation by including UV effects from quantum gravity and matter [272, 273]. General scenarios have been classified and conditions for cosmological fixed points with inflationary expansions in the early universe are known [273] (see [47, 274] for settings where inflation arises purely quantum gravitationally). It has also been speculated that inflation may arise from asymptotically safe toy models [112, 113], neglecting quantum gravity altogether [125, 275]. Compatibility with the 2015 Planck data [276] at the  $2\sigma$ -level requires a large conformal window up to  $\epsilon \approx 0.7 \dots 0.8$  if minimal coupling is assumed [125]. This scenario seems firmly excluded in the light of (5.27) and (5.31). Without minimal coupling, the conformal window (5.31) imposes large values for the non-minimal coupling  $\xi \gg 1$  of scalar matter to gravity (substantially larger than the conformal value  $\xi = \frac{1}{6}$ ) to achieve compatibility with data [276].

It is interesting to check how finite  $N$  corrections beyond the Veneziano limit [268], higher loop corrections beyond  $2\text{NLO}'$ , higher-dimensional operators [233], or strong coupling effects, are going to modify the UV conformal window and the bounds (5.31), (5.34) and (5.35). This is left for future work.

## 5.5 Discussion

The existence of exact and interacting UV fixed points in particle physics offers many opportunities for model building [121]. For any practical applications, however, it is equally important to understand the size of the corresponding conformal window. Here, we have investigated the conformal window for the gauge-Yukawa theory (5.1). Extending the findings of [112] we have obtained exact results for fixed points, anomalous dimensions, and scaling exponents up to second order in the small parameter (5.4), the highest order in perturbation theory presently available. The underlying ordering principle, which due to the fixed point is different from what one would expect normally, is also explained in detail (Tab. 5.1).

The conformal window follows from fixed points and beta functions. We have also compared different approximation orders and clarified the role of subleading corrections (Tab. 5.2). Limits invariably arise through a competition of fluctuations. Higher loops in the Yukawa sector enhance the conformal window, countered by higher loops in the gauge sector. Higher loops in the scalar sector tend to destabilise the quantum vacuum. With increasing coupling strength, the conformal window terminates either through fixed point mergers or via the onset of vacuum instability. Despite their qualitatively different origins, constraints are quantitatively similar, with vacuum stability offering the tightest one, (5.31). Moreover, the conformal window based on the convergence of fixed points and scaling exponents (Fig. 5.1) is less constrained than the one

based on beta functions (Fig. 5.2). Some phenomenological implications have been worked out for particle physics and cosmology.

It has also been noted that another conformal window may exist in the regime where the parameter  $\epsilon$  becomes large [112, 127–129]. If so, the underlying mechanism is non-perturbative. Presently, results are available at the leading order in  $1/\epsilon$ . Assuming the fixed point exists at finite  $1/\epsilon$ , a rough estimate for its conformal window has been given based on perturbation theory, (5.32).

As a final point, we note that the theory remains perturbative in the entire conformal window, much unlike the IR conformal windows in QCD-like theories [261]. The culprit for this is the scalar sector which controls the stability of the ground state. It would be good to confirm these results non-perturbatively, also in view of higher dimensional operators and finite  $N$  corrections.

## Technicalities

In Sec. 5.2, and starting from known general expressions in the  $\overline{\text{MS}}$  renormalisation scheme [182–185, 187], we have derived all beta functions and anomalous dimensions for our model both manually, and with the help of a purpose-made algebraic code. In this appendix we provide some details on the extraction of the two-loop contributions to the running of the scalar quartic couplings. We follow closely the notation of [185] and [182–184]. Our conventions for the most general Yukawa and quartic scalar selfinteractions are

$$\begin{aligned} L_{\text{Yuk.}} &= -\frac{1}{2}(Y_{jk}^a \Phi^a \Psi_j \Psi_k + \text{h.c.}), \\ L_{\text{pot.}} &= -\frac{1}{4!} \lambda_{abcd} \Phi^a \Phi^b \Phi^c \Phi^d, \end{aligned} \quad (5.36)$$

where  $\Psi_j$  denote Weyl fermions, and  $\Phi^a$  real scalars. Below, we will find it convenient to view the Yukawa couplings as symmetric matrices in the fermionic indices  $Y^a$ , with  $(Y^a)_{jk} = Y_{jk}^a$ .

Due to the scalars being gauge singlets in our model (5.1), (5.2), the number of non-zero contributions reduces drastically, and a general expression for the two-loop beta function of the quartics can be given. Writing the scalar beta functions as  $\beta_{abcd} = \mu \partial_\mu \lambda_{abcd}$ , and also using conventions as in (5.6), we have

$$\begin{aligned} \beta_{abcd}^{(2)} &= \sum_{e=a,b,c,d} \frac{1}{2} \left( \Lambda_{ee}^2 - 3H_{ee}^2 - 2\overline{H}_{ee}^2 + 10Y_{ee}^{2F} \right) \lambda_{abcd} \\ &\quad - \overline{\Lambda}_{abcd}^3 - 2\overline{\Lambda}_{abcd}^{2Y} + \overline{H}_{abcd}^\lambda + 2H_{abcd}^Y + 4\overline{H}_{abcd}^Y + 4H_{abcd}^3 - 2H_{abcd}^F. \end{aligned} \quad (5.37)$$

For convenience, we have scaled the loop factor  $(4\pi)^4$  into the couplings. The terms in the first line of (5.37) are the two-loop corrections to the scalar legs, with

$$\begin{aligned} \Lambda_{ab}^2 &= \frac{1}{6} \lambda_{acde} \lambda_{bcde}, \\ H_{ab}^2 &= \frac{1}{2} \text{Tr} \left[ Y^a Y^{\dagger b} Y^c Y^{\dagger c} + Y^{\dagger a} Y^b Y^{\dagger c} Y^c \right], \\ \overline{H}_{ab}^2 &= \frac{1}{2} \text{Tr} \left[ Y^a Y^{\dagger c} Y^b Y^{\dagger c} + Y^{\dagger a} Y^c Y^{\dagger b} Y^b \right], \\ Y_{ab}^{2F} &= \frac{1}{2} g^2 \text{Tr} \left[ C_2(F) (Y^a Y^{\dagger b} + Y^b Y^{\dagger a}) \right]. \end{aligned} \quad (5.38)$$

The terms in the second line of (5.37) are the various vertex corrections, defined as

$$\begin{aligned}
\bar{\Lambda}_{abcd}^3 &= \frac{1}{4} \sum_{\text{perms}} \lambda_{abef} \lambda_{cegh} \lambda_{dfgh}, \\
\bar{\Lambda}_{abcd}^{2Y} &= \frac{1}{16} \sum_{\text{perms}} \lambda_{abef} \lambda_{cdeg} \text{Tr} [Y^{\dagger f} Y^g + Y^{\dagger g} Y^f], \\
\bar{H}_{abcd}^\lambda &= \frac{1}{8} \sum_{\text{perms}} \lambda_{abef} \text{Tr} [Y^c Y^{\dagger e} Y^d Y^{\dagger f} + (Y \leftrightarrow Y^\dagger)], \\
H_{abcd}^Y &= \sum_{\text{perms}} \text{Tr} [Y^{\dagger a} Y^b Y^{\dagger c} Y^d Y^{\dagger e} Y^e], \\
\bar{H}_{abcd}^Y &= \frac{1}{2} \sum_{\text{perms}} \text{Tr} [Y^{\dagger a} Y^e Y^{\dagger b} Y^c Y^{\dagger d} Y^e + (Y \leftrightarrow Y^\dagger)], \\
H_{abcd}^3 &= \frac{1}{2} \sum_{\text{perms}} \text{Tr} [Y^a Y^{\dagger b} Y^e Y^{\dagger c} Y^d Y^{\dagger e}], \\
H_{abcd}^F &= g^2 \sum_{\text{perms}} \text{Tr} [\{C_2(F), Y^a\} Y^{\dagger b} Y^c Y^{\dagger d}],
\end{aligned} \tag{5.39}$$

where  $\sum_{\text{perms}}$  denotes the sum over all permutations of the indices  $a, b, c, d$ . Traces are taken over all fermion indices, and the matrix  $C_2(F)$  is the quadratic Casimir for the fermions.

Next, we need to map and evaluate expressions in the conventions of our model (5.1), (5.2) and (5.3). The algebra is somewhat tedious since the scalar couplings  $\lambda_{abcd}$  in (5.36) are fully symmetrised, differently normalised than those in the model considered here, and defined in terms of fields decomposed into real degrees of freedom. One simplification is that the contribution from the field strength renormalisation is, of course, equal for each of the quartic couplings  $\lambda_{abcd}$ . By a suitable choice of outer indices, renormalisation group equations for  $\alpha_u, \alpha_v$  in (5.3) are obtained. For example, for the double-trace coupling, taking the outer legs as  $\Phi^a, \Phi^b = (\text{Re } H)_{ii}$  and  $\Phi^c, \Phi^d = (\text{Re } H)_{jj}$  with  $i \neq j$ , leads to  $\frac{1}{4!} \lambda_{aacc} = \alpha_v / (12N_F^2)$ . For the single trace coupling, taking  $\Phi^a = (\text{Re } H)_{ii}, \Phi^b = (\text{Re } H)_{ij}, \Phi^c = (\text{Re } H)_{jj}$  and  $\Phi^d = (\text{Re } H)_{ji}$  with  $i \neq j$  leads to  $\frac{1}{4!} \lambda_{abcd} = \alpha_u / (24N_F)$ , and similarly for the map from  $Y_{jk}^a$  onto  $\alpha_y$ .

With these considerations in mind we find the two loop contributions to  $\mu \partial_\mu \alpha_{u,v}$  from (5.37), (5.38) and (5.39). In terms of (5.4), and neglecting subleading terms of  $\mathcal{O}(1/N)$  in the Veneziano limit, we obtain from (5.38)

$$\begin{aligned}
\sum_e \Lambda_{ee}^2 &= 16\alpha_u^2, & \sum_e H_{ee}^2 &= 2(11 + 2\epsilon)\alpha_y^2, \\
\sum_e \bar{H}_{ee}^2 &= 0, & \sum_e Y_{ee}^{2F} &= 2\alpha_g \alpha_y,
\end{aligned} \tag{5.40}$$

where the sum runs over any four scalar indices. The two-loop vertex corrections (5.39) to the flow of the single-trace quartic coupling  $\mu \partial_\mu \alpha_u$ , normalised to account for the map from  $\lambda_{abcd}$  to  $\alpha_u$  in (5.37), are

$$\begin{aligned}
H_u^F &= (11 + 2\epsilon)\alpha_g \alpha_y^2, & \bar{\Lambda}_u^3 &= 32\alpha_u^3, \\
H_u^Y &= \frac{1}{2}(11 + 2\epsilon)^2 \alpha_y^3, & \bar{\Lambda}_u^{2Y} &= 8\alpha_y \alpha_u^2, \\
\bar{H}_u^Y &= 0, & H_u^3 &= 0, & \bar{H}_u^\lambda &= 0.
\end{aligned} \tag{5.41}$$

Similarly, the vertex corrections (5.39) to the flow of the double-trace coupling  $\mu \partial_\mu \alpha_v$ , now nor-

malised to account for the map from  $\lambda_{abcd}$  to  $\alpha_v$ , are given by

$$\begin{aligned}
 \bar{\Lambda}_v^3 &= 48 \alpha_u^2 (2\alpha_u + \alpha_v), & \bar{H}_v^\lambda &= 4(11 + 2\epsilon) \alpha_y^2 \alpha_u, \\
 \bar{\Lambda}_v^{2Y} &= 4 \alpha_y (3\alpha_u^2 + 4\alpha_u \alpha_v + \alpha_v^2), & H_v^3 &= \frac{1}{4}(11 + 2\epsilon)^2 \alpha_y^3, \\
 H_v^Y &= 0, & \bar{H}_v^Y &= 0, & H_v^F &= 0.
 \end{aligned} \tag{5.42}$$

Combining (5.40), (5.41) and (5.42) leads to the final result (5.9) and (5.10). The expressions for the two-loop anomalous dimensions (5.11), (5.12) have been deduced from general expressions using similar techniques.

## 6 Majorana fermions and large- $N$ equivalences

### 6.1 Introduction

Equivalences or dualities between seemingly different theories can provide valuable insights into the dynamics of quantum fields at weak and strong coupling. Well-known examples include equivalences between  $SU$ ,  $SO$ , and  $Sp$  gauge theories in the limit where the rank of the gauge group is large [277], electric-magnetic duality in supersymmetric theories [278], the seminal AdS/CFT conjecture [279], or equivalences between theories related by orbifold/orientifold projections [280–285] where parent and child theories achieve coinciding perturbative expansions in the planar limit, and, under some conditions, non-perturbative equivalence [286, 287]. Large  $N$  equivalences have also seen many applications in QCD-like theories including on the lattice [288–290].

On a different tack, the discovery of interacting ultraviolet fixed points in QCD-like theories, first conjectured in [89], has sparked a lot of interest [2, 4, 67, 110–115, 121–123, 233, 258, 291]. It has led to a general classification of  $4d$  quantum field theories including necessary and sufficient conditions and strict no-go theorems for weakly interacting fixed points [110, 111]. In the large  $N$  limit, proofs for asymptotic safety with Dirac fermions are available with [115] and without supersymmetry [2, 112, 114, 233]. Key ingredients are Yukawa interactions which can stabilise non-free gauge couplings [110]. At finite  $N$ , these ideas are used to UV complete the Standard Model [121, 122, 291] and to study aspects of flavour and vacuum stability [4, 123].

In this paper, we explain how asymptotic safety materialises in theories with Majorana fermions and elementary mesons, and how this compares to settings with Dirac fermions.<sup>15</sup> With the help of perturbation theory, the renormalisation group (RG), negative dimensionality theorems, and ideas from string theory, we also put forward new classes of large  $N$  equivalences amongst gauge-Yukawa theories with different gauge or global symmetries, and different types of matter fields. Results include a triality of asymptotically safe theories with  $SU$ ,  $SO$  or  $Sp$  gauge groups with identical phase diagrams and scaling exponents at ultraviolet critical points, and dualities between asymptotically free gauge-matter theories with identical infrared critical points, and more.

---

<sup>15</sup>Here we distinguish theories with Dirac and Majorana fermions by the Yukawa interaction. If the scalar acquires a vacuum expectation value, the Yukawa term gives rise to either a Dirac or a Majorana mass in terms of the Weyl components for each fermion.



Invariant	$SU(N)$	$SO(N)$	$Sp(N)$
$d_R$	$N$	$N$	$N$
$C_2^R$	$\frac{1}{2}(N - 1/N)$	$\frac{1}{4}(N - 1)$	$\frac{1}{4}(N + 1)$
$d_G$	$N^2 - 1$	$\frac{1}{2}N(N - 1)$	$\frac{1}{2}N(N + 1)$
$C_2^G$	$N$	$\frac{1}{2}(N - 2)$	$\frac{1}{2}(N + 2)$

**Table 6.1:** Dimensions and quadratic Casimirs of fundamental and adjoint representations with Dynkin index  $S_2^R = \frac{1}{2}$ .

## 6.2 Majorana fermions

We consider non-abelian gauge theories coupled to Majorana fermions  $\Psi_i$  and singlet complex scalar fields  $H_{ij}$ . Majorana fermions are their own charge conjugates  $\Psi^c = \Psi$  whose left- and right-handed chiral components

$$\Psi = \frac{1}{\sqrt{2}} (\psi, \psi^c)^\top \quad (6.1)$$

relate to the same Weyl field  $\psi$  with charge conjugation  $\psi^c = \varepsilon \psi^*$  and  $\varepsilon = \begin{pmatrix} 0 & 1 \\ -1 & 0 \end{pmatrix}$ . Real representations ensure that both Weyl components undergo identical gauge transformations, whose generators are purely imaginary and antisymmetric  $t^a = -(t^a)^\top = -(t^a)^*$ . For theories with chiral Yukawa interactions the requirement for real representations can be weakened to include pseudo-real ones which are real up to a transformation  $(t^a)^\top = -M t^a M^{-1}$ . In either case chiral gauge anomalies cancel due to the vanishing of

$$d^{abc} \equiv \frac{1}{2} \text{tr} [t^a \{t^b, t^c\}] = 0. \quad (6.2)$$

To ensure strict perturbative control, we use a suitable large  $N$  limit [228] which necessitates the Majorana fermions to be in the fundamental representation. The latter implies that unitary or any of the exceptional gauge groups are excluded, which leaves us with orthogonal or symplectic gauge groups.

**Orthogonal gauge symmetry  $SO(N)$ .** We begin with a theory of  $N_f$  Majorana fermions in the fundamental representation of an  $SO(N)$  gauge theory, interacting with gauge-singlet complex scalar fields  $H$ . The theory has a global  $SU(N_f)$  flavour symmetry with the Weyl components transforming in the fundamental and the scalars in the two-index symmetric representation  $H_{ij} =$

	$\alpha_g^*$	$\alpha_y^*$	$\alpha_u^*$	$\alpha_v^*$	$\mathfrak{P}_1$	$\mathfrak{P}_2$	$\mathfrak{P}_3$	$\mathfrak{P}_4$	Type
<b>FP<sub>1</sub></b>	$-\frac{8}{75}\epsilon$	0	0	0	$\frac{16}{225}\epsilon^2$	$\frac{8}{25}\epsilon$	0	0	<b>IR</b>
<b>FP<sub>2</sub></b>	$\frac{52}{57}\epsilon$	$\frac{8}{19}\epsilon$	$\frac{2(\sqrt{23}-1)}{19}\epsilon$	$a_{UV}\epsilon$	$-\frac{104}{171}\epsilon^2$	$\frac{52}{19}\epsilon$	$\frac{8}{19}\sqrt{20+6\sqrt{23}}\epsilon$	$\frac{16}{19}\sqrt{23}\epsilon$	<b>UV</b>
<b>FP<sub>3</sub></b>	$-\frac{10}{3}\epsilon$	$-\frac{4}{3}\epsilon$	$\frac{1-2\sqrt{3}}{3}\epsilon$	$a_{IR}\epsilon$	$\frac{20}{9}\epsilon^2$	$-10\epsilon$	$-8\left(1+\frac{4}{3}\sqrt{3}\right)^{1/2}\epsilon$	$-\frac{32}{\sqrt{3}}\epsilon$	<b>IR</b>

**Table 6.2:** Interacting fixed points and scaling exponents to leading order in  $\epsilon$ , with  $a_{UV} = \frac{2}{19}[(20 + 6\sqrt{23})^{1/2} - 2\sqrt{23}]$  and  $a_{IR} = \frac{4}{3}\sqrt{3} - (1 + \frac{4}{3}\sqrt{3})^{1/2}$ . The fixed points FP<sub>2</sub> (FP<sub>1,3</sub>) are UV (IR) and physical for small positive (negative)  $\epsilon$ , respectively.

$H_{(ij)}$ . The Lagrangian reads

$$L = -\frac{1}{4}F_{\mu\nu}^a F^{a\mu\nu} + \text{tr}(\psi^\dagger i\sigma^\mu D_\mu \psi) + \text{tr}(\partial_\mu H^\dagger \partial^\mu H) - \frac{1}{2}y \text{tr}(\psi^\dagger h H \epsilon \psi + \psi^\dagger h H^\dagger \epsilon \psi^*) - u \text{tr}(H^\dagger H)^2 - v(\text{tr} H^\dagger H)^2 \quad (6.3)$$

where  $F_{\mu\nu}^a$  denotes the non-abelian field strength, the trace sums over gauge and flavour indices, and gauge-contractions of fermion bilinears  $(\chi \xi) = \chi_\alpha h^{\alpha\beta} \xi_\beta$  are symmetric with  $h^{\alpha\beta} = h^{\beta\alpha}$  and  $h^{\alpha\beta} h_{\beta\gamma} = \delta^\alpha_\gamma$ . The four canonically marginal couplings  $\{g, y, u, v\}$  of the perturbatively renormalisable theory are the gauge, Yukawa, single, and double trace quartic, respectively. Next, we investigate the renormalisation group equations for the running couplings [182–185] and search for perturbative fixed points of the theory [110]. Perturbative control is achieved using a Veneziano limit [228] where the dimension of the fundamental representation  $d_R$  and the number of fermion flavours  $N_f$  are sent to infinity while their ratio is kept fixed (see Tab. 6.1 for our conventions of group-theoretical parameters). The parameter

$$\epsilon = \frac{N_f}{N} - \frac{11}{2} \quad (6.4)$$

becomes continuous and may take any value within the range  $-\frac{11}{2} < \epsilon < \infty$ . For  $\epsilon < 0$ , the theory is asymptotically free, while asymptotic freedom is absent for  $\epsilon > 0$ . Following 't Hooft [230], we introduce rescaled couplings suitable for a planar or large  $N$  limit

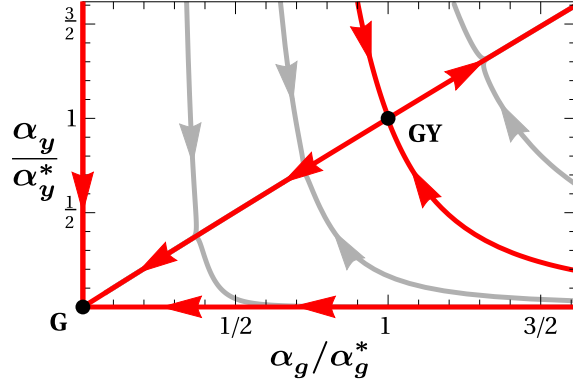
$$\alpha_x = \frac{d_R x^2}{(4\pi)^2}, \quad \alpha_u = \frac{N_f u}{(4\pi)^2}, \quad \alpha_v = \frac{N_f^2 v}{(4\pi)^2}, \quad (6.5)$$

where  $x = g$  or  $y$ , and beta functions  $\beta_i \equiv d\alpha_i/d\ln\mu$ . To the leading non-trivial orders in perturbation theory which is two loop in the gauge and one loop in the Yukawa and quartic beta functions, we find

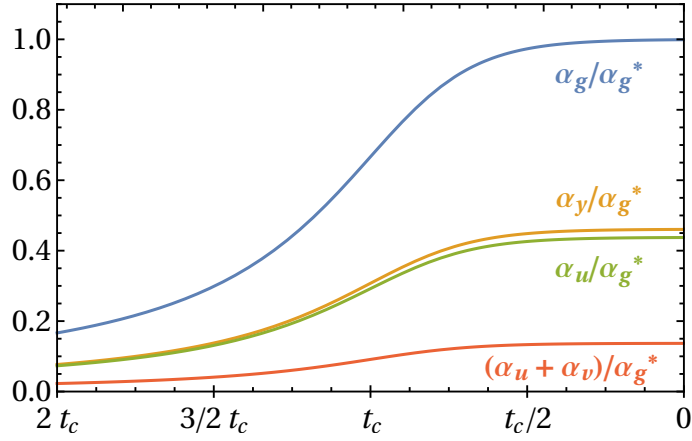
$$\begin{aligned} \beta_g &= \alpha_g^2 \left[ \frac{2}{3}\epsilon + \left( \frac{25}{4} + \frac{13}{6}\epsilon \right) \alpha_g - \frac{1}{2} \left( \frac{11}{2} + \epsilon \right)^2 \alpha_y \right], \\ \beta_y &= \alpha_y \left[ \left( \frac{13}{2} + \epsilon \right) \alpha_y - 3\alpha_g \right], \\ \beta_u &= 4\alpha_u^2 + 2\alpha_y \alpha_u - \left( \frac{11}{2} + \epsilon \right) \alpha_y^2, \\ \beta_v &= 2\alpha_v^2 + 8\alpha_u \alpha_v + 6\alpha_u^2 + 2\alpha_y \alpha_v. \end{aligned} \quad (6.6)$$

In any  $4d$  quantum field theory, the weakly coupled fixed point solutions to  $\beta_i = 0$  are either of the Banks-Zaks or of the gauge-Yukawa type [110, 111]. For small  $\epsilon$  they arise as a strict power series in  $\epsilon$  where subleading terms up to order  $\epsilon^n$  are obtained from the loop order  $(n+1, n, n)$  in the gauge, Yukawa, and quartic beta functions [2, 114]. Also, any weakly coupled fixed point corresponds to a (unitary) conformal field theory [138]. Our results are summarised in Tab. 6.2. In the regime with asymptotic freedom the theory (6.3) with (6.6) displays a Banks-Zaks fixed point  $\text{FP}_1$ . Infrared gauge-Yukawa fixed points are absent. In the regime where asymptotic freedom is lost, the gauge-Yukawa fixed point  $\text{FP}_2$  arises with  $(\alpha_g^*, \alpha_y^*, \alpha_u^*, \alpha_u^* + \alpha_v^*) \approx (0.91, 0.42, 0.40, 0.13) \epsilon$  and a stable quantum vacuum [113, 292]

$$\alpha_u^* \geq 0, \quad \alpha_u^* + \alpha_v^* \geq 0. \quad (6.7)$$



**Figure 6.1:** Phase diagram with asymptotic safety ( $\epsilon = 0.01$ ), projected onto the  $(\alpha_g, \alpha_y)$  plane. Arrows point from the UV to the IR. Asymptotically safe trajectories emanate from the gauge-Yukawa fixed point  $\text{FP}_2$  and run along a separatrix towards either a weakly or a strongly coupled IR regime.



**Figure 6.2:** Cross-over of running couplings from asymptotic safety to infrared freedom in units of  $\alpha_g^*$  with  $\mu_c = \Lambda \exp t_c$ .

A secondary fixed point in the scalar sector does not lead to a stable vacuum and has been discarded. The universal exponents  $\vartheta_1 < 0 < \vartheta_{2,3,4}$  establish that the fixed point is UV and the scaling power-law rather than logarithmic, and that the UV critical surface is one-dimensional corresponding to a single relevant coupling. The phase diagram with RG trajectories in the  $(\alpha_g, \alpha_y)$ -plane is displayed in Fig. 6.1. Switching on mass terms for the vector-like fermions or the scalars adds additional relevant directions (not shown), because perturbatively small anomalous dimensions cannot turn these into irrelevant operators. By the same token, higher dimensional interactions remain strictly irrelevant [233]. The separatrix which connects the UV fixed point with the free IR fixed point is shown in Fig. 6.2. The scale  $\mu_c = \Lambda \exp t_c$  with  $\Lambda$  the high scale and  $\alpha_g(t_c) = \frac{2}{3} \alpha_g^*$  [113] characterises the cross-over between the two fixed points and is the analogue of  $\Lambda_{\text{QCD}}$  in QCD. A second separatrix exists towards a regime with strong coupling and confinement in the IR (not shown). Finally, we note that all previously known quantum field theories in four dimensions with exact asymptotic safety involve unitary gauge symmetry and Dirac fermions [2, 112, 114, 115]. In this light, the theory (6.3) with (6.6) offers the first proof of existence for asymptotic safety in gauge theories with  $SO(N)$  gauge symmetry, and in theories with Majorana fermions.

**Symplectic gauge symmetry  $Sp(N)$ .** Next, we turn to a theory of  $N_f$  Majorana fermions in the fundamental representation of an  $Sp(N)$  gauge theory interacting with gauge-singlet complex scalar fields  $H$ . In our conventions  $N$  is an even integer, and  $Sp(2) \simeq SO(3) \simeq SU(2)$ . The theory has a global  $SU(N_f)$  flavour symmetry with Weyl components transforming in the fundamental and  $H$  in the two-index antisymmetric representation  $H_{ij} = H_{[ij]}$ . To avoid a Witten anomaly [293]  $N_f$  has to be an even integer as well. The perturbatively renormalisable Lagrangian of the theory takes the form

$$\begin{aligned} L = & -\frac{1}{4}F_{\mu\nu}^a F^{a\mu\nu} + \text{tr}(\psi^\dagger i\sigma^\mu D_\mu \psi) + \text{tr}(\partial_\mu H^\dagger \partial^\mu H) \\ & -\frac{1}{2}y \text{tr}(\psi^\dagger f H \epsilon \psi + \psi^\dagger f H^\dagger \epsilon \psi^*) - u \text{tr}(H^\dagger H)^2 - v(\text{tr} H^\dagger H)^2 \end{aligned} \quad (6.8)$$

where we recall that gauge-contractions of fermion bilinears  $(\chi \xi) = \chi_\alpha f^{\alpha\beta} \xi_\beta$  are antisymmetric with  $f^{\alpha\beta} = -f^{\beta\alpha}$  and  $f^{\alpha\beta} f_{\beta\gamma} = -\delta^\alpha_\gamma$ . A Veneziano limit is established using (6.4) and rescaled couplings (6.5). Introducing the parameter  $\epsilon$  as in (6.4), we find the RG beta functions for all couplings to the leading non-trivial order in perturbation theory. Denoting the 't Hooft couplings (6.5) for the theories (6.3) and (6.8) as  $\alpha_i^{SO}$  and  $\alpha_i^{Sp}$  respectively, we find the remarkable result that the RG beta functions (6.6) for the theory (6.3) agree exactly with those of the theory (6.8), after the identification of couplings

$$\alpha_i^{SO} = \alpha_i^{Sp}. \quad (6.9)$$

Consequently the fixed points and scaling exponents (FP<sub>1</sub> and FP<sub>2</sub> in Tab. 6.2), and the RG trajectories and phase diagrams (Figs. 6.1 and 6.2) of the theories (6.3) and (6.8) are *identical* in the Veneziano limit. However, we also note that the equivalence is mildly violated beyond the Veneziano limit at large yet finite  $N$  and  $N_f$  due to subleading corrections of order  $1/N$  and  $1/N_f$  which arise with the same magnitude but opposite sign. Finally, we emphasise that the theory (6.8) yields the first rigorous example for asymptotic safety in a symplectic gauge theory coupled to matter. The result thus establishes that asymptotic safety can be achieved in  $4d$  quantum field theories with any of the non-exceptional gauge groups, and for sufficiently large  $N$ .

### 6.3 Dirac fermions

Next, we consider theories of  $N_f$  Dirac fermions  $\Psi_i$  interacting with non-abelian gauge fields and gauge-singlet complex scalar fields  $H_{ij}$ . The theories have a global  $SU(N_f) \times SU(N_f)$  flavour symmetry with the elementary scalars  $H$  transforming in the bifundamental. The perturbatively renormalisable Lagrangian is given by

$$\begin{aligned} L = & -\frac{1}{4}F_{\mu\nu}^a F_a^{\mu\nu} + \text{tr}(\bar{\Psi} i \not{D} \Psi) + \text{tr}(\partial_\mu H^\dagger \partial^\mu H) \\ & -y \text{tr}(\bar{\Psi}_L H \Psi_R + \bar{\Psi}_R H^\dagger \Psi_L) - u \text{tr}(H^\dagger H)^2 - v(\text{tr} H^\dagger H)^2 \end{aligned} \quad (6.10)$$

where  $F_{\mu\nu}^a$  denotes the non-abelian field strength, the trace sums over all indices and the decomposition  $\Psi = \Psi_L + \Psi_R$  with  $\Psi_{L/R} = \frac{1}{2}(1 \pm \gamma_5)\Psi$  is understood. Due to the fermions being vector-like, gauge-anomalies cancel by design and no restriction on their representations apply. In addition to the gauge coupling  $g$  and the Yukawa coupling  $y$ , we observe two independent quartic self interactions  $u$  and  $v$ , which provides us with a set of four canonically marginal couplings.

plings  $\{g, y, u, v\}$ . In the following, we consider the Dirac fermions in the fundamental gauge representation of  $SU(N)$ ,  $SO(2N)$  and  $Sp(2N)$ . We also establish a Veneziano limit using the parameter (6.4) and adopt the same set of 't Hooft couplings (6.5) as in the cases with Majorana fermions.

**Unitary gauge symmetry  $SU(N)$ .** For unitary gauge groups, the theory (6.10) has been studied in a number of works [2, 112, 113, 294, 295]. In the regime with asymptotic freedom, it can display a Banks-Zaks fixed point. Once asymptotic freedom is lost, it develops a weakly interacting asymptotically safe UV fixed point [112] with a stable quantum vacuum [113]. The corresponding UV conformal window has been determined up to the complete next-to-next-to-leading order in perturbation theory which is three loop in the gauge and two loop in the Yukawa and quartic couplings [2]. The main observation here is that the theory (6.10) with  $SU$  gauge symmetry and Dirac fermions is intimately related to the theories (6.3) with  $SO$  and to (6.8) with  $Sp$  gauge symmetry and Majoranas. Introducing the parameter  $\epsilon$  as in (6.4) and denoting the couplings (6.5) for the theory (6.10) with unitary gauge symmetry as  $\alpha_i^{SU}$ , we find that beta functions in the Veneziano limit are *identical* to those of the theories (6.3) and (6.8), given by (6.6), provided we rescale the 't Hooft couplings by a factor of two,

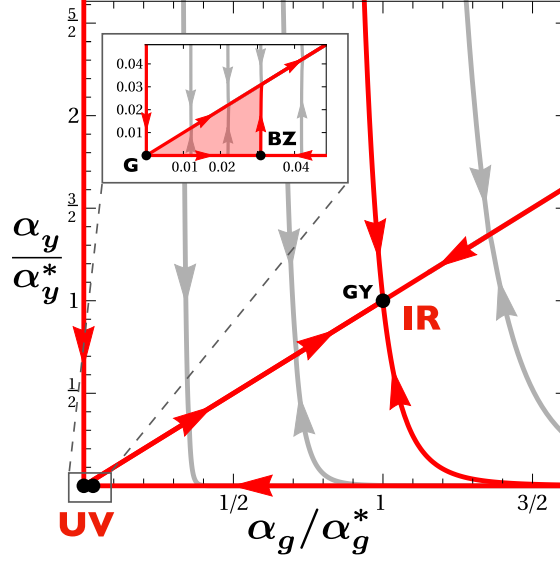
$$\alpha_i^{SO} = \alpha_i^{Sp} = 2 \alpha_i^{SU}. \quad (6.11)$$

Consequently fixed points are either of the Banks-Zaks ( $FP_1$ ) or the gauge-Yukawa-type ( $FP_2$ ) and take the values given in Tab. 6.2 after rescaling. Phase diagrams and RG trajectories in these theories are also identical up to (6.11), and given by Figs. 6.1 and 6.2. Most notably, universal scaling exponents, which are insensitive to the normalisation of couplings, are identical between the two theories, and take the values given in Tab. 6.2.

**$SO(2N)$  gauge symmetry.** Next, we consider settings with  $N_f$  Dirac fermions in the fundamental representation of  $SO(2N)$  gauge symmetry, again coupled to scalars in the bifundamental two-index representation of the global  $SU(N_f) \times SU(N_f)$  flavour symmetry, and with action (6.10). Notice that since Dirac fermions have twice as many degrees of freedom as Majorana fermions, and to ensure that the definition for the small parameter  $\epsilon$  (6.4) remains unchanged, the dimension of the gauge group has been taken twice as large as in the case with  $SU$  gauge symmetry. Then, to the leading order in perturbation theory and in the Veneziano limit, we find

$$\begin{aligned} \beta_g &= \alpha_g^2 \left[ \frac{2}{3}\epsilon + \left( \frac{25}{4} + \frac{13}{6}\epsilon \right) \alpha_g - \frac{1}{2} \left( \frac{11}{2} + \epsilon \right)^2 \alpha_y \right], \\ \beta_y &= \alpha_y \left[ \left( \frac{15}{2} + \epsilon \right) \alpha_y - 3\alpha_g \right], \\ \beta_u &= 8\alpha_u^2 + 4\alpha_y\alpha_u - \left( \frac{11}{2} + \epsilon \right) \alpha_y^2, \\ \beta_v &= 4\alpha_v^2 + 16\alpha_u\alpha_v + 12\alpha_u^2 + 4\alpha_y\alpha_v \end{aligned} \quad (6.12)$$

for models (6.10) with orthogonal gauge symmetry. In stark contrast to the previous examples, no interacting UV fixed points are found as soon as asymptotic freedom is absent [110]. However, the beta functions (6.12) admit interacting fixed points provided the theory is asymptotically free ( $\epsilon < 0$ ). These are either of the Banks-Zaks ( $FP_1$ ) or of the gauge-Yukawa-type ( $FP_3$ ), with fixed point coordinates and scaling exponents summarised in Tab. 6.2. The gauge-Yukawa fixed point  $FP_3$  at  $(\alpha_g^*, \alpha_y^*, \alpha_u^*, \alpha_u^* + \alpha_v^*) \approx -(3.33, 1.33, 1.23, 0.58) \epsilon$  also displays a stable quantum vacuum (6.7).



**Figure 6.3:** Phase diagram with asymptotic freedom ( $\epsilon = -0.01$ ) projected onto the  $(\alpha_g, \alpha_y)$  plane. Arrows point from the UV to the IR. Dots show the Gaussian (G), the Banks-Zaks (BZ), and the infrared gauge-Yukawa (GY) fixed points. The inset highlights the two-dimensionality of the UV critical surface (red shaded area) which becomes effectively one-dimensional in the cross-over to the IR.

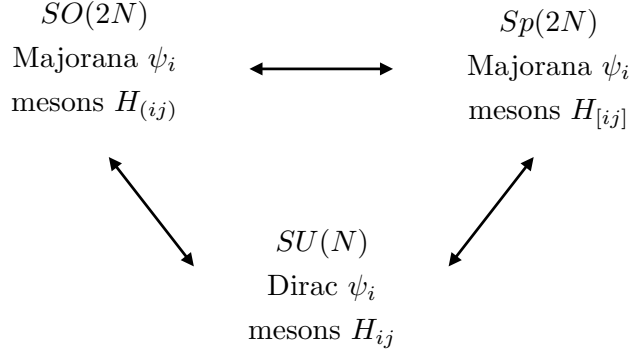
The universal exponents  $0 < \vartheta_{1,2,3,4}$  establish that the fixed point  $\text{FP}_3$  is fully attractive in all canonically marginal couplings thus corresponding to an IR sink [121], and that the scaling is power-law rather than logarithmic. The phase diagram in regimes with asymptotic freedom is shown in Fig. 6.3. We notice that the Banks-Zaks fixed point is parametrically small compared to the gauge-Yukawa fixed point (see the inset in Fig. 6.3). It implies that the UV critical surface at the Gaussian fixed point, which is two-dimensional, *effectively* becomes one-dimensional, given by the separatrix connecting the Gaussian and the GY fixed point.

**$Sp(2N)$  gauge symmetry.** Finally, we turn to the models (6.10) with  $N_f$  Dirac fermions in the fundamental of  $Sp(2N)$  gauge symmetry, coupled to scalars in the bifundamental two-index representation of the global  $SU(N_f) \times SU(N_f)$  flavour symmetry. Using (6.4), introducing couplings as in (6.5), and following the same steps as before, we find once more that the beta functions in the Veneziano limit come out *identical* to those found in (6.12) after a straight identification of couplings (6.9). It follows that the running of couplings, the phase diagrams, and the conformal critical points of theories (6.10) are identical, irrespective of whether we impose an orthogonal or symplectic gauge symmetry.

## 6.4 Large $N$ equivalences

In this section, we investigate the kinematical equivalences detected in the previous sections from the point of view of weak-coupling dualities and orbifold projections, and discuss implications for asymptotic safety.

**Negative dimensionality theorems.** Some of our results can be understood with the help of so-called negative dimensionality theorems [231, 296–299]. They state that for any  $SO(L)$  in-



**Figure 6.4:** Triality of asymptotic safety, and large  $N$  equivalences amongst matter-gauge theories with global  $SU(2N_f)$  flavour symmetry and Majorana fermions (top), and a theory with a global  $SU(N_f) \times SU(N_f)$  flavour symmetry and Dirac fermions (bottom). The horizontal arrow emphasises that RG flows, phase diagrams, and critical points are identical. Top-down arrows indicate equivalence after orbifold reduction.

variant scalar there exists a corresponding  $Sp(L)$  invariant scalar, and vice versa, obtained by exchanging symmetrisations and antisymmetrisations, replacing the  $SO(L)$  symmetric bilinear invariant  $h_{\alpha\beta}$  by the  $Sp(L)$  antisymmetric bilinear invariant  $f_{\alpha\beta}$ , and replacing  $L$  by  $-L$ . Similarly, for any  $SU(M)$  invariant scalar exchanging symmetrisations and antisymmetrisations is equivalent to replacing  $M$  by  $-M$ . Schematically, we write the theorems as

$$SO(L) = \overline{Sp}(-L), \quad SU(M) = \overline{SU}(-M), \quad (6.13)$$

where overlines indicate the transposition of Young tableaux for all representations, corresponding precisely to the interchange of symmetrisation and antisymmetrisation [231, 296–299].

**Symplectic vs orthogonal gauge groups.** Let us now clarify how the negative dimensionality theorems impact on our models. On the level of the local symmetries in the models with Majorana fermions (6.3), (6.8), the relations (6.13) interchange orthogonal and symplectic gauge theories. When applied to the global  $SU(N_f)$  symmetry the transposition of global representations accounts for the different symmetrisations of the scalars, interchanging  $H_{(ij)}$  with  $H_{[ij]}$ , and all of this accompanied by the analytic continuation of field multiplicities towards negative values<sup>16</sup>

$$N \mapsto -N, \quad N_f \mapsto -N_f. \quad (6.14)$$

Fingerprints of the negative dimensionality theorems (6.13) can be seen on the level of the renormalisation group equations. For theories with Majorana fermions, we have confirmed at the leading orders in perturbation theory that the beta functions for the gauge, Yukawa and quartic couplings of the theory (6.3) are *identical* to the beta functions of the theory (6.8) for any  $N$  and  $N_f$ , provided we make the replacement (6.14) in the latter together with  $\{g^2, y^2, u, v\} \mapsto \{-g^2, -y^2, -u, v\}$ . This implies that the gauge, Yukawa, and the single and double trace quartic

<sup>16</sup>Note that this analytic continuation is a purely mathematical feature, the existence of a consistent QFT with negative degrees of freedom or flipped spin statistics is not implied.

$$\begin{array}{ccc}
SO(2N) & & Sp(2N) \\
\text{Dirac } \psi_i & \longleftrightarrow & \text{Dirac } \psi_i \\
\text{mesons } H_{ij} & & \text{mesons } H_{ij}
\end{array}$$

**Figure 6.5:** Duality of conformal fixed points, and large  $N$  equivalences of matter-gauge theories with global  $SU(N_f) \times SU(N_f)$  flavour symmetry.

Model	Lagr.	Gauge symmetry	Global symmetry	Gauge bosons	Fermion type	Weyl components	Scalars	Real scalar components
1	(6.3)	$SO(2N)$	$SU(2N_f)$	$2N^2$	Majorana	$2N \cdot 2N_f$	$H_{(ij)}$	$4N_f^2$
2	(6.8)	$Sp(2N)$	$SU(2N_f)$	$2N^2$	Majorana	$2N \cdot 2N_f$	$H_{[ij]}$	$4N_f^2$
3	(6.10)	$SU(N)$	$SU(N_f) \times SU(N_f)$	$N^2$	Dirac	$N \cdot 2N_f$	$H_{ij}$	$2N_f^2$
4	(6.10)	$SO(2N)$	$SU(N_f) \times SU(N_f)$	$2N^2$	Dirac	$2N \cdot 2N_f$	$H_{ij}$	$2N_f^2$
5	(6.10)	$Sp(2N)$	$SU(N_f) \times SU(N_f)$	$2N^2$	Dirac	$2N \cdot 2N_f$	$H_{ij}$	$2N_f^2$

**Table 6.3:** Gauge, fermionic, and scalar degrees of freedom in the Veneziano limit of models discussed in the main text.

‘t Hooft couplings

$$\{N g^2, N y^2, N_f u, N_f^2 v\} \quad (6.15)$$

are strictly invariant and remain positive even within the theory which has negative  $N$  and  $N_f$ , as they must [300]. For pure quantum gauge theories the invariance of  $N g^2$  under (6.13) is explained in [297]. Moreover, we have also confirmed that the exact same equivalence holds true for beta functions and running couplings in theories with Dirac fermions (6.10) coupled to orthogonal or symplectic gauge fields. In summary, we conclude that the negative dimensionality theorems manifest themselves in the quantum theory through the equivalence of ‘t Hooft couplings and their beta functions for any  $N$  and any  $N_f$ . We expect this equivalence to hold true to any order in the perturbative loop expansion. For positive  $N$  and  $N_f$ , the large  $N$  equivalence of the theories (6.3) and (6.8), and of the theories (6.10) with either  $SO$  or  $Sp$  gauge symmetry, is now simple to understand, the key point being that the explicit dependence of beta functions on field multiplicities arises, in the Veneziano limit, only through the parameter  $\epsilon$  given in (6.4). Since  $\epsilon$  is insensitive to the combined sign change (6.14), the mapping of negative field multiplicities in the partner theory back to positive ones leaves all beta functions for ‘t Hooft couplings (6.15) invariant. The price to pay (for having positive field multiplicities on either side of the duality) is that the equivalence holds only in the large  $N$  limit. In fact, in either theory the subleading corrections start at order  $1/N$  and  $1/N_f$  and enter with the same magnitude but opposite signs (once more owing to the negative dimensionality theorems) thus breaking the duality beyond large  $N$ . This pattern explains the equivalence of beta functions for ‘t Hooft couplings as well as the structure of subleading corrections found in the previous sections, and illustrated in Figs. 6.4 and 6.5. There are two further points worth noting with regards to large  $N$  equivalences. First, counting the number of gauge fields, Weyl fermions, and real scalar fields in either of these, we find that dual theories have the exact same number of degrees of freedom (see Model 1 vs Model



2, and Model 4 vs Model 5 in Tab. 6.3). This no longer holds true beyond large  $N$ . Second, we also emphasize that dual theories described here, in all cases, have the same global symmetry but different gauge symmetry. This supports the view that global symmetry is a property of the system, whereas gauge symmetry is a property of the description of the system [301].

**Unitary gauge groups.** For the theories with Dirac fermions (6.10) and  $SU$  gauge symmetry we confirm that beta functions for 't Hooft couplings are mapped onto themselves under the replacement (6.13), (6.14), valid for all  $N$ . Moreover, subleading corrections in the large  $N$  limit arise as inverse even powers of field multiplicities  $1/N^2$  and  $1/N_f^2$  and are insensitive to a change in sign (6.14), meaning that the theory is effectively self-dual and mapped onto itself for any  $N$ ,  $N_f$ , as it must. The result generalises to  $SU$  gauge theories with matter sectors different from (6.10).

**Orbifold equivalence.** We now turn to the equivalence of theories between Dirac fermions coupled to unitary gauge fields, and Majorana fermions coupled to orthogonal or symplectic gauge fields, illustrated in Fig. 6.4. Theories have different global symmetries, and those with Dirac fermions contain exactly half as many gauge, Weyl, and scalar degrees of freedom as those with Majorana fermions in the Veneziano limit (see Models 1 and 2 vs Model 3 in Tab. 6.3). Still, after the identification of couplings via the map (6.11), all three theories have identical beta functions, phase diagrams, conformal fixed points, and scaling exponents. This pattern suggests that the theories are related by orbifolding. Orbifold projections in quantum field theory link a parent theory to a child theory with the help of a discrete subgroup of the parent's global symmetry [281–286, 288, 289] (see [287, 290] for reviews). "Orbifolding" eliminates those degrees of freedom from the parent theory which are not invariant under the discrete subgroup, leading to the child theory. At the perturbative level, orbifold equivalence is based on the observation that planar diagrams of the parent and child theories coincide to all loop orders, possibly up to a rescaling of couplings, and that correlation functions of gauge-invariant operators obey the same set of closed equations [281]. It has also been shown that the equivalence of theories holds non-perturbatively as long as the global symmetry used for the orbifolding is not broken spontaneously [288]. In the setting illustrated in Fig. 6.4, the Majorana models (6.3) and (6.8) with  $SO(2N)$  or  $Sp(2N)$  gauge symmetry and  $SU(2N_f)$  global symmetry represent parent theories. Then, using a suitable  $\mathbb{Z}_2$  symmetry in the gauge and flavour groups [289] leads in both cases to the child theory (6.10) with Dirac fermions,  $SU(N)$  gauge symmetry, and  $SU(N_f) \times SU(N_f)$  global symmetry [302]. In the Veneziano limit, the orbifold equivalence between parent and child theories is exact, explaining the links observed in Fig. 6.4. The factor of two which appears in the rescaling (6.11) reflects that the parent theories contain twice as many gauge, Weyl, and scalar degrees of freedom as the child theory, see Tab. 6.3. In the literature, some orbifold/orientifold reductions have been reported which relate supersymmetric with non-supersymmetric theories [285, 287]. On the account that asymptotic safety in supersymmetry necessitates the gauge group to be semi-simple [115, 227], however, we do not expect to find a supersymmetric parent for the non-supersymmetric theories with weakly coupled ultraviolet fixed points and simple gauge group studied here.

**Dirac vs Majorana fermions.** Another important observation of this study is that  $SO$  and

$Sp$  gauge theories with Majorana fermions and elementary mesons can develop asymptotically safe UV fixed points while their counterparts with Dirac fermions cannot. To appreciate the origin for this we write the leading loop contributions to the gauge and Yukawa beta functions as  $\partial_t \alpha_g = \alpha_g^2(-B + C\alpha_g - D\alpha_y)$  and  $\partial_t \alpha_y = \alpha_y(E\alpha_y - F\alpha_g)$  with  $C, D$  and  $B, E, F$  denoting universal two-loop and one-loop coefficients respectively. A necessary condition for weakly interacting UV fixed points is given by [110]

$$C' \equiv C - DF/E < 0. \quad (6.16)$$

A generic asymptotically non-free theory ( $B < 0$ ) has loop coefficients  $C, D, E, F > 0$  [110], implying  $C' \leq C$ . The condition (6.16) states that asymptotic safety requires the (Yukawa-shifted) two loop term to become negative,  $C' < 0$ . In all theories with exact asymptotic safety (meaning  $FP_2$  in Tab. 6.2) we find the universal shift

$$C'/C = -\frac{38}{325}, \quad (6.17)$$

assuming small  $0 < \epsilon \ll 1$ . Hence, the Yukawa interactions roughly induce a  $-112\%$  correction to the two-loop gauge coefficient, which is large enough to change the sign of  $C$  and to enable asymptotic safety. Replacing Majorana by Dirac fermions in the theories with  $SO$  or  $Sp$  gauge symmetry effectively changes the scalar matter content. In fact, adjusting  $N$  and  $N_f$  such that theories display the same number of gauge fields and Weyl fermions, we find that the settings with Dirac fermions only feature half as many scalar degrees of freedom (see Models 1 and 2 vs Models 4 and 5 in Tab. 6.3). Although scalars are gauge singlets, they propagate in loops and modify the Yukawa loop coefficient  $E$  which is proportional to the number of degrees of freedom [224]. Here, the coefficient  $E|_{\text{Majorana}} \propto 2N_f + 2N$  reduces down to  $E|_{\text{Dirac}} \propto N_f + 2N$  and gives the first term in  $\beta_y$  of (6.6) and (6.12), respectively, after 't Hooft normalisation. With all other coefficients untouched, we find

$$C'/C = \frac{4}{125} \quad (6.18)$$

instead of (6.17). This corresponds to a  $-97\%$  correction of the two-loop gauge coefficient  $C$ , which is narrowly too small to change the overall sign of  $C$ . The result (6.18) explains why models with Dirac fermions and  $SO$  or  $Sp$  gauge symmetry may display interacting infrared fixed points, but cannot develop interacting ultraviolet ones, much unlike their counterparts with Majoranas.

As a final remark, we note that the ratio (6.18) also dictates the ratio of gauge couplings at the Banks-Zaks fixed point compared to the gauge-Yukawa fixed point in asymptotically free  $SO$  and  $Sp$  gauge theories with Dirac fermions (6.10). There, we found that  $\alpha_g^{\text{BZ}}/\alpha_g^{\text{GY}}|_* = C'/C$  provided that  $0 < -\epsilon \ll 1$  (see  $FP_1$  and  $FP_3$  in Tab. 6.2). Hence, the parametric smallness of the ratio of fixed point couplings, as observed in Fig. 6.3, can now be attributed to the "near-miss" of asymptotic safety due to (6.18).

## 6.5 Discussion and conclusions

As a proof of principle, we have established that asymptotic safety arises in matter-gauge theories with Majorana fermions, and in theories with  $SO$  and  $Sp$  gauge symmetry (6.3), (6.8). Together with the earlier discovery of asymptotic safety with Dirac fermions in  $SU$  gauge theories (6.10), our results clarify that interacting ultraviolet fixed points can readily be realised for either type of fermions and for any of the classical gauge groups. Intriguingly though,  $SU$  gauge symmetry does require fermions to be Dirac, whereas  $SO$ ,  $Sp$  gauge symmetry does require fermions to be Majorana. We have also put forward new classes of large  $N$  equivalences between seemingly different gauge-matter theories. Equivalences between pure  $SU$ ,  $SO$  and  $Sp$  gauge theories in the planar limit have been known for a long time. Here, we have explained how equivalences arise amongst theories with different local symmetries, different matter content, and, possibly, different global symmetries. Invariably, they imply identical all-order RG flows, phase diagrams, and conformal critical points (Tab. 6.2). Examples (Tab. 6.3) include a triality of asymptotic safety (Figs. 6.1 and 6.4) or dualities amongst theories with identical infrared critical points (Figs. 6.3 and 6.5). Based on the underlying structure, many more large  $N$  equivalences arise in gauge theories with matter and Yukawa interactions, also offering new directions for orbifold reductions [287, 302]. Finally, we note that our theories, at interacting fixed points, correspond to unitary conformal field theories. This link allows the extraction of conformal data such as scaling dimensions [2, 112, 114, 115] or structure coefficients [303] directly from the renormalisation group [140], and in a manner complementary to the conformal bootstrap [147]. It will be interesting to see whether the equivalences discovered here (Figs. 6.4 and 6.5) extend to all conformal data. This is left for future work.

## 7 Asymptotic safety beyond the Standard Model

### 7.1 Model

In this chapter, we will consider more realistic QFT descriptions of asymptotically safe particle physics. This means each candidate theory has to be effectively described by the Standard Model (SM) within experimentally accessible energy regimes. Before the electroweak symmetry break-

Field		Gen.	$U(1)_Y$	$SU(2)_W$	$SU(3)_C$
Fermions	$L$	3	$-1/2$	2	1
	$E$	3	$-1$	1	1
	$Q$	3	$+1/6$	2	3
	$U$	3	$+2/3$	1	3
	$D$	3	$-1/3$	1	3
Scalars	$H$	1	$+1/2$	2	1

**Table 7.1:** Field content of the Standard Model of particle physics with number of generations and gauge multiplicities.

ing, the SM consists of a  $U(1)_Y \times SU(2)_W \times SU(3)_C$  gauge group, describing hypercharge, weak isospin and colour charge, as well as the matter content is listed in Tab. 7.1. Besides the gauge interactions, there is also a Yukawa and scalar sector due to interactions the Higgs field  $H$ :

$$\begin{aligned} \mathcal{L}_{\text{yuk, SM}} &= -Y_e^{ij} H L_i^\dagger E_j - Y_d^{ij} H Q_i^\dagger D_j - Y_u^{ij} H^\dagger Q_i^\dagger U_j + \text{h.c.}, \\ \mathcal{L}_H &= -\mu^2 H^\dagger H - \lambda (H^\dagger H)^2. \end{aligned} \quad (7.1)$$

**SM extensions.** As stated above, the goal is to construct a suitable extension of the Standard Model. The strategy to achieve asymptotic safety is to use the model (1.50) as a building block, and embed it into the BSM theory. The advantage of this approach is that the mechanism of asymptotic safety is well understood. Although the Veneziano limit  $N_{f,c} \rightarrow \infty$  as a key ingredient is not realistic, it has been shown in Ch. 5 that finite values of  $N_{f,c}$  within a reasonable magnitude are compatible with the asymptotic safety phenomenon.

Several ansätze for the embedding may be pursued. For instance, gauge and flavour groups as well as particle sectors of both SM and the safe template theory can be kept distinct. This retains the quantities  $N_{f,c}$  to ensure asymptotic safety. However, interactions of both sectors are limited to a few portal terms, which may lead to decoupling in the UV and narrows corrections to the SM in the IR.

To avoid this, both SM and template sector can be coupled together by gauge interactions. The  $U(1)$  triviality problem can also be addressed in that manner. For instance, the SM gauge group

may be embedded in a GUT scenario, or the template gauge group may be replaced with the SM one, an alley pursued in [121, 122]. In the latter case, the SM field content of Tab. 7.1 are supplemented by  $N_f$  BSM fermions  $\psi_i^{L,R}$ , in the representations  $(Y, R_2, R_3)$ , as well as a completely uncharged  $N_f \times N_f$  scalar matrix  $S_{ij}$ . In addition to the SM interactions (7.1), the BSM ones

$$\begin{aligned} \mathcal{L}_{\text{yuk, BSM}} &= -y \psi_i^{L\dagger} S_{ij} \psi_j^R + \text{h.c.}, \\ \mathcal{L}_S &= -\mu_S^2 \text{tr} [S^\dagger S] - u \text{tr} [S^\dagger S S^\dagger S] - v \text{tr} [S^\dagger S]^2 - \delta H^\dagger H \text{tr} [S^\dagger S] \end{aligned} \quad (7.2)$$

are also included in the action. This approach does not violate flavour symmetry of the BSM sector explicitly and retains the quantity  $N_f$ , while trading  $N_c$  for  $Y$  and  $R_{2,3}$ , forfeiting perturbative exactness. Although strict perturbative control is lost [122], many potential fixed points can be identified that allow for matching onto the SM as low as at the TeV scale. This gives experimental access to signatures such as long-lived particles, R-hadrons and Drell-Yan production [121].

**Connecting flavour.** So far, only the gauge symmetries of the SM and BSM sector have been joined, while keeping the flavour symmetries decoupled. In the SM, each Weyl fermion contributes its own subgroup, yielding  $U(3)_L \times U(3)_E \times U(3)_Q \times U(3)_U \times U(3)_D$  overall. These groups are being broken by the SM Yukawa interactions (7.1) except for  $U(1)$  groups for lepton and baryon number as well as hypercharge.

On the BSM side, the flavour symmetry is  $U(N_f)_{\psi^L} \times U(N_f)_{\psi^R} \times U(N_f)_{S^L} \times U(N_f)_{S^R}$ , which gives rise to a general Yukawa interaction  $y_{ijkl} \psi_i^L S_{jk} \psi_l^R + \text{h.c.}$  The Yukawa term  $y_{ijkl} = y \delta_{ij} \delta_{kl}$  breaks this group down to  $U(N_f)_{\psi^L} \times U(N_f)_{\psi^R} \times U(1)_{\text{PQ}}$ .

We will now seek to interweave the SM and BSM global symmetries by adding a new Yukawa interaction, coupling to the SM Higgs,  $\psi^L$  or  $\psi^R$  and one of the SM fermions. This will also provide a connection phenomena of flavour physics. In order to identify flavour groups, we fix  $N_f = 3$ . The weak hypercharge, weak isospin and colour representation of the BSM fermions are constrained by writing down the aforementioned Yukawa interaction. Tab. 7.1 is supplementing by a  $3 \times 3$  gauge singlet scalar matrix  $S$ , and 3 vector-like fermions  $\psi^{L,R}$  in representations listed in Tab. 7.2.

In all of the models A-M of Tab. 7.2, we can formulate Yukawa interactions and scalar potentials

$$\begin{aligned} \mathcal{L}_{\text{yuk}} &= \mathcal{L}_{\text{yuk, SM}} + \left( \mathcal{L}_\kappa - y \psi_i^{L\dagger} S_{ij} \psi_j^R + \text{h.c.} \right), \\ \mathcal{L}_{\text{pot}} &= \mu_H^2 H^\dagger H + \mu_S^2 \text{tr} [S^\dagger S] + \mu_{\text{det}} [\det S + \det S^\dagger] \\ &\quad - \lambda (H^\dagger H)^2 - \delta H^\dagger H \text{tr} [S^\dagger S] - u \text{tr} [S^\dagger S S^\dagger S] - v \text{tr} [S^\dagger S]^2, \end{aligned} \quad (7.3)$$

where  $y$  is the pure BSM Yukawa interaction inherited from the template theory,  $\lambda$  the SM Higgs quartic,  $u$  and  $v$  are the single and double trace BSM quartics and  $\delta$  a scalar portal coupling between the sectors. Mass terms  $\mu_H$  and  $\mu_S$  are present for the Higgs and the BSM scalar alike, as well as a cubic interaction  $\mu_{\text{det}}$  owing to the choice  $N_f = 3$ .

**Yukawa sector.** Mixing between the Higgs and the BSM scalar is implied through the portal  $\delta$ , while SM–BSM fermion mixing occurs through Yukawa terms within  $\mathcal{L}_\kappa$ , which is model dependent. In the following, we will focus on models A-F where the BSM fermions are lepton-

Model	$U(1)_Y$	$SU(2)_W$	$SU(3)_C$	#	BSM Yukawas
A	-1	1	1	3	$L^\dagger H \psi^R$ $\psi^{L\dagger} S E$
B	-1	3	1	2	$L^\dagger \otimes H \psi^R$
C	-1/2	2	1	3	$\psi^{L\dagger} H E$ $L^\dagger S \psi^R$
D	-3/2	2	1	2	$\psi^{L\dagger} H^\dagger E$
E	0	1	1	2	$L^\dagger H^\dagger \psi^R$
F	0	3	1	2	$L^\dagger \otimes H^\dagger \psi^R$
G	+2/3	1	3	3	$Q^\dagger H \psi^R$ $\psi^{L\dagger} S D$
H	+2/3	3	3	2	$Q^\dagger \otimes H \psi^R$
I	-1/3	1	3	3	$Q^\dagger H^\dagger \psi^R$ $\psi^{L\dagger} S U$
J	-1/3	3	3	2	$Q^\dagger \otimes H^\dagger \psi^R$
K	+1/6	2	3	4	$\psi^{L\dagger} H D$ $\psi^{L\dagger} H^\dagger U$ $Q^\dagger S \psi^R$
L	+5/6	2	3	2	$\psi^{L\dagger} H^\dagger D$
M	-7/6	2	3	2	$\psi^{L\dagger} H U$

**Table 7.2:** Representations of  $\psi^{L,R}$  and number of BSM Yukawa coupling matrices for each model. By design, this number is at least two, the term  $\psi^{L\dagger} S \psi^R$  is always present. For models C,D and K-M with weak doublets, one may choose to replace the representation 2  $\mapsto \bar{2}$ , which can be absorbed into a field redefinition  $\psi^{L,R} \mapsto \varepsilon \psi^{L,R}$ . The symbol  $\otimes$  indicates a bilinear in the adjoint representation of  $SU(2)_W$ .

like colour singlets, giving rise to the Yukawa sector

$$\begin{aligned}
\mathcal{L}_\kappa^A &= -\kappa_{ij} L_{ia}^\dagger H_a \psi_j^R - \kappa' \psi_i^{L\dagger} S_{ij} E_j, & \mathcal{L}_\kappa^B &= -\kappa_{ij} L_{ia}^\dagger t_{ab}^A H_b \psi_{jA}^R, \\
\mathcal{L}_\kappa^C &= -\kappa_{ij} \psi_{ia}^{L\dagger} H_a E_j - \kappa' L_a^\dagger S_{ij} \psi_{ja}^R, & \mathcal{L}_\kappa^D &= -\kappa_{ij} \psi_{ia}^{L\dagger} \varepsilon_{ab} H_b^\dagger E_j, \\
\mathcal{L}_\kappa^E &= -\kappa_{ij} L_{ia}^\dagger \varepsilon_{ab} H_b^\dagger \psi_j^R, & \mathcal{L}_\kappa^F &= -\kappa_{ij} L_{ia}^\dagger \varepsilon_{ab} t_{bc}^A H_c^\dagger \psi_{jA}^R,
\end{aligned} \tag{7.4}$$

where  $a, b, \dots$  denote  $SU(2)_W$  fundamental indices. In the following, we will simplify the RG analysis by assuming

$$\kappa_{ij} = \kappa \delta_{ij} \quad \text{for models A-F.} \tag{7.5}$$

This melds SM and BSM flavour symmetries by identifying  $U(3)_L$  with  $U(3)_{\psi^R}$  groups in models A, B, E, F and  $U(3)_E$  with  $U(3)_{\psi^L}$  in models C and D. Models A and C are special, BSM fermions  $\psi^R$  and  $\psi^L$  have the same representations as the SM fields  $E$  and  $L$ , respectively. Hence, an additional Yukawa term  $\propto \kappa'$  to be formulated, which breaks the flavour symmetry even further, by identifying  $U(3)_E[U(3)_L]$  with  $U(3)_{\psi^R}[U(3)_{\psi^L}]$  in model A [C]. Together with (7.5), this absorbs the entire BSM flavour group into the SM one. A third such theory is not realised in the set of colour singlets A-F, as a sterile neutrino is missing in the SM. This leaves model E without a  $\kappa'$ -interaction, and  $\psi^R$  takes the place of a right-handed neutrino.

**Scalar potential.** For each of the models A-M in Tab. 7.2, the scalar potential  $\mathcal{L}_{\text{pot}}$  is universal. Its classical moduli space implies the existence of two distinct vacua  $V^\pm$ , which depend on the sign of the BSM quartic  $u$ . In accordance with [113, 267], conditions for the stability of the potential are found to be

$$V^+ : \quad \begin{cases} \lambda > 0, & u > 0, & u + 3v > 0, \\ \delta > -2\sqrt{\lambda(u/3 + v)} \end{cases} \quad V^- : \quad \begin{cases} \lambda > 0, & u < 0, & u + v > 0, \\ \delta > -2\sqrt{\lambda(u + v)} \end{cases}. \tag{7.6}$$

When the BSM scalar acquires a vacuum expectation value (VEV), the remaining  $U(N_f)_{\psi^L} \times U(N_f)_{\psi^R}$  BSM symmetry group is softly broken dependent on the vacuum configuration

$$\langle S_{ij} \rangle = \begin{cases} v_s \delta_{ij} & \text{for } V^+ \\ v_s \delta_{i\bar{n}} \delta_{j\bar{n}} \text{ (no sum)} & \text{for } V^- \end{cases}, \quad (7.7)$$

where in  $V^+$ , a diagonal  $U(3)$  flavour symmetry is retained, while for  $V^-$  a single one of the diagonal components acquires a VEV, violating flavour universality. In particular, this breaks SM flavour symmetries via the  $\kappa, \kappa'$  Yukawa interactions. In general, off-diagonal mass terms are introduced through VEVs and the portal coupling  $\delta$ , resulting in scalar mixing between SM and BSM sector. In the same manner, BSM fermions acquire mass and mix with the SM ones via  $\kappa'$  and  $\kappa$  Yukawas as the Higgs acquires a VEV as well.

## 7.2 Running couplings

Next, we will investigate the RG flows  $\beta_i = \partial \alpha_i / \partial \ln \mu$  in terms of the quantities  $\alpha_c = c^2/(4\pi)^2$ , for  $c$  being gauge or Yukawa interactions, and  $\alpha_q = q/(4\pi)^2$  with quartics  $q$ .

### 7.2.1 Top-down approach

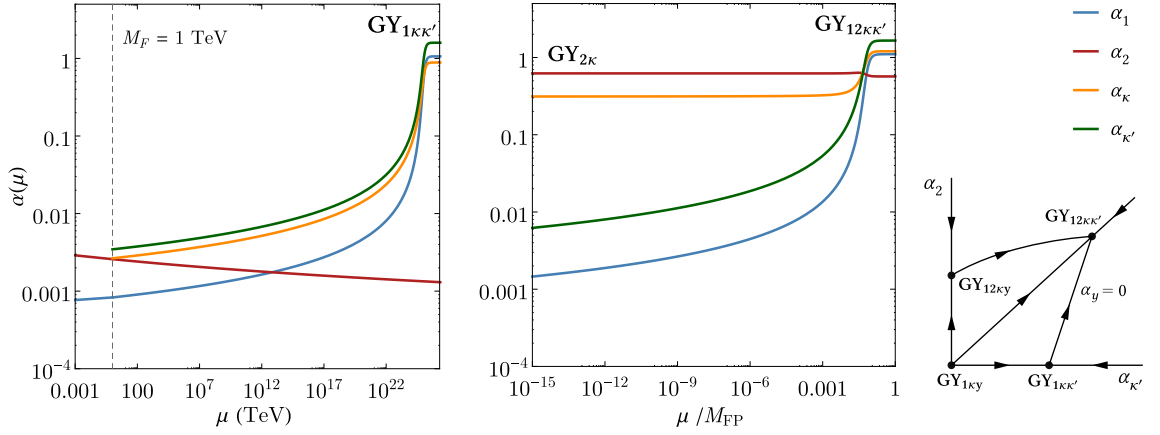
Starting on the side of the full theory,  $\beta$ -functions can be solved directly to gain a set of potential fixed point. Their UV critical surface is computed and trajectories towards the IR analysed for matching against the SM.

**Leading order.** Now, we will investigate the two-loop gauge and one-loop Yukawa system of RGEs. As quartics decouple algebraically, we can solve the gauge-Yukawa sector first. This will be referred to as the (2,1,0) approximation. As all BSM matter in models A-F is colourless, the strong coupling  $\alpha_3$  is expected to remain asymptotically free, suggesting  $\alpha_3^* = 0$ . To avoid the triviality problem, the hypercharge coupling needs to have an interacting fixed point  $\alpha_1^* \neq 0$ , or be stabilised by the weak coupling as in (1.44). Both of those mechanisms require Yukawa contributions  $\alpha_{\kappa, \kappa', y}^*$  to be sizeable. In models E and F,  $\beta_1$  is independent of  $\alpha_y$ , and  $\alpha_\kappa^*$  is too small to avert the triviality of  $\alpha_1$ . Surprisingly, model C does not provide a fixed point solving this problem either, leaving only A, B and D with viable fixed point candidates.

For model A, these candidates are listed in Tab. 7.3, see there for details of the notation. The Gaussian is a saddle point due to the coefficients (1.29)  $B_1 < 0 < B_2$ , no  $\mathbf{BZ}_1$  and  $\mathbf{BZ}_{12}$  can exist for the  $U(1)_Y$  gauge group.  $\mathbf{BZ}_2$  is infrared, with only  $\alpha_\kappa$  being relevant, as BSM fermions are  $SU(2)_W$  singlets. The fixed point  $\mathbf{GY}_{2\kappa}$  is a complete infrared sink. Moreover, there is a line of fixed points covering all solutions  $\mathbf{GY}_{1\kappa'}$ ,  $\mathbf{GY}_{1y}$  and  $\mathbf{GY}_{1\kappa'y}$ , fixing a value of the quantity  $\propto (\alpha_{\kappa'} + \alpha_y)$ . Any other linear combination of these couplings then represents a second, degenerate parameter giving rise to a marginal eigendirection. However, this phenomenon is lifted by higher-order corrections. Taking into account the relation  $\beta_y/\alpha_y = \beta_{\kappa'}/\alpha_{\kappa'} + 2\alpha_\kappa$ , the points  $\mathbf{GY}_{1\kappa\kappa'y}$  and  $\mathbf{GY}_{12\kappa\kappa'y}$  cannot occur. This leaves only four candidates of which  $\mathbf{GY}_{1\kappa\kappa'}$  and  $\mathbf{GY}_{1\kappa y}$  can be matched onto the SM, while  $\mathbf{GY}_{12\kappa\kappa'}$  and  $\mathbf{GY}_{12\kappa y}$  cannot, see Fig. 7.1. In models B and D, similar observations can be made, a complete discussion is contained in [304].

FP	$\alpha_1^*$	$\alpha_2^*$	$\alpha_\kappa^*$	$\alpha_{\kappa'}^*$	$\alpha_y^*$	rel.	irrel.	Matching
<b>G</b>	$0^{(+)}$	$0^{(-)}$	$0^{(+)}$	$0^{(+)}$	$0^{(+)}$	1	4	–
<b>BZ<sub>2</sub></b>	$0^{(+)}$	0.543	$0^{(+)}$	$0^{(+)}$	$0^{(+)}$	1	4	–
<b>GY<sub>2<math>\kappa</math></sub></b>	$0^{(+)}$	0.623	0.311	$0^{(+)}$	$0^+$	0	5	–
<b>GY<sub>1<math>\kappa'</math>y</sub></b>	2.746	$0^{(+)}$	$0^-$	$4.120 - \alpha_y^*$	$\alpha_y^*$	2	2	–
<b>GY<sub>1<math>\kappa\kappa'</math></sub></b>	1.063	$0^{(-)}$	0.886	1.594	$0^+$	2	3	✓
<b>GY<sub>12<math>\kappa\kappa'</math></sub></b>	1.105	0.569	1.205	1.657	$0^+$	1	4	✗
<b>GY<sub>1<math>\kappa y</math></sub></b>	2.151	$0^{(-)}$	0.782	$0^-$	3.032	3	2	✓
<b>GY<sub>12<math>\kappa y</math></sub></b>	2.267	0.200	0.933	$0^-$	3.165	2	3	✗

**Table 7.3:** Real fixed points of model A in the (2,1,0) approximation. FP indicates if the fixed point is the Gaussian (**G**), Bankz-Zaks (**BZ**) or gauge-Yukawa (**GY**) type. Non-vanishing couplings at each fixed point are given as indices. Fixed point values, as well as number of relevant (rel.) and irrelevant (irrel.) eigendirections are listed. For vanishing couplings, a superscript  $-/+$  indicates if it is relevant/irrelevant, parentheses mean that the flow is logarithmic rather than a power law. The entry **GY<sub>1 $\kappa'$ y</sub>** is actually a line of fixed points, giving rise to an exactly marginal coupling. A dash in the last column indicates that a point is not a fitting UV candidate, a ✓ means that it can be matched against the SM, while ✗ denotes the opposite.



**Figure 7.1:** Matching of model A in the (2,1,0) approximation. Right panel: schematic phase diagram of various fixed points from Tab. 7.3 in the  $(\alpha_{\kappa'}, \alpha_2)$  plane, arrows point from the UV to the IR. Middle panel: RG flow from of UV fixed point **GY<sub>12 $\kappa\kappa'$</sub>** , which cannot be matched against the SM, as the coupling  $\alpha_2$  is captured in the IR sink **GY<sub>2 $\kappa$</sub>** . Left panel: RG flow from **GY<sub>12 $\kappa\kappa'$</sub>**  which is matched against the SM around at the TeV scale.

**Higher loop orders.** The potential UV fixed points **GY<sub>1 $\kappa\kappa'$</sub>** , **GY<sub>12 $\kappa\kappa'$</sub>** , **GY<sub>1 $\kappa y$</sub>**  and **GY<sub>12 $\kappa y$</sub>**  in Tab. 7.3 all have components of order one, suggesting that the (2,1,0) approximation in perturbation theory is not sufficient. Indeed, fixing all gauge groups, representation and  $N_f = 3$  has carried us far away from the perturbative control of earlier chapters [121, 122]. This brings the applicability of perturbation theory into question. Nevertheless, we will proceed cautiously about the result obtained, in good faith that the foundational principle of Yukawa couplings stabilising the gauge sector may still hold in this regime. However, there is no reason to believe that the  $(\ell + 1, \ell, \ell)$  approximation scheme is reliable. Studies of fixed points in various combinations of loop orders are tedious and show little evidence of recurring patterns. Moreover, the complexity of solving the RG system grows exponentially with the number of couplings and loop orders, which becomes numerically challenging. This leads us to switch strategy in the next section.



### 7.2.2 Bottom-up approach

**Planck safety.** To overcome the shortcomings of the previous section, we will follow the diametrical approach of starting at the SM matching scale, and investigate the RG running towards the deep UV. This requires the adopting of a more practical notion of safety until the Planck scale, instead of the existence of a UV fixed point. We will subsequently refer to the property as *Planck safety*. Consequently we demand that no singularities in the RG evolution such as Landau poles arise. Moreover, no vacuum instability between the SM matching and the Planck scale must occur. In this range, an agnostic view toward quantum gravity is justified, as its dynamics are suppressed by the Planck mass, and their influence beyond it are not clear.

**BSM critical surface.** At the matching scale  $\mu_0$ , some running couplings are predicted by the SM, while the rest are free parameters. The set of initial conditions of these pure BSM couplings at  $\mu_0$  corresponding to Planck-safe trajectories form the *BSM critical surface* in parameter space. In our particular search, we assume that the BSM fermions acquire a universal mass  $\propto M_F \psi_i^{L\dagger} \psi_i^R + \text{h.c.}$ , which represents our matching scale, and is set to

$$\mu_0 = M_F = 1 \text{ TeV}. \quad (7.8)$$

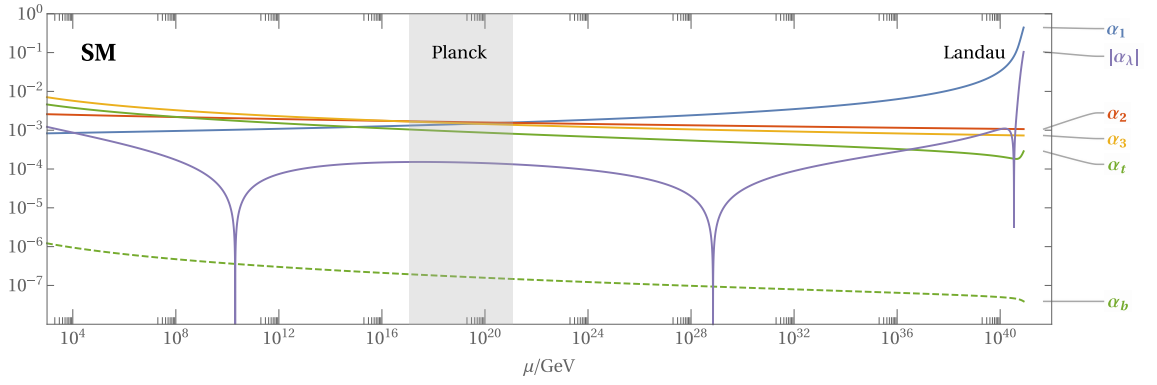
We will suppress any threshold corrections and higher order operators in the matching procedure, consistent with  $M_F$  being assumed large with respect to the electroweak scale. Utilising [20, 24], we fix six SM parameters

$$\begin{aligned} \alpha_1(\mu_0) &\approx 8.30 \cdot 10^{-4}, & \alpha_2(\mu_0) &\approx 2.58 \cdot 10^{-3}, & \alpha_3(\mu_0) &\approx 7.08 \cdot 10^{-3}, \\ \alpha_t(\mu_0) &\approx 4.61 \cdot 10^{-3}, & \alpha_b(\mu_0) &\approx 1.22 \cdot 10^{-6}, & \alpha_\lambda(\mu_0) &\approx 6.09 \cdot 10^{-4}, \end{aligned} \quad (7.9)$$

where we have only considered top and bottom Yukawas and completely neglected any lepton Yukawa in  $Y_e$ , due to its small size. As a consequence, our models assume the lepton flavour symmetry to be approximately restored in the UV, which is compatible with the (7.5).

Hence, five dimensionless parameters  $\alpha_{\kappa, \gamma, \delta, u, v}(\mu_0)$  remain in models B and D-F, while A and C have six, also including  $\alpha_{\kappa'}(\mu_0)$ . This means the BSM critical surface is a 5 or 6 - dimensional manifold to scan over. With a fixed matching scale a certain (direction dependent) reliability radius of the BSM critical surface around  $\alpha_{\text{BSM}} = 0$  is implied for each configuration of  $\beta$ -function loop orders utilised in the running. The bottom-up approach provides therefore a more systematic control than the top-down one. In our case, two-loop running is used for all couplings, but before BSM theories are studied, the pure SM case is revisited, for which three-loop corrections are available.

**Standard Model running.** The RG evolution of SM is displayed in Fig. 7.2 from the matching scale of  $10^3$  GeV, past the Planck scale at  $M_{\text{Pl}} \approx 10^{19}$  GeV (grey band) until the deep UV for demonstrational purposes, ignoring contributions from quantum gravity. All parameters remain weakly coupled  $|\alpha_i| \leq 10^{-2}$  before  $M_{\text{Pl}}$  and run relatively slowly, with  $\alpha_{2,3}$  as well as  $\alpha_{t,b}$  being asymptotically free, while  $\alpha_1$  exhibits a Landau pole beyond the Planck scale around  $\mu \approx 10^{41}$  GeV. Mainly driven by  $\alpha_t$  contributions, the Higgs coupling  $\alpha_\lambda$  becomes negative around  $10^{10}$  GeV but recovers at  $10^{29}$  GeV until the Landau pole. The negativity heralds the metastability of the Higgs



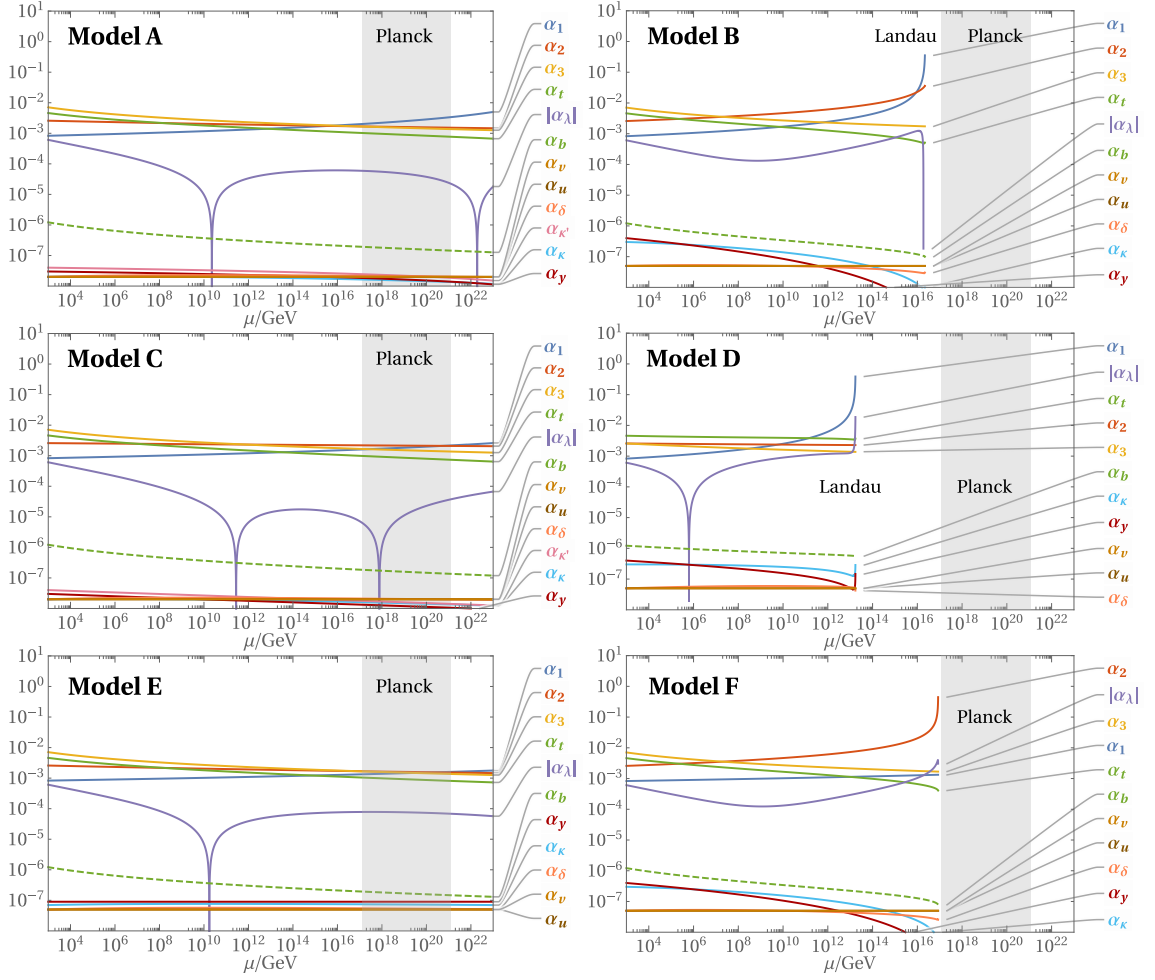
**Figure 7.2:** RG running of the hypercharge (blue), weak (red) and strong (yellow) gauge couplings, the norm of the Higgs quartic (purple) and top and bottom Yukawas (green, solid and dashed) in the SM at three-loop order over the renormalisation scale  $\mu$ . The grey band marks the range two orders of magnitude around the Planck scale, where quantum gravity effects take hold. Trajectories are extended past this region to illustrate their stability. The fate of the Landau pole therein is unknown.

potential [23–25] and will be utilised as an indicator. If we allow for metastability, the SM already fits the criterion of Planck-safety.

**Feeble BSM couplings.** A natural starting point for exploring the BSM critical surface is around vanishing BSM couplings when the running is most insensitive to the loop order. If the BSM couplings are chosen feebly small, e.g.  $\alpha_{\text{BSM}} < 10^{-6}$ , their influence is negligible for the SM running and they effectively decouple, remaining in the feeble regime. This is displayed in Fig. 7.3. The models A-F are then SM extensions with additional electro-weakly charged matter. This shifts the Landau pole of  $\alpha_1$  closer to the IR, and in models B, D and F even introduces one for  $\alpha_2$ . Consequently models A, C and E remain Planck safe with Higgs metastability, while in model B [D and F] Landau poles in  $\alpha_1$  [ $\alpha_2$ ] occur before the Planck scale. Curiously, for the weak triplet models B and F, the Higgs sector appears to be stabilised. In all cases the behaviour does not change significantly when BSM couplings are increased but remain one order of magnitude smaller than the SM ones. In order to move Landau poles in models B, D and F, one needs to advance to a weakly coupled BSM regime.

**Weakly coupled regime.** Scanning the BSM critical surface regions where couplings are allowed in the same order of magnitude or higher as SM ones is tedious due to its high dimensionality. However, a loose classification certain regions by the magnitude of BSM Yukawa couplings  $\alpha_{\kappa,\kappa',y}$  is possible. In fact, these Yukawas play a double role: they slow down the RG running in the gauge sector and move Landau poles towards the UV, while they may also stabilise the quartic sector of the scalars they couple to. This stabilisation is only visible beyond the leading orders in perturbation theory. We even find *walking regions* where the RG evolutions of Yukawas and quartics are almost deadlocked due to the vicinity of (pseudo) fixed points, moving Landau poles and ensuring stable potentials. This causes certain cases to stand out like isles of stability, in particular:

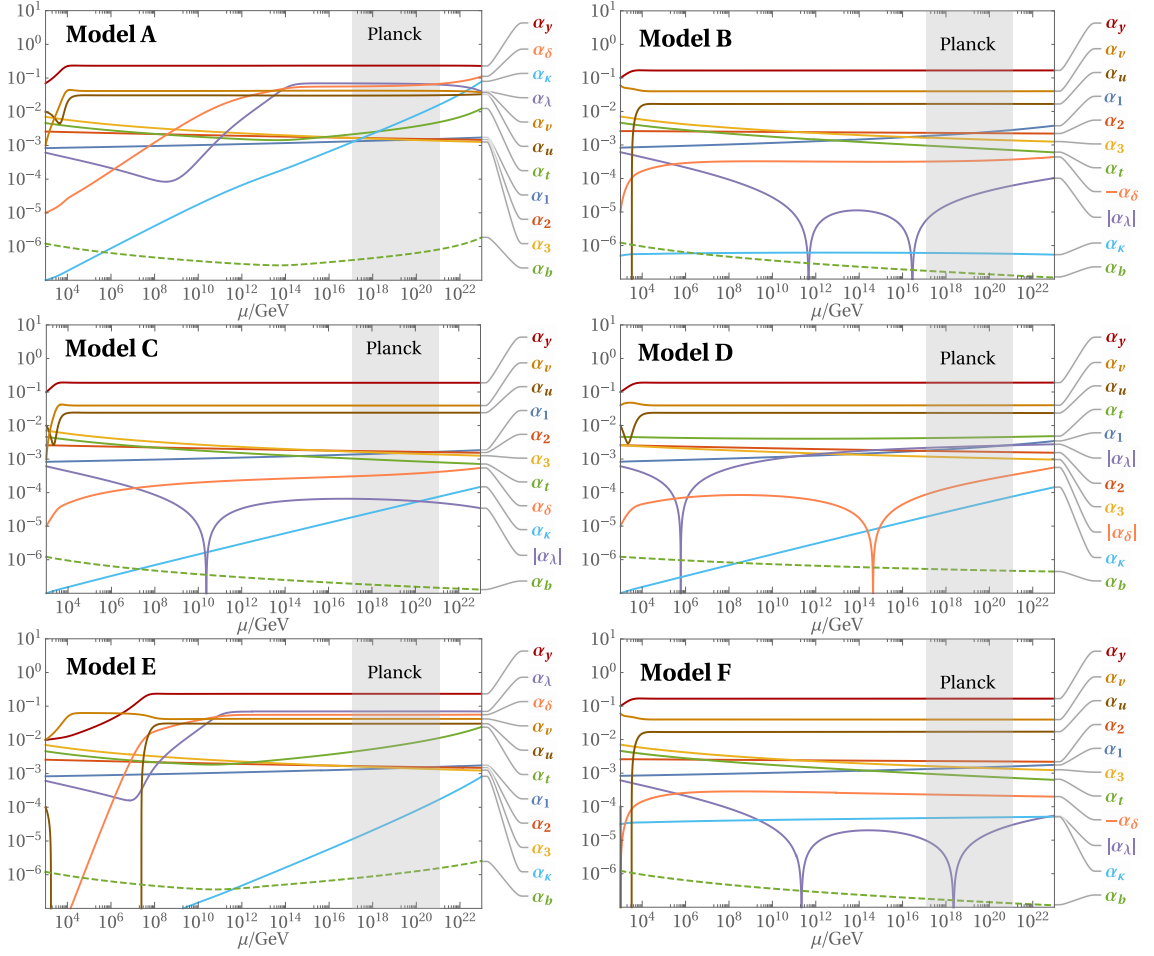
- (a)  $\alpha_y \neq 0$ ,  $\alpha_{\kappa,\kappa'} \approx 0$ : This scenario, depicted in Fig. 7.4, is most similar to the mechanism of asymptotic safety in the template theory. The value of  $\alpha_y|_{M_F}$  slows down the running of  $\alpha_{1,2}$  and moves all Landau poles past  $M_{\text{Pl}}$ .  $\alpha_y|_{M_F}$  is fixed on a broad range of scales by



**Figure 7.3:** RG running of all gauge couplings, Yukawas and quartics at two-loop order over the renormalisation scale for models A-F. All BSM couplings are feebly small  $\alpha_{\text{BSM}} < 10^{-6}$ .

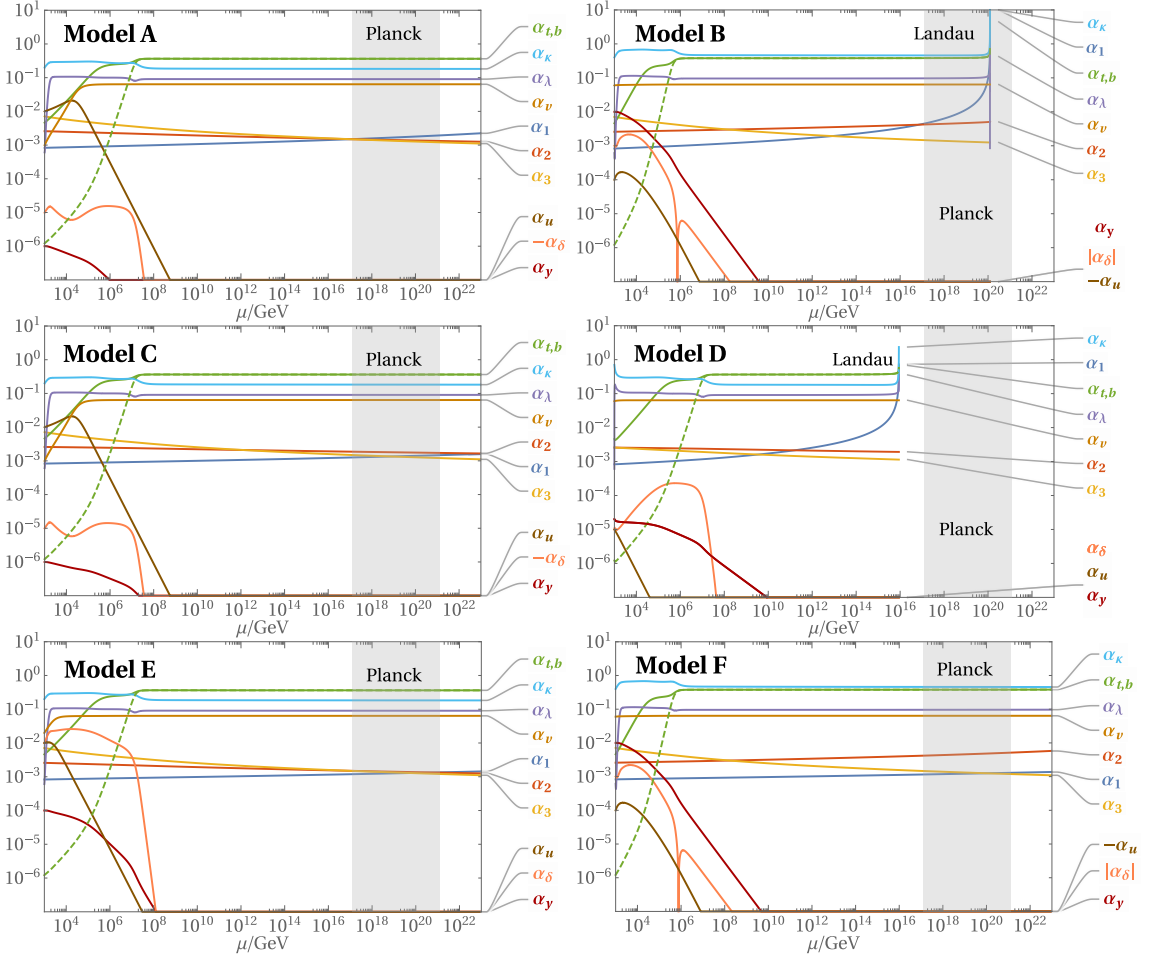
a walking regime also stabilising the BSM potential  $\alpha_{u,v}$ . The Higgs on the other hand remains metastable, unless  $\alpha_\delta|_{M_F}$  is larger than a model-dependent value. Except for the triplet models B and F, non-zero values of  $\alpha_\kappa$  eventually destabilise the walking and lead into poles.

- (b)  $\alpha_\kappa \neq 0$ ,  $\alpha_{y,\kappa'} \approx 0$ : The opposite case to (a) is plotted in Fig. 7.5. A walking regime occurs on the SM side, driven by  $\alpha_\kappa$ . This stabilises the Higgs potential, while  $\alpha_v$  self-stabilises on the BSM side. Small initial values of BSM couplings are driven to zero. However, a Landau pole still occurs before  $M_{\text{Pl}}$  in model D, and is barely moved past it in B.
- (c)  $\alpha_{\kappa,\kappa'} \neq 0$ ,  $\alpha_y \approx 0$ : For model A and C, the additional Yukawa coupling allows to have a walking regime involving SM and BSM sectors, see Fig. 7.6, stabilising both at the same time. This locks all couplings except for  $\alpha_{1,2,3,\delta}$  which run only slowly from below until far beyond the Planck scale. When finally the trajectory breaks free from the pseudo fixed point with  $\alpha_{1,2,3,y,\delta}^* = 0$ , it is absorbed into a proper UV one. Smaller values for  $\alpha_\kappa|_{M_F}$  require larger  $|\alpha_\delta|_{M_F}$ , but Higgs stability is not guaranteed.

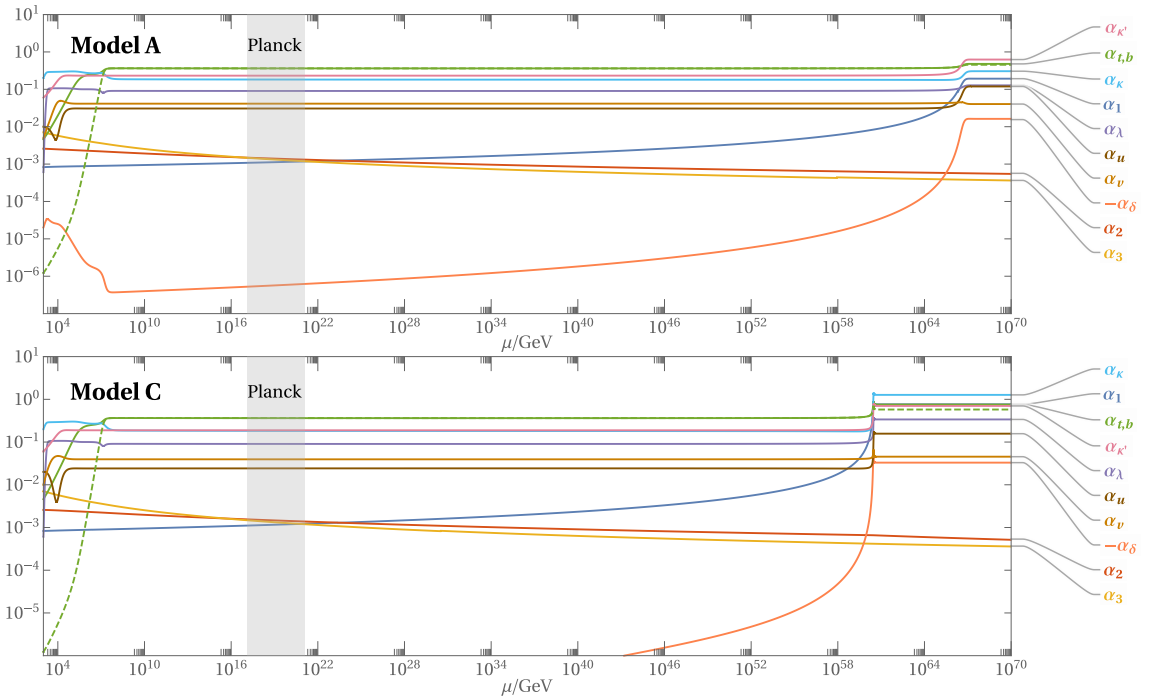


**Figure 7.4:** Two-loop RG evolution of gauge, Yukawa and quartic couplings in models A-F with  $\alpha_y|_{M_F} \approx 10^{-2}$  to  $10^{-1}$  and  $\alpha_{\kappa, \kappa'}|_{M_F} \approx 0$ . The grey band marks the range two orders of magnitude around the Planck scale. Corrections due to quantum gravity are neglected.

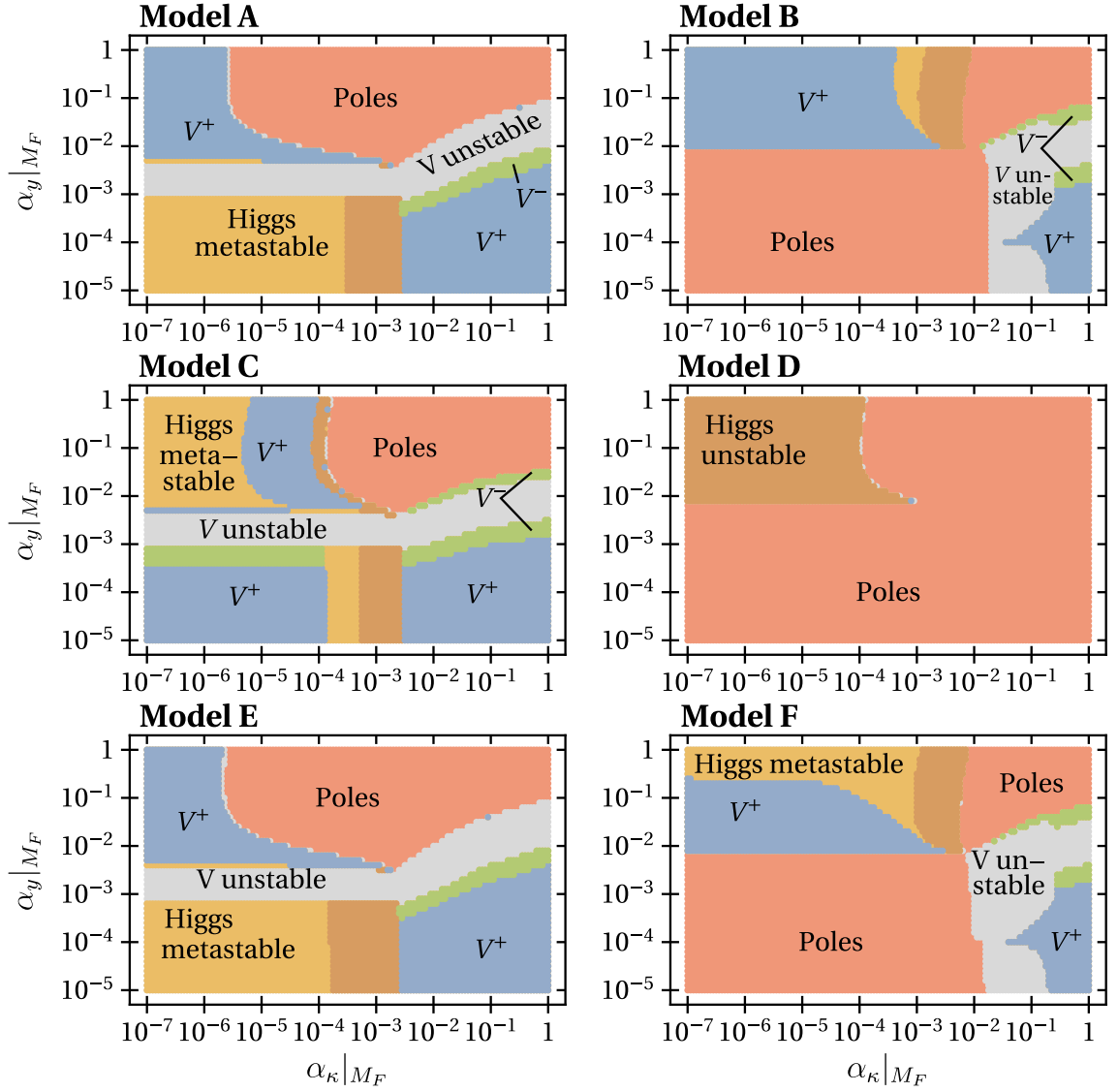
**BSM critical survey.** As the BSM Yukawa coupling play a key role for Planck safety, slices of the BSM critical surface can be visualised by scanning over ranges of  $\alpha_{\kappa, y}|_{M_F}$  and  $\alpha_{\kappa, \kappa'}|_{M_F}$  for model A and C, while fixing the other BSM parameters e.g. to orders of magnitude below the SM ones. This is shown in Fig. 7.7 and Fig. 7.8, wherein the colours indicate the vacuum at the Planck scale of the RG trajectory with these matching conditions. Both plots reflect that for very small Yukawas, models A, C and D are either in the stable vacua  $V^\pm$  (depending if  $\alpha_u|_{M_F} \gtrless 0$ , blue or green) or with the Higgs coupling metastable  $0 > \alpha_\lambda > -10^{-4}$  (yellow) at the Planck scale. In models B, D and F however poles are reached before  $M_{Pl}$  (red). For small  $\alpha_\kappa|_{M_F}$  and larger  $\alpha_y|_{M_F}$ , the case (a) is visible in Fig. 7.7, but it turns out to have an unstable Higgs potential for model D ( $\alpha_\lambda < -10^{-4}$ , brown). There is also a remarkable band for certain values of  $\alpha_y|_{M_F}$  where the BSM potential is unstable (grey). In the same manner, case (b) can be found in each figures. The interference of both cases cause poles around the region  $\alpha_{\kappa, y}|_{M_F} \gtrsim 10^{-2}$ . In Fig. 7.8, case (c) with  $\alpha_{\kappa, y}|_{M_F} \gtrsim 10^{-2}$  exhibits a stable  $V^+$  vacuum. For smaller  $\alpha_\kappa|_{M_F}$ , model A remains stable, but the Higgs potential in model C does not for the fixed values of  $\alpha_\delta|_{M_F}$ . This concludes and summarises our survey of the BSM critical surface.



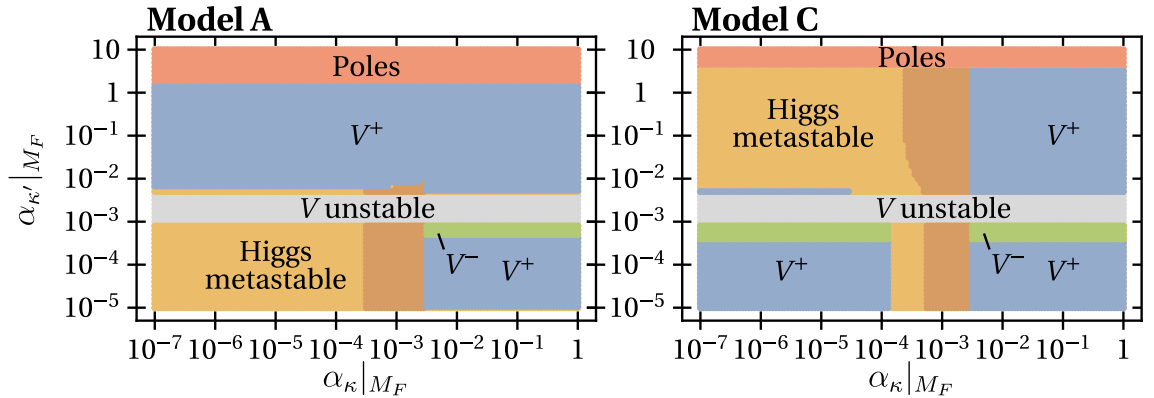
**Figure 7.5:** Renormalisation group flow of all dimensionless parameters in models A-F at two-loop order.  $\alpha_\kappa$  is larger than  $\alpha_y$  and  $\alpha'_\kappa = 0$ . Quantum gravity corrections are neglected.



**Figure 7.6:** Two-loop running couplings over the renormalisation scale in models A and C with  $\alpha_y = 0$  and  $\alpha_{\kappa,\kappa'} \neq 0$ . The stability of the trajectories beyond  $M_{\text{Pl}}$  without gravity is also shown.



**Figure 7.7:** BSM critical surface for models A-F with  $\{\alpha_{\kappa'}, \alpha_\delta, \alpha_u, \alpha_v\}|_{M_F} = \{0, 5, 1, 4\} \cdot 10^{-5}$ . Depending on values  $\{\alpha_\kappa, \alpha_y\}|_{M_F}$  the colours indicate if the vacuum at  $M_{Pl}$  is stable in  $V^\pm$  (blue, green),  $\alpha_{u,v}|_{M_{Pl}}$  are stable but  $\alpha_\lambda|_{M_{Pl}} < 0$  (yellow for  $\alpha_\lambda|_{M_{Pl}} > -10^{-4}$ , otherwise brown), unstable (grey) or poles are reached before this scale (red).



**Figure 7.8:** BSM critical surface for models A and C with matching conditions  $\{\alpha_y, \alpha_\delta, \alpha_u, \alpha_v\}|_{M_F} = \{0, 5, 1, 4\} \cdot 10^{-5}$  in dependence of  $\{\alpha_\kappa, \alpha_{\kappa'}\}|_{M_F}$ . The colouring is the same as for Fig. 7.7.

### 7.3 Phenomenology

In this section, we will highlight a few phenomenological aspects of models A-F in Tab. 7.2. An extended discussion can be found in [304].

**Scalar mixing.** After electroweak symmetry breaking, mixing between the SM Higgs  $h$  and the BSM scalar component  $s$  occurs. Both are related to the unbroken fields  $H, S$  via

$$H = \frac{1}{\sqrt{2}} \begin{pmatrix} \sqrt{2} h^+ \\ v_h + h + ih' \end{pmatrix}, \quad S_{kk} = \frac{1}{\sqrt{2}} (v_{s_k} + s_k + i s'_k). \quad (7.10)$$

In the case of a flavour- $n$  specific vacuum  $V^-$ , we have  $v_{s_i} = v_s \delta_{in}$  and the BSM scalar  $s = s_n$ , while for  $V^+$  one obtains  $v_{s_i} = v_s/\sqrt{3}$  and  $s_i \mapsto s/\sqrt{3}$  for all  $i$ . The rotation into mass eigenstates  $h_{1,2}$  is parametrised by the mixing angle  $\beta$

$$\begin{pmatrix} h_1 \\ h_2 \end{pmatrix} = \begin{pmatrix} \cos \beta & -\sin \beta \\ \sin \beta & \cos \beta \end{pmatrix} \begin{pmatrix} h \\ s \end{pmatrix}. \quad (7.11)$$

The mass matrix can be extracted from (7.3) and is given by

$$V_{\mathcal{M}s} = \frac{1}{2} \begin{pmatrix} h \\ s \end{pmatrix}^\top \begin{pmatrix} m_{hh}^2 & m_{sh}^2 \\ m_{sh}^2 & m_{ss}^2 \end{pmatrix} \begin{pmatrix} h \\ s \end{pmatrix}. \quad (7.12)$$

In the following, we introduce the auxiliary variable  $n$  with  $n = 1$  for vacuum  $V^-$  and  $n = 3$  for  $V^+$ . Inserting the relations

$$\mu_H^2 = \lambda v_h^2 + \frac{1}{2} \delta v_s^2, \quad \mu_S^2 = \frac{1}{2} \delta v_h^2 + (u/n + v) v_s^2 + \frac{n-1}{4} \sqrt{6} \mu_{\text{det}} v_s \quad (7.13)$$

from expanding the potential (7.3) around the minima in  $h$  and  $s$  at tree level gives the components

$$m_{hh}^2 = 2\lambda v_h^2, \quad m_{sh}^2 = \delta v_s v_h, \quad m_{ss}^2 = 2(u/n + v) v_s^2 + 3 \frac{n-1}{4} \sqrt{6} \mu_{\text{det}} v_s, \quad (7.14)$$

which yield the mass eigenvalues

$$m_{1,2}^2 = \frac{1}{2} \left[ m_{ss}^2 + m_{hh}^2 \mp \sqrt{(m_{ss}^2 - m_{hh}^2)^2 + 4 m_{sh}^4} \right] \quad (7.15)$$

of the respective scalars  $h_{1,2}$ . This gives rise to the mixing angle

$$\tan 2\beta = \frac{2 m_{sh}}{m_{ss}^2 - m_{hh}^2} \approx \frac{\delta}{\sqrt{\lambda(u/n + v)}} \frac{m_{hh}}{m_{ss}} + \mathcal{O} \left( \frac{m_{hh}^2}{m_{ss}^2} \right), \quad (7.16)$$

where the latter part is obtained in the limit of large mass splitting with  $m_{ss} \gg m_{hh}$  and  $\mu_{\text{det}} = 0$ . The mixing angle enters each SM vertex when rotating into the mass basis. In particular, it is detectable as a deviation from SM decay rates, which become  $\Gamma(h_1 \rightarrow X) = \cos^2 \beta \Gamma(h \rightarrow X)$ . Higgs signal strength measurements [20] then suggest

$$\sin 2\beta < 0.2, \quad (7.17)$$

implying a lower mass bound on the BSM scalar  $s$ . The 17 additional scalar degrees of freedom give rise to a plethora of interactions, which are very distinct from those of e.g. Two-Higgs-Doublet models.

**Fermion mixing.** In a similar vein, mass mixing also occurs among the left- and right-chiral SM and BSM fermions,

$$\begin{pmatrix} f_L^i \\ F_L^i \end{pmatrix} = \begin{pmatrix} \cos \theta_L^i & -\sin \theta_L^i \\ \sin \theta_L^i & \cos \theta_L^i \end{pmatrix} \begin{pmatrix} L_i \\ \psi_i^L \end{pmatrix}, \quad \begin{pmatrix} f_R^i \\ F_R^i \end{pmatrix} = \begin{pmatrix} \cos \theta_R^i & -\sin \theta_R^i \\ \sin \theta_R^i & \cos \theta_R^i \end{pmatrix} \begin{pmatrix} E_i \\ \psi_i^R \end{pmatrix}. \quad (7.18)$$

Here the index  $i$  counts both flavours and  $SU(2)_W$  components. The exact values of  $\theta_{L,R}^i$  do not only depend on the model A–F, but also the vacuum  $V^\pm$ . For instance, model A in  $V^+$  gives rise to a mass matrix

$$V_{\mathcal{M}_F} = \begin{pmatrix} L_{\ell i} \\ \psi_i^L \end{pmatrix}^\dagger \begin{pmatrix} Y_e^{ij} \frac{v_h}{\sqrt{2}} & \kappa_{ij} \frac{v_h}{\sqrt{2}} \\ \kappa' \delta_{ij} \frac{v_s}{\sqrt{6}} & y \delta_{ij} \frac{v_s}{\sqrt{6}} + M_F \delta_{ij} \end{pmatrix} \begin{pmatrix} E_j \\ \psi_j^R \end{pmatrix} + \text{h.c.}, \quad (7.19)$$

while the neutrino  $L_{\nu i}$  is not involved in the mixing. In the limit of large BSM masses  $v_h \ll v_s, M_F$  and small SM Yukawas  $Y_e \approx 0$ , the mixing angles read

$$\tan \theta_L^{\ell_i} = \frac{v_h \kappa}{\sqrt{2} M_F + \frac{v_s}{\sqrt{3}} y + \frac{v_s^2 \kappa'^2}{3 \sqrt{2} M_F}} + \mathcal{O}(v_h^3), \quad \tan \theta_R^{\ell_i} = \frac{v_s \kappa'}{\sqrt{6} M_F + y v_s} + \mathcal{O}(v_h^2), \quad (7.20)$$

and give rise to the mass eigenvalues

$$m_{f_i} = \frac{v_h}{\sqrt{2}} \left[ y_{\ell_i} - \frac{v_s \kappa \kappa'}{\sqrt{6} M_F + y v_s} \right] + \mathcal{O}(v_h^3), \quad m_{F_i} = M_F + \frac{v_s}{\sqrt{6}} y + \frac{v_s \kappa \kappa'}{\sqrt{6} M_F + y v_s} \frac{v_h}{\sqrt{2}} + \mathcal{O}(v_h^2), \quad (7.21)$$

where  $Y_e^{ij} = y_{\ell_i} \delta^{ij}$  and  $\kappa_{ij} = \kappa \delta_{ij}$ . The mixing affects SM interactions in each of the models. In particular, the coupling to the  $Z^0$  boson is modified in the electroweak sector. In general, this yields

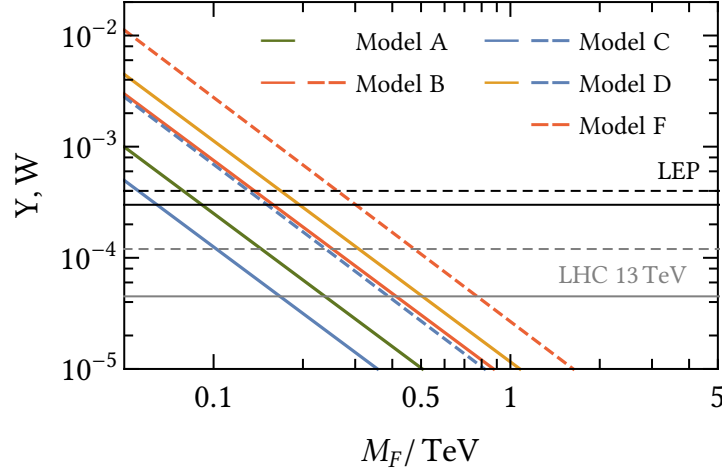
$$\begin{aligned} V_{Zff} &= \frac{g_2}{2 \cos \theta_W} Z_\mu \left[ \bar{\ell}_i \gamma^\mu (g_{\ell,V} + g_{\ell,A} \gamma_5) \ell_i + g_\nu \bar{\nu}_i \gamma^\mu (1 - \gamma_5) \nu_i + g_\psi \bar{\psi}_i \gamma^\mu \psi_i \right] \\ &= \frac{g_2}{2 \cos \theta_W} Z_\mu \left[ \bar{f}_{\ell i} \gamma^\mu (\tilde{g}_{\ell,V} + \tilde{g}_{\ell,A} \gamma_5) f_{\ell i} + \tilde{g}_{\nu i} \bar{f}_{\nu i} \gamma^\mu (1 - \gamma_5) f_{\nu i} + \dots \right] \end{aligned} \quad (7.22)$$

where the modified coupling prefactors read

$$\begin{aligned} \tilde{g}_{\ell,V} &= \frac{1}{2} (g_{\ell,V} + g_{\ell,A}) \cos^2 \theta_R^{\ell_i} + \frac{1}{2} (g_{\ell,V} - g_{\ell,A}) \cos^2 \theta_L^{\ell_i} + \frac{1}{2} g_\psi (\sin^2 \theta_R^{\ell_i} + \sin^2 \theta_L^{\ell_i}), \\ \tilde{g}_{\ell,A} &= \frac{1}{2} (g_{\ell,V} + g_{\ell,A}) \cos^2 \theta_R^{\ell_i} - \frac{1}{2} (g_{\ell,V} - g_{\ell,A}) \cos^2 \theta_L^{\ell_i} + \frac{1}{2} g_\psi (\sin^2 \theta_R^{\ell_i} - \sin^2 \theta_L^{\ell_i}), \\ \tilde{g}_{\nu i} &= g_\nu \cos^2 \theta_L^{\nu_i} + \frac{1}{2} g_\psi \sin^2 \theta_L^{\nu_i}. \end{aligned} \quad (7.23)$$

Experimental constraints for each  $|\tilde{g}_X - g_X| \lesssim 10^{-3}$  [20] suggest that the fermion mixing is small. In combination with the observation that one of the mixing angles follows  $\theta_{L/R} \propto \frac{\kappa v_h}{M_F}$  in each of





**Figure 7.9:** Drell-Yan observables  $Y$  (solid lines) and  $W$  (dashed) (7.25) at the leading order (7.26) for models A (green), B (red), C (blue), D (solid yellow, dashed blue) and F (dashed red). Due to BSM fermions being uncharged, model A [F] does not contribute to  $W$  [ $Y$ ], and model E provides no predictions for either. Doublet [triplet] models C and D [B and F] give identical contributions to  $W$ . Lowest experimental bounds from data LEP are marked in black and projections for LHC sensitivity at 13 TeV in grey [306].

the models for  $v_s \rightarrow 0$ , an upper bound

$$\alpha_\kappa \lesssim 4 \cdot 10^{-4} \left( \frac{\text{TeV}}{M_F} \right)^2 \quad (7.24)$$

on the Yukawa  $\kappa$  is implied.

As the BSM sector is colourless, mixing with SM quarks and constraints from the strong sector are avoided. Moreover,  $U(1)_{B-L}$  remains intact, which protects the stability of the proton.

**Fermion mass bounds.** The BSM fermions in models A-F are colourless, but carry weak isospin and hypercharge, rendering them detectable in electroweak precision measurements. The only exception is model E, where the BSM matter sector is completely uncharged. The fermion mass  $M_F$  can be constrained from charged and neutral current Drell-Yan processes through the parameters  $Y$  and  $W$  [305], given by

$$Y, W = \frac{1}{10} \alpha_{1,2} c_{1,2} \frac{M_W^2}{M_F^2} (B_{1,2}^{\text{eff,SM}} - B_{1,2}^{\text{eff}}) \quad \text{with } c_1 = \frac{3}{5} \text{ and } c_2 = 1. \quad (7.25)$$

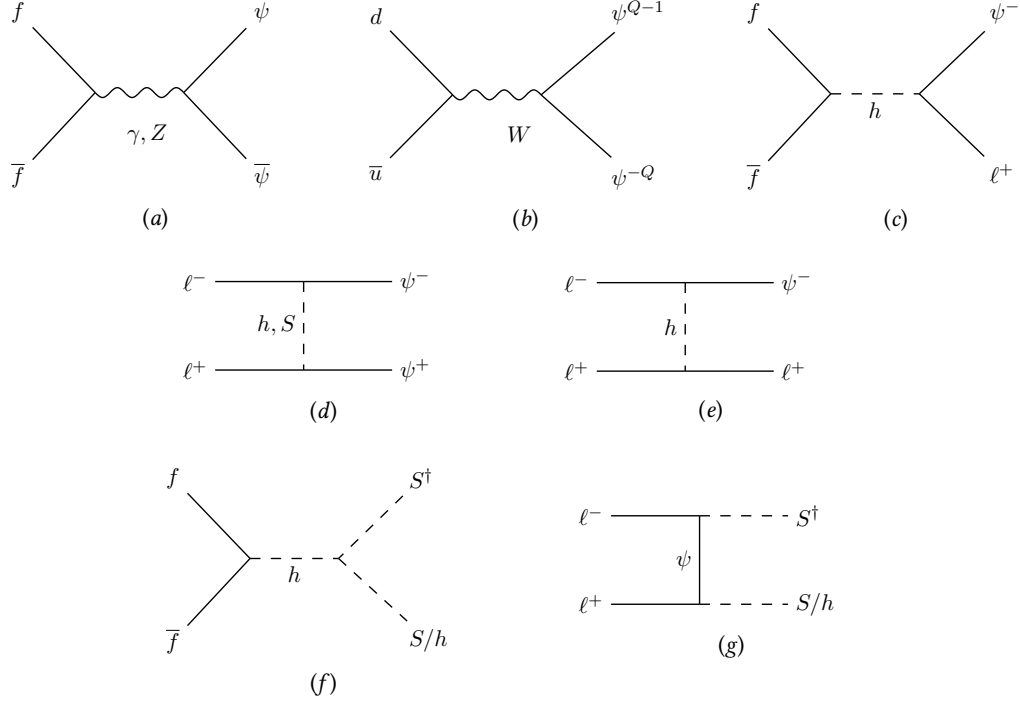
Here,  $B_{1,2}^{\text{eff}}$  are the effective one-loop coefficients from  $\beta_{1,2}$  as in (1.44), which are

$$(B_1^{\text{eff,SM}} - B_1^{\text{eff}}) = 8 d_{R_2} Y_F^2 + \mathcal{O}(\alpha), \quad (B_2^{\text{eff,SM}} - B_2^{\text{eff}}) = 8 S_2^{R_2} + \mathcal{O}(\alpha), \quad (7.26)$$

depending on the hypercharge as well as dimension and Dynkin index of the  $SU(2)_W$  representation for the BSM fermions. Experimental bounds [306] then suggest  $M_F$  to be in the order of a few hundred GeV, see Fig. 7.9. This justifies the choice  $M_F = 1$  TeV in the previous section. No similar bounds arise for the BSM scalar as it is uncharged.

**Production.** Tree-level production channels are listed as processes  $a - g$  in Fig. 7.10. Due to all

BSM matter being colourless, s-channel productions of  $\psi$  in either  $pp$ - or  $\ell\ell$ -colliders are only due to electroweak vector boson fusion (a, b) or Higgs exchange (c). For  $\ell\ell$ -machines, t-channel processes with Higgs or BSM scalar exchanges are also available (d, e). The BSM scalar may be produced via the Higgs portal  $\alpha_\delta$  (f) at any collider, or for models A and C via the second Yukawa  $\alpha'_\kappa$ , again for an  $\ell\ell$  experiment (g).



**Figure 7.10:** Production channels of the BSM particles at  $pp$  and  $\ell\ell$  colliders, with  $f = \ell, q$ . In diagram (f) the  $S$  and  $S^\dagger$  labels are schematic for model A.

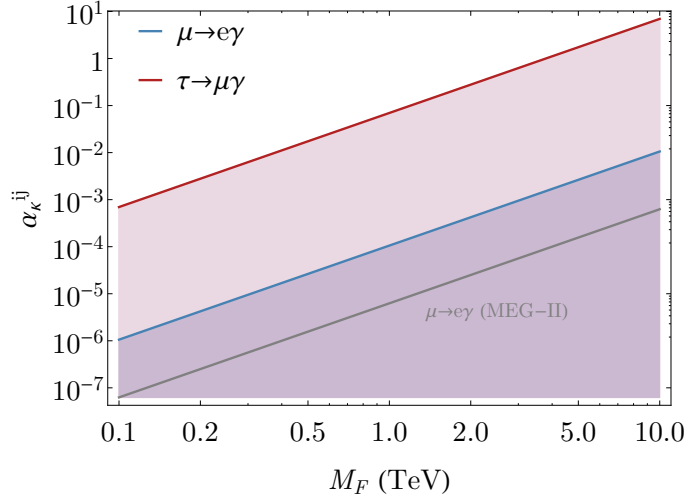
**Decay.** As the BSM fermions are heavy, the leading decay channel is through the Yukawa interaction coupling to the Higgs

$$\Gamma(\psi^q \rightarrow \ell^q h) = \frac{\pi}{4} C_{\psi\ell}^2 \alpha_\kappa M_F \left(1 - \frac{m_h^2}{M_F^2}\right)^2 \quad \text{and} \quad C_{\psi\ell}^2 = \begin{cases} 1/2 & \text{in models B, F} \\ 1 & \text{otherwise} \end{cases}. \quad (7.27)$$

For  $\alpha_\kappa \approx 10^{-4}$  and  $M_F \approx 1$  TeV, this implies a prompt decay  $\Gamma^{-1} \approx 10^{-24}$  s. As each model has a different  $\kappa$ -interaction, the decay channel allows to differentiate between them. The fermionic components not coupling to the Higgs decay via  $\psi^q \rightarrow \psi^{q\mp 1} W^\pm$  first, leaving displaced vertex signatures [307]. Models A and C also permit decay via the second Yukawa with the decay rate

$$\Gamma(\psi^q \rightarrow \ell^q S) = \frac{\pi}{2} \alpha_{\kappa'} M_F \left(1 - \frac{M_S^2}{M_F^2}\right)^2. \quad (7.28)$$

if the BSM scalar is light. In the same manner, the BSM scalar decays via the Yukawas  $y$  and  $\kappa'$  in the channel  $S \rightarrow \bar{\psi}\psi$  for  $M_S > 2M_F$  as well as  $S \rightarrow \ell\psi$  for  $M_S > M_F$ . Decays into gauge bosons are loop suppressed. Moreover, mixing in both BSM fermions (7.18) and scalars (7.11) open up more decay channels with Higgs and leptonic final states for the heavy mass eigentstates  $F_{L,R}$  and  $h_2$ . These are kinetically favourable, but suppressed by the mixing angles  $\theta_{L,R}^i$  and  $\beta$ , which



**Figure 7.11:** Allowed regions for  $\alpha_\kappa^{\mu e}, \alpha_\kappa^{\tau \mu}$  and  $M_F$  from LFV decays. Due to the proximity of upper limits on the branching ratios  $\mathcal{B}(\tau \rightarrow e\gamma)$  and  $\mathcal{B}(\tau \rightarrow \mu\gamma)$  only the latter is shown. The projected sensitivity of the MEG-II experiment [309] is denoted by the grey line.

are bound to be small. Nevertheless, this means that none of the heavy BSM fields are stable in general. However, the plethora of gauge and Yukawa interactions as well as the Higgs portal complicates the discussion of dark matter. Suitable candidates are the BSM scalar in either theory, or the electrically neutral BSM fermions in models C, D, E and F. In fact, the entire BSM sector in model E is uncharged, with  $\psi$  resembling a sterile neutrino that avoids the bounds in Fig. 7.9, and could be subject to additional Majorana mass terms. If dark matter candidates can be made suitably stable by adjusting the parameter space of couplings and masses is a non-trivial issue, that will be explored in future works.

**More Yukawa bounds.** We have already argued that the magnitude of  $\kappa$  is bounded from above via (7.24). Moreover, off-diagonal components of  $\kappa_{ij}$  may give rise to charged lepton flavour violation (LFV) via decays  $\ell_i \rightarrow \ell_j \gamma$ . Assuming  $m_{\ell_{ij}}, m_h \ll M_F$  and  $m_j \ll m_i$ , the decay width reads [308]

$$\Gamma(\ell_i \rightarrow \ell_j \gamma) = \frac{\alpha_e}{576} (\alpha_\kappa^{ij})^2 \frac{m_i^5}{M_F^4} \quad \text{with} \quad \alpha_\kappa^{ij} = (4\pi)^{-2} \sum_n \kappa_{in}^* \kappa_{jn}, \quad (7.29)$$

where  $n$  sums over all BSM flavours.<sup>17</sup> Experimental bounds on branching ratios for  $\mu$  and  $\tau$  decays are available [20], as well as projections for the MEG-II experiment [309], see Fig. 7.11. Finally, models A and C introduce an electric dipole moment  $d_\ell$  of SM leptons at one-loop order. The current experimental bounds on  $d_e$  and  $d_\mu$ , posed by the ACME and Muon g-2 collaborations respectively [310, 311] result in the constraints

$$\begin{aligned} \left| \sin 2\beta \operatorname{Im} [\kappa_{e\psi_1} \kappa'] \right| &< 2.2 \cdot 10^{-13} \cdot (4\pi)^2 \frac{M_F}{\text{TeV}}, \\ \left| \sin 2\beta \operatorname{Im} [\kappa_{\mu\psi_2} \kappa'] \right| &< 3.0 \cdot 10^{-2} \cdot (4\pi)^2 \frac{M_F}{\text{TeV}}, \end{aligned} \quad (7.30)$$

<sup>17</sup>Hence,  $\kappa \mapsto \kappa^T$  in (7.29) is required for some models.

which is the formulation for model A, the same conditions with  $\kappa_{\ell i} \kappa' \mapsto \kappa_{i\ell} \kappa'$  hold for model C. Another important prediction are the anomalous magnetic moments of electron and muon  $a_{e,\mu}$ , as the Yukawa  $\kappa$  present in each model gives a new contributions. To account for  $a_\mu$ , models A, C and D require  $\alpha_\kappa \approx (1.4 \pm 0.4)(M_F/\text{TeV})^2$  while B and F necessitate  $\alpha_\kappa \approx (4.2 \pm 1.2)(M_F/\text{TeV})^2$ , all of which are excluded due to the bound (7.24). Moreover, model E cannot explain the muon discrepancy at all. In summary, only models A and C are not excluded a priori, having a second interaction via  $\kappa'$  at their disposal. In Ch. 8 we will show that they can even explain both  $a_{e,\mu}$  without explicitly breaking lepton flavour universality.

## 7.4 Conclusion

In this chapter, we have explored a novel approach for model building, connecting ideas of asymptotic safety and flavour physics. Investigating a subset with colourless BSM matter, our results indicate that these models may remain well-defined until the Planck scale and the Higgs potential could be stabilised. Due to electroweak interactions and mixing with the leptonic and SM Higgs sector, the models are predictive and verifiable within the current experimental reach.

## 8 Anomalous magnetic moments from asymptotic safety

### 8.1 Prelude

This chapter is concerned with leptonic anomalous magnetic moments, for which we will provide a small overview here, mostly neglecting experimental aspects. A comprehensive review with focus on the muon can be found in [312, 313].

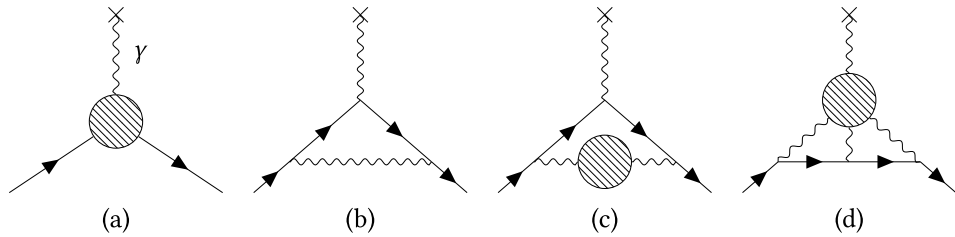
Semi-classically, the intrinsic magnetic dipole moment  $\vec{\pi}$  of a spin- $\frac{1}{2}$  fermion  $\Psi$  with charge  $q$ , momentum  $\vec{p}$ , mass  $m$  and spin  $\vec{S}$  can be read off from the Pauli equation

$$i\partial_t\Psi = \left[ \frac{1}{2m} \left( \vec{p} - q\vec{A} \right)^2 + q\Phi - \vec{\pi} \cdot \vec{B} \right] \Psi \quad \text{with} \quad \vec{\pi} = \frac{q}{2m} g \vec{S}. \quad (8.1)$$

Here,  $\Phi$  and  $\vec{A}$  are an external electric and magnetic potential, and  $\vec{B} = \vec{\nabla} \times \vec{A}$  the corresponding magnetic field. The gyromagnetic factor  $g$  is predicted by expanding the Dirac equation around  $|\vec{p} - q\vec{A}|^2 \ll m^2$  to  $g = 2$ . What is commonly referred to as the anomalous magnetic moment is the relative deviation from this value

$$a = (g - 2)/2. \quad (8.2)$$

In QFT, the corresponding interaction of an external (classical) field  $\bar{A}_\mu$  is contained in the effective operator  $\bar{\Psi} \Gamma^\mu \Psi \bar{A}_\mu$ . This corresponds to diagram Fig. 8.1(a).



**Figure 8.1:** Some diagrams related to anomalous magnetic moments: (a) generic vertex diagram, (b) Schwinger contribution, (c) hadronic vacuum polarisation, (d) hadronic light-by-light scattering. For (a), the blob stands for any interaction, while in (c) and (d) hadronic ones are denoted.

In momentum space, one obtains

$$\bar{u}(p) \Gamma^\mu u(p') = (iq) \bar{u}(p) \left[ F_1(k^2) \gamma^\mu + \frac{i}{2m} [F_2(k^2) + F_3(k^2) \gamma_5] \sigma^{\mu\nu} k_\nu \right] u(p'), \quad (8.3)$$

where  $k_\mu = p_\mu - p'_\mu$  and  $\sigma^{\mu\nu} = \frac{i}{2} [\gamma^\mu, \gamma^\nu]$  is the spin operator. In the classical limit with vanishing

momentum transfer to the external field, one obtains

$$F_1(0) = 1, \quad F_2(0) = a. \quad (8.4)$$

In fact, only the knowledge of leading and subleading coefficients in  $\Gamma^\mu$  around  $k^2 = 0$  is required, and the anomalous magnetic moment can be projected out [312] via

$$a = \text{tr} \left[ \frac{(\not{p} + m)[\gamma^\mu, \gamma^\nu](\not{p} + m)}{8(d-2)(d-1)(iq)m} \left( \frac{\partial}{\partial k^\nu} \Gamma_\mu \Big|_{k^2=0} \right) + \frac{m^2 \gamma^\mu - (d-1)m \not{p}^\mu - d \not{p} \not{p}^\mu}{4(d-1)(iq)m^2} \left( \Gamma_\mu \Big|_{k^2=0} \right) \right]. \quad (8.5)$$

Especially the muon anomalous magnetic moment  $a_\mu$  has been determined to high precision both in experimental measurements as well as theory prediction [20]. However, a discrepancy prevails:

$$\begin{aligned} a_\mu^{\text{exp}} &= 116592091(54)(33) \cdot 10^{-11}, \\ a_\mu^{\text{SM}} &= 116591803(42)(26) \cdot 10^{-11}. \end{aligned} \quad (8.6)$$

On the theory side, the contributions can be classified as pure QED parts, electroweak interactions involving massive vector bosons and scalars, and hadronic terms involving strong interactions

$$a_\mu^{\text{SM}} = a_\mu^{\text{QED}} + a_\mu^{\text{EW}} + a_\mu^{\text{Had}}. \quad (8.7)$$

The QED corrections amount the main contribution to  $a_\mu^{\text{SM}}$  and are computed up to 5-loop order in perturbation theory [314]:

$$\begin{aligned} a_\mu^{\text{QED}} &= \frac{\alpha}{2\pi} + 0.765857425(17) \left( \frac{\alpha}{\pi} \right)^2 + 24.05050996(32) \left( \frac{\alpha}{\pi} \right)^3 \\ &\quad + 130.8796(63) \left( \frac{\alpha}{\pi} \right)^4 + 753.3(1.0) \left( \frac{\alpha}{\pi} \right)^5 \\ &= 116584718.95(0.08) \cdot 10^{-11} \end{aligned} \quad (8.8)$$

where  $\alpha^{-1} = 137.035999049(90)$  is the fine structure constant. The leading term, corresponding to diagram Fig. 8.1(b) was computed by Schwinger [157] and gives by far the largest correction with  $\alpha/(2\pi) = 116140973.3(2.5) \cdot 10^{-11}$ , which is already 99.6% of  $a_\mu^{\text{SM}}$ .

The electroweak contributions are suppressed by the very mass scale, and have been computed to two-loop order with three-loop leading logarithms, amounting to

$$a_\mu^{\text{EW}} = 153.6(1.0) \cdot 10^{-11}. \quad (8.9)$$

The hadronic part  $a_\mu^{\text{Had}}$  is less straightforward to compute due to its non-perturbative nature. The leading order in  $\alpha$  is given by hadronic vacuum polarisation, as displayed in Fig. 8.1(c). Using dispersion relation techniques [315, 316], the quantity can be related to the cross section  $\sigma(e^+ e^- \rightarrow \text{hadrons})$  via the optical theorem. This provides at leading order [20]:

$$a_\mu^{\text{Had, LO}} = 6923(42)(3) \cdot 10^{-11}, \quad (8.10)$$

which is in fact the largest contribution after (8.8). At next-to-leading order, the contribution is negative  $a_\mu^{\text{HVP, NLO}} = -(98.4 \pm 0.6) \cdot 10^{-11}$ . However, hadronic light-by-light corrections, shown in

Fig. 8.1(d), also play a role, introducing large theoretical uncertainties [20]

$$a_\mu^{\text{Had, NLO}} = 7(26) \cdot 10^{-11}. \quad (8.11)$$

Collecting the results (8.8), (8.9), (8.10) and (8.11) reproduces (8.6).

## 8.2 Introduction

Measurements of the electron and muon anomalous magnetic moments exhibit intriguing discrepancies from standard model (SM) predictions [20–22]. Adding uncertainties in quadrature, the deviations

$$\begin{aligned} \Delta a_\mu &\equiv a_\mu^{\text{exp}} - a_\mu^{\text{SM}} = 268(63)(43) \cdot 10^{-11}, \\ \Delta a_e &\equiv a_e^{\text{exp}} - a_e^{\text{SM}} = -88(28)(23) \cdot 10^{-14} \end{aligned} \quad (8.12)$$

amount to  $3.5 \sigma$  ( $2.4 \sigma$ ) for the muon (electron). Recent theory predictions for  $a_\mu$  find up to  $4.1 \sigma$  [317, 318]. There are two stunning features in the data. First, the deviations  $\Delta a_\mu$  and  $\Delta a_e$  have opposite sign. Second, their ratio  $\Delta a_e / \Delta a_\mu = -(3.3 \pm 1.6) \cdot 10^{-4}$  is an order of magnitude smaller than the lepton mass ratio  $m_e / m_\mu$  and an order of magnitude larger than the square of the mass ratio  $(m_e / m_\mu)^2$ . Theory explanations of the data (8.12) with either new light scalars [319–322], supersymmetry [323–325], or bottom-up models [326, 327] invariably involve a manifest breaking of lepton flavour universality.

In recent years, asymptotic safety has been put forward as a new idea for model building [121, 291]. It is based on the discovery [112] that particle theories may very well remain fundamental and predictive in the absence of asymptotic freedom due to interacting high energy fixed points [32, 89, 171]. For weakly coupled theories, general theorems for asymptotic safety are available [110, 111] with templates covering simple [2, 112], semi-simple [114], and supersymmetric gauge theories [115]. Yukawa interactions and new scalar fields play a prominent role because they slow-down the growth of asymptotically non-free gauge couplings, which can enable interacting fixed points [110] including in extensions of the standard model [121–123, 291].

In this letter, we show that asymptotically safe extensions of the SM may offer a natural explanation for the data (8.12). The primary reason for this is that Yukawa interactions, which help generate interacting fixed points, can *also* contribute to lepton anomalous magnetic moments. We demonstrate this idea in two concrete models by introducing Yukawa couplings between ordinary leptons and new vector-like fermions, and by adding new scalar fields which admit either a flavourful or flavour universal ground state. The stability of SM extensions all the way up to the Planck scale is exemplified using the renormalisation group (RG) running of couplings for a wide range of BSM parameters.

## 8.3 New vector-like fermions and scalar matter

In the spirit of [112], we are interested in SM extensions involving  $N_F$  flavours of vector-like colour-singlet fermions  $\psi_i$  and  $N_F^2$  complex scalar singlets  $S_{ij}$ . In their simplest form, the new fermions couple to SM matter only via gauge interactions [121, 291]. The new ingredient in this letter are Yukawa couplings between SM and BSM matter. To make contact with SM flavour we

set  $N_F = 3$ . We then consider singlet or doublet models where the new fermions are either  $SU(2)$  singlets with hypercharge  $Y = -1$ , or  $SU(2)$  doublets with  $Y = -\frac{1}{2}$ . In our conventions, electric charge  $Q$  and weak isospin  $T_3$  relate as  $Q = T_3 + Y$ . Within these choices, and denoting the SM lepton singlets, doublets and Higgs as  $E, L$  and  $H$ , respectively, we find three possible Yukawa couplings  $\kappa, \kappa'$  and  $y$  with

$$\begin{aligned}\mathcal{L}_Y^{\text{singlet}} &= -\kappa \bar{L} H \psi_R - \kappa' \bar{E} S^\dagger \psi_L - y \bar{\psi}_L S \psi_R + \text{h.c.} \\ \mathcal{L}_Y^{\text{doublet}} &= -\kappa \bar{E} H^\dagger \psi_L - \kappa' \bar{L} S \psi_R - y \bar{\psi}_L S \psi_R + \text{h.c.}\end{aligned}\quad (8.13)$$

and flavour traces are understood to simplify the subsequent RG analysis. Effects of the Yukawa coupling  $y$  have been studied in [121, 122, 291]. The scalar potential of either model reads

$$V = \lambda (H^\dagger H)^2 + \delta H^\dagger H \text{tr} [S^\dagger S] + u \text{tr} [S^\dagger S S^\dagger S] + v (\text{tr} [S^\dagger S])^2, \quad (8.14)$$

where  $u, v, \lambda$  and  $\delta$  are quartic and portal couplings. We further introduce mass terms for the scalars and vector-like fermions. The potential (8.14) admits vacuum configurations  $V^+$  and  $V^-$  characterized by

$$\begin{aligned}V^+ : & \begin{cases} \lambda > 0, & u > 0, & u + 3v > 0, \\ \delta > -2\sqrt{\lambda(u/3 + v)}, \end{cases} \\ V^- : & \begin{cases} \lambda > 0, & u < 0, & u + v > 0, \\ \delta > -2\sqrt{\lambda(u + v)}. \end{cases}\end{aligned}\quad (8.15)$$

Either of these allow for electroweak symmetry breaking. Moreover, in  $V^+$ , and for suitable mass parameters, the diagonal components of  $S$  each acquire the same vacuum expectation value  $\langle S_{\ell\ell} \rangle \neq 0$  and the ground state is flavour universal. In  $V^-$  a finite vacuum expectation value  $\langle S_{\ell\ell} \rangle \neq 0$  arises only for one flavour direction giving rise to a flavourful vacuum.

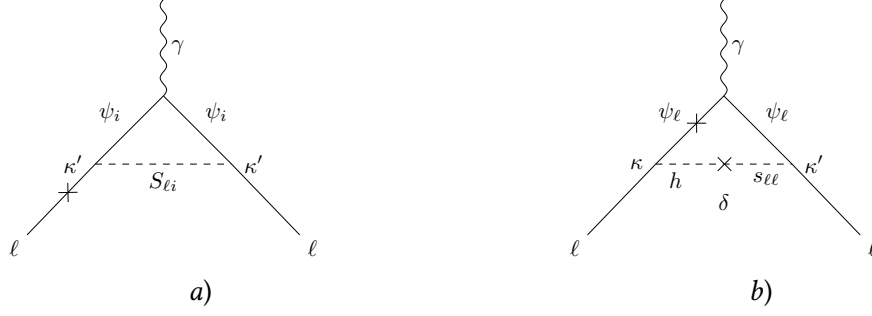
## 8.4 Explaining anomalous magnetic moments

We are now in a position to explain the data (8.12) in SM extensions with (8.13) and (8.14). The relevant leading loop effects due to the couplings  $\kappa, \kappa'$ , and  $\delta$  are shown in Fig. 8.2, also using  $S = \langle S \rangle + s$ . Any lepton flavour  $\ell = e, \mu, \tau$  receives a contribution from BSM scalar-fermion loops with chiral flip on the lepton line induced by the coupling  $\kappa'$  (see Fig. 8.2a). It scales quadratically with the lepton mass,

$$\Delta a_\ell = \frac{N_F \kappa'^2}{96\pi^2} \frac{m_\ell^2}{M_F^2} f_1 \left( \frac{M_S^2}{M_F^2} \right), \quad (8.16)$$

and represents a minimal lepton flavour dependence with  $f_1(t) = (2t^3 + 3t^2 - 6t^2 \ln t - 6t + 1)/(t-1)^4$  positive for any  $t$ , and  $f_1(0) = 1$ . This manifestly positive contribution is the dominant one for  $a_\mu$ . Contributions through  $Z$ - and  $W$ -loops are parametrically suppressed as  $\mathcal{O}(g_2^2)$  and by fermion mixing [304]. Comparing (8.16) with the muon data for small scalar-to-fermion mass ratio  $M_S^2/M_F^2 \ll 1$  yields the Yukawa coupling  $\alpha_{\kappa'}$  within  $(0.48 \pm 0.15)(\frac{M_F}{\text{TeV}})^2$ , which is large for TeV-range fermion masses  $M_F$ . Fixing  $\Delta a_\mu$  to the muon data (8.12)) confirms that the corresponding contribution (8.16) for the electron would come out too small and with the wrong sign  $\Delta a_e \simeq$





**Figure 8.2:** Leading loop contributions to  $\Delta a_\ell$  ( $\ell = e, \mu, \tau$ ), including a) BSM scalar-fermion loops with a lepton chiral flip (cross on solid line), and b) chirally enhanced contributions through scalar mixing (cross on dashed line) provided  $\langle S_{\ell\ell} \rangle \neq 0$ , and a BSM fermion  $\psi_\ell$  chiral flip (cross on solid line).

$6 \cdot 10^{-14}$  (see Fig. 8.3).

Additionally, chirally enhanced contributions, which are linear in the lepton mass, may arise through a portal-mediated scalar mixing where the chiral flip is shifted to a  $\psi$  line (Fig. 8.2b). The key observation is that chiral enhancement naturally explains the electron data (Fig. 8.3). In practice, this can be realized with either  $V^+$  or  $V^-$ .<sup>18</sup> If the ground state is  $V^-$ , it must point into the electron direction (only  $\langle S_{ee} \rangle \neq 0$ ) or else (8.12) cannot be satisfied. Overall, this leads to

$$\Delta a_e = \frac{m_e}{M_F} \frac{\kappa \kappa' \sin 2\beta}{32\pi^2} \left[ f_2 \left( \frac{m_s^2}{M_F^2} \right) - f_2 \left( \frac{m_h^2}{M_F^2} \right) \right] + \frac{m_e^2}{m_\mu^2} \Delta a_\mu \quad (8.17)$$

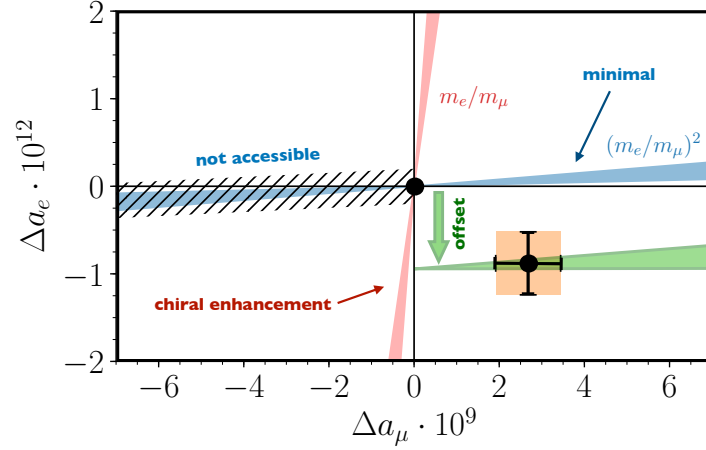
where  $m_{h,s}$  are the Higgs and the BSM scalar mass, and the last term accounts for (8.16). The loop function  $f_2(t) = (3t^2 - 2t^2 \ln t - 4t + 1)/(1 - t)^3$  is positive for any  $t$  and  $f_2(0) = 1$ . The mixing angle  $\beta$  between the scalar  $s_{\ell\ell}$  and the physical Higgs  $h$  is fixed via

$$\tan 2\beta = \frac{\delta}{\sqrt{\lambda(u+v)}} \frac{m_h}{m_s} \left( 1 + \mathcal{O}(m_h^2/m_s^2) \right). \quad (8.18)$$

In (8.17), the term linear in the electron mass provides a unique offset for the electron  $\Delta a_e$ , sketched in Fig. 8.3. It dominates parametrically over the quadratic term and can have either sign set by the Yukawas  $\kappa, \kappa'$  and the portal coupling  $\delta$ .

As an estimate, comparing (8.17) with the electron data assuming  $m_h^2/M_F^2 \ll 1$  and simultaneously fixing (8.16) to match the muon data, we find  $|\kappa \sin 2\beta| \approx (2.9 \pm 1.2) \cdot 10^{-4} \left( \frac{M_F}{\text{TeV}} \right)^2$ . The full parameter window explaining the data is indicated in Fig. 8.4 assuming  $V^-$ . Corrections from  $Z$ - and  $W$ -exchange, which contribute differently in the singlet and doublet models, are suppressed by small fermion mixing angles and not sizeable enough to be seen in Fig. 8.4. Also shown are limits on  $M_F$  (grey) from Drell-Yan processes [123, 305, 306] and on perturbativity in  $\alpha_{\kappa'}$  (red). We observe  $M_F$  within  $(0.05 - 2)$  TeV for  $\alpha_{\kappa'}$  within  $(10^{-2} - 1)$ , with  $\kappa \sin 2\beta/(4\pi)$  deeply perturbative (green) for small portal coupling  $\delta$ . The dual parameter space ( $\kappa' \ll \kappa$ ) where Fig. 8.2a is replaced by the corresponding Higgs-fermion loops, is ruled out by  $Z \rightarrow \ell\ell$  data [20], which constrains left-handed (right-handed) fermion mixing angles in the singlet (doublet) model to be of  $\mathcal{O}(10^{-2})$  or smaller.

<sup>18</sup>Hence, lepton flavour universality is either intact ( $V^+$ ) or broken spontaneously ( $V^-$ ).



**Figure 8.3:** Leading contributions to  $\Delta a_{e,\mu}$  from Fig. 8.2a (blue band) and Fig. 8.2b (red band), which, in combination (green band), explain the electron and muon data (cross) simultaneously. The chirally enhanced offset is either flavour universal or points into the electron direction (green arrow). Band widths are indicative of a 20% mass splitting between fermion flavours from leading loops; the hatched region is inaccessible.

If the vacuum is  $V^+$ , all lepton anomalous magnetic moments receive a chirally enhanced contribution from Fig. 8.2b, similar to the first term in (8.17). The offset in Fig. 8.3 is then slightly tilted and points along the direction of the red band. Due to the smallness of the tilt, results and constraints are similar to those for  $V^-$  in Fig. 8.4. As either of the relevant contributions in Fig. 8.2 are flavour-diagonal and real irrespective of the vacuum configurations, they do not contribute to lepton decay and electric dipole moments [304].

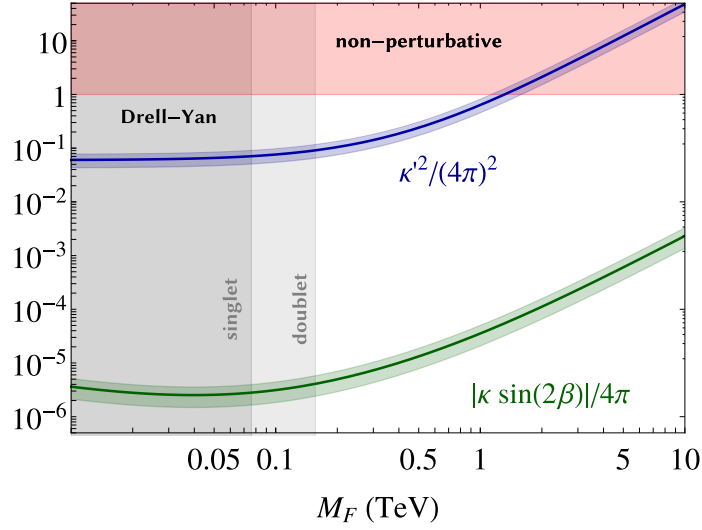
## 8.5 Running of couplings up to the Planck scale

We now turn to the RG running of couplings and conditions under which models are stable and predictive up to the Planck scale. We normalize couplings to loop factors,

$$\alpha_x = \frac{x^2}{(4\pi)^2}, \quad \alpha_z = \frac{z}{(4\pi)^2}, \quad (8.19)$$

where  $x = g_1, g_2, g_3, y_t, y_b, y, \kappa, \kappa'$  are any of the gauge, top, bottom or BSM Yukawa couplings, and  $z = \lambda, u, v, \delta$  are the quartic and portal couplings. Models are matched onto the SM at the scale set by the fermion mass. For the running above  $M_F$ , we retain all 12 RG beta-functions up to two-loop order in all couplings [182–185].

The left panel of Fig. 8.5 shows benchmark trajectories up to the Planck scale  $M_{\text{Pl}}$  for models starting in the vacuum  $V^-$  at the scale  $M_F$ . For some initial conditions  $\alpha_{\text{BSM}}|_{M_F}$  at the low scale, such as those used in Fig. 8.5, we find that the running is stable up to the Planck scale. We also observe from Fig. 8.5 that the Higgs potential becomes stable (remains metastable) in the singlet (doublet) model. Higgs stability in the doublet model can be achieved for larger portal and quartic couplings. Some couplings in Fig. 8.5 run slowly all the way up to the Planck scale. Others



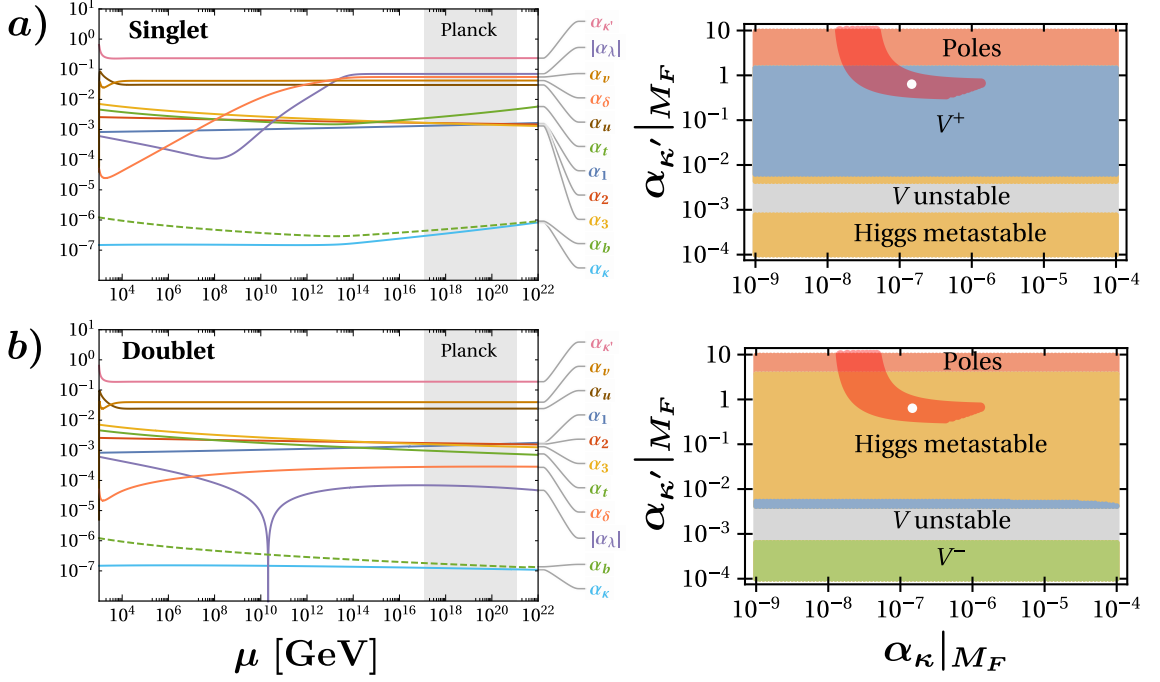
**Figure 8.4:** Window for Yukawa and portal couplings which simultaneously explain the muon and electron data (8.12) as functions of the BSM fermion mass  $M_F$ , and  $M_S = 0.5$  TeV. Grey-shaded areas are excluded by Drell-Yan searches, the red-shaded area indicates strong coupling. All results refer to  $V^-$ , very similar ones are found for  $V^+$  (not shown).

show a slow or fast cross-over to near-constant values due to near-zeros of beta functions [328] which arise from a competition between SM and BSM matter. In the absence of quantum gravity, the evolution of couplings ultimately terminates in an interacting UV fixed point corresponding to asymptotic safety (singlet benchmark) with asymptotic freedom prevailing in the weak and strong sectors [110, 121, 291]. In some cases, trajectories remain safe up to the Planck scale (doublet benchmark) but blow up at transplanckian energies. For other initial conditions we also find unsafe trajectories which terminate in subplanckian Landau poles (see [304] for a detailed study of initial conditions  $\alpha_{\text{BSM}}|_{M_F}$ ).

The right panel of Fig. 8.5 shows the vacua of singlet and doublet models at the Planck scale in terms of the Yukawa couplings  $(\alpha_\kappa, \alpha_{\kappa'})|_{M_F}$  at the matching scale. Integrating the RG between  $M_F$  and  $M_{\text{Pl}}$ , we find wide ranges of models whose vacua at the Planck scale are either  $V^+$  (blue), or a stable  $V$  with a metastable Higgs sector ( $\alpha_\lambda \gtrsim -10^{-4}$ ) such as in the SM [23, 24] (yellow). For other parameter ranges we also find  $V^-$  (green), or unstable BSM potentials (grey), or Landau poles below the Planck scale (light red). Most importantly, the anomalous magnetic moments (8.12) are matched for couplings in the red-shaded areas. Here, constraints from Higgs signal strength [20] imply an upper bound on  $\alpha_\kappa$  corresponding to a lower bound for the scalar mass of about 226 GeV (for  $M_F = 1$  TeV). Similar results are found for  $V^+$  at the low scale (not shown) except that regions with  $V^-$  in Fig. 8.5 turn into  $V^+$ . We conclude that models are stable and Planck-safe for a range of parameters  $\alpha_{\text{BSM}}|_{M_F}$ .

## 8.6 Collider production and decay

Models predict new scalars and fermions in the TeV energy range. Their phenomenology is characterized by an enlarged flavour sector with a large Yukawa coupling  $\kappa'$  and moderate or



**Figure 8.5:** Benchmark trajectories ( $M_F = 2M_S = 1$  TeV) between the matching scale  $M_F$  and the Planck scale (left), and parameter scans of vacua at the Planck scale (right) for *a*) the singlet model (top) and *b*) the doublet model (bottom) using  $(\alpha_\delta, \alpha_u, \alpha_v, \alpha_y)|_{M_F} = (5, -1, 4, 0) \cdot 10^{-5}$ . High scale vacua are shown as functions of the Yukawa couplings  $(\alpha_\kappa, \alpha_{\kappa'})|_{M_F}$ . Parameters within the red-shaded areas are compatible with data (8.12); white dots refer to the benchmarks on the left.

small couplings  $\kappa$ ,  $\delta$ . We identify collider signatures through production and decay [304]. We denote the fermions in the singlet model by  $\psi_s^{-1}$  and the isospin components in the doublet model by  $\psi_d^0$  and  $\psi_d^{-1}$ ; superscripts show electric charge. The  $\psi_d^0$  is lighter than the  $\psi_d^{-1}$  by  $\Delta m = M_{\psi^{-1}} - M_{\psi^0} = g_2^2 \sin^2 \theta_W^2 m_Z / (8\pi) \simeq 0.4 \text{ GeV}$  [329]. All fermion flavours can be pair-produced in  $pp$  and  $\ell\ell$  machines via  $s$ -channel  $\gamma$  or  $Z$  exchange, and through  $W^\pm$  exchange at  $pp$ -colliders (doublet model only). Lepton colliders allow for pair-production from  $t$ -channel  $S$  at order  $\kappa'^2$ , which is sizeable (see Fig. 8.4). Single  $\psi$  production together with a lepton arises from  $s$ -channel  $Z$ - and  $W$ -boson contributions via fermion mixing.  $S$  production occurs only via the Higgs portal, or at lepton colliders with  $t$ -channel  $\psi$  in association with  $h$  at order  $\kappa \kappa'$  or in pairs at order  $(\kappa')^2$ . If kinematically allowed, the charged fermions decay as  $\psi^{-1} \rightarrow S\ell$  and the neutral ones as  $\psi_d^0 \rightarrow S\nu$ . If these channels are closed, the  $\psi^{-1}$  decay to Higgs plus lepton instead. The decay rate  $\Gamma(\psi^{-1} \rightarrow h\ell^-) = \frac{\kappa^2}{64\pi} M_F (1 - m_h^2/M_F^2)^2$  provides the lifetime estimate  $\Gamma^{-1} \approx 10^{-27} \alpha_\kappa^{-1} M_F^{-1} \text{ TeVs}$ . The neutral fermion  $\psi_d^0$  cascades down slower, yet still promptly through  $W$ -emission with  $\psi_{d,i}^0 \rightarrow \psi_{d,i}^{-1*} W^{++} \rightarrow h\ell_i^- W^{++}$ . If kinematically allowed, the BSM scalars  $S$  undergo tree level decay into  $\psi\bar{\psi}$  via  $y$ , and into  $\psi\ell$  via  $\kappa'$ . At one-loop arise the decays  $S \rightarrow \gamma\gamma$ ,  $ZZ$ ,  $Z\gamma$ , and  $S \rightarrow WW$  (doublet model only) from  $y$ . Although there is no genuine lepton flavour violation (LFV) as flavour in the  $S$ -decay process is conserved, the mixing between the  $\psi$  and the SM leptons introduces very distinct LFV-like final states  $S_{ij} \rightarrow \ell_i^\pm \ell_j^\mp$ . The LFV-like decays at the order  $\kappa\kappa' v_h/M_F$  or  $(\kappa')^2 (v_s v_h/2M_F)^2$  are the leading ones for negligible  $y$  and  $M_S/M_F \ll 1$ .

## 8.7 Discussion

We have shown that extensions of the standard model with new vector-like leptons and singlet scalars (8.13), (8.14) explain the muon and electron anomalous magnetic moments (8.12) simultaneously. Yukawa couplings mixing SM and BSM matter and a Higgs portal coupling are instrumental to generate both minimal (8.16) and chirally enhanced (8.17) contributions, which, when taken together, match the data naturally (Fig. 8.3). Another salient feature is that the Higgs potential remains stable up to the Planck scale, unlike in the SM [23, 24]. Further predictions are a strongly and a weakly coupled Yukawa sector, and new matter fields with masses in the TeV range (Fig. 8.4) which can be tested at colliders.

An intriguing aspect of our models is that they predict the deviation of the tau anomalous magnetic moment from its standard model value solely based on the data (8.12) and the vacuum, and irrespective of any other specifics. Provided the ground state distinguishes electron flavour we have

$$\Delta a_\tau \equiv a_\tau^{\text{exp}} - a_\tau^{\text{SM}} = (7.5 \pm 2.1) \cdot 10^{-7}, \quad (8.20)$$

and  $\Delta a_\tau = (8.1 \pm 2.2) \cdot 10^{-7}$  otherwise. Although the present limit on  $\Delta a_\tau$  is four orders of magnitude away [20], it would be very interesting to test this in the future. We also note that with small CP phases, the electric dipole moment of the electron can be as large as the present bound  $d_e < 1.1 \cdot 10^{-29} e \text{ cm}$  [310]. In settings with flavour universal vacua the bound extends to all lepton electric dipole moments  $d_\ell$ , which would make an experimental check for the muon and the tau very challenging.

The new ingredients to address the anomalous magnetic moments are key for achieving safe and controlled SM extensions up to the Planck scale (Fig. 8.5), and extend the ideas for asymptotically safe model building initiated in [121, 291]. More work is required to explore the full potential of asymptotic safety for flavour and particle physics.

## 9 Conclusion

This thesis contains several landmarks of the journey from formal aspects of a general RG analysis, through the realm of asymptotic safety in perturbative exact toy models and towards realistic UV completions of particle physics.

**Renormalisation group analysis.** Ch. 2 revisits the theoretical backbone to compute perturbative RGEs. Among the main results are equations (2.22)–(2.26), (2.55), (2.56), (2.67) and (2.79), correcting several errors in the pre-existing literature. These formulas are very powerful, as they apply to any perturbatively renormalisable QFT. In particular, there are no restriction regarding the field content and interactions. Hence, the results benefit the wider research community – either being employed directly or as the backend of scientific software tools.

There are only two reservations of this framework. Firstly, it is manifestly perturbative and limited by the loop orders available for each of the master formulas. This boundary can be stretched by future computational efforts. Moreover, mapping the template expressions onto the theory of interest is a very complex and error-prone task that requires automation. This is addressed in Ch. 3, introducing the software package ARGES. As we have highlighted, ARGES is a general-purpose framework for computing RG equations, competitive with existing software available. However, due to various design differences, ARGES also works with QFTs that cannot be processed by any alternative tools. Hence, the program enables the automated extraction of RGEs not only for models specific to this thesis, but almost any renormalisable QFT.

**Perturbatively exact asymptotic safety.** After the removal of technical hurdles, Ch. 4–Ch. 6 are concerned with weakly coupled asymptotic safety. We follow the footsteps of the Litim-Sannino model [112,113], where this property has been proven rigorously in the Veneziano limit. However, it was neither known if other QFTs with such an interacting UV fixed points exist, nor if there are strict exclusion principles. Hence, Ch. 4 combines the requirements for asymptotic safety and the Veneziano limit, classifying models with a simple gauge group and single Yukawa interaction. The results indicate that only theories featuring charged fermions, coupling to a sufficiently large number of neutral scalars via a Yukawa term, allow for weakly interacting UV fixed points. Gathered evidence suggests that this might hold beyond the limitations of this ansatz. A quantification of asymptotic safety is introduced, identifying that the safest QFTs are those with infinitely many scalar fields per fermion. However, no example could be constructed. Instead, we argue that the Litim-Sannino model and equivalent formulations are maximally asymptotically safe. Hence the question arises whether this model and its unitary gauge symmetry is of unique importance. This is addressed in Ch. 6, which uncovers two similar theories in the same universality class. Exact asymptotic safety appears to require complex scalars and Dirac fermions transforming under a unitary gauge group, or Majorana ones with either orthogonal or symplectic gauge. Remarkably, all three families are equivalent even away from the fixed point. Hence,

the results obtained in Ch. 5 are universal among them. All renormalisation group equations are computed up to the highest available loop order. Based on this, it was possible to probe the extent of the UV conformal window. A systematic study has strengthened the lore that Yukawa interactions are crucial for asymptotic safety. At higher loop order, they are found to widen the window while gauge and quartic interactions narrow it.

**BSM model building.** The last two chapters abandon the exact regime in favour of realistic UV completions for Standard Model of particle physics. The guiding principle is to achieve asymptotic safety until the Planck scale. A set of models is presented in Ch. 7, extending the SM field content by electroweakly charged vector-like fermions and a neutral scalar meson. Another novel ingredient was an additional Yukawa coupling between BSM fermions and SM Higgs, intertwining both flavour sectors. A bottom-up approach from SM matching to the Planck scale lent itself quite naturally to this analysis. It is found that the mechanism of Yukawa couplings slowing the running of gauge interaction prevails, to the point where Landau poles are shifted beyond the Planck scale. Moreover, beyond the leading order running, these Yukawas stabilise the scalar potential. Remarkably, this may even remove the metastability of the SM Higgs, due to the BSM portal Yukawa sector. The key role to stabilise both gauge and quartic quantum corrections hints at a fundamental necessity of Yukawa interactions. Several (partial) walking regimes around pseudo-fixed points are identified, which enable this double-stabilisation, and are visible as isles of stability on the BSM critical surface. Additionally, a basic overview of phenomenological implications and constraints are provided.

In this regard, Ch. 8 demonstrates how open questions of the SM can be addressed. The discrepancies in both muon and electron anomalous magnetic moments between SM prediction and experimental data can be accounted for simultaneously in two of the models. This is achieved without explicitly breaking lepton flavour universality or introducing supersymmetry, as required by other ansätze. Instead, scalar mixing provides two distinct contributions that can be tuned to explain the anomalies, while providing stability and safety until the Planck scale.

Many avenues of research connected to this thesis remain open for future endeavours. For instance, it would be interesting to further pursue the webs of equivalences that have become apparent among various QFTs in the large- $N$  limit. Moreover, the discovered triality of asymptotic safety could be employed for constructing BSM theories with orthogonal or symplectic gauge symmetries. However, some questions also remain in the BSM theory presented here, for instance about stability of the Higgs potential. Additional candidate theories featuring coloured fermions have been neglected so far.

## Bibliography

- [1] I. Schienbein, F. Staub, T. Steudtner and K. Svirina, *Revisiting RGEs for general gauge theories*, *Nucl. Phys.* **B939** (2019) 1 [1809.06797].
- [2] A. D. Bond, D. F. Litim, G. Medina Vazquez and T. Steudtner, *UV conformal window for asymptotic safety*, *Phys. Rev.* **D97** (2018) 036019 [1710.07615].
- [3] A. D. Bond, D. F. Litim and T. Steudtner, *Asymptotic safety with Majorana fermions and new large  $N$  equivalences*, *Phys. Rev.* **D101** (2020) 045006 [1911.11168].
- [4] G. Hiller, C. Hormigos-Feliu, D. F. Litim and T. Steudtner, *Anomalous magnetic moments from asymptotic safety*, 1910.14062.
- [5] S. Glashow, *Partial Symmetries of Weak Interactions*, *Nucl. Phys.* **22** (1961) 579.
- [6] S. Weinberg, *A Model of Leptons*, *Phys. Rev. Lett.* **19** (1967) 1264.
- [7] A. Salam, *Weak and Electromagnetic Interactions*, *Conf. Proc. C* **680519** (1968) 367.
- [8] S. Glashow, J. Iliopoulos and L. Maiani, *Weak Interactions with Lepton-Hadron Symmetry*, *Phys. Rev. D* **2** (1970) 1285.
- [9] H. Fritzsch, M. Gell-Mann and H. Leutwyler, *Advantages of the Color Octet Gluon Picture*, *Phys. Lett. B* **47** (1973) 365.
- [10] F. Englert and R. Brout, *Broken Symmetry and the Mass of Gauge Vector Mesons*, *Phys. Rev. Lett.* **13** (1964) 321.
- [11] P. W. Higgs, *Broken Symmetries and the Masses of Gauge Bosons*, *Phys. Rev. Lett.* **13** (1964) 508.
- [12] G. Guralnik, C. Hagen and T. Kibble, *Global Conservation Laws and Massless Particles*, *Phys. Rev. Lett.* **13** (1964) 585.
- [13] G. 't Hooft, *Renormalizable Lagrangians for Massive Yang-Mills Fields*, *Nucl. Phys. B* **35** (1971) 167.
- [14] ATLAS collaboration, *Observation of a new particle in the search for the Standard Model Higgs boson with the ATLAS detector at the LHC*, *Phys. Lett. B* **716** (2012) 1 [1207.7214].
- [15] CMS collaboration, *Observation of a New Boson at a Mass of 125 GeV with the CMS Experiment at the LHC*, *Phys. Lett. B* **716** (2012) 30 [1207.7235].



- [16] ATLAS, CMS collaboration, *Combined Measurement of the Higgs Boson Mass in pp Collisions at  $\sqrt{s} = 7$  and 8 TeV with the ATLAS and CMS Experiments*, *Phys. Rev. Lett.* **114** (2015) 191803 [1503.07589].
- [17] A. Sakharov, *Violation of CP Invariance, C asymmetry, and baryon asymmetry of the universe*, *Sov. Phys. Usp.* **34** (1991) 392.
- [18] S. Weinberg, *Cosmology*. Oxford Univ. Pr., 9, 2008.
- [19] A. Strumia and F. Vissani, *Neutrino masses and mixings and...*, hep-ph/0606054.
- [20] PARTICLE DATA GROUP collaboration, *Review of Particle Physics*, *Phys. Rev.* **D98** (2018) 030001.
- [21] D. Hanneke, S. Fogwell and G. Gabrielse, *New Measurement of the Electron Magnetic Moment and the Fine Structure Constant*, *Phys. Rev. Lett.* **100** (2008) 120801 [0801.1134].
- [22] R. H. Parker, C. Yu, W. Zhong, B. Estey and H. Müller, *Measurement of the fine-structure constant as a test of the Standard Model*, *Science* **360** (2018) 191 [1812.04130].
- [23] G. Degrandi, S. Di Vita, J. Elias-Miro, J. R. Espinosa, G. F. Giudice, G. Isidori et al., *Higgs mass and vacuum stability in the Standard Model at NNLO*, *JHEP* **08** (2012) 098 [1205.6497].
- [24] D. Buttazzo, G. Degrandi, P. P. Giardino, G. F. Giudice, F. Sala, A. Salvio et al., *Investigating the near-criticality of the Higgs boson*, *JHEP* **12** (2013) 089 [1307.3536].
- [25] A. Bednyakov, B. Kniehl, A. Pikelner and O. Veretin, *Stability of the Electroweak Vacuum: Gauge Independence and Advanced Precision*, *Phys. Rev. Lett.* **115** (2015) 201802 [1507.08833].
- [26] A. Hook, *TASI Lectures on the Strong CP Problem and Axions*, *PoS TASI2018* (2019) 004 [1812.02669].
- [27] L. D. Landau, A. A. Abrikosov and I. M. Khalatnikov, *An asymptotic expression for the photon Green function in quantum electrodynamics*, *Dokl. Akad. Nauk SSSR* **95** (1954) 1177.
- [28] M. Gockeler, R. Horsley, V. Linke, P. E. Rakow, G. Schierholz and H. Stuben, *Is there a Landau pole problem in QED?*, *Phys. Rev. Lett.* **80** (1998) 4119 [hep-th/9712244].
- [29] H. Gies and J. Jaeckel, *Renormalization flow of QED*, *Phys. Rev. Lett.* **93** (2004) 110405 [hep-ph/0405183].
- [30] D. J. Callaway, *Triviality Pursuit: Can Elementary Scalar Particles Exist?*, *Phys. Rept.* **167** (1988) 241.
- [31] K. G. Wilson, *The Renormalization Group and Strong Interactions*, *Phys. Rev.* **D3** (1971) 1818.
- [32] S. Weinberg, *Ultraviolet Divergences in Quantum Theories of Gravitation*, in *General Relativity: An Einstein Centenary Survey*, pp. 790–831, (1980).

- [33] C. Wetterich, *Exact evolution equation for the effective potential*, *Phys. Lett.* **B301** (1993) 90 [1710.05815].
- [34] T. R. Morris, *The Exact renormalization group and approximate solutions*, *Int. J. Mod. Phys.* **A9** (1994) 2411 [hep-ph/9308265].
- [35] M. Reuter, *Nonperturbative evolution equation for quantum gravity*, *Phys. Rev.* **D57** (1998) 971 [hep-th/9605030].
- [36] D. Dou and R. Percacci, *The running gravitational couplings*, *Class. Quant. Grav.* **15** (1998) 3449 [hep-th/9707239].
- [37] D. F. Litim, *Fixed points of quantum gravity*, *Phys. Rev. Lett.* **92** (2004) 201301 [hep-th/0312114].
- [38] O. Lauscher and M. Reuter, *Flow equation of quantum Einstein gravity in a higher derivative truncation*, *Phys. Rev. D* **66** (2002) 025026 [hep-th/0205062].
- [39] D. Benedetti and F. Caravelli, *The Local potential approximation in quantum gravity*, *JHEP* **06** (2012) 017 [1204.3541].
- [40] J. A. Dietz and T. R. Morris, *Asymptotic safety in the  $f(R)$  approximation*, *JHEP* **01** (2013) 108 [1211.0955].
- [41] K. Falls, D. F. Litim, K. Nikolakopoulos and C. Rahmede, *A bootstrap towards asymptotic safety*, 1301.4191.
- [42] M. Demmel, F. Saueressig and O. Zanusso, *A proper fixed functional for four-dimensional Quantum Einstein Gravity*, *JHEP* **08** (2015) 113 [1504.07656].
- [43] N. Ohta, R. Percacci and G. P. Vacca, *Renormalization Group Equation and scaling solutions for  $f(R)$  gravity in exponential parametrization*, *Eur. Phys. J. C* **76** (2016) 46 [1511.09393].
- [44] K. G. Falls, D. F. Litim and J. Schröder, *Aspects of asymptotic safety for quantum gravity*, *Phys. Rev. D* **99** (2019) 126015 [1810.08550].
- [45] D. Benedetti, P. F. Machado and F. Saueressig, *Asymptotic safety in higher-derivative gravity*, *Mod. Phys. Lett. A* **24** (2009) 2233 [0901.2984].
- [46] H. Gies, B. Knorr, S. Lippoldt and F. Saueressig, *Gravitational Two-Loop Counterterm Is Asymptotically Safe*, *Phys. Rev. Lett.* **116** (2016) 211302 [1601.01800].
- [47] K. Falls, C. R. King, D. F. Litim, K. Nikolakopoulos and C. Rahmede, *Asymptotic safety of quantum gravity beyond Ricci scalars*, *Phys. Rev.* **D97** (2018) 086006 [1801.00162].
- [48] K. Falls, N. Ohta and R. Percacci, *Towards the determination of the dimension of the critical surface in asymptotically safe gravity*, 2004.04126.
- [49] P. Donà, A. Eichhorn and R. Percacci, *Matter matters in asymptotically safe quantum gravity*, *Phys. Rev. D* **89** (2014) 084035 [1311.2898].

- [50] P. Donà, A. Eichhorn and R. Percacci, *Consistency of matter models with asymptotically safe quantum gravity*, *Can. J. Phys.* **93** (2015) 988 [1410.4411].
- [51] J. Meibohm, J. M. Pawłowski and M. Reichert, *Asymptotic safety of gravity-matter systems*, *Phys. Rev. D* **93** (2016) 084035 [1510.07018].
- [52] N. Christiansen, D. F. Litim, J. M. Pawłowski and M. Reichert, *Asymptotic safety of gravity with matter*, *Phys. Rev. D* **97** (2018) 106012 [1710.04669].
- [53] M. Niedermaier and M. Reuter, *The Asymptotic Safety Scenario in Quantum Gravity*, *Living Rev. Rel.* **9** (2006) 5.
- [54] M. Niedermaier, *The Asymptotic safety scenario in quantum gravity: An Introduction*, *Class. Quant. Grav.* **24** (2007) R171 [gr-qc/0610018].
- [55] R. Percacci, *Asymptotic Safety*, 0709.3851.
- [56] A. Codello, R. Percacci and C. Rahmede, *Investigating the Ultraviolet Properties of Gravity with a Wilsonian Renormalization Group Equation*, *Annals Phys.* **324** (2009) 414 [0805.2909].
- [57] D. F. Litim, *Renormalisation group and the Planck scale*, *Phil. Trans. Roy. Soc. Lond.* **A369** (2011) 2759 [1102.4624].
- [58] A. Eichhorn, *An asymptotically safe guide to quantum gravity and matter*, *Front. Astron. Space Sci.* **5** (2019) 47 [1810.07615].
- [59] A. Bonanno, A. Eichhorn, H. Gies, J. M. Pawłowski, R. Percacci, M. Reuter et al., *Critical reflections on asymptotically safe gravity*, 2004.06810.
- [60] R. Gastmans, R. Kallosh and C. Truffin, *Quantum Gravity Near Two-Dimensions*, *Nucl. Phys.* **B133** (1978) 417.
- [61] S. M. Christensen and M. J. Duff, *Quantum Gravity in Two +  $\epsilon$  Dimensions*, *Phys. Lett.* **79B** (1978) 213.
- [62] E. Tomboulis, *1/N Expansion and Renormalization in Quantum Gravity*, *Phys. Lett. B* **70** (1977) 361.
- [63] E. Tomboulis, *Renormalizability and Asymptotic Freedom in Quantum Gravity*, *Phys. Lett. B* **97** (1980) 77.
- [64] L. Smolin, *A Fixed Point for Quantum Gravity*, *Nucl. Phys. B* **208** (1982) 439.
- [65] M. E. Peskin, *Critical Point Behavior of the Wilson Loop*, *Phys. Lett.* **94B** (1980) 161.
- [66] H. Gies, *Renormalizability of gauge theories in extra dimensions*, *Phys. Rev.* **D68** (2003) 085015 [hep-th/0305208].
- [67] A. Codello, K. Langæble, D. F. Litim and F. Sannino, *Conformal Gauge-Yukawa Theories away From Four Dimensions*, *JHEP* **07** (2016) 118 [1603.03462].

- [68] K. Gawedzki and A. Kupiainen, *Renormalizing the Nonrenormalizable*, *Phys. Rev. Lett.* **55** (1985) 363.
- [69] J. Braun, H. Gies and D. D. Scherer, *Asymptotic safety: a simple example*, *Phys. Rev.* **D83** (2011) 085012 [1011.1456].
- [70] B. Rosenstein, B. J. Warr and S. H. Park, *The Four Fermi Theory Is Renormalizable in (2+1)-Dimensions*, *Phys. Rev. Lett.* **62** (1989) 1433.
- [71] C. de Calan, P. A. Faria da Veiga, J. Magnen and R. Seneor, *Constructing the three-dimensional Gross-Neveu model with a large number of flavor components*, *Phys. Rev. Lett.* **66** (1991) 3233.
- [72] D. F. Litim and M. J. Trott, *Asymptotic safety of scalar field theories*, *Phys. Rev. D* **98** (2018) 125006 [1810.01678].
- [73] R. D. Pisarski, *Fixed point structure of  $(\phi^6)$  in three-dimensions at large  $N$* , *Phys. Rev. Lett.* **48** (1982) 574.
- [74] W. A. Bardeen, M. Moshe and M. Bander, *Spontaneous Breaking of Scale Invariance and the Ultraviolet Fixed Point in  $O(n)$  Symmetric  $(\phi^6)$  in Three-Dimensions Theory*, *Phys. Rev. Lett.* **52** (1984) 1188.
- [75] E. Brezin and J. Zinn-Justin, *Renormalization of the nonlinear sigma model in  $2 + \epsilon$  dimensions. Application to the Heisenberg ferromagnets*, *Phys. Rev. Lett.* **36** (1976) 691.
- [76] W. A. Bardeen, B. W. Lee and R. E. Shrock, *Phase Transition in the Nonlinear  $\sigma$  Model in  $2 + \epsilon$  Dimensional Continuum*, *Phys. Rev.* **D14** (1976) 985.
- [77] E. Brezin, J. Zinn-Justin and J. C. Le Guillou, *Renormalization of the Nonlinear Sigma Model in (Two + Epsilon) Dimension*, *Phys. Rev.* **D14** (1976) 2615.
- [78] E. Brezin and J. Zinn-Justin, *Spontaneous Breakdown of Continuous Symmetries Near Two-Dimensions*, *Phys. Rev.* **B14** (1976) 3110.
- [79] M. Shaposhnikov and C. Wetterich, *Asymptotic safety of gravity and the Higgs boson mass*, *Phys. Lett. B* **683** (2010) 196 [0912.0208].
- [80] A. Eichhorn and A. Held, *Top mass from asymptotic safety*, *Phys. Lett. B* **777** (2018) 217 [1707.01107].
- [81] A. Eichhorn and F. Versteegen, *Upper bound on the Abelian gauge coupling from asymptotic safety*, *JHEP* **01** (2018) 030 [1709.07252].
- [82] A. Eichhorn and A. Held, *Mass difference for charged quarks from asymptotically safe quantum gravity*, *Phys. Rev. Lett.* **121** (2018) 151302 [1803.04027].
- [83] R. Alkofer, A. Eichhorn, A. Held, C. M. Nieto, R. Percacci and M. Schröfl, *Quark masses and mixings in minimally parameterized UV completions of the Standard Model*, 2003.08401.

- [84] D. J. Gross and F. Wilczek, *Ultraviolet Behavior of Nonabelian Gauge Theories*, *Phys. Rev. Lett.* **30** (1973) 1343.
- [85] H. D. Politzer, *Reliable Perturbative Results for Strong Interactions?*, *Phys. Rev. Lett.* **30** (1973) 1346.
- [86] T. P. Cheng, E. Eichten and L.-F. Li, *Higgs Phenomena in Asymptotically Free Gauge Theories*, *Phys. Rev.* **D9** (1974) 2259.
- [87] G. F. Giudice, G. Isidori, A. Salvio and A. Strumia, *Softened Gravity and the Extension of the Standard Model up to Infinite Energy*, *JHEP* **02** (2015) 137 [1412.2769].
- [88] B. Holdom, J. Ren and C. Zhang, *Stable Asymptotically Free Extensions (SAFEs) of the Standard Model*, *JHEP* **03** (2015) 028 [1412.5540].
- [89] D. Bailin and A. Love, *Asymptotic Near Freedom*, *Nucl. Phys.* **B75** (1974) 159.
- [90] W. E. Caswell, *Asymptotic Behavior of Nonabelian Gauge Theories to Two Loop Order*, *Phys. Rev. Lett.* **33** (1974) 244.
- [91] T. Banks and A. Zaks, *On the Phase Structure of Vector-Like Gauge Theories with Massless Fermions*, *Nucl. Phys.* **B196** (1982) 189.
- [92] Y. Iwasaki, K. Kanaya, S. Sakai and T. Yoshie, *Quark confinement and number of flavors in strong coupling lattice QCD*, *Phys. Rev. Lett.* **69** (1992) 21.
- [93] M. Velkovsky and E. V. Shuryak, *QCD with large number of quarks: Effects of the instanton - anti-instanton pairs*, *Phys. Lett. B* **437** (1998) 398 [hep-ph/9703345].
- [94] H. Gies and J. Jaeckel, *Chiral phase structure of QCD with many flavors*, *Eur. Phys. J. C* **46** (2006) 433 [hep-ph/0507171].
- [95] T. A. Ryttov and F. Sannino, *Supersymmetry inspired QCD beta function*, *Phys. Rev. D* **78** (2008) 065001 [0711.3745].
- [96] T. Appelquist, G. T. Fleming and E. T. Neil, *Lattice study of the conformal window in QCD-like theories*, *Phys. Rev. Lett.* **100** (2008) 171607 [0712.0609].
- [97] T. Appelquist, G. T. Fleming and E. T. Neil, *Lattice Study of Conformal Behavior in SU(3) Yang-Mills Theories*, *Phys. Rev. D* **79** (2009) 076010 [0901.3766].
- [98] A. Hasenfratz, *Investigating the critical properties of beyond-QCD theories using Monte Carlo Renormalization Group matching*, *Phys. Rev. D* **80** (2009) 034505 [0907.0919].
- [99] A. Hasenfratz, *Conformal or Walking? Monte Carlo renormalization group studies of SU(3) gauge models with fundamental fermions*, *Phys. Rev. D* **82** (2010) 014506 [1004.1004].
- [100] Y. Kusafuka and H. Terao, *Fixed point merger in the SU(N) gauge beta functions*, *Phys. Rev. D* **84** (2011) 125006 [1104.3606].

- [101] Z. Fodor, K. Holland, J. Kuti, D. Nogradi, C. Schroeder, K. Holland et al., *Twelve massless flavors and three colors below the conformal window*, *Phys. Lett. B* **703** (2011) 348 [1104.3124].
- [102] T. Nunes da Silva, E. Pallante and L. Robroek, *Conformal or Confining*, 1506.06396.
- [103] LATKMI collaboration, *Conformality in twelve-flavor QCD*, *PoS LATTICE2014* (2015) 256 [1501.06660].
- [104] A. G. Cohen and H. Georgi, *Walking Beyond the Rainbow*, *Nucl. Phys. B* **314** (1989) 7.
- [105] T. Appelquist, J. Terning and L. Wijewardhana, *The Zero temperature chiral phase transition in  $SU(N)$  gauge theories*, *Phys. Rev. Lett.* **77** (1996) 1214 [hep-ph/9602385].
- [106] T. Appelquist, J. Terning and L. Wijewardhana, *Postmodern technicolor*, *Phys. Rev. Lett.* **79** (1997) 2767 [hep-ph/9706238].
- [107] V. Miransky and K. Yamawaki, *Conformal phase transition in gauge theories*, *Phys. Rev. D* **55** (1997) 5051 [hep-th/9611142].
- [108] T. Appelquist, A. Ratnaweera, J. Terning and L. Wijewardhana, *The Phase structure of an  $SU(N)$  gauge theory with  $N(f)$  flavors*, *Phys. Rev. D* **58** (1998) 105017 [hep-ph/9806472].
- [109] L. Di Pietro and M. Serone, *Looking through the QCD Conformal Window with Perturbation Theory*, 2003.01742.
- [110] A. D. Bond and D. F. Litim, *Theorems for Asymptotic Safety of Gauge Theories*, *Eur. Phys. J.* **C77** (2017) 429 [1608.00519].
- [111] A. D. Bond and D. F. Litim, *Price of Asymptotic Safety*, *Phys. Rev. Lett.* **122** (2019) 211601 [1801.08527].
- [112] D. F. Litim and F. Sannino, *Asymptotic safety guaranteed*, *JHEP* **12** (2014) 178 [1406.2337].
- [113] D. F. Litim, M. Mojaza and F. Sannino, *Vacuum stability of asymptotically safe gauge-Yukawa theories*, *JHEP* **01** (2016) 081 [1501.03061].
- [114] A. D. Bond and D. F. Litim, *More asymptotic safety guaranteed*, *Phys. Rev.* **D97** (2018) 085008 [1707.04217].
- [115] A. D. Bond and D. F. Litim, *Asymptotic safety guaranteed in supersymmetry*, *Phys. Rev. Lett.* **119** (2017) 211601 [1709.06953].
- [116] S. Abel and F. Sannino, *Radiative symmetry breaking from interacting UV fixed points*, *Phys. Rev.* **D96** (2017) 056028 [1704.00700].
- [117] N. Christiansen, A. Eichhorn and A. Held, *Is scale-invariance in gauge-Yukawa systems compatible with the graviton?*, *Phys. Rev.* **D96** (2017) 084021 [1705.01858].

- [118] D. H. Rischke and F. Sannino, *Thermodynamics of asymptotically safe theories*, *Phys. Rev. D* **D92** (2015) 065014 [1505.07828].
- [119] N. A. Dondi, V. Prochazka and F. Sannino, *Conformal Data of Fundamental Gauge-Yukawa Theories*, *Phys. Rev. D* **D98** (2018) 045002 [1712.05388].
- [120] F. Sannino and V. Skrinjar, *Instantons in asymptotically safe and free quantum field theories*, *Phys. Rev. D* **D99** (2019) 085010 [1802.10372].
- [121] A. D. Bond, G. Hiller, K. Kowalska and D. F. Litim, *Directions for model building from asymptotic safety*, *JHEP* **08** (2017) 004 [1702.01727].
- [122] D. Barducci, M. Fabbrichesi, C. M. Nieto, R. Percacci and V. Skrinjar, *In search of a UV completion of the standard model — 378,000 models that don't work*, *JHEP* **11** (2018) 057 [1807.05584].
- [123] G. Hiller, C. Hormigos-Feliu, D. F. Litim and T. Steudtner, *Asymptotically safe extensions of the Standard Model with flavour phenomenology*, in *54th Rencontres de Moriond on Electroweak Interactions and Unified Theories (Moriond EW 2019) La Thuile, Italy, March 16-23, 2019*, 2019, 1905.11020.
- [124] F. Sannino and I. M. Shoemaker, *Asymptotically Safe Dark Matter*, *Phys. Rev. D* **D92** (2015) 043518 [1412.8034].
- [125] N. G. Nielsen, F. Sannino and O. Svendsen, *Inflation from Asymptotically Safe Theories*, *Phys. Rev. D* **D91** (2015) 103521 [1503.00702].
- [126] D. Espriu, A. Palanques-Mestre, P. Pascual and R. Tarrach, *The  $\gamma$  Function in the  $1/N_f$  Expansion*, *Z. Phys. C* **C13** (1982) 153.
- [127] A. Palanques-Mestre and P. Pascual, *The  $1/N_f$  Expansion of the  $\gamma$  and Beta Functions in QED*, *Commun. Math. Phys.* **95** (1984) 277.
- [128] J. A. Gracey, *The QCD Beta function at  $O(1/N_f)$* , *Phys. Lett. B* **B373** (1996) 178 [hep-ph/9602214].
- [129] B. Holdom, *Large  $N$  flavor beta-functions: a recap*, *Phys. Lett. B* **B694** (2011) 74 [1006.2119].
- [130] O. Antipin and F. Sannino, *Conformal Window 2.0: The large  $N_f$  safe story*, *Phys. Rev. D* **D97** (2018) 116007 [1709.02354].
- [131] K. Kowalska and E. M. Sessolo, *Gauge contribution to the  $1/N_F$  expansion of the Yukawa coupling beta function*, *JHEP* **04** (2018) 027 [1712.06859].
- [132] G. M. Pelaggi, A. D. Plascencia, A. Salvio, F. Sannino, J. Smirnov and A. Strumia, *Asymptotically Safe Standard Model Extensions?*, *Phys. Rev. D* **D97** (2018) 095013 [1708.00437].
- [133] T. Alanne and S. Blasi, *The  $\beta$ -function for Yukawa theory at large  $N_f$* , *JHEP* **08** (2018) 081 [1806.06954].

- [134] O. Antipin, N. A. Dondi, F. Sannino, A. E. Thomsen and Z.-W. Wang, *Gauge-Yukawa theories: Beta functions at large  $N_f$* , *Phys. Rev.* **D98** (2018) 016003 [1803.09770].
- [135] N. A. Dondi, G. V. Dunne, M. Reichert and F. Sannino, *Towards the QED beta function and renormalons at  $1/N_f^2$  and  $1/N_f^3$* , 2003.08397.
- [136] T. Alanne, S. Blasi and N. A. Dondi, *Critical Look at  $\beta$ -Function Singularities at Large  $N$* , *Phys. Rev. Lett.* **123** (2019) 131602 [1905.08709].
- [137] J. Polchinski, *Scale and Conformal Invariance in Quantum Field Theory*, *Nucl. Phys. B* **303** (1988) 226.
- [138] M. A. Luty, J. Polchinski and R. Rattazzi, *The  $a$ -theorem and the Asymptotics of 4D Quantum Field Theory*, *JHEP* **01** (2013) 152 [1204.5221].
- [139] G. Mack, *All unitary ray representations of the conformal group  $SU(2,2)$  with positive energy*, *Commun. Math. Phys.* **55** (1977) 1.
- [140] J. Cardy, *Scaling and Renormalization in Statistical Physics*, Cambridge Lecture Notes in Physics. Cambridge University Press, 1996, 10.1017/CBO9781316036440.
- [141] S. Ferrara, A. Grillo and R. Gatto, *Tensor representations of conformal algebra and conformally covariant operator product expansion*, *Annals Phys.* **76** (1973) 161.
- [142] A. Polyakov, *Nonhamiltonian approach to conformal quantum field theory*, *Zh. Eksp. Teor. Fiz.* **66** (1974) 23.
- [143] A. Belavin, A. M. Polyakov and A. Zamolodchikov, *Infinite Conformal Symmetry in Two-Dimensional Quantum Field Theory*, *Nucl. Phys. B* **241** (1984) 333.
- [144] R. Rattazzi, V. S. Rychkov, E. Tonni and A. Vichi, *Bounding scalar operator dimensions in 4D CFT*, *JHEP* **12** (2008) 031 [0807.0004].
- [145] Z. Li and D. Poland, *Searching for gauge theories with the conformal bootstrap*, 2005.01721.
- [146] D. Simmons-Duffin, *The Conformal Bootstrap*, in *Theoretical Advanced Study Institute in Elementary Particle Physics: New Frontiers in Fields and Strings*, pp. 1–74, 2017, DOI [1602.07982].
- [147] D. Poland, S. Rychkov and A. Vichi, *The Conformal Bootstrap: Theory, Numerical Techniques, and Applications*, *Rev. Mod. Phys.* **91** (2019) 015002 [1805.04405].
- [148] J. L. Cardy, *Is There a  $c$  Theorem in Four-Dimensions?*, *Phys. Lett. B* **215** (1988) 749.
- [149] H. Osborn, *Derivation of a Four-dimensional  $c$  Theorem*, *Phys. Lett. B* **222** (1989) 97.
- [150] I. Jack and H. Osborn, *Analogues for the  $c$  Theorem for Four-dimensional Renormalizable Field Theories*, *Nucl. Phys.* **B343** (1990) 647.



- [151] Z. Komargodski and A. Schwimmer, *On Renormalization Group Flows in Four Dimensions*, *JHEP* **12** (2011) 099 [1107.3987].
- [152] H. Osborn, *Weyl consistency conditions and a local renormalization group equation for general renormalizable field theories*, *Nucl. Phys. B* **363** (1991) 486.
- [153] I. Jack and H. Osborn, *Constraints on RG Flow for Four Dimensional Quantum Field Theories*, *Nucl. Phys.* **B883** (2014) 425 [1312.0428].
- [154] S. R. Coleman and E. J. Weinberg, *Radiative Corrections as the Origin of Spontaneous Symmetry Breaking*, *Phys. Rev.* **D7** (1973) 1888.
- [155] T. Appelquist and J. Carazzone, *Infrared Singularities and Massive Fields*, *Phys. Rev. D* **11** (1975) 2856.
- [156] S. Tomonaga, *On a relativistically invariant formulation of the quantum theory of wave fields*, *Prog. Theor. Phys.* **1** (1946) 27.
- [157] J. S. Schwinger, *On Quantum electrodynamics and the magnetic moment of the electron*, *Phys. Rev.* **73** (1948) 416.
- [158] J. S. Schwinger, *Quantum electrodynamics. I A covariant formulation*, *Phys. Rev.* **74** (1948) 1439.
- [159] J. S. Schwinger, *Quantum electrodynamics. 2. Vacuum polarization and selfenergy*, *Phys. Rev.* **75** (1948) 651.
- [160] J. S. Schwinger, *Quantum electrodynamics. III: The electromagnetic properties of the electron: Radiative corrections to scattering*, *Phys. Rev.* **76** (1949) 790.
- [161] R. Feynman, *Space - time approach to quantum electrodynamics*, *Phys. Rev.* **76** (1949) 769.
- [162] R. Feynman, *The Theory of positrons*, *Phys. Rev.* **76** (1949) 749.
- [163] R. Feynman, *Mathematical formulation of the quantum theory of electromagnetic interaction*, *Phys. Rev.* **80** (1950) 440.
- [164] F. Dyson, *The S matrix in quantum electrodynamics*, *Phys. Rev.* **75** (1949) 1736.
- [165] F. Dyson, *The Radiation theories of Tomonaga, Schwinger, and Feynman*, *Phys. Rev.* **75** (1949) 486.
- [166] E. C. G. Stueckelberg de Breidenbach and A. Petermann, *La normalisation des constantes dans la théorie des quanta* *Normalizaton of constants in the quanta theory*, *Helv. Phys. Acta* **26** (1953) 499.
- [167] M. Gell-Mann and F. Low, *Quantum electrodynamics at small distances*, *Phys. Rev.* **95** (1954) 1300.
- [168] K. Symanzik, *Small distance behavior in field theory and power counting*, *Commun.Math.Phys.* **18** (1970) 227.

- [169] J. Callan, Curtis G., *Broken scale invariance in scalar field theory*, *Phys.Rev.D* **2** (1970) 1541.
- [170] L. Kadanoff, *Scaling laws for ising models near  $t(c)$* , *Physics Physique Fizika* **2** (1966) 263.
- [171] K. G. Wilson, *Renormalization group and critical phenomena. 1. Renormalization group and the Kadanoff scaling picture*, *Phys. Rev.* **B4** (1971) 3174.
- [172] K. G. Wilson, *Renormalization group and critical phenomena. 2. Phase space cell analysis of critical behavior*, *Phys. Rev. B* **4** (1971) 3184.
- [173] K. Wilson and J. B. Kogut, *The renormalization group and the epsilon expansion*, *Phys.Rept.* **12** (1974) 75.
- [174] K. G. Wilson, *The Renormalization Group: Critical Phenomena and the Kondo Problem*, *Rev. Mod. Phys.* **47** (1975) 773.
- [175] J. Polchinski, *Renormalization and effective lagrangians*, *Nucl.Phys.B* **231** (1984) 269.
- [176] G. 't Hooft, *Dimensional regularization and the renormalization group*, *Nucl.Phys.B* **61** (1973) 455.
- [177] D. V. Shirkov, *The Renormalization Group Method and Functional Selfsimilarity in Physics*, *Theor. Math. Phys.* **60** (1985) 778.
- [178] O. J. Rosten, *Fundamentals of the Exact Renormalization Group*, *Phys. Rept.* **511** (2012) 177 [1003.1366].
- [179] I. Jack and H. Osborn, *General Two Loop Beta Functions for Gauge Theories With Arbitrary Scalar Fields*, *J. Phys.* **A16** (1983) 1101.
- [180] I. Jack and H. Osborn, *Two Loop Background Field Calculations for Arbitrary Background Fields*, *Nucl. Phys.* **B207** (1982) 474.
- [181] I. Jack and H. Osborn, *General Background Field Calculations With Fermion Fields*, *Nucl. Phys.* **B249** (1985) 472.
- [182] M. E. Machacek and M. T. Vaughn, *Two Loop Renormalization Group Equations in a General Quantum Field Theory. 1. Wave Function Renormalization*, *Nucl. Phys.* **B222** (1983) 83.
- [183] M. E. Machacek and M. T. Vaughn, *Two Loop Renormalization Group Equations in a General Quantum Field Theory. 2. Yukawa Couplings*, *Nucl. Phys.* **B236** (1984) 221.
- [184] M. E. Machacek and M. T. Vaughn, *Two Loop Renormalization Group Equations in a General Quantum Field Theory. 3. Scalar Quartic Couplings*, *Nucl. Phys.* **B249** (1985) 70.
- [185] M.-x. Luo, H.-w. Wang and Y. Xiao, *Two loop renormalization group equations in general gauge field theories*, *Phys. Rev.* **D67** (2003) 065019 [hep-ph/0211440].
- [186] T. Curtright, *Three loop charge renormalization effects due to quartic scalar selfinteractions*, *Phys.Rev.D* **21** (1980) 1543.

- [187] A. G. M. Pickering, J. A. Gracey and D. R. T. Jones, *Three loop gauge beta function for the most general single gauge coupling theory*, *Phys. Lett.* **B510** (2001) 347 [hep-ph/0104247].
- [188] L. N. Mihaila, J. Salomon and M. Steinhauser, *Renormalization constants and beta functions for the gauge couplings of the standard model to three-loop order*, *Phys.Rev.D* **86** (2012) 096008 [1208.3357].
- [189] L. Mihaila, *Three-loop gauge beta function in non-simple gauge groups*, *PoS RADCOR2013* (2013) 060.
- [190] C. Poole and A. E. Thomsen, *Constraints on 3- and 4-loop  $\beta$ -functions in a general four-dimensional quantum field theory*, *JHEP* **09** (2019) 055 [1906.04625].
- [191] M. Sperling, D. Stöckinger and A. Voigt, *Renormalization of vacuum expectation values in spontaneously broken gauge theories*, *JHEP* **07** (2013) 132 [1305.1548].
- [192] M. Sperling, D. Stöckinger and A. Voigt, *Renormalization of vacuum expectation values in spontaneously broken gauge theories: Two-loop results*, *JHEP* **01** (2014) 068 [1310.7629].
- [193] I. Jack and C. Poole, *Scheme invariants in  $\phi^4$  theory in four dimensions*, *Phys. Rev. D* **98** (2018) 065011 [1806.08598].
- [194] E. Mølgaard, *Decrypting gauge-yukawa cookbooks*, *Eur.Phys.J.Plus* **129** (2014) 159 [1404.5550].
- [195] S. P. Martin and M. T. Vaughn, *Two loop renormalization group equations for soft supersymmetry breaking couplings*, *Phys. Rev.* **D50** (1994) 2282 [hep-ph/9311340].
- [196] Y. Yamada, *Two loop renormalization group equations for soft SUSY breaking scalar interactions: Supergraph method*, *Phys. Rev.* **D50** (1994) 3537 [hep-ph/9401241].
- [197] I. Jack, D. R. T. Jones and A. Pickering, *Renormalization invariance and the soft Beta functions*, *Phys. Lett.* **B426** (1998) 73 [hep-ph/9712542].
- [198] I. Jack, D. R. T. Jones, S. P. Martin, M. T. Vaughn and Y. Yamada, *Decoupling of the epsilon scalar mass in softly broken supersymmetry*, *Phys. Rev.* **D50** (1994) R5481 [hep-ph/9407291].
- [199] I. Jack, D. Jones and C. North,  *$N=1$  supersymmetry and the three loop gauge beta function*, *Phys.Lett.B* **386** (1996) 138 [hep-ph/9606323].
- [200] I. Jack, D. Jones and C. North, *Scheme dependence and the nsvz beta function*, *Nucl.Phys.B* **486** (1997) 479 [hep-ph/9609325].
- [201] I. Jack, D. Jones and C. North,  *$N=1$  supersymmetry and the three loop anomalous dimension for the chiral superfield*, *Nucl.Phys.B* **473** (1996) 308 [hep-ph/9603386].
- [202] T. van Ritbergen, J. Vermaseren and S. Larin, *The four loop beta function in quantum chromodynamics*, *Phys.Lett.B* **400** (1997) 379 [hep-ph/9701390].

- [203] M. Czakon, *The four-loop qcd beta-function and anomalous dimensions*, *Nucl.Phys.B* **710** (2005) 485 [hep-ph/0411261].
- [204] F. Herzog, B. Ruijl, T. Ueda, J. Vermaseren and A. Vogt, *The five-loop beta function of yang-mills theory with fermions*, *JHEP* **02** (2017) 090 [1701.01404].
- [205] T. Luthe, A. Maier, P. Marquard and Y. Schroder, *The five-loop beta function for a general gauge group and anomalous dimensions beyond feynman gauge*, *JHEP* **10** (2017) 166 [1709.07718].
- [206] J. A. Gracey, T. Luthe and Y. Schroder, *Four loop renormalization of the Gross-Neveu model*, *Phys. Rev.* **D94** (2016) 125028 [1609.05071].
- [207] N. Zerf, L. N. Mihaila, P. Marquard, I. F. Herbut and M. M. Scherer, *Four-loop critical exponents for the Gross-Neveu-Yukawa models*, *Phys. Rev.* **D96** (2017) 096010 [1709.05057].
- [208] J. A. Gracey, *Large  $N$  critical exponents for the chiral Heisenberg Gross-Neveu universality class*, *Phys. Rev.* **D97** (2018) 105009 [1801.01320].
- [209] O. Schnetz, *Numbers and Functions in Quantum Field Theory*, *Phys. Rev.* **D97** (2018) 085018 [1606.08598].
- [210] M. Kompaniets and E. Panzer, *Renormalization group functions of  $\phi^4$  theory in the  $\overline{MS}$ -scheme to six loops*, *PoS* **LL2016** (2016) 038 [1606.09210].
- [211] D. V. Batkovich, K. G. Chetyrkin and M. V. Kompaniets, *Six loop analytical calculation of the field anomalous dimension and the critical exponent  $\eta$  in  $O(n)$ -symmetric  $\phi^4$  model*, *Nucl. Phys.* **B906** (2016) 147 [1601.01960].
- [212] A. Pelissetto, P. Rossi and E. Vicari, *Large  $n$  critical behavior of  $O(n) \times O(m)$  spin models*, *Nucl. Phys. B* **607** (2001) 605 [hep-th/0104024].
- [213] P. Calabrese and P. Parruccini, *Five loop epsilon expansion for  $O(n) \times O(m)$  spin models*, *Nucl. Phys. B* **679** (2004) 568 [cond-mat/0308037].
- [214] M. Kompaniets, A. Kudlis and A. Sokolov, *Six-loop  $\epsilon$  expansion study of three-dimensional  $O(n) \times O(m)$  spin models*, *Nucl. Phys. B* **950** (2020) 114874 [1911.01091].
- [215] L. N. Mihaila, J. Salomon and M. Steinhauser, *Gauge Coupling Beta Functions in the Standard Model to Three Loops*, *Phys. Rev. Lett.* **108** (2012) 151602 [1201.5868].
- [216] A. V. Bednyakov, A. F. Pikelner and V. N. Velizhanin, *Anomalous dimensions of gauge fields and gauge coupling beta-functions in the Standard Model at three loops*, *JHEP* **01** (2013) 017 [1210.6873].
- [217] A. V. Bednyakov, A. F. Pikelner and V. N. Velizhanin, *Yukawa coupling beta-functions in the Standard Model at three loops*, *Phys. Lett.* **B722** (2013) 336 [1212.6829].

- [218] A. V. Bednyakov, A. F. Pikelner and V. N. Velizhanin, *Higgs self-coupling beta-function in the Standard Model at three loops*, *Nucl. Phys.* **B875** (2013) 552 [1303.4364].
- [219] K. G. Chetyrkin and M. F. Zoller, *Three-loop  $\beta$ -functions for top-Yukawa and the Higgs self-interaction in the Standard Model*, *JHEP* **06** (2012) 033 [1205.2892].
- [220] K. G. Chetyrkin and M. F. Zoller,  *$\beta$ -function for the Higgs self-interaction in the Standard Model at three-loop level*, *JHEP* **04** (2013) 091 [1303.2890].
- [221] J. Davies, F. Herren, C. Poole, M. Steinhauser and A. E. Thomsen, *Gauge coupling beta functions to four-loop order in the standard model*, 1912.07624.
- [222] S. R. Coleman and D. J. Gross, *Price of asymptotic freedom*, *Phys. Rev. Lett.* **31** (1973) 851.
- [223] N. Brambilla et al., *QCD and Strongly Coupled Gauge Theories: Challenges and Perspectives*, *Eur. Phys. J.* **C74** (2014) 2981 [1404.3723].
- [224] A. D. Bond, D. F. Litim and T. Steudtner, , *in preparation* (2020) .
- [225] A. Held, *Effective asymptotic safety and its predictive power: Gauge-Yukawa theories*, 2003.13642.
- [226] K. Intriligator and F. Sannino, *Supersymmetric asymptotic safety is not guaranteed*, *JHEP* **11** (2015) 023 [1508.07411].
- [227] S. P. Martin and J. D. Wells, *Constraints on ultraviolet stable fixed points in supersymmetric gauge theories*, *Phys. Rev.* **D64** (2001) 036010 [hep-ph/0011382].
- [228] G. Veneziano, *U(1) Without Instantons*, *Nucl. Phys.* **B159** (1979) 213.
- [229] K. G. Wilson and M. E. Fisher, *Critical exponents in 3.99 dimensions*, *Phys. Rev. Lett.* **28** (1972) 240.
- [230] G. 't Hooft, *A Planar Diagram Theory for Strong Interactions*, *Nucl. Phys.* **B72** (1974) 461.
- [231] P. Cvitanovic, *Group theory: Birdtracks, Lie's and exceptional groups*. Princeton, USA: Univ. Pr. (2008) 273 p, 2008.
- [232] S. Keppeler, *Birdtracks for SU(N)*, in *QCD Master Class 2017 Saint-Jacut-de-la-Mer, France, June 18-24, 2017*, 2017, DOI [1707.07280].
- [233] T. Buyukbese and D. F. Litim, *Asymptotic safety of gauge theories beyond marginal interactions*, *PoS LATTICE2016* (2017) 233.
- [234] T. Büyükbeşe, *Asymptotic safety of gauge theories and gravity: adventures in large group dimensions*, Ph.D. thesis, University of Sussex, 2018.
- [235] F. Staub, *SARAH*, 0806.0538.
- [236] F. Staub, *From Superpotential to Model Files for FeynArts and CalcHep/CompHep*, *Comput. Phys. Commun.* **181** (2010) 1077 [0909.2863].

- [237] F. Staub, *Automatic Calculation of supersymmetric Renormalization Group Equations and Self Energies*, *Comput. Phys. Commun.* **182** (2011) 808 [1002.0840].
- [238] F. Staub, *SARAH 3.2: Dirac Gauginos, UFO output, and more*, *Comput. Phys. Commun.* **184** (2013) 1792 [1207.0906].
- [239] F. Staub, *SARAH 4 : A tool for (not only SUSY) model builders*, *Comput. Phys. Commun.* **185** (2014) 1773 [1309.7223].
- [240] F. Lyonnet, I. Schienbein, F. Staub and A. Wingerter, *PyR@TE: Renormalization Group Equations for General Gauge Theories*, *Comput. Phys. Commun.* **185** (2014) 1130 [1309.7030].
- [241] F. Lyonnet and I. Schienbein, *PyR@TE 2: A Python tool for computing RGEs at two-loop*, *Comput. Phys. Commun.* **213** (2017) 181 [1608.07274].
- [242] R. M. Fonseca, M. Malinský and F. Staub, *Renormalization group equations and matching in a general quantum field theory with kinetic mixing*, *Phys. Lett.* **B726** (2013) 882 [1308.1674].
- [243] S. P. Martin and M. T. Vaughn, *Regularization dependence of running couplings in softly broken supersymmetry*, *Phys. Lett.* **B318** (1993) 331 [hep-ph/9308222].
- [244] J. Braathen, M. D. Goodsell, M. E. Krauss, T. Opferkuch and F. Staub, *N-loop running should be combined with N-loop matching*, *Phys. Rev.* **D97** (2018) 015011 [1711.08460].
- [245] A. V. Bednyakov, *On three-loop RGE for the Higgs sector of 2HDM*, 1809.04527.
- [246] Wolfram Research, Inc., *Mathematica, Version 12.0*, <https://www.wolfram.com/mathematica> (Champaign, IL, 2020) .
- [247] T. Steudtner, *ARGES*, <https://github.com/tomsteu/ARGES> (2020) .
- [248] Free Software Foundation, *GNU General Public License v3*, <https://www.gnu.org/licenses/gpl-3.0.html> (2007) .
- [249] R. M. Fonseca, *Calculating the renormalisation group equations of a SUSY model with Susyno*, *Comput. Phys. Commun.* **183** (2012) 2298 [1106.5016].
- [250] F. Lyonnet, *PyLie*, <https://github.com/dibus2/pylie> (2016) .
- [251] D. F. Litim, *On fixed points of quantum gravity*, *AIP Conf. Proc.* **841** (2006) 322 [hep-th/0606044].
- [252] D. F. Litim, *Fixed Points of Quantum Gravity and the Renormalisation Group*, 0810.3675.
- [253] K. Falls, D. F. Litim, K. Nikolakopoulos and C. Rahmede, *Further evidence for asymptotic safety of quantum gravity*, *Phys. Rev.* **D93** (2016) 104022 [1410.4815].

- [254] D. F. Litim, M. C. Mastaler, F. Synatschke-Czerwonka and A. Wipf, *Critical behavior of supersymmetric  $O(N)$  models in the large- $N$  limit*, *Phys. Rev.* **D84** (2011) 125009 [1107.3011].
- [255] M. Heilmann, D. F. Litim, F. Synatschke-Czerwonka and A. Wipf, *Phases of supersymmetric  $O(N)$  theories*, *Phys. Rev.* **D86** (2012) 105006 [1208.5389].
- [256] D. F. Litim, E. Marchais and P. Mati, *Fixed points and the spontaneous breaking of scale invariance*, *Phys. Rev.* **D95** (2017) 125006 [1702.05749].
- [257] B. H. Wellegehausen, D. Körner and A. Wipf, *Asymptotic safety on the lattice: The Nonlinear  $O(N)$  Sigma Model*, *Annals Phys.* **349** (2014) 374 [1402.1851].
- [258] A. Bond and D. F. Litim, *Interacting ultraviolet completions of four-dimensional gauge theories*, *PoS LATTICE2016* (2017) 208.
- [259] D. D. Dietrich and F. Sannino, *Conformal window of  $SU(N)$  gauge theories with fermions in higher dimensional representations*, *Phys. Rev.* **D75** (2007) 085018 [hep-ph/0611341].
- [260] J. Braun and H. Gies, *Scaling laws near the conformal window of many-flavor QCD*, *JHEP* **05** (2010) 060 [0912.4168].
- [261] L. Del Debbio, *The conformal window on the lattice*, *PoS Lattice2010* (2014) 004 [1102.4066].
- [262] E. Pomoni and L. Rastelli, *Large  $N$  Field Theory and AdS Tachyons*, *JHEP* **04** (2009) 020 [0805.2261].
- [263] O. Antipin, M. Gillioz, E. Mølgaard and F. Sannino, *The  $a$  theorem for gauge-Yukawa theories beyond Banks-Zaks fixed point*, *Phys. Rev.* **D87** (2013) 125017 [1303.1525].
- [264] O. Antipin, M. Gillioz, J. Krog, E. Mølgaard and F. Sannino, *Standard Model Vacuum Stability and Weyl Consistency Conditions*, *JHEP* **08** (2013) 034 [1306.3234].
- [265] D. F. Litim and E. Marchais, *Critical  $O(N)$  models in the complex field plane*, *Phys. Rev.* **D95** (2017) 025026 [1607.02030].
- [266] A. Jüttner, D. F. Litim and E. Marchais, *Global Wilson–Fisher fixed points*, *Nucl. Phys.* **B921** (2017) 769 [1701.05168].
- [267] A. J. Paterson, *Coleman-Weinberg Symmetry Breaking in the Chiral  $SU(N) \times SU(N)$  Linear Sigma Model*, *Nucl. Phys.* **B190** (1981) 188.
- [268] G. Medina Vazquez, *Asymptotic safety in gauge theories under various representations*, Master’s thesis, University of Sussex, 2016.
- [269] C. Pica and F. Sannino, *Beta Function and Anomalous Dimensions*, *Phys. Rev.* **D83** (2011) 116001 [1011.3832].
- [270] R. Shrock, *Study of Possible Ultraviolet Zero of the Beta Function in Gauge Theories with Many Fermions*, *Phys. Rev.* **D89** (2014) 045019 [1311.5268].

- [271] H. Georgi and S. L. Glashow, *Unity of All Elementary Particle Forces*, *Phys. Rev. Lett.* **32** (1974) 438.
- [272] S. Weinberg, *Asymptotically Safe Inflation*, *Phys. Rev.* **D81** (2010) 083535 [0911.3165].
- [273] M. Hindmarsh, D. Litim and C. Rahmede, *Asymptotically Safe Cosmology*, *JCAP* **1107** (2011) 019 [1101.5401].
- [274] K. Falls, D. F. Litim, K. Nikolakopoulos and C. Rahmede, *On de Sitter solutions in asymptotically safe  $f(R)$  theories*, *Class. Quant. Grav.* **35** (2018) 135006 [1607.04962].
- [275] O. Svendsen, H. Bazrafshan Moghaddam and R. Brandenberger, *Preheating in an Asymptotically Safe Quantum Field Theory*, *Phys. Rev.* **D94** (2016) 083527 [1603.02628].
- [276] PLANCK collaboration, *Planck 2015 results. XX. Constraints on inflation*, *Astron. Astrophys.* **594** (2016) A20 [1502.02114].
- [277] C. Lovelace, *UNIVERSALITY AT LARGE  $N$* , *Nucl. Phys.* **B201** (1982) 333.
- [278] N. Seiberg, *Electric - magnetic duality in supersymmetric nonAbelian gauge theories*, *Nucl. Phys.* **B435** (1995) 129 [hep-th/9411149].
- [279] J. M. Maldacena, *The Large  $N$  limit of superconformal field theories and supergravity*, *Int. J. Theor. Phys.* **38** (1999) 1113 [hep-th/9711200].
- [280] S. Kachru and E. Silverstein, *4-D conformal theories and strings on orbifolds*, *Phys. Rev. Lett.* **80** (1998) 4855 [hep-th/9802183].
- [281] M. Bershadsky and A. Johansen, *Large  $N$  limit of orbifold field theories*, *Nucl. Phys.* **B536** (1998) 141 [hep-th/9803249].
- [282] M. Schmaltz, *Duality of nonsupersymmetric large  $N$  gauge theories*, *Phys. Rev.* **D59** (1999) 105018 [hep-th/9805218].
- [283] J. Erlich and A. Naqvi, *Nonperturbative tests of the parent / orbifold correspondence in supersymmetric gauge theories*, *JHEP* **12** (2002) 047 [hep-th/9808026].
- [284] M. J. Strassler, *On methods for extracting exact nonperturbative results in nonsupersymmetric gauge theories*, hep-th/0104032.
- [285] A. Armoni, M. Shifman and G. Veneziano, *Exact results in non-supersymmetric large  $N$  orientifold field theories*, *Nucl. Phys.* **B667** (2003) 170 [hep-th/0302163].
- [286] P. Kovtun, M. Unsal and L. G. Yaffe, *Necessary and sufficient conditions for non-perturbative equivalences of large  $N(c)$  orbifold gauge theories*, *JHEP* **07** (2005) 008 [hep-th/0411177].
- [287] G. V. Dunne and M. Ünsal, *New Nonperturbative Methods in Quantum Field Theory: From Large- $N$  Orbifold Equivalence to Bions and Resurgence*, *Ann. Rev. Nucl. Part. Sci.* **66** (2016) 245 [1601.03414].



- [288] P. Kovtun, M. Unsal and L. G. Yaffe, *Volume independence in large  $N(c)$  QCD-like gauge theories*, *JHEP* **06** (2007) 019 [hep-th/0702021].
- [289] M. Hanada and N. Yamamoto, *Universality of Phases in QCD and QCD-like Theories*, *JHEP* **02** (2012) 138 [1103.5480].
- [290] B. Lucini and M. Panero,  *$SU(N)$  gauge theories at large  $N$* , *Phys. Rept.* **526** (2013) 93 [1210.4997].
- [291] K. Kowalska, A. Bond, G. Hiller and D. Litim, *Towards an asymptotically safe completion of the Standard Model*, *PoS EPS-HEP2017* (2017) 542.
- [292] E. Gildener, *Radiatively Induced Spontaneous Symmetry Breaking for Asymptotically Free Gauge Theories*, *Phys. Rev.* **D13** (1976) 1025.
- [293] E. Witten, *An  $SU(2)$  Anomaly*, *Phys. Lett.* **117B** (1982) 324.
- [294] H. Terao and A. Tsuchiya, *Conformal dynamics in gauge theories via non-perturbative renormalization group*, 0704.3659.
- [295] D. B. Kaplan, J.-W. Lee, D. T. Son and M. A. Stephanov, *Conformality Lost*, *Phys. Rev.* **D80** (2009) 125005 [0905.4752].
- [296] R. C. King, *Modification rules and products of irreducible representations of the unitary, orthogonal, and symplectic groups*, *J. Math. Phys.* **12** (1971) 1588.
- [297] R. L. Mkrтчian, *The Equivalence of  $Sp(2N)$  and  $SO(-2N)$  Gauge Theories*, *Phys. Lett.* **105B** (1981) 174.
- [298] P. Cvitanovic and A. D. Kennedy, *Spinors in Negative Dimensions*, *Phys. Scripta* **26** (1982) 5.
- [299] R. L. Mkrтчyan and A. P. Veselov, *On duality and negative dimensions in the theory of Lie groups and symmetric spaces*, *J. Math. Phys.* **52** (2011) 083514 [1011.0151].
- [300] F. J. Dyson, *Divergence of perturbation theory in quantum electrodynamics*, *Phys. Rev.* **85** (1952) 631.
- [301] E. Witten, *Symmetry and Emergence*, *Nature Phys.* **14** (2018) 116 [1710.01791].
- [302] D. F. Litim and T. Steudtner, , *in preparation* (2020) .
- [303] A. Codello, M. Safari, G. P. Vacca and O. Zanusso, *Functional perturbative RG and CFT data in the  $\epsilon$ -expansion*, *Eur. Phys. J.* **C78** (2018) 30 [1705.05558].
- [304] G. Hiller, C. Hormigos-Feliu, D. F. Litim and T. Steudtner, *Model building from asymptotic safety with flavor and Higgs portals, (in prep.)* (2020) .
- [305] D. S. M. Alves, J. Galloway, J. T. Ruderman and J. R. Walsh, *Running Electroweak Couplings as a Probe of New Physics*, *JHEP* **02** (2015) 007 [1410.6810].

- [306] M. Farina, G. Panico, D. Pappadopulo, J. T. Ruderman, R. Torre and A. Wulzer, *Energy helps accuracy: electroweak precision tests at hadron colliders*, *Phys. Lett.* **B772** (2017) 210 [1609.08157].
- [307] J. A. Evans and J. Shelton, *Long-Lived Staus and Displaced Leptons at the LHC*, *JHEP* **04** (2016) 056 [1601.01326].
- [308] L. Lavoura, *General formulae for  $f(1) \rightarrow f(2)$  gamma*, *Eur. Phys. J. C* **29** (2003) 191 [hep-ph/0302221].
- [309] G. Cavoto, A. Papa, F. Renga, E. Ripiccini and C. Voena, *The quest for  $\mu \rightarrow e\gamma$  and its experimental limiting factors at future high intensity muon beams*, *Eur. Phys. J. C* **78** (2018) 37 [1707.01805].
- [310] ACME collaboration, *Improved limit on the electric dipole moment of the electron*, *Nature* **562** (2018) 355.
- [311] MUON (G-2) collaboration, *An Improved Limit on the Muon Electric Dipole Moment*, *Phys. Rev. D* **80** (2009) 052008 [0811.1207].
- [312] F. Jegerlehner and A. Nyffeler, *The Muon g-2*, *Phys. Rept.* **477** (2009) 1 [0902.3360].
- [313] T. Aoyama et al., *The anomalous magnetic moment of the muon in the Standard Model*, 2006.04822.
- [314] T. Aoyama, M. Hayakawa, T. Kinoshita and M. Nio, *Complete Tenth-Order QED Contribution to the Muon g-2*, *Phys. Rev. Lett.* **109** (2012) 111808 [1205.5370].
- [315] C. Bouchiat and L. Michel, *La résonance dans la diffusion méson  $\pi$ — méson  $\pi$  et le moment magnétique anormal du méson  $\mu$* , *J. Phys. Radium* **22** (1961) 121.
- [316] S. J. Brodsky and E. De Rafael, *Suggested Boson - Lepton Pair Couplings and the Anomalous Magnetic Moment of the Muon*, *Phys. Rev.* **168** (1968) 1620.
- [317] F. Jegerlehner, *Muon g - 2 theory: The hadronic part*, *EPJ Web Conf.* **166** (2018) 00022 [1705.00263].
- [318] M. Davier, *Update of the Hadronic Vacuum Polarisation Contribution to the muon g-2*, *Nucl. Part. Phys. Proc.* **287-288** (2017) 70 [1612.02743].
- [319] H. Davoudiasl and W. J. Marciano, *Tale of two anomalies*, *Phys. Rev.* **D98** (2018) 075011 [1806.10252].
- [320] J. Liu, C. E. M. Wagner and X.-P. Wang, *A light complex scalar for the electron and muon anomalous magnetic moments*, *JHEP* **03** (2019) 008 [1810.11028].
- [321] S. Gardner and X. Yan, *Light scalars with lepton number to solve the  $(g - 2)_e$  anomaly*, 1907.12571.
- [322] M. Bauer, M. Neubert, S. Renner, M. Schnubel and A. Thamm, *Axion-like particles, lepton-flavor violation and a new explanation of  $a_\mu$  and  $a_e$* , 1908.00008.

- [323] B. Dutta and Y. Mimura, *Electron  $g - 2$  with flavor violation in MSSM*, *Phys. Lett.* **B790** (2019) 563 [1811.10209].
- [324] M. Endo and W. Yin, *Explaining electron and muon  $g - 2$  anomaly in SUSY without lepton-flavor mixings*, *JHEP* **08** (2019) 122 [1906.08768].
- [325] M. Badziak and K. Sakurai, *Explanation of electron and muon  $g-2$  anomalies in the MSSM*, *JHEP* **10** (2019) 024 [1908.03607].
- [326] A. Crivellin, M. Hoferichter and P. Schmidt-Wellenburg, *Combined explanations of  $(g - 2)_{\mu,e}$  and implications for a large muon EDM*, *Phys. Rev.* **D98** (2018) 113002 [1807.11484].
- [327] A. Crivellin and M. Hoferichter, *Combined explanations of  $(g - 2)_{\mu}$ ,  $(g - 2)_e$  and implications for a large muon EDM*, in *33rd Rencontres de Physique de La Vallée d'Aoste (LaThuile 2019) La Thuile, Aosta, Italy, March 10-16, 2019*, 2019, 1905.03789.
- [328] B. Holdom, *Technicolor*, *Phys. Lett.* **150B** (1985) 301.
- [329] M. Cirelli, N. Fornengo and A. Strumia, *Minimal dark matter*, *Nucl. Phys.* **B753** (2006) 178 [hep-ph/0512090].